2014

Characterisation of group A streptococcal innate immune resistance and host response mechanisms

James Anthony Tsatsaronis
University of Wollongong

Characterisation of group A streptococcal innate immune resistance and host response mechanisms

A thesis submitted in fulfilment of the requirements for the award of the degree

Doctor of Philosophy (PhD)

From the

University of Wollongong

By

James Anthony Tsatsaronis

Bachelor of Biotechnology (Adv) (Hons)

Illawarra Health and Medical Research Institute (IHMRI)

School of Biological Sciences

2014

CERTIFICATION

I, James A. Tsatsaronis, declare that this thesis, submitted in fulfilment of the requirements for the award of Doctor of Philosophy, in the Department of Biological Sciences, University of Wollongong, is wholly my own work unless otherwise referenced and acknowledged. The document has not been submitted for qualifications at any other academic institution.

_____

James Anthony Tsatsaronis

May, 2014

ACKNOWLEDGEMENTS

A PhD is not an endeavour that one undertakes alone, or is completed solely due to the work of one person. This PhD was no different. As such, I would like to thank Martina Sanderson-Smith for being the greatest source of advice, inspiration, and support over the last few years. I cannot imagine a supervisor who is as caring and nurturing of her students. You gave me the guidance and confidence necessary to be the “beautiful scientific flower” that I hope I now resemble.

Many others have also helped shape the work contained herein. I am always grateful to my co-supervisor Mark Walker for your insightful wisdom and input. To Eva Medina I cannot express too much gratitude for hosting me not once, but twice at the HZI during this project. Oliver Goldmann, my discussions with you during these visits were probably more help than you realise. I thank Scott Beatson for hosting me in those early days at UQ, and for the assistance of your entire bioinformatic lab group. I also thank my collaborators and others who contributed to the project, either directly or indirectly, particularly Jude Taylor, Andrew Hollands, Jason Cole and Manfred Rohde for exquisite electron microscopy.

I would like to thank the past and present members of the Walker/Sanderson-Smith/McArthur labs, particularly Jason McArthur for constantly being a source of advice. I thank Ron Sluyter for his excellent and often unacknowledged advice. Others from within and without the lab; Amanda, Di ly, Bodgy, Corky, Simon, Flynn, Aleta, David, Carola, Blake, Cortny, Mari, Pan, Jeff, to name a few. I thank you all for your friendship and support. We all know what a labour a PhD is, but that burden was much easier to bear thanks to you all. I also thank my distant friends in Braunschweig, Andrew, Mel, Diego, Giuseppe, Marcia, Bahram, Rolf and the entire thirsty crew. You made my months in Germany feel more welcoming and fun than I can express.

Finally, to my family and friends outside the research world. I thank you all for your love and patience. Without your support and encouragement, I doubt that I could have come to where I am now.

ABSTRACT

Group A Streptococcus (GAS, *Streptococcus pyogenes*) is a Gram-positive bacterial pathogen responsible for life-threatening, invasive human diseases, including necrotising fasciitis and streptococcal toxic shock syndrome. In the last 30 years, a global increase in the rates of severe and fatal forms of GAS infection has been noted. Coinciding with this epidemiological trend has been a pandemic spread of particularly hypervirulent GAS, notably a clone of the M1T1 serotype. Studies investigating this serotype highlight the unique genetic makeup of M1T1 GAS and its interactions with the host innate immune response as key elements coordinating the virulence of this serotype. Phage-mediated horizontal gene transfer and selective pressure exerted by polymorphonuclear leukocytes (PMNs) for mutations in the control of virulence regulator operon (*covRS*) bestow M1T1 GAS with enhanced pathogenic capacity. However, isolates of virulent GAS also occur in genetic backgrounds lacking phage-encoded factors, such as *sda1,* and other M1T1-specific core genomic elements necessary for *covRS* mutation. In this study, high-throughput next-generation sequencing was utilised to generate a draft genome sequence of NS88.2, an *emm*98.1 GAS isolate exhibiting a hypervirulent and PMN resistant phenotype. The multi-locus sequence type (MLST) was determined from the NS88.2 draft genome sequence, which was compared to fully sequenced GAS strains by whole genome BLAST alignment. NS88.2 was found to have a MLST sequence type of 205, and regions of nucleotide sequence divergence between NS88.2 and other GAS included the multiple gene regulator (MGA) and fibronectin, collagen and T-antigen (FCT) loci. The NS88.2 MGA locus showed low sequence similarity to GAS of other *emm*-types, and the FCT locus corresponded to an FCT type 3. A ~30 kb region containing putative prophage-like elements constituted the majority of NS88.2 novel sequence data, however

interrogation of these elements did not reveal novel genes with obvious roles in modulating PMN responses. Bioinformatic prediction of genes encoding cell surface and secreted proteins was conducted, and identified 10 putative cell surface proteins and 190 putative proteins with secretion signal peptides. The addition of this genome draft to public databases will facilitate other studies of GAS genome biology, and further in-depth analyses of the NS88.2 isolate described here.

The phage-encoded extracellular DNase streptodornase 1 (Sda1) has previously been shown as essential for M1T1 GAS acquisition of *covRS* mutations. Mutations of *covRS* in M1T1 GAS bestow hypervirulent and PMN resistant qualities. These phenotypes are also observed in the NS88.2 isolate, which encodes a truncated, non-functional *covS* gene, but not the *sda1* gene. In this study, NS88.2 and derivative strains with intact *covS* (NS88.2*rep*) or reverse complemented inactive *covS* (NS88.2*covS*) were examined to determine potential novel mechanisms by which these strains interact with the innate immune response. Phenotypic comparison of NS88.2, NS88.2*rep* and NS88.2*covS* to M1T1 GAS demonstrated that similar to M1T1 GAS, mutation of *covS* impairs the ability of NS88.2 and NS88.2*covS* to adhere to HEp-2 cells *in vitro*, murine skin *in vivo*, and to biofilm production relative to NS88.2*rep*. The ability of NS88.2 strains to degrade neutrophil extracellular traps (NETs) was determined, and in congruence with previously described genome data describing the absence of *sda1*, these strains showed significantly reduced ability to degrade NETs over virulent M1T1 GAS. In extension to the NS88.2 genomic sequence draft, proteomic and transcriptomic approaches utilising 2D-PAGE and transcriptional microarray analyses were undertaken. Proteomics revealed that *covS*-mutation lead to increased amounts of streptococcal collagen-like protein A (SclA), general stress protein 24 (Gls24) and other known or potential virulence factors in culture supernatants. Analysis of the NS88.2 transcriptome demonstrated that *sclA* was upregulated by *covS* mutation, and

that *gls24* was highly upregulated in response to incubation in whole blood. NS88.2 isogenic deletion mutants of *sclA* and *gls24* exhibited significantly reduced ability to proliferate in whole blood, and reduced ability to resist killing by purified PMNs. This study describes genomic, transcriptomic and proteomic characterisation of a non-M1T1 GAS isolate, and identification of a novel role for two GAS virulence determinants in modulating interactions with PMNs.

Infection of PMNs with M1T1 GAS rapidly triggers an apoptotic cell death program, however the impact of differentially PMN-resistant GAS strains on PMN cell death responses is unclear. In this study, the interactions of PMNs with PMN-resistant (NS88.2) and PMN-sensitive (NS88.2*rep*) GAS were characterised to determine the effect on PMN cell death modality. *In vitro* infection of purified PMNs demonstrated that PMNs phagocytosed significantly less virulent NS88.2 than avirulent NS88.2*rep* and subsequently generated less reactive oxygen species. PMNs that had phagocytosed NS88.2*rep* also underwent a higher degree of mitochondrial membrane depolarisation than NS88.2. Scanning electron microscopy of NS88.2*rep* infected PMNs indicated morphological signs of apoptotic cell death, which was supported by biochemical evidence of nuclear DNA fragmentation and caspase-3 activation. Conversely, apoptotic markers were absent in NS88.2 infected PMNs, which displayed ultra-structural markers of oncotic cell death and loss of plasma membrane integrity. Intradermal infection of C57BL/6 mice determined that phagocytosis of NS88.2 was impaired *in vivo*, which contributed to the survival and virulence of this strain. Immunohistological analysis of murine dermal tissue showed that infection by NS88.2*rep* lead to migration of murine PMNs, and cells associated with infection stained strongly for apoptotic markers associated with a pro-resolution of inflammation phenotype. Murine dermal tissue infected with NS88.2 also exhibited murine PMN influx, however was absent for apoptotic markers and exhibited adverse

histopathologies. This study indicates that the manner of PMN cell death program induced by GAS infection may enhance GAS virulence and affect disease pathologies.

The work described here illustrates interactions between the human innate immune response and GAS in a non-M1T1 genetic background. These findings emphasise heterologous mechanisms by which GAS of different serotypes resist killing by PMNs, and how PMN cell death responses are shaped by virulent and avirulent GAS. A deepened understanding of both host and GAS cellular and molecular interactions during infection holds high potential to identify novel targets that can be exploited for the development of improved diagnostics and therapeutics for GAS diseases.

TABLE OF CONTENTS

PUBLICATIONS INCLUDED IN THIS THESIS

This thesis includes chapters that have been published in the following journal articles:

James A. Tsatsaronis, Mark J. Walker, Martina L. Sanderson-Smith (2014). Host Responses to Group A *Streptococcus*: Cell Death and Inflammation. *Invited for revision for PLoS Pathogens.* Incorporated in part as Chapter 1.

Contributor	**Extent of contribution**
J. A. Tsatsaronis	Wrote the paper (100%) Preparation of figures (100%)
M. J. Walker	Edited the paper (50%)
M. L. Sanderson-Smith	Edited the paper (50%)

James A. Tsatsaronis, Andrew Hollands, Jason N. Cole, Peter G. Maamary, Christine M. Gillen, Nouri L. Ben Zakour, Malak Kotb, Victor Nizet, Scott A. Beatson, Mark J. Walker, Martina L. Sanderson-Smith (2013). Streptococcal collagen-like protein A and general stress protein 24 are immuno-modulating virulence factors of group A Streptococcus. *FASEB J.* **7:** 2633-43. Incorporated as Chapter 4.

Contributor	**Extent of contribution**
J. A. Tsatsaronis	Genome sequence analysis (90%)* 2D-PAGE and mass spectrometry (100%) Quantitative PCR (100%) Cloning, protein expression and purification (100%) LIC cloning (95%) Allelic exchange mutagenesis (100%) Hyaluronic acid capsule measurement (100%) Growth curves (100%) Whole blood growth kinetics (100%) Neutrophil killing (100%) Wrote the paper (100%)
A. Hollands	Murine skin adherence (100%) Biofilm formation (100%) HEp-2 adherence (100%)
J. N. Cole	NET degradation (100%)

	Transcriptomic microarray (50%)
P. G. Maamary	Transcriptomic microarray (50%)
C. M. Gillen	LIC cloning (5%)
N. L. Ben Zakour	Genome sequence analysis (5%)*
M. Kotb	Directed and supervised research (5%)
V. Nizet	Directed and supervised research (10%) Edited the paper (10%)
S. A. Beatson	Genome sequence analysis (5%)* Edited the paper (10%)
M. J. Walker	Directed and supervised research (35%) Edited the paper (10%)
M. L. Sanderson-Smith	Directed and supervised research (50%) Edited the paper (70%)

*Genome assembly and analyses are presented in detail in Chapter 3.

James A. Tsatsaronis, Oliver Goldmann, Manfred Rohde, Jude Taylor, Diane Ly, Robert Geffers, Mark J. Walker, Eva Medina, Martina L. Sanderson-Smith. (2014) Group A Streptococcus modulates tissue inflammation by manipulating polymorphonuclear cell death responses. *In preparation for submission to the Journal of Infectious Disease.* – Incorporated as Chapter 5.

Contributor	**Extent of contribution**
J. A. Tsatsaronis	Generation of GFP strains (50%) Phagocytosis assays (100%) Mitochondrial membrane potential assessment (100%) ROS assessment (100%) Cytotoxicity assays (100%) Western blotting (100%) Transcriptomic microarray (50%) TUNEL staining (90%) Confocal microscopy (90%) Survival curve (100%) Murine intradermal infection (80%)

	Histology (100%) Wrote the paper (100%)
O. Goldmann	Directed and supervised research (15%)
M. Rohde	Electron microscopy (100%)
J. Taylor	TUNEL staining (10%) Murine intra-dermal infection (10%) Confocal microscopy (10%)
D. Ly	Generation of GFP strains (50%) Murine intra-dermal infection (10%)
R. Geffers	Transcriptomic microarray (50%)
M. J. Walker	Directed and supervised research (5%) Edited the paper (15%)
E. Medina	Directed and supervised research (20%) Edited the paper (15%)
M. L. Sanderson-Smith	Directed and supervised research (60%) Edited the paper (70%)

As the primary supervisor, I, Dr. Martina Sanderson-Smith, declare that the greater part of the work in each article listed above is attributed to the candidate, James Anthony Tsatsaronis. In the above manuscripts, James contributed to study design, and was primarily responsible for data collection, data analysis and data interpretation, as described above. The first draft of each manuscript was written by the candidate, and James was then responsible for responding to the editing suggestions of his co-authors. James has been primarily responsible for submitting these manuscripts for publication to the relevant journals, and has been involved in responding to reviewers' comments with assistance from his co-authors.

Dr. Martina Sanderson-Smith

Principle Supervisor

OTHER PUBLICATIONS

Diane Ly, Jude M. Taylor, James A. Tsatsaronis, Mercedes M. Monteleone, Amanda S. Skora, Cortny A. Donald, Tracy Maddocks, Victor Nizet, Nicholas P. West, Marie Ranson, Mark J. Walker , Jason D. McArthur, Martina L. Sanderson-Smith. (2014) Plasmin Acquisition by Group A Streptococcus Protects Against C3b-Mediated Neutrophil Killing. *Journal of Innate Immunity.* **6:** 240-250.

CONFERENCE PROCEEDINGS

Tsatsaronis J.A., Hollands A., Cole J., Maamary P.G., Ben Zakour N.L., Kotb M., Nizet V., Beatson S.A., Sanderson-Smith M.L., Walker M.J. Systems Biology Characterisation of Invasive Non-M1T1 Serotype Group A Streptococcus. XVIII Lancefield International Symposium on Streptococci and streptococcal Diseases. Palermo, Italy. September 4 - 8, 2011. *Oral Presentation.*

Ly D., Taylor J., Tsatsaronis J.A., Monteleone M., Skora A., Donald C., Maddocks T., Nizet V., West N., Ranson M., Walker M.J., McArthur J.D., Sanderson-Smith M.L. Plasmin acquisition by group A Streptococcus protects against C3b-mediated neutrophil phagocytosis. XIVth International Workshop Molecular and Cellular Biology of Plasminogen Activation. June 4 – 8 2013. *Oral Presentation.*

Tsatsaronis J.A., Goldmann O., Rohde M., Taylor J., Ly D., Geffers R., Walker M.J., Medina E., Sanderson-Smith M.L. Group A Streptococcus induces a polarity in polymorphonuclear leukocyte cell-death responses that contributes to inflammatory tissue destruction. BacPath 12: Molecular Analysis of Bacterial Pathogens, Moreton Island, Queensland, Australia, September 29 – October 2 2013. *Oral Presentation*.

Tsatsaronis, J.A., Walker M.J., Sanderson-Smith M.L. Interactions of the innate immune response and Group A Streptococcus. Humboldt Colloquium, “Looking to the Future: International Research in a Changing World”. October 17 – 19 2013. Sydney, New South Wales, Australia. *Poster Presentation*.

Underlined: Presenting author.

LIST OF FIGURES

LIST OF TABLES

ABBREVIATIONS

2D	Two-dimensional
α	Anti-
APSGN	Acute post-streptococcal glomerulonephritis
ARF	Acute rheumatic fever
ATP	Adenosine tri-phosphate
BLAST	Basic local alignment search tool
bp	Base pairs
BSA	Bovine serum albumin
CDS	Coding sequence
CFU	Colony forming units
Da	Dalton
DAMP	Damage associated molecular pattern
DC	Dendritic cell
DNA	Deoxyribonucleic acid
DNase	Deoxyribonuclease
DTT	Dithiothreitol
ECM	Extracellular matrix
EDTA	Ethylenediamine tetra-acetic acid
FCS	Fetal calf serum
g	Gram
g	Gravitational force
GAPDH	Glyceraldehyde 3-phosphate dehydrogenase
GAS	Group A *Streptococcus*
h	Hour(s)
HBP	Heparin binding protein
HCl	Hydrochloride
HRP	Horse radish peroxidase
Ig	Immunoglobulin
IPG	Immobilised pH gradient
IPTG	Isopropyl-β-D-thiogalactopyranoside
k	Kilo
L or l	Litre(s)
LB	Lysogeny broth
LDH	Lactate-*D*-hydrogenase
LTA	Lipoteichoic acid
µ	Micro
ψ_m	Mitochondrial outer membrane potential
m (prefix)	Milli
m (suffix)	Metre(s)
M	Molar
m/*z*	Mass to charge ratio
MAC	Membrane attack complex
MALDI	Matrix assisted laser desorption/ionisation

MFI	Mean fluorescence intensity
min	Minute(s)
MLST	Multi locus sequence typing
MOI	Multiplicity of infection
MS	Mass spectrometry
n	Nano
NET	Neutrophil extracellular trap
NF	Necrotising fasciitis
NGS	Next generation sequencing
NK	Natural killer cell
ºC	Degrees Celsius
OD	Optical density
PAGE	Polyacrylamide gel electrophoresis
PBS	Phosphate buffered saline
PBST	Phosphate buffered saline with 0.05% Tween-20
PCR	Polymerase chain reaction
pI	Isoelectric point
PMN	Polymorphonuclear leukocyte
RFLP	Restriction fragment length polymorphism
RNA	Ribonucleic acid
ROS	Reactive oxygen species
s	Second(s)
SDS	Sodium dodecyl sulphate
SNP	Single nucleotide polymorphism
SSS	Standard sample solubilisation
ST	Sequence type
STSS	Streptococcal toxic shock syndrome
TAE	Tris-acetate EDTA
TCA	Trichloroacetic acid
THY	Todd-Hewitt broth 1% yeast
TUNEL	Terminal deoxynucleotidyl transferase dUTP nick end labelling
V	Volt(s)
v/v	Volume per volume
W	Watt(s)
w/v	Weight per volume

CHAPTER 1: REVIEW OF THE LITERATURE

1.1 Overview

Streptococcus pyogenes (Group A Streptococcus, GAS) is the etiological agent of mild skin and mucosal conditions such as impetigo and pharyngitis (Bisno and Stevens, 1996), in addition to life-threatening invasive diseases such as the "flesh eating disease" necrotising fasciitis (Donaldson *et al.*, 1993) and streptococcal toxic shock syndrome (McCormick *et al.*, 2001). Invasive GAS infections frequently lead to mortality, with over 500,000 deaths annually resulting from GAS infections and their sequelae (Carapetis *et al.*, 2005). In recent decades, higher rates of GAS diseases have been reported despite the efficacy of antimicrobial agents (Efstratiou, 2000). Paralleling this resurgence, the globally disseminated M1T1 GAS serotype is frequently isolated from severe invasive infections (Aziz and Kotb, 2008). Virulence of the M1 serotype and other serotypes is promoted by multiple virulence factors contributing to innate immune avoidance and systemic dissemination throughout the host (Cunningham, 2000; Walker *et al*., 2014). Evasion of the innate immune response is an essential precursor to invasive disease, and while the pathogenic mechanisms underlying M1T1 virulence continue to be studied intensively, non-M1T1 GAS immune interactions are less understood. A mounting body of evidence suggests critical roles for host immune mediators in determining the severity of infection (Norrby-Teglund and Johansson, 2013). Cellular agents of the innate immune response mediate the initial host interactions with GAS, and are responsible for orchestrating subsequent antimicrobial responses (Goldmann *et al.*, 2004; Loof *et al.*, 2007). Numerous genetic elements coordinate both the susceptibility of the host to infection, and the virulence of GAS isolates (Abdeltawab *et al.*, 2008; Walker *et al.*, 2007). This duality of pathogen and host derived genetic factors suggest that in-depth analyses encompassing both sides of infection are requisite to understanding the complete disease process.

Presented here is a review of the literature regarding GAS epidemiology and disease pathologies, host responses to GAS infection and GAS virulence factors which mitigate innate immune responses during infection.

1.2 Classification of streptococci

Streptococcus is a genus of Gram-positive, chain forming, non-motile coccal bacteria, phylogenetically divided into more than 50 species and subspecies. Many streptococcal species are pathogenic agents of humans and domesticated animals (Facklam, 2002). Historically, classification of streptococcal species was based upon their haemolytic potential, and was later expanded to differentiate between the carbohydrate "group" antigens of the bacteria (Lancefield, 1928; Schottmüller, 1903).

1.2.1 Lancefield classification

The Lancefield system of classification groups streptococci into categories based on the presence of specific cell wall polysaccharides (groups A, B, C, F and G) or lipoteichoic acids (group D) (Cunningham, 2000). The streptococcal group A carbohydrate is composed of *N*-acetyl-*β*-*D*-glucosamine linked to a polymeric rhamnose backbone. Group A of the Lancefield classification system consists predominantly of *Streptococcus pyogenes* (Lancefield, 1962), however other streptococcal species, *Streptococcus dysgalactiae* subsp. *equisimilis* and the *Streptococcus anginosus* group may also contain the group A carbohydrate (Facklam, 2002).

1.2.2 M-typing

The GAS M protein (encoded by the *emm* gene) is a major surface protein which extends from the streptococcal cell wall (carboxy terminal) as an α-helical, coiled-coil dimer with conserved, variable and hypervariable regions (Fig. 1.1) (Fischetti, 1989). Immune selection of the variable and hypervariable regions is hypothesised to have

resulted in broad diversification of the M protein (Bessen *et al.*, 2008). This variation forms the basis of GAS serological M-typing, and uses standardised typing sera (Cunningham, 2000; Fischetti, 1989). However, many difficulties with M serotyping have arisen, including achieving full coverage of >100 M serospecificities of GAS (Cunningham, 2000), difficulty in the preparation of M protein antisera (Vitali *et al.*, 2002) and notably, the lack of reactivity of some GAS isolates to reference M-antisera (Relf *et al.*, 1992). Simultaneous serotyping of the surface T-antigen, encoded by the *tee* gene, is occasionally performed in conjunction with M typing to differentiate between M-nontypeable strains (Jones *et al.*, 1991). Assignment of a T-serotype can distinguish between M-nontypeable GAS strains, however issues in interpreting T-serotyping results can arise through cross-reactivity of many GAS strains to reference T antisera (Johnson *et al*., 2006).

1.2.3 emm-typing

Due to the difficulties in serologically typing streptococcal M protein, molecular typing methods based upon analysis of the 5' sequence of the *emm* gene, encoding the hypervariable amino terminus of M protein, are now routinely used (Beall *et al.*, 1996; Vitali *et al.*, 2002). The heterogeneous 5' end of *emm* genes encoding the hypervariable region, determines the serotype specificity of the M protein. Sequencing this region provides more discriminatory data over serological methods for distinguishing between GAS isolates. *Emm*-typing is conducted by sequencing ~150 bases from the 5' end of the *emm* PCR product and grouping together sequences showing >95% homology as *emm* types, whilst separating *emm*-types showing a maximum of 80% homology (Efstratiou, 2000). Currently, >250 *emm* types and subtypes have been collected, emphasising the hypervariability of the *emm* gene (Smeesters *et al.*, 2010). Other *emm* based typing methods rely on PCR using *emm* type specific oligonucleotides (Vitali *et al.*, 2002).

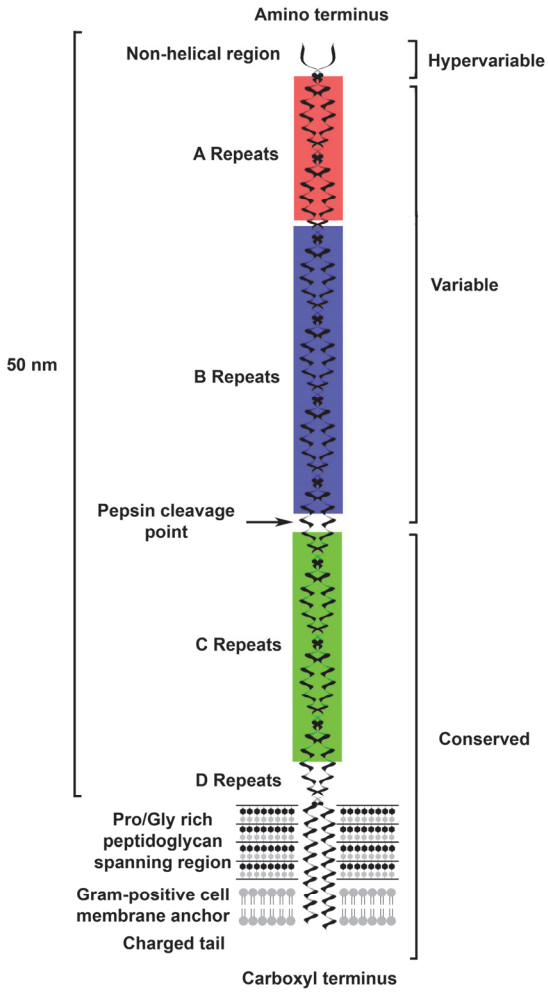

Fig. 1.1 General structure of the group A streptococcal M protein. The α-helical, coiled-coil region extends approximately 50 nm away from the bacterial cell wall. Indicated are the amino-terminal hypervariable and variable (containing A and B repeats) regions which dictate the M serotype specificity and the conserved (containing C and D repeats) region which also contains the LPxTG Gram-positive cell wall anchor and positively charged tail. The number and sequence of the A and B repeats is dependent on the M type. Adapted from Fischetti (1989).

1.2.4 emm-patterning

Many GAS strains encode multiple *emm* or *emm*-family genes, forming the basis for grouping of *emm* chromosomal patterns or subfamilies (Hollingshead *et al.*, 1993). The five major pattern groupings (A - E) are defined by the number of *emm* genes encoded, the subfamily content of each gene and their relative order (Fig. 1.2) (Hollingshead *et al.*, 1993). Designation of an *emm* pattern is determined by PCR amplification patterns using *emm* subfamily specific primer sets (Hollingshead *et al.,* 1993). Strains of the

same M serotype may encode different *emm* patterns, and *vice versa* as a single M pattern encompasses many M serotypes (Bessen *et al.*, 1996).

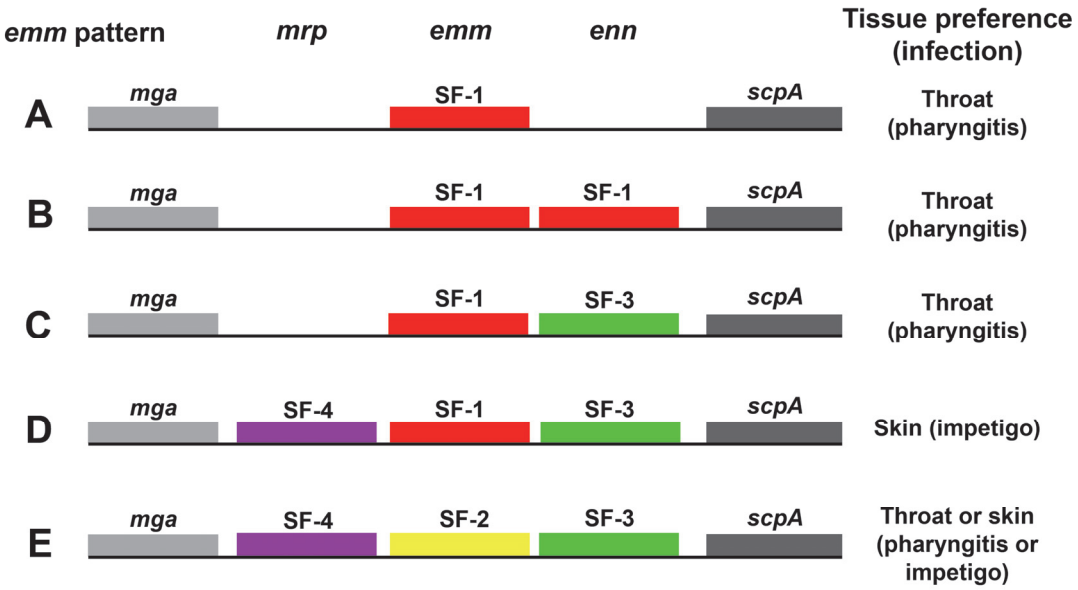

Fig. 1.2 Chromosomal arrangement of the five major *emm* pattern groups A - E. *emm* pattern groups are designated according to amplification using *emm* and *emm*-family (*mrp* and *enn*) gene subfamily (SF) specific primers. Bordering the *emm* and *emm*-family genes are the *mga* regulator and C5a peptidase (*scpA*) genes. Intergenic distances between *emm* genes in *emm* patterns A and B may vary due to large DNA insertions. The tissue tropism classically associated with each *emm* pattern is also indicated. Figure is adapted from Hollingshead *et al.* (1993) and Cunningham (2000).

1.2.5 Vir-typing

An alternative molecular method utilising long PCR and restriction fragment length polymorphisms (RFLPs) to differentiate between GAS strains has also been proposed (Gardiner *et al.*, 1995). This approach is applied to the multiple gene regulator (MGA) region of GAS, the same region dictating GAS M patterns, which comprises of the M-protein family genes *mrp* (M-protein related protein, also known as *fcrA*), *emm* and *enn*, which are flanked by C5a peptidase (*scpA*) and a regulatory gene *mga* (also known as *virR* or *mry*) (Gardiner *et al.*, 1995). A strong correlation between RFLPs of many GAS isolates and *emm* sequence types was found using this technique, and provides advantages over routine *emm* sequencing as a more rapid method of typing in response to outbreaks (Gardiner *et al.*, 1998).

1.3 Pathologies and epidemiology of GAS disease

1.3.1 Non-invasive GAS disease

Group A streptococci are responsible for a diverse range of mild, superficial diseases including streptococcal pharyngitis ("strep throat"), scarlet fever and impetigo. While GAS may asymptomatically colonise host epithelia, acute symptomatic streptococcal infection is the most common bacterial cause of pharyngitis, causing approximately 15 - 30% of cases in children and 5 - 10% of cases in adults (Bisno, 2001). Streptococcal pharyngitis results from symptomatic bacterial colonisation of the oropharyngeal epithelium, typically manifesting as a sudden onset of throat pain, fever, headache and nausea or vomiting (Bisno, 2001). Scarlet fever is often linked with pharyngitis and is exhibited symptomatically as large red rashes and bright red tongue discolouration. Investigations utilising molecular typing have found that streptococcal superantigens, SSA, SpeC and SpeA may mediate the virulence of scarlet fever and contribute to scarlet fever outbreaks (Perea-Mejia *et al.*, 2002; Tse *et al.*, 2012). Group A streptococci frequently colonise the skin to cause impetigo. Impetigo, also known as pyoderma, is caused by symptomatic infection of the epidermis by GAS, commonly occurring at exposed surfaces such as the face or extremities. Impetigo is characterised by suppurative lesions which rupture to form yellow crusts (Bisno and Stevens, 1996). Deeper invasion through local trauma, abrasions, severe acne or eczema, may cause conditions such as erysipelas or cellulitis, depending on the degree of penetration of the superficial and subcutaneous layers (Bisno and Stevens, 1996).

1.3.2 Invasive GAS disease

The entry of GAS into deeper, sterile tissue from superficial infection sites or direct inoculation from penetrating injuries, burns, trauma or surgery, may lead to the development of severe, invasive GAS diseases such as necrotising fasciitis (NF),

sepsis and streptococcal toxic shock syndrome (STSS) (Bisno and Stevens, 1996; Stevens *et al*., 2005). NF, otherwise known as the "flesh eating disease", results from GAS infection and subsequent necrosis of subcutaneous fat, superficial fascia and superficial-deep fascia. Initial symptoms often present the skin as intact, however secondary gangrene commonly follows late in the course of infection (Donaldson *et al.*, 1993). NF and other soft tissue infections are routinely treated by surgical debridement of necrotic tissues, with amputation as an emergency measure (Stevens *et al*., 2005). Soft tissue infections such as NF and cellulitis may develop concurrent STSS (McCormick *et al.*, 2001). STSS is mediated by secretion of streptococcal superantigens or pyrogenic toxins that initiate massive, non-specific stimulation of T-cell populations, leading to overwhelming cytokine release (McCormick *et al.*, 2001; Lappin and Ferguson, 2009). STSS is exhibited clinically as hypotension, renal dysfunction, erythematous macular rash, coagulopathy, soft tissue necrosis or respiratory stress (Lappin and Ferguson, 2009). Despite the sensitivity of GAS to penicillin, large quantities of the pathogen are able to reach stationary growth phase in invasive infections such as STSS, reducing the antimicrobial efficacy of this antibiotic (Baxter and McChesney, 2000). Currently, paired penicillin and clindamycin treatment is recommended for soft-tissue and systemic GAS infections, due to suppression of GAS toxins and modulation of cytokine production (Stevens *et al.*, 2005).

1.3.3 Immunologically-mediated sequelae

Recurring GAS infections may give rise to immunologically-mediated complications such as acute rheumatic fever (ARF) and acute post-streptococcal glomerulonephritis (APSGN). ARF stems from the production of auto-reactive antibodies and T cells following GAS infection, leading to inflammation of heart muscle (carditis), joints (arthritis), central nervous system (chorea) and skin (erythema marginatum) (Cunningham, 2008). Molecular mimicry between streptococcal M-protein epitopes and

host tissue, particularly heart muscle myosin, is believed to be a major underlying cause of ARF. This hypothesis is supported by evidence that T-cell clones from rheumatic heart disease patients possess cross-reactivity between myosin, mitral valve associated proteins and streptococcal M peptides (Fae *et al.*, 2006). Other potential mechanisms underlying ARF include immune cross-reactivity of other GAS molecules including the group A carbohydrate, and the accumulation of type IV collagen on ARF-associated GAS, triggering the production of collagen-specific autoantibodies (Dinkla *et al.*, 2003; Dinkla *et al.*, 2009). Development of ARF is triggered 1 - 5 weeks after primary infection by GAS, commonly in the form of streptococcal pharyngitis (Walker *et al*., 2014). APSGN describes post-infection, immune-mediated sequelae which may also arise following either cutaneous or pharyngeal infection. Outbreaks of APSGN have declined over the last decade however higher incidences are still reported in Africa, South America, New Zealand and Kuwait (Cunningham, 2008). APSGN is characterised by oedema, hypertension, haematuria and proteinacious sediment in urine, all of which are linked to renal impairment due to inflammation of renal glomeruli (Cunningham, 2008). Several mechanisms by which APSGN is triggered have been proposed, including immune reactions within glomeruli resulting from cross-reactive renal antigens or from the deposition of circulating streptococcal antigen-antibody immune complexes (Cunningham, 2000; Walker *et al*., 2014). Early treatment of pharyngitis with penicillin has been shown to inhibit the development of APSGN (Holm, 1988).

1.3.4 GAS disease epidemiology

It has been noted that particular GAS strains and serotypes appear to preferentially infect different tissue sites, either the epidermis of the skin, or the epithelial layer of the oropharynx (Bessen *et al.*, 1996). Tissue tropism of GAS has historically been viewed as dependent upon the specific *emm* pattern of each isolate. GAS 'specialist' strains

which preferentially infect the throat and cause pharyngitis are associated with *emm* patterns A - C, whilst strains which preferentially infect the skin and cause impetigo are typically *emm* pattern D (Fig. 1.2) (Bessen *et al.*, 1996). Strains which belong to *emm* pattern E may infect either tissue site with no recorded specificity (Bessen *et al.*, 1996). In a laboratory-based study of three regions in the U.S.A, the risk factors of invasive GAS infection for adults were: exposure to one more children with sore throats, HIV infection and a history of injecting drug use (Factor *et al.*, 2003). A larger, population-based surveillance study across Europe found environmental factors such as advanced age and overcrowding, increased the severity and likelihood of infection respectively (Lamagni *et al.*, 2008). Infection by GAS is also subject to seasonal variation, with colder or more temperate climates and seasons favouring pharyngeal infection and warmer climates and seasons favouring impetigous infection (Lamagni *et al.*, 2008).

Both mild and severe GAS infections occur in developing and developed countries worldwide. The frequency of severe GAS diseases has been increasing since the mid-1980s, with 1.78 million cases reported annually worldwide (Carapetis *et al.*, 2005). Multiple pathogenic factors are believed to have played roles in the recent resurgence of severe GAS infections, including the phage-mediated acquisition of additional virulence factors (Aziz and Kotb, 2008) and emergence of particularly virulent subclones of certain M serotypes (Musser *et al.*, 1995). A hypervirulent GAS subclone of the M1T1 serotype has spread on a global scale, which has paralleled the rise of invasive GAS infections (Aziz and Kotb, 2008). Contrasting the spread of the M1T1 serotype, the indigenous Aboriginal population of Australia's Northern Territory suffer from endemic skin and pharyngeal diseases caused by diverse serotypes and strains of GAS (Gardiner and Sriprakash, 1996). As a consequence of this endemic GAS disease, Aboriginal communities display one of the highest rates in the world of autoimmune sequelae, such as acute rheumatic fever and rheumatic heart disease, following primary GAS infection (Carapetis *et al.*, 1996). Intriguingly, GAS isolates from

Aboriginal communities do not conform to the classic *emm* pattern tissue tropism profile, as up to 70% of *emm* pattern A - C GAS isolates from these communities were taken from impetigous sores (Bessen *et al.*, 2000). However, in the same region *emm* pattern D GAS are nonetheless the most prevalent *emm* pattern isolated (Bessen *et al.*, 2000). Necrotising fasciitis isolates from rural indigenous communities also show *emm* diversification not observed in urban populations (Hassell *et al.*, 2004).

1.4 Establishment of GAS infection

1.4.1 Adhesion to the host

The initiation of superficial GAS infection requires adherence of bacteria to host epithelial cells. Humans are widely accepted to be the exclusive reservoir of GAS, with nasopharyngeal mucosa and impetigous sores serving as the primary sites of infection and routes of GAS transmission between hosts (Fiorentino *et al.*, 1997). The establishment of oropharyngeal infection is dependent on the ability of GAS to overcome mechanical obstacles, such as clearance by salivary flow and cell shedding, in order to adhere to the epithelium. To achieve this, GAS hijack host extracellular matrix (ECM) molecules such as fibronectin, fibrinogen, and laminin. GAS exhibits a bewildering array of putative adhesins which bind host ECM molecules (Table 1.1). However, not all GAS adhesins are expressed simultaneously by all strains, and some may have differing affinities for different host cell types (Courtney *et al.*, 2002). One proposed model for the adhesion of GAS to host receptors is a two-step mechanism involving a low-affinity binding mediated by GAS lipoteichoic acid (LTA) through its lipid moiety, followed by a higher-affinity binding through an adhesin such as PrtF1/SfbI or M protein, to a specific host cell membrane receptor (Hasty *et al.*, 1992) (Fig. 1.3). The second step of this adhesion model determines the tissue specificity of the interaction and would partly explain the variable propensities of GAS strains to preferentially infect different host tissue sites.

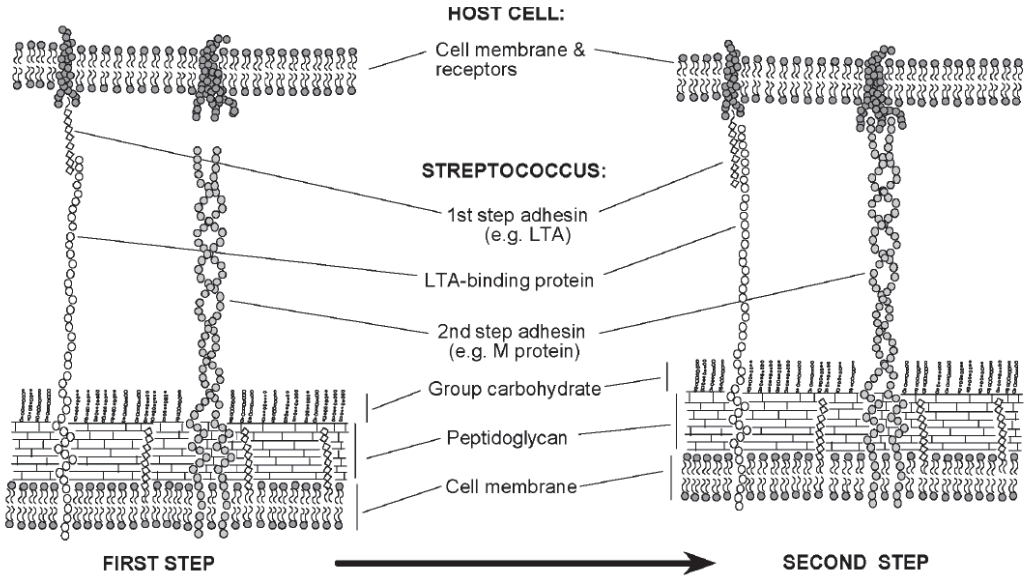

Fig. 1.3 Two-step mechanism for the attachment of group A Streptococci to host receptors. The first step of this mechanism involves the non-specific, low-affinity interaction of GAS lipoteichoic acid (LTA) with hydrophobic regions of host cell receptors. This low-affinity binding facilitates the second higher-affinity binding, bringing a specific GAS adhesin in contact with host receptors which affect a stronger irreversible adhesion of pathogen to host. Reproduced from Hasty *et al.*, 1992.

1.4.2 Adaptive response to the colonisation state

During colonisation, GAS must be able to scavenge sufficient nutrients in order to survive. Cynomologous macaques have been utilised as a non-human primate model of streptococcal pharyngitis, and during 86-day infection with M1T1 GAS the initial colonisation phase was dominated by the up-regulation of carbohydrate metabolism genes (Virtaneva *et al.*, 2005). Regulation of salivary persistence mechanisms is controlled by a two-component regulator *sptRS*, which can significantly remodel the GAS transcriptome to promote complex carbohydrate utilisation via increased starch degradation and maltose uptake (Shelburne *et al.*, 2005). GAS can utilise α-glucans degraded by human α-amylase via the maltose transporters MalE and MalT, both of which contribute to salivary nutrient uptake and enhance the ability of GAS to colonise the murine oropharynx (Shelburne *et al.*, 2008).

Table 1.1 Putative adhesins of group A streptococcus (GAS)[A]

GAS Adhesin	Host receptor(s)	Comments	References
Lipoteichoic acid	Fibronectin, macrophage scavenger receptor	Contributes to biofilm formation	Courtney *et al.*, 2009; Courtney *et al.*, 1983; Simpson *et al.*, 1980
M protein	Fibronectin, fibrinogen, laminin, CD46, galactose, fucose/fucosylated glycoprotein, collagen	Some binding propensities are serotype dependant	Akesson *et al.*, 1994; Courtney *et al.*, 1997; Cue *et al.*, 2001; Dinkla *et al.*, 2003; Okada *et al.*, 1994; Schrager *et al.*, 1998; Wang and Stinson, 1994
Mrp/FcrA	Fibronectin		Courtney *et al.*, 2006
PrtF1/SfbI	Fibronectin, integrins	FCT protein	Hanski and Caparon, 1992; Hanski *et al.*, 1992; Medina *et al.*, 1999
PrtF2 (Pfbp/FbaB)	Fibronectin	FCT protein, Pfbp and FbaB are alleles of PrtF2	Jaffe *et al.*, 1996; Ramachandran *et al.*, 2004; Terao *et al.*, 2002b
SOF/SfbII	Fibronectin, fibrinogen, fibulin	Only present in M pattern	Gillen *et al.*, 2008; Timmer *et al.*, 2006
Fbp54	Fibronectin, fibrinogen		Courtney *et al.*, 1996; Courtney *et al.*, 1994
GAPDH	Fibronectin, fibrinogen		Pancholi and Fischetti, 1992
Hyaluronic acid	CD44, collagen		Cywes *et al.*, 2000; Schrager *et al.*, 1998
Cpa/Ap1	Collagen	FCT protein, Ancillary protein 1 of GAS pili	Kreikemeyer *et al.*, 2005; Podbielski *et al.*, 1999
SlaA	Not determined		Beres *et al.*, 2002; Sitkiewicz *et al.*, 2006
SclA, SclB	Integrins		Caswell *et al.*, 2007; Humtsoe *et al.*, 2005
28 kDa protein	Fibronectin		Courtney *et al.*, 1992
Vn-binding	Vitronectin		Valentin-Weigand *et al.*, 1988
Tee/FctA	Not determined	FCT protein, Pili backbone protein/Tee	Abbot *et al.*, 2007; Manetti *et al.*, 2007; Mora *et al.*, 2005
FctB/Ap2	Not determined	FCT protein, Ancillary protein 2 of GAS pili	Abbot *et al.*, 2007; Manetti *et al.*, 2007; Mora *et al.*, 2005
SpeB	Fibronectin, laminin		Burns *et al.*, 1998; Chaussee *et al.*, 2000; Hytonen *et al.*, 2001
SfbX	Fibronectin, fibrinogen	FCT protein	Jeng *et al.*, 2003
Lbp	Laminin		Podbielski *et al.*, 1999; Terao *et al.*, 2002a
FbaA	Fibronectin	FCT protein	Terao *et al.*, 2001; Terao *et al.*, 2005

[A] Adapted from Courtney *et al.*, 2002 and Olsen *et al.*, 2009.

Abbreviations: Mrp, M-protein related protein; Sfb, streptococcal fibronectin binding protein; Fba, Fibronectin binding protein; SOF, Serum opacity factor; Fbp54, Fibronectin binding protein 54; GAPDH, glyceraldehydes-3-phosphate-dehydrogenase; Cpa, collagen binding protein; SlaA, streptococcal phospholipase A_2; Scl, streptococcal collagen-like protein; Vn, Vitronectin; Lbp, laminin binding protein; FCT, Fibrinogen, Collagen and T-antigen locus.

1.5 Interaction of GAS with the innate immune system

1.5.1 Innate immunity

Immunity can be defined as resistance to infection by external agents that would otherwise lead to a disease state. The human immune system is composed of two networks, the innate and the adaptive immune systems, that recognise and respond to infections resulting in the destruction of foreign antigens (Pommerville, 2010). The innate immune system is characterised by its rapid response time, limited antigenic specificity and lack of immunological memory (Pommerville, 2010). This system includes physical barriers against infection, constitutive chemical barriers that inhibit microbial colonisation, receptors which detect the entry of foreign microbes and specialised immune cells responsible for promoting subsequent antimicrobial responses (Gallo and Nizet, 2008). Epithelial cells cover the interface between the body and external environment, and release antimicrobial peptides (AMPs) that prevent colonisation of epithelial surfaces. Humans produce a diverse range of AMPs, such as cathelicidin (LL-37), which show broad spectrum antimicrobial activity against Gram-positive and Gram-negative bacteria, fungi and some viruses (Radek and Gallo, 2007). Commonly, AMPs possess a net cationic charge, >50% hydrophobic residues and an amphipathic nature (Diamond *et al.*, 2009). These characteristics allow AMPs to interact with bacterial outer membranes, as AMPs frequently exhibit antimicrobial activity via membrane permeation (Diamond *et al.*, 2009).

The complement system is composed of intrinsic immune molecules which 'complement' immune responses by detecting the presence of foreign antigens and promoting subsequent phagocytosis and killing of invaders. Activation of the complement system may be triggered via three separate pathways, known as the classical, mannose-binding lectin and alternative pathways (Pommerville, 2010). The alternative and the lectin pathways can be activated in the absence of antibodies, via

binding of C3b or mannose-binding lectin to the microbial cell surface (Abbas and Lichtman, 2009). The downstream effects of all three complement pathways result in generation of C5a and C5b peptides, and coating of the microbial cell surface in C3b (Abbas and Lichtman, 2009). Circulating C5a is a potent phagocyte chemo-attractant whilst bound C5b initiates formation of the membrane attack complex (MAC), a transmembrane pore effecting microbial lysis via water and ion influx. Opsonisation of the microbial cell surface by C3b is recognised by complement receptors of phagocytes, resulting in engulfment and intracellular killing.

1.5.2 Cellular innate immune mediators

Specialised immune cells known as phagocytes mediate direct killing of microbes via phagocytosis. Two major classes of professional phagocytes include mononuclear phagocytes, consisting of monocytes, macrophages and dendritic cells (DCs); and polymorphonuclear leukocytes (PMNs); consisting of neutrophil, eosinophil and basophil granulocytes (Pommerville, 2010). DCs and macrophages are derived from monocyte precursors during infectious and inflammatory episodes, and form a bridge linking innate and adaptive immunity by presenting antigenic material to T lymphocytes. Other cells, including natural killer cells (NKs), are also classified as innate immune leukocyte. NKs have numerous roles in innate immunity, primarily involving targeting of infected or ‘stressed’ cells for elimination.

PMNs are the first innate immune cells to be recruited in response to infection, and the most abundant class of PMN are neutrophil granulocytes (Athens *et al.*, 1961). Neutrophils are also the most abundant cell type circulating in the blood, after red blood cells, but have a short half-life as they are rapidly and spontaneously apoptotic (Kobayashi *et al.*, 2005). As such, the majority of haematopoiesis occurring in adult humans is devoted to maintenance of neutrophil populations (Athens *et al.*, 1961). Macrophages mature from circulating blood monocytes cells, which arise from bone marrow precursor cells. Macrophages can further differentiate into specialised resident

macrophages such as microglial cells in the central nervous system or alveolar macrophages in the lungs (Adams and Hamilton, 1984). Unlike neutrophils, macrophages are less abundant in the blood however resident macrophages persist in extravascular tissue sites for long periods of time, and so may mediate the first interactions between pathogens and the immune system prior to neutrophil recruitment (Goldmann *et al.*, 2004). Neutrophils migrate to sites of infection due to pathogen and host-derived chemo-attractant signals, such as bacterial lipopolysaccharides and complement component C5a via chemotaxis (Witko-Sarsat *et al.*, 2000). Tissue resident macrophages and dendritic cells also release cytokines in response to detecting pathogenic invasion, attracting neutrophil migration and stimulating surrounding vascular endothelial cells to produce adhesion molecules. Neutrophils and monocytes circulating in the blood weakly bind these adhesins, and via a multi-step 'rolling' process, are exposed to greater concentrations of chemokines causing them to migrate between the cells of the endothelium to the site of infection (Pommerville, 2010).

Recognition of pathogens activates phagocytes to begin phagocytosis, whereby the plasma membrane of the phagocyte is extended around the microbe forming an intracellular vesicle, referred to as a phagosome. Phagosomes are subsequently fused with lysosomes, forming phagolysosomes, which deliver a combination of AMPs produced intracellularly by the phagocyte (Witko-Sarsat *et al.*, 2000). Other enzymes are also released into phagolysosomes which synthesise reactive oxygen species (ROS) with which to counter infection (Fig. 1.4). The interaction of the chemo-attractant signals with neutrophils 'primes' the phagocyte for microbicidal activities including the production of ROS, phagocytosis and degranulation (Kobayashi *et al.*, 2005). Neutrophils also release extracellular traps (NETs) composed of DNA with associated histone and granular antimicrobial peptides which serve to ensnare bacteria, exposing them to higher local concentrations of bactericidal peptides (Brinkmann *et al.*, 2004).

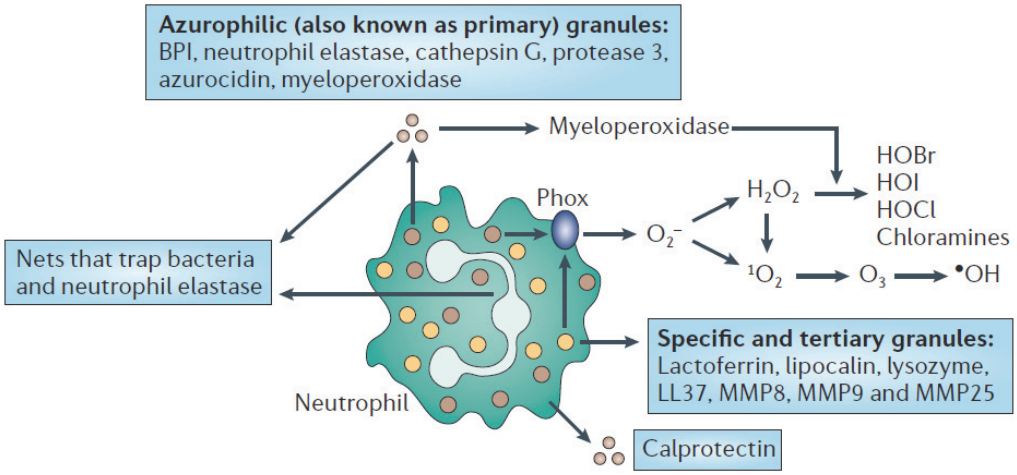

Fig. 1.4 Neutrophil synthesis and secretion of multiple anti-microbial peptides and reactive oxygen species (ROS) from varied cellular compartments. Azurophillic granules produce a potent antibacterial agent of Gram-negative bacteria, bactericidal permeability increasing protein (BPI); four broad spectrum antibacterial agents, elastase, cathepsin G, protease 3, azurocidin; and also myeloperoxidase. Specific and tertiary granules release lactoferrin and lipocalin which scavenge iron from bacterial pathogens; a peptidoglycan hydrolase lysozyme, antimicrobial peptide LL-37 and three matrix metalloproteinases (MMP) 8, MMP9 and MMP25. Myeloperoxidase and phagocyte oxidase (Phox) are responsible for the down-stream production of oxygen radicals and ROS. Figure reproduced from (Nathan, 2006).

1.5.3 Toll-like receptor recognition of GAS

Cellular surveillance and recognition of foreign agents by the innate immune system is an essential prerequisite to effector recruitment and induction of appropriate responses. One class of cell receptors involved in recognition of highly conserved microbial components are the Toll-like receptors (TLRs). There are currently more than 10 known TLRs, which recognise multiple pathogen-associated molecular patterns (PAMPs) including; LTA and peptidoglycan (recognised by TLR2), lipopolysaccharide (recognised by TLR4), and unmethylated bacterial CpG DNA (recognised by TLR9) (Takeda *et al.*, 2003). Studies investigating the receptors involved in recognition of GAS infection have shown that TLR signalling, particularly through the MyD88 adapter molecule, plays a vital role in induction of host defences and inflammation (Fig. 1.5) (Loof *et al.*, 2010; Loof *et al.*, 2008). Given that TLR2 recognises multiple Gram-positive bacterial ligands, it is likely this TLR plays a major role in GAS recognition and

responses. Indeed, induction of streptococcal cell-wall extract-induced joint inflammation is dependent on TLR2/MyD88 signalling (Joosten *et al.*, 2003). Macrophages and DCs are commonly viewed as central coordinators of immune responses, a view that has been supported by studies showing that macrophages and DCs are both essential for control of GAS infection (Goldmann *et al.*, 2004; Loof *et al.*, 2007), likely through their secretion of multiple cytokines such as IL-1ß, IL-6, TNFα and IL-12 (Goldmann *et al.*, 2005b; Loof *et al.*, 2008).

1.5.4 Leukocyte signalling events

Macrophage and DC recognition of GAS is partially mediated by TLRs, and interactions with multiple bacterial factors by different TLRs appears to provide immune redundancy in inducing cytokine responses. This is exemplified by the activation of macrophages via TLR4 signalling from non-structural elements such as GAS cytolysin streptolysin O (SLO), and the inability of singular TLR1, TLR2, TLR4 and TLR9 deficiencies to prevent stimulation of DC cytokine responses (Loof *et al.*, 2008; Park *et al.*, 2004). However, downstream signalling via MyD88 is critical for coordinated immune responses, an aspect prominent in clinical studies of patients lacking MyD88, whom are highly predisposed to pyogenic infections (von Bernuth *et al.*, 2008). MyD88 participates in macrophage and DC TLR-stimulated TNFα production (Gratz *et al.*, 2008; Loof *et al.*, 2010). MyD88 is absolutely required for DC type-1 interferon responses, which are triggered via Interferon Regulatory Factor (IRF) 5 (Gratz *et al.*, 2011). In contrast, MyD88 is partially dispensable for type 1 interferon production by macrophages, which requires IRF3, TANK-binding kinase 1 (TBK1) and the STING adaptor (Gratz *et al.*, 2011). Although GAS is typically considered an extracellular pathogen, recent studies indicate intracellular receptors such as TLR9, are important for cytokine responses via hypoxia-inducible factor 1-alpha (HIF-1α) signalling, and also contributes to macrophage GAS killing and ROS production (Zinkernagel *et al.*, 2012).

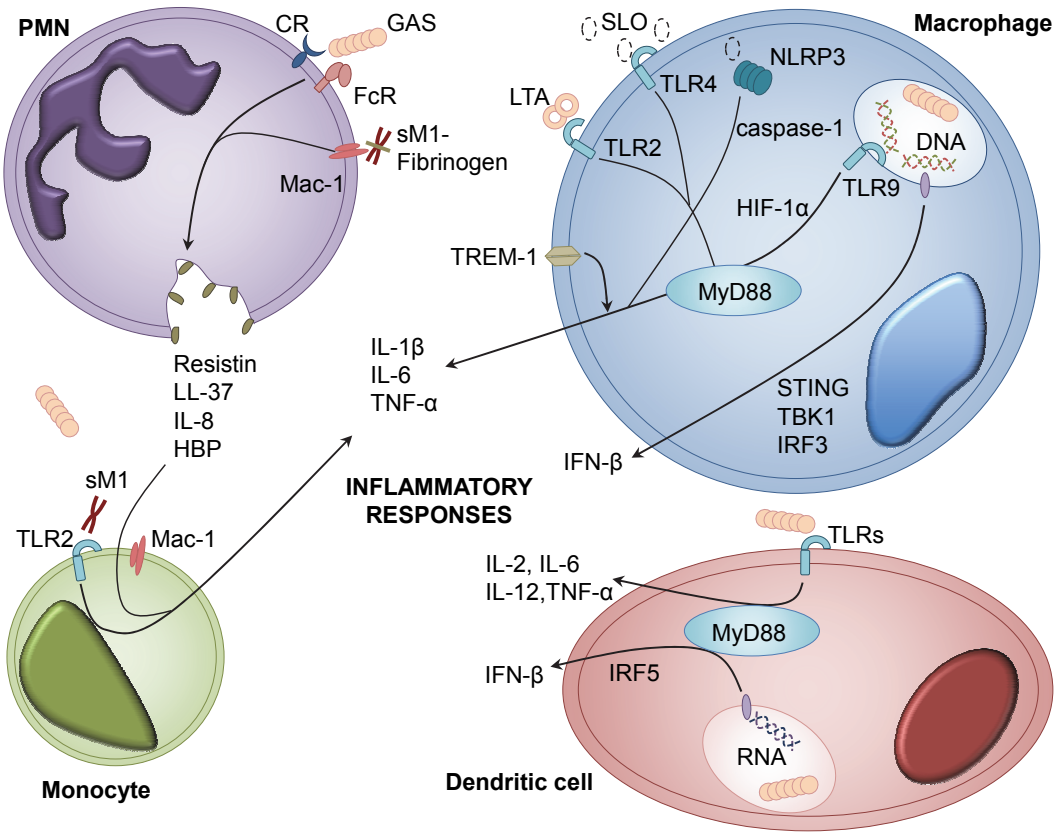

Fig. 1.5 Cellular receptors and signalling pathways involved in GAS recognition and inflammatory mediator release. Inflammatory mediators are released from multiple leukocyte types during GAS infection; including PMNs, monocytes, macrophages and dendritic cells. GAS and GAS-derived LTA; SLO, and soluble M1 protein (sM1), activate cellular responses to infection. Receptors involved in recognition of GAS include TLRs, TREM-1, complement receptors (CR), immunoglobulin receptors (FcR), Mac-1, and NLRP3. Ligand binding to these receptors leads to downstream signalling via MyD88, HIF-1α, STING, IFR3, IRF5, and TBK1. Recognition of GAS triggers release of interleukins, TNF-α, IFN-β, HBP, resistin and LL-37.

1.5.5 Non-TLR recognition of GAS

Other non-TLR receptors on macrophages have been shown to respond to GAS infection. Secretion of SLO mediates activation of the intracellular inflammasome component NLRP3 and promotes caspase-1 mediated IL-1ß secretion independently of both TLR and MyD88 signalling (Harder *et al.*, 2009). A recent report describes secondary modulation of macrophage cytokine responses by the TREM-1 receptor, which when inhibited has a therapeutic effect in murine models of GAS sepsis (Horst *et al.*, 2013). The recent work of Baruch *et al.* demonstrates SLO-mediated host signalling

via induction of endoplasmic reticulum stress (Baruch *et al.*, 2014). Adherence of *sil*-expressing GAS to epithelial cells and macrophages increases host asparagine synthetase expression and asparagine production, driving GAS proliferation and virulence (Baruch *et al.*, 2014).

1.5.6 Excessive host responses contributing to GAS disease pathology

Sufficient excitation of immune mediators is necessary to mount an adequate response to combat GAS infection. A large body of evidence suggests however, that excessive and misdirected host responses underlie damaging pathologies during severe GAS infection (Lappin and Ferguson, 2009). This effect has been historically attributed to the effects of GAS superantigenic stimulation of T-cell responses during STSS (Kotb, 1995; Norrby-Teglund *et al.*, 2000). However, the interactions of PMNs and the classic GAS virulence factor M protein have also been recently implicated in mediating this process (Norrby-Teglund and Johansson, 2013). Serotype M1 protein released from the GAS cell surface forms complexes with fibrinogen that bind to the PMN Mac-1 receptor, both activating PMNs and triggering the release of heparin binding protein (HBP) (Fig. 1.5) (Herwald *et al.*, 2004). HBP is a potent inducer of vascular permeability, and release of this protein elicits pulmonary lesion formation and vascular leakage (Gautam *et al.*, 2001; Herwald *et al.*, 2004). PMN-mediated HBP release synergistically enhances inflammatory cytokine responses from M protein-stimulated peripheral blood monocytes during necrotising infections (Pahlman *et al.*, 2006). Individuals with IgG antibodies directed towards the central region of the M protein elicit higher HBP release, and subsequently, are more at risk of suffering a pathologically excessive inflammatory response to M1 protein-fibrinogen-IgG complexes (Kahn *et al.*, 2008). Direct injection of purified M1 protein is sufficient to trigger PMN granule-mediated severe lung damage, which is markedly reduced in neutropenic mice (Soehnlein *et al.*, 2008). The M1 protein structure plays an important role in triggering HBP-mediated lung injury, as mutated, non-fibrinogen binding M1 protein exhibits

diminished capacity to cause pulmonary haemorrhage (McNamara *et al.*, 2008). The precise organisation of fibrinogen molecules into a supra-molecular, cross-like network by M1 protein is essential for PMN activation, and is conformationally distinct from normal fibrin clots (Macheboeuf *et al.*, 2011). A novel marker of septic shock severity, resistin, has also been found to predominately originate from M protein-activated PMNs during both systemic and localised severe GAS infection, and contributes to local tissue damage (Johansson *et al.*, 2009). Of particular note, resistin release is triggered by streptococcal cell wall extracts and M protein, but not by GAS superantigens (Johansson *et al.*, 2009).

Other GAS virulence factors, particularly SLO, have been found to modulate PMN responses and contribute to tissue inflammation and destruction. Expression of SLO during cutaneous infection induces toxic PMN/platelet aggregates that mediate the progression of microvascular thrombosis and ischemic tissue necrosis (Bryant *et al.*, 2005). SLO binding by PMNs has also been shown to mediate HBP, LL-37, alpha-defensin and elastase release (Nilsson *et al.*, 2006). Interestingly, host NKs have been found to increase the severity of GAS septic shock, as depletion of this cell type induces a protective reduction in systemic pro-inflammatory cytokine levels (Goldmann *et al.*, 2005a). The role of host genetic factors contributing to severe sepsis has also been investigated. Goldmann *et al.* utilised differential susceptibilities of distinct mouse strains to severe GAS infection to demonstrate that failure to control infection and evocation of excessive inflammatory responses by susceptible mice result in extensive tissue destruction (Goldmann *et al.*, 2003). This finding has been refined in studies ascribing differences in severity of STSS to host polymorphism in the human leukocyte antigen complex (Goldmann *et al.*, 2005b; Kotb *et al.*, 2002). Human MHC class II haplotype DRB*1501/DQB1*0602 is less commonly associated with STSS in the presence of NF, while DRB1*07/DQB1*0201 predisposes towards such disease manifestations. A complementary systems genetics approach was recently utilised to

identify a panel of host genes bestowing predisposition towards severe GAS sepsis (Abdeltawab *et al.*, 2008). Pathological levels of the product of one these genes, Prostaglandin E, directly influences the severity of GAS infection (Goldmann *et al.*, 2010).

1.5.7 Host leukocyte cell-death responses during GAS infection

Programmed cell death plays a decisive role in determining the outcome of microbial infections and inflammation. A variety of cell death mechanisms have been described in response to infection by different pathogens (Kennedy and DeLeo, 2009). Apoptosis limits the potential of damaged PMNs to ignite inflammatory responses. Coordinated PMN apoptotic shutdown initiates a state of cellular torpor, and administration of apoptotic PMNs actively promotes anti-inflammatory responses (Ren *et al.*, 2008). Conversely, alternative cell death mechanisms such as regulated necrosis or oncosis have been described, and are exhibited morphologically via cell and organelle swelling, cytoplasmic vacuolisation, eventual loss of plasma membrane integrity and escape of cytoplasmic content, leading to enhanced immune responses (Galluzzi *et al.*, 2012). Oncosis triggers a proinflammatory cell phenotype resulting in release of damage-associated molecular patterns (DAMPs), and prompts rapid immune responses (Kono and Rock, 2008). In a landmark study by Kobayashi *et al.*, phagocytosis-induced PMN transcriptional responses were analysed for a variety of bacterial pathogens, including GAS (Kobayashi *et al.*, 2003a). This study provided strong evidence of a common apoptotic program following bacterial uptake and ROS production. This apoptotic program is accelerated in GAS, and leads to rapid DNA fragmentation. Although GAS-induced PMN apoptosis was associated with enhanced virulence potential, the virulence determinant(s) responsible for this activity were not established (Kobayashi *et al.*, 2003a). Later work by the same group also indicated PMN phagocytosis-induced apoptosis is associated with nullified inflammatory capacity and expedites resolution of inflammation (Kobayashi *et al.*, 2003b; Kobayashi *et al.*, 2003c).

Several reports emphasise the dominant role of GAS cytolysins, and to a lesser extent hyaluronic acid capsule, in shaping PMN and other leukocyte cell-death responses. Early studies of SLO and streptolysin S (SLS) function indicate both are capable of inducing PMN lysis and skin lesion formation (Betschel *et al.*, 1998; Fontaine *et al.*, 2003; Limbago *et al.*, 2000; Sierig *et al.*, 2003). GAS strains expressing low and high amounts of SLO and SLS were used to demonstrate that cytolysins are capable of triggering caspase-dependent apoptosis of thioglycolate-induced murine PMNs (Miyoshi-Akiyama *et al.*, 2005), giving credence to the notion that the effect of GAS cytolysins is strongly concentration dependent, and that differential cytolysin expression influences strain virulence. This concept may explain, in part, conflicting reports of macrophage cell-death responses to GAS infection. A phagocytosis-independent, pro-inflammatory macrophage phenotype consistent with oncosis was reported by Goldmann *et al.*, driven by cytolysin mediated loss of mitochondrial membrane potential (ψ_m), ROS production and calpain activation (Goldmann *et al.*, 2009). Conversely, the work of Timmer *et al.* found that cytolysin expression by phagocytosed GAS also depolarises macrophage ψ_m, however leads to downstream caspase activation and initiation of the apoptotic cascade (Timmer *et al.*, 2009). Macrophages are principally responsible for the clearance of apoptotic PMNs, and either apoptotic or oncotic depletion may exacerbate damage resulting from GAS-induced cell death (Silva, 2011). Apoptotic PMNs not cleared by macrophages eventually lose cell membrane integrity, proceeding to secondary necrosis and elicitation of inflammatory responses. (Silva, 2010). These data support an emerging theme in bacterial pathogenesis, whereby direct manipulation of phagocyte cell-death responses contributes to the level of inflammation during disease (Fig. 1.6) (Kennedy and DeLeo, 2009). Programmed cell-death of other leukocyte populations in addition to PMNs has also been described, as GAS infection of DCs induces dendritic maturation, however the expression of SLO by intracellular bacteria, diverts DCs towards apoptosis (Cortes and Wessels, 2009).

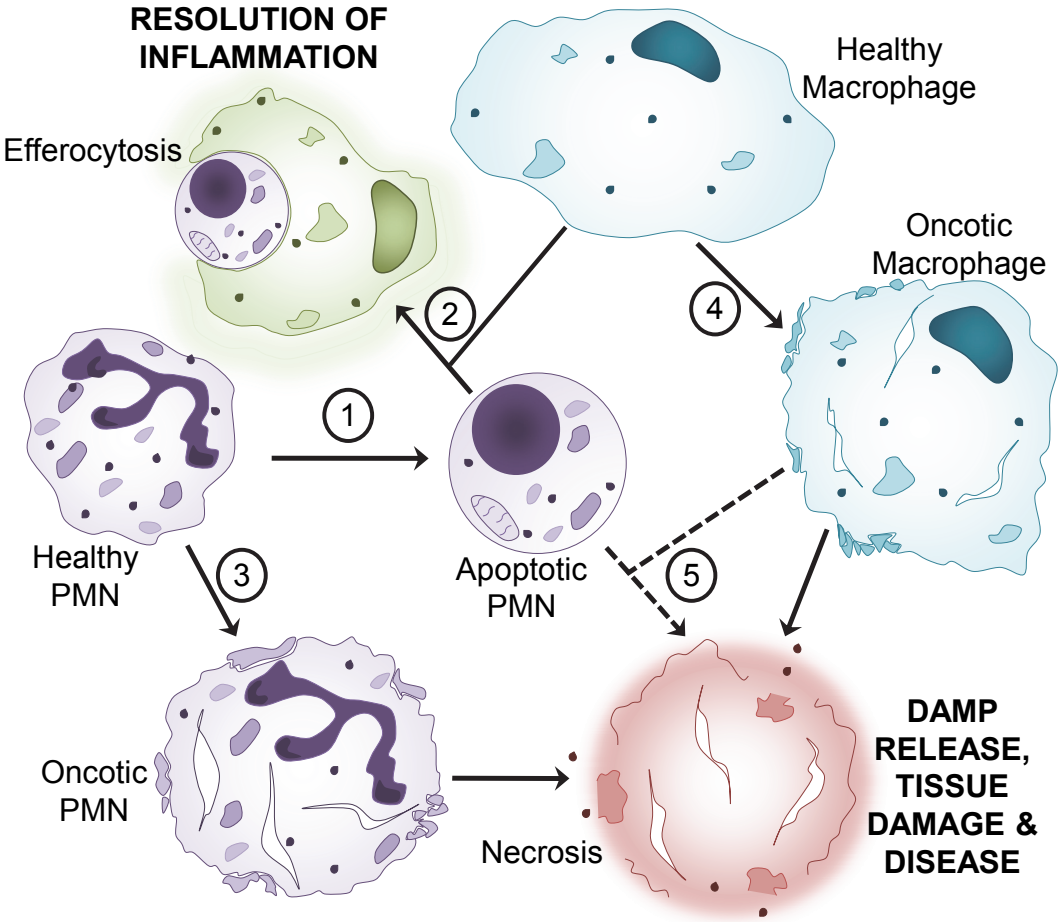

Fig. 1.6 Proposed model of PMN cell-death responses to GAS infection. Upon migration to sites of GAS infection, PMNs degranulate and generate intracellular ROS to kill phagocytosed bacteria. Under non-pathophysiological conditions, this leads to phagocytosis induced cell death (PICD) and a state of apoptotic torpor of the PMN **(1)**. Apoptotic PMNs have diminished inflammatory capacity and expose specific receptors, triggering secondary-phagocytosis of the apoptotic PMNs by mononuclear phagocytes (termed efferocytosis) **(2)**. Efferocytosis by macrophages promotes anti-inflammatory mediator release and a pro-resolution phenotype, restoring tissue homeostasis. This system is perverted by GAS at multiple levels. GAS cytolysins directly induce PMN necrosis, presumably preceded by an oncotic intermediate step **(3)**. GAS cytolysins can also induce macrophage oncosis or apoptosis **(4)**. Multiple reports also indicate GAS triggers a rapid, pathophysiological PMN apoptotic mechanism, which may lead to secondary necrosis exacerbated by apoptotic/oncotic macrophage depletion, however this remains to be conclusively tested **(5)**. PMN and macrophage necrosis triggers uncontrolled intracellular damage associated molecular patterns (DAMPs) and granule component release, and subsequent induction of hyper-inflammatory responses.

1.5.8 Epithelial cell apoptotic responses

Epithelial cells mediate the first interactions between host and bacteria. Adherence of GAS to epithelial receptors frequently precedes intracellular invasion of this bacterium (Nitsche-Schmitz *et al.*, 2007), and multiple pathways of epithelial cell death have been

reported following GAS infection (Fig. 1.7A). GAS infection of A549 and HEp-2 cells was found to elicit morphological changes consistent with apoptosis, attributable to the activity of GAS cysteine protease SpeB (Tsai *et al.*, 1999). The apoptotic Fas receptor (FasR) and $\alpha_v\beta_3$ integrins are able to bind SpeB, leading to downstream caspase-8 activation and translocation of truncated-Bid (tBid) and Bax to mitochondria (Tsai *et al.*, 2004; Tsai *et al.*, 2008). Binding of SpeB to host receptors also upregulates caspase-8 and Bax via JAK-STAT, p38 and p53 signalling (Chang *et al.*, 2009; Lee and Chang, 2010). Internalisation dependent epithelial cell apoptosis in response to GAS infection has also been reported, whereby fibronectin-mediated binding of GAS to host integrins triggers actin rearrangement and Rac1 activation (Aikawa *et al.*, 2010; Nakagawa *et al.*, 2001). Rac1 activation is hypothesised to mediate epithelial cell ROS production, leading to downstream apoptotic responses (Aikawa *et al.*, 2010; Nakagawa *et al.*, 2001). A third pathway trigged by extracellular GAS also elicits epithelial apoptosis via an SLO-dependent mechanism (Cywes Bentley *et al.*, 2005). Secretion of SLO by encapsulated GAS triggers calcium flux into the cytosol of infected cells, leading to vacuolisation of the endoplasmic reticulum and cell apoptosis (Cywes Bentley *et al.*, 2005). Central to these pathways is the role of the mitochondria, as cytochrome c release and ψ_m depolarisation are described as key events, and that overexpression of the anti-apoptotic factor Bcl-2 can inhibit mitochondrial dysfunction. In many studies, both capase-9 and caspase-3 are reported to mediate the final apoptotic cascade. Transcriptional analyses of epithelial cells also indicate overall apoptotic responses to GAS infection, and that GAS elicits upregulation of caspases and calcium regulators (Klenk *et al.*, 2005; Nakagawa *et al.*, 2004b). It is important to note that different GAS serotypes do not elicit uniform epithelial responses, and comparison of apoptotic induction by disparate GAS strains demonstrates multiple caspases are utilised (Klenk *et al.*, 2007).

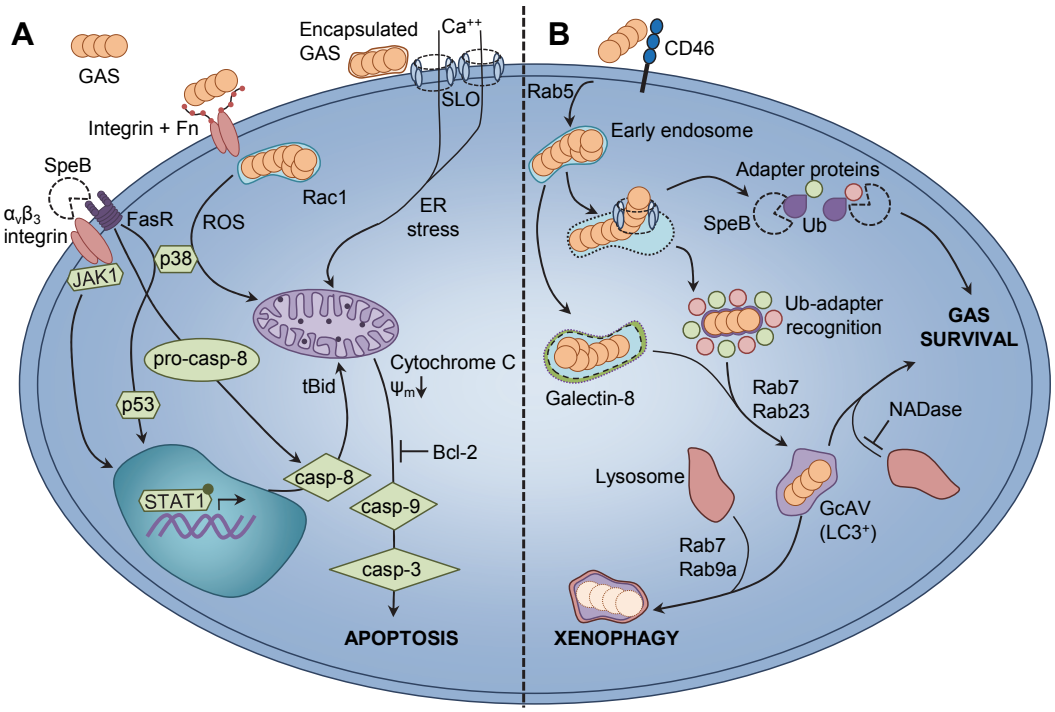

Fig. 1.7 Epithelial cellular responses to GAS infection. A GAS-induced apoptosis of epithelial cells is triggered via intrinsic and extrinsic pathways. SpeB binding to epithelial $\alpha_v\beta_3$ integrins or the Fas receptor (FasR) triggers upregulation of caspase-8 (casp-8) via JAK2, p38, p53 and STAT1 signalling. Procaspase-8 (pro-casp-8) is also activated directly due to FasR signalling, leading to truncation of cytosolic Bid (tBid) and translocation of tBid to the mitochondria. Extracellular GAS binding to host integrins is enabled via bridging molecules such as fibronectin (Fn), and enables Rac1-mediated internalisation of GAS into host epithelial cells. GAS internalisation and Rac1 activation facilitate production of ROS, leading to increased p38 phosphorylation. Encapsulated extracellular GAS are not internalised by epithelial cells and secrete the pore-forming toxin SLO. Integration of SLO into host cell membranes triggers net calcium (Ca^{++}) flux into the cytosol and endoplasmic reticulum (ER) stress. All three pathways elicit loss of ψ_m and release of cytochrome C from the mitochondria, which precedes activation of caspase-9 (casp-9) and caspase-3 (casp-3) and apoptosis. Overexpression of the anti-apoptotic factor Bcl-2 by the host can inhibit epithelial cell apoptosis. **B** GAS evades xenophagic killing by epithelial cells. GAS binding to the CD46 receptor is an early signal to activate autophagic responses, and GAS are uptaken into early endosomes in a Rab5-dependent manner, however SLO expression allows GAS to escape from endosomes into the cytosol. GAS exposure to the cytosol is recognised via ubiquitin (Ub) adapter proteins that, in conjunction with Rab7 and Rab23, facilitate shuttling of GAS into GcAVs bearing the classic autophagy LC3 marker. In the absence of SLO, streptolysin S is sufficient to damage endosomal vacuoles for targeting to GcAVs by Ub-independent, galectin-8-mediated autophagy. Lysosomal fusion with GcAVs, via Rab7 and Rab9a, effects xenophagic destruction of intracellular GAS. Expression of SpeB by cytosolic GAS degrades Ub adapter proteins and prevents targeting of bacteria to GcAVs, enhancing intracellular GAS survival. Secretion of GAS NADase also protects GAS from xenophagic killing by inhibiting fusion of GcAVs with lysosomes.

1.5.9 GAS-induced autophagy

Epithelial cell apoptosis has been suggested to protect host cells from infection, however data validating this hypothesis is lacking, and contention exists regarding whether epithelial apoptotic cell death is indeed a protective host response, or a

pathogenic mechanism utilised by GAS (Aikawa *et al.*, 2010; Cywes Bentley *et al.*, 2005). An alternative epithelial cell defence mechanism against GAS infection has been recently described. Autophagy, a stress response wherein damaged cellular components are targeted to degradative endosomal vacuoles, can protect cells from intracellular GAS (Fig. 1.7B). HeLa cells containing intracellular M6 serotype GAS recognise cytosol-exposed bacteria and target them for autophagic degradation via ubiquitinylation, LC3 labelling and the formation of GAS-containing autophagosome-like vacuoles (GcAVs) (Nakagawa *et al.*, 2004a). Expression of SLO by intracellular GAS is crucial for GAS escape from endosomes into the cytosol and subsequent targeting to GcAVs (Nakagawa *et al.*, 2004a). Binding of the cell surface CD46 receptor is an early trigger of GAS-mediated autophagy (Joubert *et al.*, 2009). The Rab-family of G-proteins is responsible for multiple aspects of GcAV formation. Rab7 protein performs numerous roles, including targeting of GAS to GcAVs and initial GcAV formation; and autophagosomal maturation (Yamaguchi *et al.*, 2009). Other Rab-enzymes; Rab5, Rab23, and Rab9a; also play distinct roles which include facilitating GAS uptake into endosomes, targeting of GAS to GcAVs, homotypic fusion of nascent GcAVs, and autophagosomal maturation (Nozawa *et al.*, 2012; Sakurai *et al.*, 2010). Recent studies report that GAS is able to subvert autophagy-mediated bacterial destruction (also called xenophagy) for intracellular survival. SLO-mediated translocation of GAS NAD-glycohydrolase (NADase) prevents efficient killing of serotype M6 GAS via inhibition of autophagosomal fusion with lysosomes (O'Seaghdha and Wessels, 2013). A novel, ubiquitin-independent pathway of GcAV formation was also described for primary human keratinocytes in this study. Ubiquitin-independent GcAV formation was mediated through SLS damage to endosomal vacuoles, leading to endosomal labelling with galectin-8, and acquisition of the autophagy specific LC3 marker (O'Seaghdha and Wessels, 2013). Infection of HEp-2 cells with M1T1 serotype GAS reveals significantly greater intracellular survival than by M6 GAS, with M1T1 GAS displaying exposure to the cell cytosol but lack of the LC3 autophagy marker

(Barnett *et al.*, 2013). Enhanced M1T1 GAS survival was found to be directly linked to SpeB activity, which degrades cytosolic ubiquitin and the adapter proteins NDP52, p62 and NBR1, to effect highly efficient evasion of cellular xenophagy (Barnett *et al.*, 2013).

1.6 GAS virulence factors bestowing innate immune resistance

GAS expresses multiple virulence factors capable of countering innate immune responses by diverse mechanisms (Fig. 1.8). Strategies of innate immune resistance and neutrophil evasion utilised by GAS include suppression of immune surveillance, interference with complement function, inhibition of antibody-mediated opsonisation, induction of phagolysis and degradation of NETs (Kwinn and Nizet, 2007).

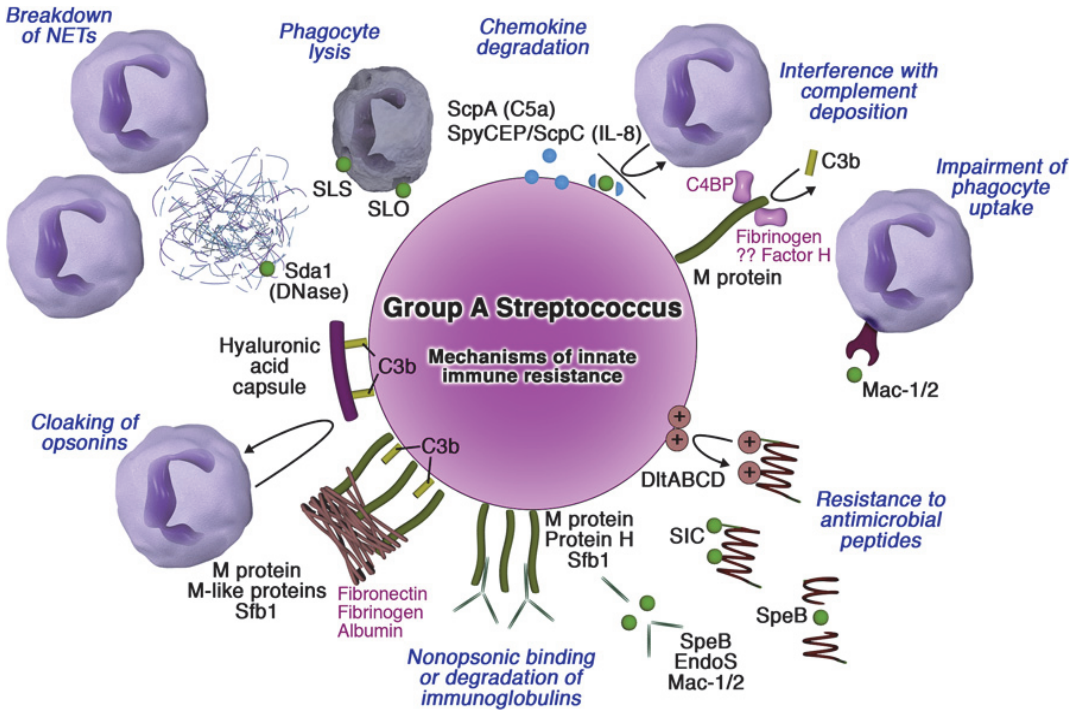

Fig. 1.8 Diverse mechanisms by which GAS circumvents elements of the innate immune response. Chemokine recruitment of polymorphonuclear leukocytes (PMNs) by C5a and interleukin-8 (IL-8) is inhibited by streptococcal C5a (ScpA) and streptococcal cell envelope (SpyCEP/ScpC) peptidases. Deposition of opsonising complement fragment C3b, C4-binding protein (C4BP) and complement factor H is blocked by M protein binding. Interaction of opsonins with host phagocyte complement receptors is cloaked by hyaluronic acid capsule and M protein bound fibrinogen, fibronectin and plasminogen. Immunoglobulins (Igs) are nonopsonically bound by Protein H and M protein, with cysteine protease SpeB, endopeptidase S and Mac-1/2 proteolytically cleaving Igs. streptococcal inhibitor of complement (SIC) inhibits phagocytosis by preventing formation of the membrane-attack complex (MAC) and inactivates cathelicidin LL-37 and neutrophil α-defensins. PMNs are lysed by the cytotoxins Streptolysin O and S (SLO and SLS). Neutrophil extracellular traps (NETs) are degraded by phage-encoded streptodornase 1 (Sda1). Reproduced from (Nizet, 2007).

1.6.1 M proteins and M-like proteins

The antiphagocytic activity of group A streptococcal M protein has been known for some decades (Lancefield, 1962). However more recently, the mechanisms underlying this activity have been ascribed to M proteins from GAS of certain serotypes that are able to bind different host factors, some of which can interfere with immune function (Smeesters *et al*., 2010). It has been shown that GAS M protein binds alternative complement pathway factor H, which regulates alternative pathway complement activity by binding fluid-phase and cell surface C3b (Horstmann *et al.*, 1988). M protein also modulates the classic complement pathway immune responses via binding to C4b-binding protein (C4BP) (Johnsson *et al.*, 1996). M protein contributes to the intracellular survival of GAS within phagocytes by inhibiting neutrophil azurophilic granule-phagosome fusion (Staali *et al.*, 2006; Staali *et al.*, 2003). M1 protein also promotes resistance to LL-37 when ensnared in PMN NETs, via binding of LL-37 to the M1 hypervariable region (Lauth *et al.*, 2009). M protein-family proteins such as Mrp and Enn are structurally similar to M protein as α-helical, coiled coil dimeric fibrils and also exhibit diverse binding ligands, including fibrinogen. Both M1 protein and Mrp can bind fibrinogen to the GAS cell surface, which interferes with complement deposition, and many Enn proteins can also bind IgA (Courtney *et al.*, 2006; Podbielski *et al.*, 1994). Approximately 15% of GAS express PAM (plasminogen-binding group A streptococcal M protein) proteins through which GAS are able to affect high-affinity plasminogen binding through specific M protein domains (Berge and Sjobring, 1993; Svensson *et al.*, 1999). Recent work has described a new role for GAS plasminogen binding in relation to GAS innate immune evasion, as bound plasminogen reduces C3b binding to the bacterial cell surface and protects GAS from neutrophil killing (Ly *et al.*, 2013).

1.6.2 Hyaluronic acid capsule

GAS expresses a capsule composed of hyaluronic acid, a high molecular weight polymer of alternating residues of *N*-acetylglucosamine and glucouronic acid (Wessels

et al., 1991). The genes encoding for capsule production are contained within the *has*ABC gene cluster, though *has*AB alone is sufficient for capsule synthesis (Ashbaugh *et al.*, 1998). The hyaluronic acid capsule aids GAS evasion of innate immune responses via resistance to phagocytosis. It is hypothesised that the capsule serves as a physical barrier to phagocytosis, as complement deposited on the GAS cell surface is unable to interact with phagocytic receptors (Dale *et al.*, 1996). Acapsular GAS mutants show decreased virulence compared to encapsulated strains in murine infection models (Wessels and Bronze, 1994). Highly upregulated expression of the *has* operon has been noted in response to animal passage through mice (Sumby *et al.*, 2006). The capsule has also been shown to inhibit internalisation of GAS by epithelial keratinocytes (Schrager *et al.*, 1996).

1.6.3 Streptococcal inhibitor of complement

Deposition of complement on bacterial cell surfaces promotes opsonisation and phagocytosis by innate immune cells. Streptococcal inhibitor of complement-mediated lysis protein (SIC) contributes to antiphagocytic activity by interfering with both the classical and alternative complement pathways in the formation of the MAC (Akesson *et al.*, 1996). SIC protein binds to the C5b67 and C5b678 complexes, preventing uptake onto cell membranes and subsequent lysis (Fernie-King *et al.*, 2001). Inactivation of the *sic* gene results in a significant reduction of mucosal surface colonisation by GAS, demonstrating that SIC enhances the colonising ability of infecting GAS strains (Lukomski *et al.*, 2000a). This hypothesis is supported by evidence that SIC is able to inhibit secretory leukocyte proteinase inhibitor, lysozyme, α-defensin and LL-37 (Fernie-King *et al.*, 2002; Frick *et al.*, 2003).

1.6.4 Modification of teichoic acid on the GAS cell surface

Most Gram-positive bacteria incorporate LTA into the cell-wall in order to maintain cell-wall shape and regulate autolytic enzyme activity. In GAS, LTA can be modified via *D*-

alanylation, increasing the net positive charge of the bacterial cell-surface via a *D*-alanine-*D*-alanyl carrier protein ligase (DltA) (Kristian *et al.*, 2005). Manipulation of the net charge of the bacterial cell surface by GAS allows this pathogen to resist polycationic AMPs such as murine cathlicidin CRAMP and polymyxin B via electro-static repulsion and thus increase antiphagocytic activity (Kristian *et al.*, 2005). *D*-alanylation of GAS LTA also affects the transcription and expression of other virulence factors such as M protein and SIC via unknown mechanisms, resulting in decreased complement deposition and higher growth rates in human blood (Cox *et al.*, 2009).

1.6.5 S. pyogenes cell envelope proteinase

Impairment of phagocyte recruitment by GAS indirectly hampers the innate immune response by crippling immune surveillance mechanisms. Previous work by Hidalgo-Grass *et al.* isolated GAS from necrotic tissue that expressed an unidentified protease capable of inhibiting neutrophil recruitment to the site of infection (Hidalgo-Grass *et al.*, 2004). This activity was later linked to *S. pyogenes* cell envelope proteinase (*Spy*CEP, also known as ScpC). *Spy*CEP promotes specific cleavage of the potent neutrophil chemokine IL-8, and strains lacking *Spy*CEP exhibit attenuated virulence in murine infection models (Edwards *et al.*, 2005; Hidalgo-Grass *et al.*, 2006). *Spy*CEP has also been shown to degrade other chemokines, including granulocyte chemotactic protein 2 and growth-related oncogene alpha, both of which are produced abundantly by human tonsillar epithelial cells (Sumby *et al.*, 2008).

1.6.6 Streptococcal C5a peptidase

The surface bound GAS virulence factor, Streptococcal C5a peptidase (ScpA) is a highly specific endopeptidase that inactivates C5a via the cleavage of six amino acids from the C terminus (Cleary *et al.*, 1992; Fernandez and Hugli, 1978; O'Connor and Cleary, 1986). ScpA inhibits the phagocytic clearance of GAS, as ScpA-deficient GAS mutants elicit significantly increased PMN recruitment during infection (Ji *et al.*, 1996).

Immunisation of mice with an enzymatically inactive peptide of serotype M49 ScpA reduced the potential of multiple serotypes to colonise the nasopharynx, presenting a possible candidate for vaccine development (Ji *et al.*, 1997).

1.6.7 Streptococcal Mac-1-like protein

Screening of the GAS secreted proteome by Lei *et al.* identified a GAS protein bearing 23% amino acid identity between amino acids E319 and V391 to the α-subunit of human leukocyte adhesion receptor Mac-1, a leukocyte β_2 integrin involved in innate immunity (Lei *et al.*, 2000). Expression of the Mac-1-like protein is regulated via the control of virulence regulatory sensor kinase (*covRS*) system (Sumby *et al.*, 2006). This protein binds CD16 (FcγRIIIB) receptor on human PMNs, inhibiting opsonophagocytosis by blocking association of C3bi and antibodies with CD16 (Lei *et al.*, 2001). The antiphagocytic activity of Mac-1-like protein (also known as immunoglobulin G-degrading enzyme of *S. pyogenes*, IdeS) is also attributed to cysteine proteolytic, IgG-specific degradation (von Pawel-Rammingen *et al.*, 2002). A variant of the Mac-1-like protein, designated Mac-2, has also been identified. Mac-2 contains ~50% sequence divergence in the central third of the molecule, and inhibits the host immune response through strong binding to both FcγRII and FcγRIII receptors (Agniswamy *et al.*, 2004; Lei *et al.*, 2002).

1.6.8 Streptolysins

Induction of neutrophil lysis is an important mechanism of GAS innate immune evasion, accomplished by the expression of cytolytic toxins. SLO secreted by GAS interacts with cholesterol in eukaryotic cell membranes, producing multi-subunit, transmembrane pores, which lead to cell death (Limbago *et al.*, 2000). A non-homologous, but functionally related haemolysin, SLS is also responsible for the cytolytic killing of mammalian cells by opening transmembrane pores that result in subsequent osmotic cell lysis, and is responsible for the typical β-haemolysis of GAS colonies on blood agar

(Betschel *et al.*, 1998; Datta *et al.*, 2005). Isogenic single and double SLS and SLO mutants have been used to show that each streptolysin may complement the role of the other with some degree of functional redundancy (Fontaine *et al.*, 2003). Expression of either streptolysin was also found to enhance the virulence of acapsular GAS, protecting more susceptible bacteria from phagocytic clearance (Sierig *et al.*, 2003).

1.6.9 Streptococcal collagen-like proteins

The Streptococcal collagen-like protein A (SclA) protein contains a collagen-like domain composed of Gly-X-X triplet amino acid motifs (Lukomski *et al.*, 2000b; Rasmussen *et al.*, 2000). Immune selection is suggested to have contributed to the evolution of the collagen-like domain of SclA, as it exhibits hypervariability analogous to M-protein, and phylogenetic analyses suggest that horizontal gene transfer of the *sclA* allele has occurred between multiple M serotypes (Lukomski *et al.*, 2000b; Rasmussen *et al.*, 2000). The putative collagen-like triple-helix structure of SclA has been confirmed experimentally, and a plethora of functions have been assigned (Xu *et al.*, 2002). SclA interacts with mammalian collagen-binding integrin $\alpha_2\beta_1$ specifically through the collagen-like region, which also enables GAS intracellular invasion, survival and re-emergence from human pharyngeal epithelial cells (Caswell *et al.*, 2007; Humtsoe *et al.*, 2005). SclA binds low-density lipoproteins through the variable non-collagenous V region (Han *et al.*, 2006) and thrombin-activatable fibrinolysis inhibitor, which is capable of inactivating complement C3a and C5a and neutrophil chemo-attractant fibrinopeptide B (Pahlman *et al.*, 2007). Recently, it has been indicated that SclA may play a role in mediating alternative complement-mediated opsonophagocytosis through binding regulatory glycoprotein factor H and factor H-related protein 1 (Caswell *et al.*, 2008). Initial characterisation of *sclA* showed that it is distally controlled by the Mga regulon (Almengor and McIver, 2004), however mutation of M1T1 *covRS* also results in up-regulated *sclA* expression (Sumby *et al.*, 2006).

1.6.10 Cysteine protease SpeB

Group A streptococci express a cysteine protease, SpeB (also known as SCP or streptopain), which has been shown to play a dynamic role in the GAS pathogenesis cycle. SpeB is an extracellular protein, secreted through the ExPortal microdomain as a 40 kDa zymogen (Rosch and Caparon, 2004), which auto-catalytically truncates to a mature 28 kDa peptide. SpeB has also been characterised as cell surface associated (Hytonen *et al.*, 2001). SpeB has a range of effects on host factors, including the activation of human IL-1β (Kapur *et al.*, 1993); the release of kinins via cleavage of kininogens (Herwald *et al.*, 1996); activation of cell matrix metalloproteases (Burns *et al.*, 1996); degradation of LL-37 and IgA, IgM, IgD and IgE (Collin and Olsen, 2003; Schmidtchen *et al.*, 2002) and specific cleavage of the IgG hinge region (Collin and Olsen, 2001). Many surface bound and extracellular GAS virulence factors are also processed by SpeB, including M protein and protein H, fragments which were detected following SpeB treatment of live GAS cells (Berge and Bjorck, 1995), in addition to proteolysing streptococcal superantigens, streptodornase and streptokinase (Aziz *et al.*, 2004b; Rezcallah *et al.*, 2004). Biologically active fragments of C5a peptidase are liberated from the GAS cell surface by SpeB, which may contribute to virulence via inhibition of phagocyte recruitment (Berge and Bjorck, 1995). However, conflicting evidence of the role of SpeB in virulence has been observed. Multiple studies implicate SpeB as critical for severe infection and dissemination (Berge and Bjorck, 1995; Lukomski *et al.*, 1998), in contrast to epidemiological evidence that SpeB expression is inversely proportional to the severity of GAS diseases (Kansal *et al.*, 2000), or that SpeB in fact, has no effect on invasive streptococcal infection (Ashbaugh and Wessels, 2001). Recent studies utilising more physiologically relevant mouse models suggest that expression of SpeB promotes bacterial colonisation, whilst the loss of SpeB expression triggers a ‘switch’ in pathogenesis to favour bacterial dissemination and invasive infection (Cole *et al.*, 2006; Walker *et al.*, 2007).

1.6.11 Streptodornases

GAS expresses four classes (subgroups A-D) of streptococcal extracellular nucleases known as streptodornases (Sda). Streptodornases are predominantly phage-acquired, and are characterised by their optimal pH and nature of substrate (DNA, RNA or both) (Wannamaker and Yasmineh, 1967; Winter and Bernheimer, 1964). Aziz *et al.* identified a streptodornase D homologue in M1T1 serotype GAS, designated Sda1 (Aziz *et al.*, 2004a). Sda1 shares two conserved domains with other extracellular nucleases and ~90% amino acid identity to SdaD but with a unique C-terminus. Sda1 is presumed to have been acquired by GAS via phage-mediated lateral gene transfer, as the *sda1* gene is located near a putative prophage attachment point, and is absent in closely related GAS strains (Aziz *et al.*, 2004a). The importance of Sda1 in virulence was established by the work of Buchanan *et al.* in which Sda1 was implicated in neutrophil resistance through degradation of NETs (Buchanan *et al.*, 2006). Increased virulence was noted in strains expressing Sda1 compared to Sda1-deficient isogenic mutants in murine infection models (Buchanan *et al.*, 2006).

1.7 Molecular basis for invasive GAS disease

1.7.1 Subversion of the host plasmin(ogen) activation system

Following host colonisation and evasion of early innate immune response, particularly invasive GAS strains or subpopulations can penetrate deeper tissues within the host, effectively transitioning from a mild to an invasive infection. The accumulation of host plasmin activity on the GAS cell surface has been associated with the development of invasive disease (Cole *et al.*, 2006). Plasminogen circulates in human plasma as an inactive zymogen, and is activated via cleavage by the host tissue-plasminogen activator (tPA) or urokinase-plasminogen activator (uPA) to plasmin. Activated plasmin is a highly potent serine protease capable of proteolysing multiple host ECM components and fibrin blood clots (Plow *et al.*, 1995). Subversion of the plasminogen

system by GAS occurs via the non-enzymatic activation of plasminogen through direct binding by secreted streptokinase (McArthur *et al.*, 2012). Bacterial cell-surface sequestration of plasmin(ogen), or the activated plasmin(ogen)-streptokinase complex is mediated by GAS plasmin(ogen) receptors PAM, streptococcal surface enolase (SEN) or glyceraldehyde-3-phosphate dehydrogenase (GAPDH) (Svensson *et al.*, 2002; Walker *et al.*, 2005). Indirect plasmin(ogen) cell-surface sequestration also occurs via the formation of a streptokinase-plasminogen-fibrinogen trimolecular complex, which also retains plasmin activity and can be bound to the GAS cell-surface through fibrinogen receptors such as Mrp (D'Costa and Boyle, 1998; Wang *et al.*, 1995). Activated human plasmin bound to the GAS cell-surface is capable of degrading fibrin clots and opening a channel for GAS to invade sterile tissue sites and cause invasive disease (Sun *et al.*, 2004; Walker *et al.*, 2005).

1.7.2 Two-component regulatory systems determining GAS virulence

Expression of GAS virulence determinants is regulated by individual transcription factors and more broadly active regulatory systems, such as the multiple gene regulator in group A streptococci (Mga) and RopB/Rgg (Chaussee *et al.*, 2003; Cunningham, 2000). GAS also encode twelve two-component gene regulatory systems, of which several have been characterised, including *sptRS*, Ihk-Irr, and *covRS* (Shelburne *et al.*, 2005; Sitkiewicz and Musser, 2006; Sumby *et al.*, 2006; Voyich *et al.*, 2004). The products of the *covRS* operon repress expression of multiple virulence genes involved in resistance to innate immune responses and tissue invasion, including *ska* (streptokinase), *slo*, the *has* operon, *scpA*, *sda1*, *mac*, *spyCEP* and *sic* (Sumby *et al.*, 2006). Conversely, mutations in *covRS* result in the up-regulation of these factors, and abolish cysteine protease SpeB expression. It has been shown that spontaneous *covRS* mutations acquired *in vivo* result in increased resistance to killing by human PMNs by M1T1 GAS (Sumby *et al.*, 2006) and that concurrent loss of *speB* expression protects the secreted proteome, including immune-

modulating virulence factors of M1T1 GAS, from degradation (Aziz *et al.*, 2004b). Therefore, it has been proposed that mutation of the *covRS* system represents a genetic trigger which enhances GAS innate immune resistance and invasive potential (Walker *et al.*, 2007).

1.7.3 Invasive disease initiation of serotype M1T1

The acquisition of *covRS* mutation in M1T1 GAS has been studied extensively, with studies elucidating that the phage-encoded Sda D2 homologue, Sda1 is critical for the selection of spontaneous *covRS* mutants during infection (Walker *et al.*, 2007). In the model proposed by Walker *et al.*, infecting M1T1 GAS express SpeB during the early stages of host colonisation, and attract neutrophils which release NETs to impede bacterial dissemination (Fig. 1.9A). However, a subpopulation of GAS acquire a mutation in *covRS*, resulting in the simultaneous up-regulation of secreted immune modulating virulence factors including Sda1 and abolition of SpeB activity, sparing these cell-surface and secreted virulence factors from degradation (Fig. 1.9A). Pressure applied by NETS results in selection of the SpeB-negative phenotype due to increased Sda1 activity, allowing the *covRS*-mutant subpopulation to proliferate and acquire cell-surface plasmin activity through streptokinase-mediated plasminogen activation and acquisition via GAS cell-surface receptors (Fig. 1.9C). Consequently, M1T1 GAS selected for by this mechanism acquire a hypervirulent phenotype which enables both evasion of the innate immune response and the initiation of invasive, systemic diseases in the host (Fig. 1.9D). This model accounts for the virulence of the invasive clone of serotype M1T1, however not for the virulence of isolates of other serotypes which lack phage-encoded virulence factors such as Sda1. Recent work by Maamary *et al*. demonstrates that mutations in *covRS* occur in a range of GAS serotypes, and result in a unanimous increase in virulence and resistance to PMN-killing (Maamary *et al*., 2010). In corroboration, other ubiquitously distributed GAS virulence factors such as M protein and capsule have been shown as critical for

acquisition of *covRS* mutations (Cole et al., 2010). However, the ability of M1T1 GAS to acquire *covRS* mutations more frequently may underlie the success of this globally disseminated serotype relative to other GAS strains (Maamary *et al*., 2010; Maamary *et al*., 2012). Mutation of M1T1 *covRS* upregulates a cohort of genes responsible for innate immune resistance and initiation of invasive disease, but this increase in virulence is counterbalanced by simultaneous detriment to colonisation ability, as upregulation of capsule via *covRS* mutation impairs M1T1 GAS adherence to HEp-2 cells and biofilm formation (Hollands *et al*., 2010). Thus, while the molecular mechanisms coordinating M1T1 GAS virulence and innate immune interactions have been precisely described, further work is required to detail these aspects of non-M1T1 GAS pathogenesis.

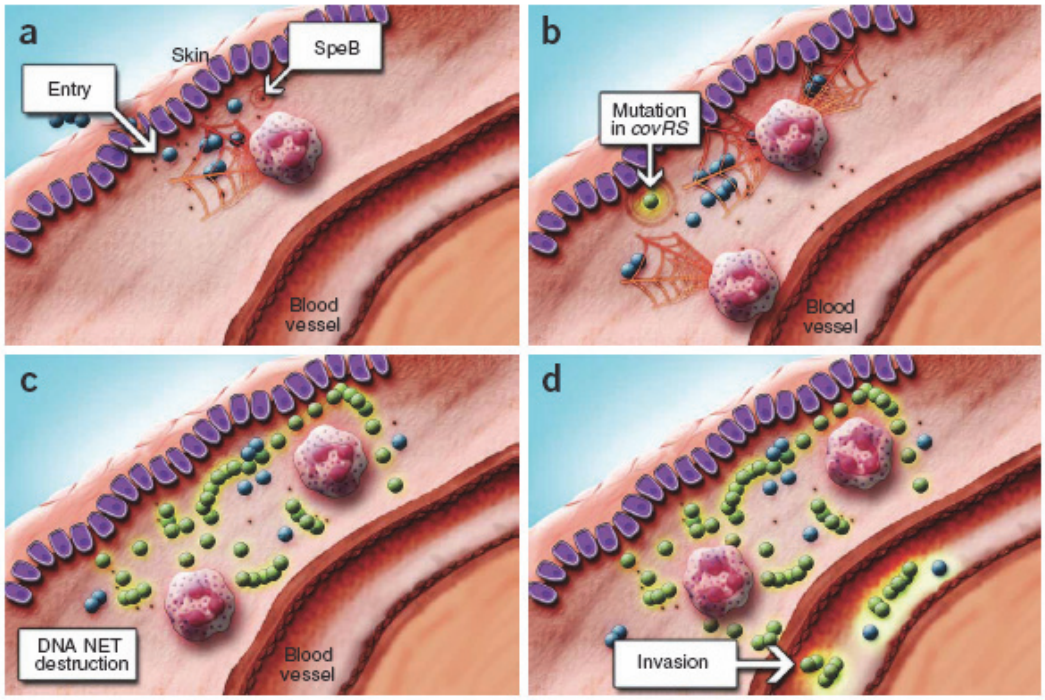

Fig. 1.9 Transition of a mild to invasive infection by group A streptococcus (GAS). A) GAS (blue) enter through a break in the epidermis and express cysteine protease SpeB (red) to aid in host colonisation. Neutrophils are recruited to the site of infection and release extracellular traps (NETs) which ensnare the bacteria. **B)** A subpopulation of GAS (green) acquire a mutation in the *covRS* regulon, resulting in downregulation of SpeB and increased activity of streptodornase 1 (Sda1). **C)** GAS *covRS* mutants with enhanced Sda1 activity are able to degrade NETs, giving an advantage over the SpeB-expressing phenotype. **D)** Loss of SpeB expression leads to the acquisition of cell surface plasmin activity, giving GAS enhanced invasive propensity and potential for dissemination. Reproduced from Walker *et al.* (2007).

1.8 Project aims

Resurgences in the rates of severe GAS diseases in urbanised areas emphasise the importance of understanding the fundamental mechanisms by which GAS initiate invasive infections. Whilst the molecular triggers for invasive disease initiation by the M1T1 serotype, a serotype which is prevalent in urbanised areas, have been recently uncovered, a dearth of knowledge remains regarding pathogenesis of serotypes from areas with more diverse epidemiology of infection. Resistance to the innate immune response is integral for the bacterium to survive and elicit severe infection. As such, in-depth analysis of non-M1 GAS interactions with the innate immune effectors, such as PMNs, will provide insight into the mechanisms that guide bacterial persistence and host responses in a less urbanised context. The clinical bacteraemia isolate NS88.2 (*emm*98.1) was isolated from Australia's Northern Territory, and exhibits virulent, neutrophil resistant phenotypes that make it a suitable representative strain to model emergent, virulent GAS isolates.

Thus, the specific aims of this study were to:

- Conduct genomic screening analysis of the virulent GAS isolate NS88.2, to identify virulence factors with putative roles in mediating PMN interactions.
- Utilise this genomic sequence to assist transcriptomic and proteomic interrogation of NS88.2 and support previous genomic analyses.
- Isogenically delete candidate virulence factors from NS88.2 and characterise the ability of mutant knock-out strains to resist innate immune killing.
- Determine differential PMN responses to infection by both PMN-resistant and PMN-sensitive GAS.

The results of this study describe in greater detail novel factors and pathways dictating both pathogen- and host-oriented interactions in the non-M1T1 GAS background.

CHAPTER 2: GENERAL MATERIALS AND METHODS

This chapter contains methods used during this project by the candidate. Other methods used by co-authors for publications are detailed in the relevant research chapters and are available in publications at the end of this thesis. Full details of all general buffer components are listed in Appendix A.

2.1 Bacterial strains, plasmids and growth conditions

Bacterial strains and plasmids utilised in this study are listed in Table 2.1. Except where otherwise noted, all GAS strains were routinely cultured at 37°C on solid horse blood agar (HBA) (Oxoid, UK), Todd-Hewitt agar (THYA) (Difco, Australia) or in liquid cultures of 1% (w/v) yeast-supplemented Todd-Hewitt broth (THY) (Difco, Australia). GAS containing pDCerm or derivative constructs were cultured in static THY cultures supplemented with 2 µg/ml erythromycin. *Escherichia coli* strains were cultured at 37°C on solid lysogeny-broth (LB) agar or liquid LB supplemented with appropriate antibiotic.

2.2 Bacterial transformation

2.2.1 Preparation of electro-competent Escherichia coli

A single colony of each *E. coli* strain to be made competent was inoculated into 100 ml of LB broth followed by subsequent overnight culture at 37°C with shaking at 200 rpm. Each culture was expanded to 1 L of LB, and incubated at 37°C with shaking at 200 rpm until reaching OD_{600}: 0.8. Cultures were harvested via centrifugation (4,650 *x g*, 10 min, 4°C) and supernatants decanted prior to resuspension in 200 ml of cold sterile dH_2O. Cell resuspensions were pelleted (6,690 *x g*, 10 min, 4°C), and the previous washing step repeated twice with 100 ml of cold sterile H_2O. After washing, cell pellets were resuspended in 4 ml of cold sterile 10% glycerol and re-pelleted (3,020 *x g,* 10 min, 4°C). Supernatants were decanted, and sufficient cold sterile 10% glycerol used to resuspend cell pellets prior to storage at -80°C

Table 2.1 Bacterial strain and plasmids utilised in this study.

Bacterial strain or plasmid	Features	Reference or Source
Streptococcus pyogenes		
NS88.2	Invasive blood isolate. *emm*98.1, *emm* pattern D, encodes an inactivating point mutation in base number 1585 of the *covS* gene.	Maamary *et al.*, 2010; McKay *et al.*, 2004
NS88.2*rep*	NS88.2 derivative strain with the inactivating point mutation in *covS* repaired to restore *covRS* functionality	Maamary *et al.*, 2010
NS88.2*covS*	NS88.2*rep* derivative strain with *covS* reverse complemented by allelic exchange, re-inactivating *covS*	Maamary *et al.*, 2010
NS88.2 (eGFP)	NS88.2 derivative expressing eGFP via pDCerm	Ly *et al.*, 2014
NS88.2*rep* (eGFP)	NS88.2*rep* derivative expressing eGFP via pDCerm	This study
NS88.2Δ*sclA*	NS88.2 derivative with *sclA* replaced with *cat* via allelic exchange	This study
NS88.2Δ*gls24*	NS88.2 derivative with *gls24* replaced with *cat* via allelic exchange	This study
NS88.2Δ*sclA (*pDC-*sclA)*	NS88.2Δ*sclA* derivative with the *sclA* deficiency complemented via heterologous expression in pDCerm	This study
NS88.2Δ*gls24* (pDC-*gls24*)	NS88.2Δ*gls24* derivative with the *gls24* deficiency complemented via heterologous expression in pDCerm	This study
Escherichia coli		
JM109	*end*A1 *gln*V44 *thi*-1 *rel*A1 *gyr*A96 *rec*A1 mcrB$^+$ Δ(*lac-pro*AB) e14- [F' traD36 proAB$^+$ *lac*I^q lacZΔM15]	Lab stock
M15 (pREP4)	His-tagged protein expression strain	Lab stock
DH5α	F$^-$ *end*A1 *gln*V44 *thi*-1 recA1 *rel*A1 *gyr*A96 *deo*R *nup*G Φ80d*lac*ZΔM15 Δ(*lacZYA-argF*)U169 *hsd*R17(r_K^- m_K^+)	Lab stock
XL10-Gold Kan^r ultra-competent cells	Tet^r Δ(*mcrA*)*183* Δ(*mcrCB-hsdSMR-mrr*)*173 endA1 supE44 thi-1 recA1 gyrA96 relA1 lac* Hte [F´ *proAB lac*IqZΔ*M15* Tn*10* (Tet^r) Tn5 (Kan^r) Amy]	Agilent, USA
TOP10 chemically competent cells	F- *mcr*A Δ(*mrr-hsd*RMS-*mcr*BC) Φ80*lac*ZΔM15 Δ*lac*X74 *rec*A1 *ara*D139 Δ(*araleu*) 7697 *gal*U *gal*K *rps*L (Str^R) *end*A1 *nup*G	Invitrogen, USA
Plasmids		
pPCR-Script	Ap^r, pUC origin, *lac* promoter, *lacZ*', T7 promoter,	Agilent, USA
pQE-30	Ap^r, ColE1 origin, 6xHis affinity tag, T5 promoter, t_0 and T1 transcriptional terminators	Qiagen, USA
pCR2.1-TOPO	Ap^r, Km^r, pUC origin, *lac* promoter, *lacZα*, T7 transcription promoter site.	Qiagen, USA
pDCerm	Erm^r, *phoZ*, gram-positive origin of replication	Jeng *et al.* 2003
pHY304-LIC	Erm^r, Cm^r, temperature sensitive replication protein *repB*, *ccdB* encoded toxin	Cook *et al.* 2012
pHSG398	Cm^r, *lac*Z	Takeshita *et al.* 1987
pPCR-*gls24*	pPCR-Script derivative containing NS88.2 *gls24* coding sequence	This study
pQE-*gls24*	pQE-30 derivative containing NS88.2 *gls24* coding sequence	This study
pCR-*gls24*	pCR2.1 derivative containing NS88.2 *gls24* coding sequence	This study
pCR-*sclA*	pCR2.1 derivative containing NS88.2 *sclA* coding sequence	This study
pDC-*gls24*	pDCerm derivative containing NS88.2 *gls24* coding sequence	This study
pDC-*sclA*	pDCerm derivative containing NS88.2 *sclA* coding sequence	This study
pHY-Δ*gls24*	pHY304-LIC derivative containing a *cat* fusion with 250 bp NS88.2 *gls24* genomic flanking regions	This study
pHY-Δ*sclA*	pHY304-LIC derivative containing a *cat* fusion with 250 bp NS88.2 *sclA* genomic flanking regions	This study

2.2.2 Preparation of chemically-competent Escherichia coli

Single colonies of *E. coli* strains to be made competent were inoculated into 10 ml of LB, and cultured overnight at 37°C. Starter cultures were inoculated into 225 ml of TSS medium and grown to OD_{600}: 0.3. Cultures were then cooled on ice for 10 min, and centrifuged in pre-chilled sterile tubes (3000 *x g*, 10 min, 4°C). Excess media was decanted and cell pellets resuspended in 5 ml of TSS medium, of which 200 µl aliquots were snap frozen in liquid nitrogen and stored at -80°C.

2.2.3 Preparation of electro-competent GAS

Single colonies of *S. pyogenes* strains to be made competent were inoculated into 5 ml of THY, and cultured overnight at 37°C. Two millilitre volumes of overnight cultures were inoculated into pre-warmed 40 ml THY cultures and grown with gentle shaking to OD_{600}: ~0.25, after which cells were harvested by centrifugation (5000 *x g*, 10 min). Excess media was decanted and cell pellets resuspended in 5 ml of cold sterile 0.625 M sucrose. Cells were pelleted (5000 *x g*, 10 min) and the previous washing step repeated twice. Cell pellets were resuspended in 300 µl of cold sterile 0.625 M sucrose, and 50 µl aliquots used immediately for transformations.

2.2.4 Transformation of electro-competent bacteria

Electro-competent bacteria were electroporated using a Bio-Rad Gene Pulser (Bio-Rad, USA) according to the manufacturer's instructions. Electro-competent *E. coli* (2.2.1) were gently mixed on ice with approximately 10 ng of plasmid DNA and pulsed at 2.5 kV, 25 µFD and 200 Ω, prior to transferral to 500 µl of LB media and incubated at 30°C (pHY304-LIC based vectors) or 37°C (all other constructs) for 1 h with shaking before plating on selective LB media. Electro-competent GAS (2.2.3) were gently mixed on ice with 1-2 µg of plasmid DNA and pulsed at 2.5 kV, 25 µFD and 200 Ω, prior to resuspension in 500 µl of THY media containing 0.25 M sucrose and incubated at 30°C or 37°C for 2 h without shaking before plating on selective THYA media.

2.2.5 Transformation of chemically-competent Escherichia coli

Chemically competent *E. coli* (2.2.2) were transformed by heat shock. Frozen cell aliquots were slowly thawed on ice and incubated with DNA ligase reactions for 30 min. Cell were subsequently heat shocked at 42ºC for 3 min, prior to dilution in 500 µl of LB media and incubated at either 30ºC (pHY304-derived vectors) or 37ºC (all other vectors) for 1 h. Cells were then plated onto LB media supplemented with appropriate antibiotics to select transformant colonies.

2.3 DNA manipulations

2.3.1 Wizard Plus SV Genomic DNA extraction

GAS genomic DNA was prepared for routine PCR using a Wizard Plus SV Genomic DNA extraction kit (Promega, USA) according to the manufacturer's instructions. Single GAS colonies were inoculated into 1 ml cultures of THY media with overnight incubation at 37°C. Planktonic GAS cells were then collected (16,000 *x g*, 2 min) and supernatants discarded, prior to resuspension in 480 µl of 50 mM EDTA, with 10 mg/ml lysozyme added and samples incubated at 37°C for 60 min to promote bacterial cell lysis. Cell nuclei and debris were pelleted (16,000 *x g*, 2 min), supernatants discarded, and resulting pellets resuspended in 600 µl of nuclei lysis solution. Samples were incubated at 80°C for 5 min, and cooled to room temperature before 3 µl of RNase solution was added to lysates with mixing via inversion, prior to further incubation at 37°C for 60 min. A 200 µl volume of protein precipitation solution was added to the RNase-treated cell lysate, mixed vigorously for 20 s and incubated on ice for 5 min before centrifugation (16,000 *x g*, 3 min). Supernatants were transferred to clean 1.5 ml microcentrifuge tubes containing 600 µl of room temperature isopropanol and mixed via gentle inversion to precipitate purified genomic DNA. DNA was collected at 16,000 *x g* for 2 min, supernatants gently decanted, and DNA pellets washed with 600 µl of room temperature 70% ethanol. After washing, samples were centrifuged (16,000 *x g*, 2

min), excess ethanol aspirated, DNA pellets completely air dried and resuspended in 100 µl of DNA Rehydration Solution overnight at room temperature. Aliquots of each sample were taken and stored at -20°C.

2.3.2 Polymerase chain reaction (PCR) conditions

Amplification of *cat, gls24* and *sclA* coding sequences; and the flanking regions of each gene for cloning into sub-cloning and allelic exchange vectors was conducted using polymerase chain reaction (PCR). All PCRs were carried out using an Eppendorf Mastercycler thermal cycler (Eppendorf, Germany). PCRs for cloning were prepared in 0.2 ml PCR tubes with reaction mixtures consisting of: 2.5 U of *PfuUltra* II fusion Hotstart proof-reading DNA polymerase (Agilent, USA), 1X *PfuUltra* II reaction buffer (Agilent, USA), 250 µM of each dNTP, 1 µM forward primer, 1 µM reverse primer, 70 ng template DNA, with sterile Milli-Q water made up to a final volume of 20 µl. Routine PCR screening of *E. coli* and GAS transformants for cloning and allelic exchange mutagenesis was conducted with reaction mixtures consisting of: 2 U of Mango *Taq* polymerase (Bioline, Australia), 1X Mango *Taq* reaction buffer (Bioline, Australia), 250 µM of each dNTP, 1 µM forward primer, 1 µM reverse primer, 2 mM $MgCl_2$, and single bacterial colonies used as template DNA in 10 µl reactions. The thermocycling conditions for PCR were initiated with a denaturing step of 95°C for 2 min; followed by 30 cycles of 30 sec denaturation at 95°C, 30 sec annealing at 55-60°C (2-3°C below the minimum melting temperature for each primer pair) and 1 min 30 sec elongation at 72°C; with a final elongation step of 72°C for 3 min followed by a 4 °C hold cycle. Details of primer sequences used for all PCRs are given in Appendix B.

2.3.3 Wizard Plus SV Gel and PCR clean up purification

Excess nucleotides, primers and restriction enzymes from PCR reactions and restriction enzyme digestions were removed using a Wizard Plus SV Gel and PCR Clean-up system (Promega, USA) according to the manufacturer's instructions.

Agarose gel slices were mixed with membrane binding solution (10 µl to 10 mg agarose) and heated to 65°C for 10 min, or until dissolving of the gel slice occurred. PCR mixtures or molten gel slices mixed with an equal volume of membrane binding solution were added to SV Minicolumns, incubated at room temperature for 1 min and bound to column membranes by centrifugation (16,000 *x g*, 1 min). Flow-through was then discarded and Minicolumn membranes washed twice with 700 µl of membrane wash solution (16,000 *x g* for 1 min) and 500 µl of membrane wash solution (16,000 *x g*, 5 min). Minicolumns were transferred to fresh microcentrifuge tubes and membranes dried (16,000 x g, 2 min) prior to the addition of 30 µl of nuclease-free water and incubation at room temperature for 1 min. DNA was eluted via centrifugation (16,000 *x g*, 2 min) and DNA stored at -20°C.

2.3.4 pPCRScript cloning

Cloning of *gls24* into qQE-30 for recombinant protein expression and purification was facilitated via step-wise sub-cloning into pPCR-Script (Agilent, USA). Cloning into pPCR-Script was initiated by PCR amplification using the proof-reading polymerase *PfuUltra II* as described (2.3.2), after which PCR amplicons underwent blunt-end ligation. Amounts of PCR products to be used in ligation reactions was calculated according to the equation ng insert DNA = bp of insert DNA x 10 ng pPCR-Script/ 2961 bp pPCR-Script. Ligation mixtures therefore contained: 10 ng pPCR-Script, 1X pPCR-Script reaction buffer, 0.5 µl of 10 mM rATP, 1.5 ng of *gls24* blunt-ended PCR product, 1 µl of *Srf*I restriction enzyme, 1 µl T4 DNA ligase and distilled H_2O to a final volume of 10 µl. Ligation mixtures were mixed gently and incubated at room temperature for 1 h, followed by incubation at 65°C for 10 min and storage on ice. Following ligation, recombinant plasmid DNA was transformed into XL10-Gold ultra-competent cells. XL10-Gold cells were thawed on ice, prior to gently mixing 40 µl of competent cells with 1.6 µl β-mercaptoethanol. A 2 µl volume of each ligation reaction was then mixed with competent cell aliquots and incubated on ice for 30 min. Each transformation mixture

was heat pulsed in a 42°C water bath for 30 s, followed by incubation on ice for 2 min. Transformation mixtures were then resuspended in 450 µl of pre-warmed LB media and incubated at 37°C for 1 h with gentle shaking. Following incubation, cells were plated onto solid LB media containing 1% (v/v) X-gal-IPTG and 100 µg/ml ampicillin, and incubated overnight at 37°C. Resulting white transformant colonies were screened for the presence of insert DNA via alkaline lysis and agarose gel electrophoresis (Appendix C).

2.3.5 pCR2.1-TOPO cloning

Cloning of *gls24* and *sclA* into pDCerm for complementation of *gls24* and *sclA* deficient GAS was facilitated via step-wise sub-cloning into pCR2.1-TOPO vector (Invitrogen, USA). PCR amplification of *gls24* and *sclA* was conducted using *PfuUltra II* polymerase and specific primers (Appendix B), as previously described (2.3.2). Adenosine overhangs were added to the 3' ends of blunt-end PCR amplicons via treatment with 1 U of Taq polymerase at 72°C for 10 min. Cloning reactions were prepared with 0.5 - 4 µl of *Taq* treated PCR products, 1 µl of salt solution, 1 µl of pCR2.1-TOPO vector and dH_2O to 6 µl. Reaction mixtures were permitted to anneal for 30 min at room temperature, prior to transformation of TOP10 chemically competent cells (Invitrogen, USA). Two microlitre volumes of cloning reactions were added to 20 µl of chemically competent cells, and incubated on ice for 30 min prior to heat shock at 42°C for 30 s. Heat shocked cells were immediately transferred to ice, and diluted in 250 µl of SOC medium prior to incubation at 37°C for 1 h with agitation. Transformant *E. coli* were selected for on LB containing 100 µg/ml ampicillin overnight at 37°C, and resultant colonies containing the *gls24* or *sclA* insert were screened for by PCR and restriction enzyme digestion (Appendix C).

2.3.6 Restriction enzyme digestion

Sub-cloning vectors; pPCR-Script and pCR2.1-TOPO containing insert *gls24* and *sclA* genes, pQE-30 and pDCerm, were routinely subject to restriction enzyme digestion to obtain double-stranded insert DNA with complementary single stranded overhangs suitable for downstream ligation (Appendix C). Approximately 5 µg of pPCR-*gls24* and 3 µg pQE-30 were digested in reactions containing 10 U of *Sma*I, 10 U of *Pae*I restriction enzymes (Fermentas, Lithuania), in 1X Buffer B (Fermentas, Lithuania) with dH_2O to 30 µl at 30°C for 1 h, followed by 37°C for 1 h. Approximately 7 µg of pCR-*gls24*, pCR-*sclA* and pDCerm were digested in reactions containing 20 U of *Xba*I and 10 U of *Eco*RI restriction enzymes (Fermentas, Lithuania), in 2X Tango buffer (Fermentas, Lithuania) with dH_2O added to 30 µl and incubated at 37°C for 1 h. In restriction enzyme digests of cloning vectors (pQE-30 and pDCerm), 2 U of Fast AP Thermosensitive Alkaline Phosphatase (Fermentas, Lithuania) was added to dephosphorylate 3'-overhangs and prevent recircularisation during downstream ligation. All digests were performed with appropriate single enzyme controls, after which all reactions were heat inactivated at 75-85°C for 10 min as appropriate for each enzyme, and digested DNA purified by Wizard Plus SV gel purification as previously described (2.3.3).

2.3.7 Ligation conditions

Ligation of restriction enzyme digested inserts from sub-cloning vectors was conducted using T4 ligase. Optimal ligation efficiency was obtained using a 3:1 (insert:vector) molar ratio calculated from the equation ng insert DNA = (3/1)*[(bp of insert DNA x 70 ng vector DNA)/ bp of vector]. Ligation reactions therefore contained: 16-60 ng insert DNA, 70 ng vector DNA, 1X T4 ligation buffer, 5 U T4 ligase with dH_2O to 30 µl. Reactions were incubated overnight at approximately 13°C and used to transform chemically competent or electro-competent *E. coli* (2.2.4, 2.2.5).

2.3.8 Ligation independent cloning (LIC)

Cloning of the chloramphenicol acetyltransferase (*cat*) gene into pHY304-LIC for performing precise allelic exchange mutagenesis of *gls24* and *sclA* was accomplished via a Ligation Independent Cloning (LIC) strategy (Fig. 2.1). NS88.2 genomic DNA was used as the template for PCRs amplifying 250 bp regions directly upstream and downstream of *gls24* and *sclA*, with each homology fragment modified via primer 5' extensions to bear overlapping, complementary sequence to pHY304-LIC or *cat* (Appendix B). The *cat* gene was PCR amplified from pHSG398, and pHY304-LIC digested with the *Pme*I restriction enzyme. To enable DNA recombination, 200 ng of *Pme*I treated pHY304 LIC, *cat* gene and homology fragments were treated with T4 polymerase in the presence of a deoxynucleotide (dTTP for pHY304-LIC and *cat*, dATP for the homology fragments). T4 polymerase reaction mixtures contained: 200 ng of template DNA, 6 U of T4 polymerase (New England Biolabs, USA), 1X NEBuffer 2 (New England Biolabs, USA), 5 mM of either dTTP or dATP, 5 mM DTT, 1 mg/ml BSA and dH_2O to 20 µl. T4 polymerase treatment resulted in the generation of 15-16 bp single stranded overhangs at the end of each DNA fragment. The overhangs at the ends of the pHY304-LIC were complementary to the 5' overhang of the upstream homology fragment and 3' overhang of the downstream homology fragment. The overhangs of the *cat* gene were complementary to the 3' overhang of the upstream homology fragment and the 5' overhang of the downstream homology fragment. The DNA fragments were mixed on ice and allowed to anneal for 30 min, prior to transformation into chemically competent DH5α *E. coli* (2.2.5). The successful construction of each LIC vector was confirmed by alkaline lysis of transformants and sequencing analysis (Appendix C).

2.3.9 Plasmid extraction via alkaline lysis

E. coli transformant colonies were routinely screened for the presence of recombinant plasmid DNA via alkaline lysis. Transformants were re-streaked onto appropriate

selective LB media and incubated overnight at 37°C. A loopful of each transformant was resuspended in 200 µl of cold Solution 1 and incubated for 5 min at room temperature, followed by addition of 200 µl volume of fresh Solution 2, gentle mixing via inversion and incubation for 5 min on ice. A 200 µl volume of Solution 3 was then added, the samples mixed gently via inversion and incubated for a further 5 min on ice before pelleting precipitated protein (16,000 *x g*, 10 min). Supernatants containing plasmid DNA were carefully aspirated from each sample, added to 400 µl of room temperature isopropanol and incubated for 10 min at room temperature to precipitate DNA prior to centrifugation (16,000 *x g*, 5 min). DNA pellets were then washed with 1 ml of 70% ethanol (16,000 *x g*, 1 min) and the pellet air dried before resuspension in 40 µl of dH_2O and size separation via agarose gel electrophoresis.

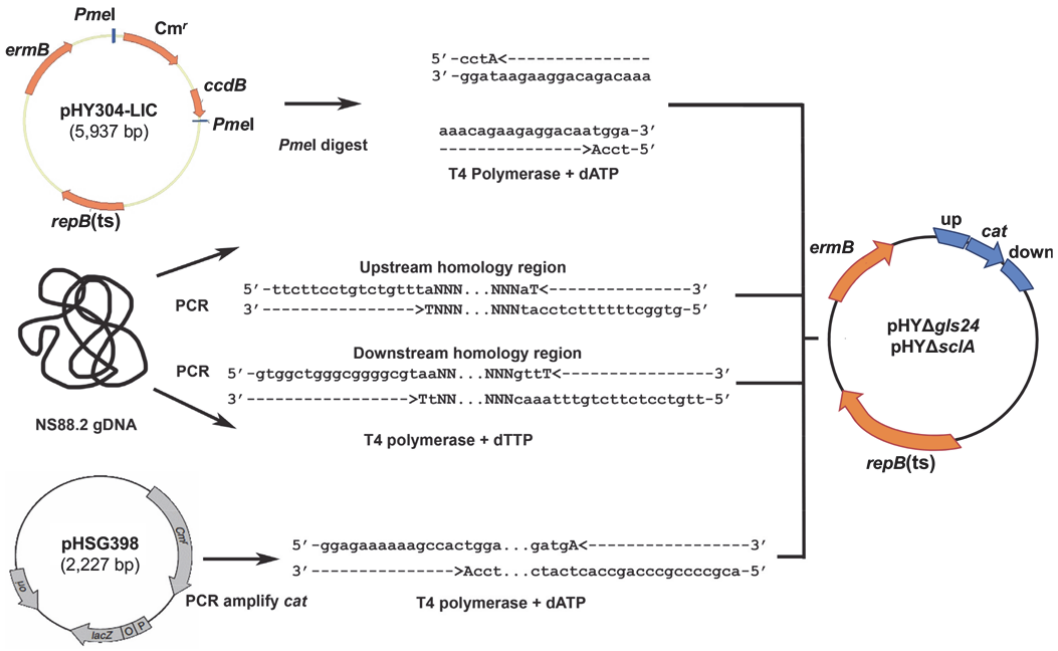

Fig. 2.1 Schematic of Ligation Independent Cloning (LIC) Strategy. pHY304-LIC based knock-out vectors for allelic exchange were generated via LIC. Upstream and downstream genomic regions flanking genes of interest and the *cat* gene were amplified by PCR from NS88.2 genomic DNA (gDNA) and pHSG398. These amplicons and *Pme*I restriction digested pHY304-LIC, were 3'-5' exonuclease treated using T4 polymerase, generating complementary single strand overhangs between pHY304-LIC vector, homology regions and the *cat* gene. These fragments were combined, permitted to anneal and transformed into chemically competent *E. coli*, generating intact vectors with in-frame gene fusions of the homology regions to *cat*.

2.3.10 Wizard Plus SV Mini-prep DNA purification

Plasmid DNA for use in restriction enzyme digestions, transformations and Sanger DNA sequencing reactions was prepared using a Wizard Plus SV Mini-prep DNA purification kit (Promega, USA) according to the manufacturer's instructions. Each strain undergoing plasmid extraction was struck out onto appropriate selective LB media overnight at 37°C. A loopful of each strain was then resuspended in 250 µl of cell resuspension solution with vigorous mixing. A 250 µl volume of cell lysis solution was added to each sample and mixed four times via inversion, prior to adding 10 µl of alkaline protease solution and mixing a further four times. Each sample was incubated for 5 min at room temperature prior to adding 350 µl of neutralisation solution and mixed four times via inversion. Cell lysates were cleared (16,000 *x g*, 10 min) and loaded into silicone membranes, prior to binding DNA to the membrane (16,000 *x g*, 1 min). Flowthrough from each sample was discarded and the membrane columns washed twice with 750 µl of column wash solution (16,000 *x g*, 1 min) and 250 µl of column wash solution (16,000 *x g* for 5 min). Spin columns were then transferred to fresh microcentrifuge tubes and dried (16,000 *x g*, 2 min), prior to transferral to a fresh microcentrifuge tube. A 50 µl volume of nuclease free H_2O was added to each spin column and incubated at room temperature for 1 min, followed by elution of bound plasmid DNA (16,000 *x g*, 2 min) and storage at -20°C.

2.3.11 Agarose gel electrophoresis

DNA samples were routinely size separated using 1% (w/v) agarose gels. DNA samples were mixed with one fifth volume of DNA loading dye prior to being deposited in each well. Agarose gels were electrophoresed using a Bio-Rad Power Pack (Bio-Rad, USA) at 100 V for approximately 1 h in 1X TAE buffer. Following agarose gel electrophoresis, agarose gels were stained in an excess volume of ethidium bromide staining solution for 20 min with gentle agitation. Once sufficiently stained, gels were destained in dH_2O for 5 min followed by visualisation using a UVP EC3 bioilluminator

with Gel HR/camera (UVP BioImaging Systems, USA). HyperLadder-1 (Bioline, USA) DNA molecular size markers were used to estimate DNA size.

2.3.12 Ethanol precipitation of DNA

Concentration of DNA samples or removal of excess dye terminators prior to Sanger capillary sequencing was conducted by ethanol precipitation. To each DNA sample, 2 M Sodium Citrate (pH 4.5) was added to a final concentration of 0.4 M. A 3.5 volume of 95% ethanol was subsequently added, samples inverted to mix and incubated on ice for 20 min. DNA was pelleted via centrifugation (16,000 *x g*, 20 min) and supernatant discarded. Each DNA pellet was then washed with 1 ml of 70% ethanol, centrifuged at 16,000 *x g* for 10 min and pellets air dried prior to resuspension in dH_2O or storage at -20°C.

2.3.13 Sanger DNA sequencing

Routine confirmation of correct insert sequence of sub-cloning, expression and allelic exchange vectors was conducted by chain terminating fluorescent dideoxynucleotide sequencing (Sanger method). Sequencing reactions were prepared on ice with 200-400 ng of plasmid DNA, 0.5 µl of BigDye v3.1 Ready Reaction Mix (Applied Biosystems, USA), 1X sequencing buffer (Applied Biosystems, USA), 3.2 pmol sequencing primer and dH_2O to 10 µl. Sequencing reactions were then subjected to a thermocycling program of an initial denaturation cycle of 96°C for 2 min; 25 cycles of denaturation at 96°C for 30 s, primer annealing at 50°C for 20 s and elongation at 60°C for 4 min; followed by a final extension cycle of 72°C for 1 min and a holding cycle of 4°C. Excess dye terminators were removed by ethanol precipitation as described previously (2.3.12) and reactions read via capillary electrophoresis using an Applied Biosystems 3130 Genetic Analyser (Applied Biosystems, USA). Electrophoragrams were read and initial base calls assigned using Applied Biosystems Analysis software

(Applied Biosystems, USA) with additional manual sequence curation and contig assembly using Geneious Pro Trial v5.6 (Biomatters, New Zealand).

2.4 Allelic exchange mutagenesis

Isogenic deletion of *gls24* and *sclA* from the NS88.2 genome was conducted via precise allelic exchange of a *cat* gene fusion with the upstream and downstream *gls24* and *sclA* homologous regions encoded in pHY-Δ*gls24* and pHY-Δ*sclA* (Appendix C). Electro-competent NS88.2 were transformed with 1 – 2 µg of allelic exchange vector DNA as described previously (2.2.4) and transformants selected for at 30°C to permit plasmid replication on THYA containing 2 µg/ml erythromycin (48 – 96 h incubation). GAS transformants were PCR screened for the presence of the *ermB* gene and inoculated into 3 ml liquid cultures of THY containing 2 µg/ml erythromycin overnight at 30°C. Post-incubation, cultures were diluted serially ten-fold onto THYA containing 2 µg/ml erythromycin and passaged overnight at the non-permissive plasmid replication temperature of 37°C to encourage plasmid integration into the chromosome. Putative GAS colonies with single cross-over allelic exchanges into the chromosome were cultured overnight at 30°C in THY to allow for plasmid disintegration from the chromosome, followed by serial dilution onto THYA in the absence of antibiotics and overnight passage at 37°C, encouraging both single and double cross-over homologous recombination events to occur. Single colonies from 37°C passages were picked using sterile toothpicks and patched onto two individual THYA plates with and without 2 µg/ml chloramphenicol. GAS colonies exhibiting chloramphenicol resistance were PCR screened for the presence of cat and absence of *ermB* and the gene of interest to confirm complete allelic exchange of *gls24* or *sclA* with *cat* (Appendix C).

2.5 Sodium dodecyl sulphate-polyacrylamide gel electrophoresis

Protein samples were routinely separated via sodium dodecyl sulphate-polyacrylamide gel electrophoresis (SDS-PAGE). Samples were prepared by mixing with one fifth

volume of protein cracking buffer and were boiled for 10 min to denature the proteins and reduce disulphide linkages. Samples were then analysed by SDS-PAGE using a PROTEAN Cell System (Bio-Rad, USA). Equivalent amounts of protein were loaded and separated on 12% acrylamide gels at 185 V for ~45 min using a PowerPac 300 supply unit (Bio-Rad, USA) in 1X SDS-PAGE running buffer. Molecular sizes of proteins were estimated using Unstained PageRuler Protein Ladder (Fermentas, Lithuania). Visualisation of protein bands was conducted after staining the gel with an excess volume of Coomassie Blue Rapid Stain overnight at room temperature with gentle agitation. Background staining of gels was then removed using an excess volume of Rapid Destain overnight with agitation and regular changing of destain solution. Destained gels were scanned using a GS-800 calibrated densitometer (Bio-Rad, USA).

2.6 Western transfer analysis

Detection of cleaved caspase-3 or actin in PMN lysates was conducted via transferral of lysate samples separated by SDS-PAGE to a nitrocellulose membrane, with subsequent chemiluminescent detection. Western transfers were routinely conducted using a Mini Trans-Blot apparatus (Bio-Rad, USA). Cassettes were set up as shown in Fig. 2.2, loaded into the gel tank, the tank filled with Western Transfer Buffer and proteins transferred at 100 V for 1 h at 4°C with constant stirring to ensure even buffer temperature and ion distribution. Post-transfer, membranes were blocked in PBST with 10% (w/v) skim milk powder (Difco, Australia) and incubated overnight at 4°C. Following blocking, membranes were washed twice for 5 min in PBST and probed using either mouse anti-caspase-3 antibody (Clone: 4-2-18, Biolegend, USA) diluted 1:1000 or polyclonal rabbit anti-actin antibodies (Sigma-Aldrich, USA) diluted 1:5000 in PBST with 1% (w/v) skim milk powder (Difco, Australia). Primary antibodies were incubated for 1 h with agitation at room temperature. Membranes were washed thrice for 5 min in PBST and bound primary antibodies probed using either goat anti-rabbit

IgG or goat anti-mouse IgG-horseradish peroxidise (HRP) conjugate antibodies (Bio-Rad, USA) diluted 1:1000 in PBST containing 1% (w/v) skim milk powder, followed by incubation for 1 h at room temperature. Excess secondary antibodies were washed from the membrane thrice for 5 min with PBST, followed by a subsequent 1 X PBS wash for 5 min. Bound antibodies were detected using Pierce SuperSignal West Pico Chemiluminescence substrate (Thermo Scientific, USA) and Amersham Hyperfilm (GE Healthcare, Sweden). Exposed X-ray films were scanned using a GS-800 calibrated densitometer (Bio-Rad, USA).

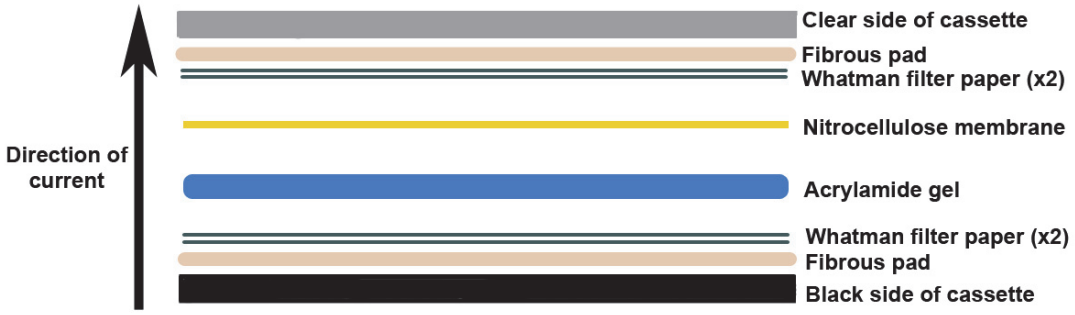

Fig. 2.2 Schematic of the apparatus for Western blotting. All components were pre-soaked in western transfer buffer prior to the loading of transfer apparatus. Transfers were conducted with current applied from the acrylamide gel to the nitrocellulose membrane resulting in the transfer of proteins to the membrane.

2.7 Protein purification

Recombinant His-tagged Gls24 protein was expressed within M15 (pREP4) *E. coli* and purified by Nickel ion affinity chromatography (Appendix C). Single *E. coli* colonies containing pQE-*gls24* were inoculated into shaking 100 ml overnight cultures of liquid LB media containing 100 µg/ml of ampicillin. The 100 ml culture was expanded to 1 L in prewarmed LB media containing 50 ug/ml of ampicillin, and cultured with shaking to OD_{600}: >0.6. Upon reaching optical density, protein expression was induced via the addition of 1 mM IPTG and 1 mM PMSF and cultures incubated for 4 h at 37°C with shaking. Post-induction, cultures were pelleted via centrifugation (4000 x *g*, 20 min, 4°C) and stored at -20°C. Native cell lysis was conducted via thawing of the cell pellet

on ice, followed by resuspension in 50 ml of ice cold native cell lysis buffer. Samples were then incubated on ice for 20 min and lysed by cycling the sample approximately 10 times at 140,000 kPa, with interspersed cooling on ice, using an Avestin EmulsiFlex-C5 Homogeniser (ATA Scientific, Australia). Complete solubilisation of protein was then encouraged via inverted mixing for 20 min at room temperature, followed by sedimentation of insoluble material via centrifugation (12,000 x *g*, 20 min, 4°C) and filtration of the cleared lysate through 0.44 µm pore size filtration units (Millipore, USA). Filtered cell lysate containing recombinant protein was bound to Ni-NTA resin via the addition of 2 ml 50% Ni-NTA resin in batch to lysate samples and subsequently mixed via inversion at 4°C for 1 h. Resin slurry was then recovered in a 10 ml column and the resin bed washed with 10 column volumes of native wash buffer, followed by elution in two 2 ml volumes of native elution buffer. Elution fractions containing purified His-tagged protein were pooled and dialysed thrice against 2 L of 1 X PBS over 48 h.

2.8 SpeB degradation assays

SpeB protease activity was assayed as described in (Cole *et al.*, 2006). Purified mature SpeB protease (5 µg, Toxin Technologies, Australia) was mixed with 5 µg of purified Gls24 or 25 µg of Casein (Sigma, USA), adjusted to a final volume of 25 µl with PBS and incubated at 37°C for 3 h. Proteolysis of casein and Gls24 was determined by SDS-PAGE analysis. Negative control assays containing casein, Gls24 or SpeB only were also included.

2.9 Isolation of GAS supernatant protein

Single GAS colonies were inoculated into 3 ml of THBY and grown overnight with parallel cultures containing 28 µM of cysteine protease inhibitor E64. Two millilitre aliquots of starter cultures were used to inoculate 100 ml of THBY (± E64) and grown overnight to early stationary phase (~20 h). Cultures were pelleted (5,400 x g, 15 min,

4°C) and filtered using 0.22 µm pore-size filter units (Millipore, Ireland). Supernatant proteins were precipitated via the addition of equal volumes of 10% trichloroacetic acid (TCA), followed by incubation on ice for 20 min and centrifugation (11,000 x *g*, 15 min). Supernatants were then discarded and protein pellets washed with an equal volume of 95% ethanol followed by centrifugation (11,000 x *g*, 5 min) and air drying. Protein pellets were resuspended in a 1 ml volume of 100 mM Tris base (pH 7.6) and transferred to fresh 2 ml microcentrifuge tubes, where supernatant proteins were TCA-precipitated as described above and resulting pellets stored at -20°C

2.10 Two-dimensional polyacrylamide gel electrophoresis (2D-PAGE)

GAS culture supernatant proteins were separated via two-dimensional-polyacrylamide gel electrophoresis (2D-PAGE) prior to mass spectrometry analysis. Supernatant protein samples were resuspended in 500 µl Standard Sample Solubilisation (SSS) buffer and sonicated at 14 W for 30 sec using a Microson ultrasonic liquid processor XL2000 (Misonix, USA) followed by 15 sec of vortexing to facilitate complete solubilisation of proteins. Sonication and vortexing steps were repeated a further three times, with unsolubilised proteins pelleted by centrifugation (16,000 x *g*, 15 min), and supernatants transferred to fresh 2 ml microcentrifuge tubes. Equal amounts of protein were expanded to 250 µl with SSS buffer, 2 µl quantities of bromophenol blue solution added to each sample, mixed thoroughly via gentle vortexing and pipetted along each lane of the reswelling tray. IPG strips (11 cm, pH 4-7, Bio-Rad, USA) were placed gel side down over each sample, and overlaid with 1 ml of paraffin oil to prevent matrix desiccation. Strips were then allowed to rehydrate overnight at room temperature, resulting in the uptake of supernatant proteins into the IPG gel matrices. Following rehydration, electrode wicks (four per IPG strip) were equilibrated in Milli-Q prior loading onto the electrodes of an isoelectric focussing (IEF) tray. Rehydrated IPG strips were placed gel side down over the wicks, overlayed with 1 ml of paraffin oil and focused using a Protean IEF Cell (Bio-Rad, USA) according to the following program:

100 V, 1 h; 300 V, 1 h; 600 V, 1 h; 1,000 V, 1 h; 2,000 V, 1 h; 4,000 V, 10 h with 100 V hold. IPG strips were removed from the IEF cell and incubated with 3 ml of equilibration buffer for 20 min with gentle rocking. Once equilibrated, strips were washed three times with 1 X SDS-PAGE running buffer, placed between the glass plates on top of 12.5% acrylamide gels and overlayed with 2 ml of molten 0.5% agarose in 1 X SDS-PAGE running buffer. Marker paper soaked with 10 µl of PageRuler Prestained protein ladder (Fermentas, Lithuania) was used as a molecular size marker. Gels were electrophoresed in 1 X SDS-PAGE running buffer using a PowerPac (Bio-Rad, USA) at 90 V for ~21 h and stained for 48 h in an excess volume of colloidal Coomassie stain, with destaining in colloidal Coomassie destain buffer.

2.11 Peptide mass fingerprinting analysis

To identify protein spots separated by 2D-PAGE, matrix-assisted laser desorption ionisation time-of-flight mass spectrometry (MALDI-TOF MS) and peptide mass fingerprinting (PMF) analyses were employed. 2D-PAGE gels were placed on a light box and the spots of interest excised using a 200 µl pipette tip. The pipette tip was rinsed thoroughly with 100% methanol between samples to prevent cross-contamination and the gel spots transferred to 96-well V-bottomed plates. Spots were destained by the addition of 100 µl of Coomassie blue destain Buffer with shaking for 1 h at room temperature. Excess destain buffer was aspirated and gel pieces dried via vacuum desiccation for 1.5 h. Proteins embedded in the gel were tryptically digested by overlaying each gel spot with 133 ng of sequencing grade modified trypsin (Promega, USA) and incubating the plate for 1 h at 4°C with gentle shaking. Excess trypsin was aspirated and discarded, followed by the release of digested peptides in 20 µl of 50 mM NH_4HCO_3 (pH 7.8) overnight at 37°C with gentle shaking. Shimadzu MALDI-TOF MS target plates were prepared by thorough rinsing with methanol and were air-dried prior to sample loading. Each sample well was thinly layered with mass spectrometry matrix by pipetting a 2 µl volume of matrix on and off the well. A 0.7 µl volume of

tryptically digested protein was then added and overlaid with 0.5 µl of mass spectrometry matrix containing 0.25 pM of MALDI-TOF calibration standards (Angiotensin, 1046.5423 Da; Pro_{14}-Arg, 1533.8582 Da; Adrenocorticotropic hormone fragment, 2465.1981 Da). Mass spectra were generated using an AXIMA Confidence MALDI-TOF MS (Shimadzu Biotech, USA). Spectra were analysed using Shimadzu Biotech Launchpad version 2.8.3 (Kratos Analytical Ltd, USA). The mass/charge peaks corresponding to tryptically digested proteins were used as the search query for interrogation of a custom Mascot database provided by the Australian Computational Proteomics Facility (http://www.apcf.edu.au). This database was constructed using a multiple-entry FASTA file of protein coding sequence exported from the NS88.2 genome draft subject to theoretical tryptic digestion, giving a indexed catalogue of mass/charge values for each protein (Chapter 3). Positive identification of proteins was based upon the highest number of experimental peptides from MALDI-TOF spectra correlating with peptide masses generated from theoretical tryptic digestion of translated GAS genomic data. As additional confirmation, mass spectral data was also searched using the public Mascot database available via Matrix Science (http://www.matrixscience.com). A minimum of two experimental peptide matches was required for positive identification of each protein. A representative MALDI-TOF spectrum and results from Matrix Science PMF are presented in Appendix D.

2.12 Whole blood growth kinetics

Estimation of GAS ability to survive and replicate in whole blood was conducted via the Lancefield method as described previously (Humtsoe *et al.*, 2005). Venous blood from healthy donors was collected and inoculated with a one-tenth volume of mid-logarithmic (OD_{600}: 0.4) phase GAS culture and incubated at 37°C for 3 h with gentle agitation on a rotating mixer. Fold growth was calculated as resultant CFU/ml after 3 h over initial CFU/ml. All individual assays were conducted in triplicate, with a minimum of 3 donors for calculation of growth kinetics for each strain assayed.

2.13 Hyaluronic acid capsule determination

Measurement of hyaluronic capsule production by the NS88.2 strains was conducted as previously described in (Schrager *et al.*, 1996). Two millilitre overnight GAS cultures were inoculated into 25 ml of THBY and grown to OD_{600}: 0.5. Ten millilitre volumes of mid-logarithmic phase cultures were sedimented (6000 x *g*, 10 min) and supernatants discarded prior to resuspension of GAS cell pellets in 500 µl sterile dH_2O. Determination of colony forming units (CFU) per ml was conducted by serial dilution of the GAS cell resuspension on THYA with subsequent overnight incubation. Hyaluronic acid capsule was released by shaking the remaining culture with 1 ml of chloroform for 5 min. Aqueous and organic solvent phases were separated by centrifugation (16,000 x *g*, 10 min) and the aqueous phase containing hyaluronic acid capsule harvested. Capsule extracts were serially-diluted in sterile dH_2O and stained using Stains-all solution, prior to spectrophotometric reading at A_{640} using a SpectraMax 250 microtitre plate reader (Molecular Devices, USA). Amounts of hyaluronic acid capsule were interpolated from a standard curve of hyaluronic acid standards against absorbance and the amount of hyaluronic acid of each strain expressed as femtograms per CFU (fg/CFU).

2.14 RNA extraction from GAS

RNA from mid-logarithmic phase GAS cultures in THY or blood were isolated using an RNeasy minikit (Qiagen, Germany) essentially as per the manufacturer's instructions. Single colonies of GAS were inoculated into 5 ml of THY media with subsequent overnight incubation at 37°C. One millilitre of starter cultures were used to subinoculate into 40 ml of THY and grown to OD_{600}: 0.4. Ten millilitres of GAS culture was pelleted via centrifugation (5000 *x g*, 10 min) and resuspended into 600 µl of RLT buffer containing β-mercaptoethanol for immediate RNA extraction. For RNA extracted from GAS blood cultures, 10 ml of mid-logarithmic phase GAS cultures were resuspended in 200 µl of sterile 1X PBS, inoculated into 1.8 ml of freshly drawn blood and incubated for

1 h at 37°C with gentle agitation. Blood cultures were hypotonically lysed using 40 ml of sterile Milli-Q and GAS harvested via centrifugation (7000 *x g*, 5 min) before being resuspended into 600 µl of RLT buffer containing 6 µl of β-mercaptoethanol. Bacteria from THY or blood cultures were homogenised using 0.1 mm silicon bead homogenisation vials shaken twice at 10 m/s for 45 s using a FastPrep-24 homogeniser (MP Biomedical, USA). Post-homogenisation, RNA samples were transferred to 1.5 ml microcentrifuge tubes containing 300 µl of 70% ethanol, mixed thoroughly and RNA bound to the membranes of RNeasy spin columns via centrifugation (14,000 *x g*, 15 s). Column membranes were washed with 350 µl volumes of RW1 buffer (14,000 *x g*, 15 s), flow through discarded and the RNA DNase treated on the RNeasy column with 10 µl of DNase I solution and 70 µl of RDD buffer for 15 min at room temperature. DNase protein was removed via washing with 350 µl of RW1 buffer via centrifugation (14,000 *x g*, 15 s). RNeasy spin columns were then washed twice with 500 µl of RPE buffer via centrifugation (14,000 *x g*, 15 s and 2 min) and a further time without buffer to eliminate ethanol carry-over (14,000 *x g*, 1 min). RNA samples were eluted from RNeasy columns using 40 µl of RNase-free water (14,000 *x g*, 2 min). Samples were then subjected to a second round of DNase treatment in solution using 2.5 µl of DNase I in 10 µl of RDD buffer diluted with 55 µl of RNase free water for 10 min at 22°C. Post-DNase treatment, RNA clean up was initiated by the addition of 350 µl of RLT buffer, followed by 250 µl of absolute ethanol and transferral of RNA samples to fresh RNeasy spin columns with RNA bound via subsequent centrifugation (14,000 *x g*, 15 s). RNeasy spin columns were then washed twice with 500 µl of RPE buffer via centrifugation as previously (14,000 *x g*, 15 s and 2 min) and a further time without buffer to eliminate ethanol carry-over (14,000 *x g*, 1 min). RNA samples were eluted from RNeasy columns using 40 µl of RNase-free water (14,000 *x g*, 2 min).

2.15 qPCR analysis of GAS gene expression

Purified GAS RNA was prepared for quantitative PCR analysis by conversion to cDNA using a Tetro cDNA Synthesis kit (Bioline, UK). cDNA synthesis reactions contained 1 - 2 µg of GAS RNA, 1X RT buffer, 1 µl random hexamer primers, 1 µl Ribosafe RNase inhibitor, 200 U Tetro Reverse Transcriptase, 0.5 mM dNTPs and DEPC-treated water to 20 µl. Reactions were incubated for 10 min at 25ºC, followed by 45ºC for 60 min and 85ºC for 10 min. NS88.2 transcripts were quantified by qPCR using a SensiFAST SYBR No-Rox kit (Bioline, UK). qPCR reactions contained 1X SensiFAST reaction buffer, 0.5 µM forward and reverse primers, 20 ng of reverse transcribed GAS total RNA and DEPC-treated water to 15 µl. Reactions were read on a LightCycler 480 instrument (Roche, Switzerland) using a 2-step thermocycling protocol of 95ºC for 2 min, followed by 40 cycles of 95º for 5 s and 60ºC for 30 s. Melt curve analysis was performed following amplification of each sample to confirm generation of single amplicons via continuous fluorescent acquisition from 55ºC to 95ºC. The absence of contaminating chromosomal DNA in RNA samples was confirmed via standard PCR analysis of purified RNA samples. Fold changes in expression were normalised according to amplification efficiency for each gene as described (Pfaffl, 2001), and to the house-keeping gene *proS*, the expression of which does not vary with *covS* mutation or growth cycle (Graham *et al.*, 2002). Primer sequences for each gene analysed are listed in Appendix B. Representative melt curves and efficiency calculations for each primer are shown in Appendix E.

2.16 Human polymorphonuclear leukocyte assays

2.16.1 Ethics statement

Permission to collect human blood under informed consent was approved by the University of Wollongong Human Ethics Committee protocol number HE08/250.

2.16.2 Preparation of human polymorphonuclear leukocytes

Human PMNs were purified from peripheral venous blood for use in PMN killing assays and other PMN-GAS association assays. Volumes of PolyMorphPrep (Axis-Shield, Norway) equal to the volume of blood taken were brought to room temperature as 5 ml aliquots in 15 ml centrifuge tubes. Blood was taken via venepuncture from healthy consenting donors into sterile tubes containing sodium citrate to a final concentration of 10 μM or heparin coated silicon beads as an anti-coagulant. Drawn blood was allowed to cool to room temperature, 5 ml of blood overlaid onto 5 ml of PolyMorphPrep and centrifuged at 500 *x g* for 30 min at room temperature without deceleration brakes applied. Cleared plasma was aspirated from each centrifuge tube and complement inactivated via heating at 55°C, incubation on ice for 30 min and centrifugation at 5000 *x g* to remove precipitate. Contaminating mononuclear leukocytes fractions from each centrifuge tube were removed via aspiration and the PMN fraction collected into a sterile 50 ml centrifuge tube. Isolated PMNs were equilibrated in 50 ml of sterile 1X PBS, pelleted (380 *x g*, 10 min) and the supernatant gently decanted. Contaminating erythrocytes in the PMN fraction were removed via hypotonic lysis in ~5 ml of sterile Milli-Q water for approximately 20 s prior to restoration of isomolarity via addition of 45 ml of sterile 1X PBS. PMNs were pelleted (380 *x g*, 10 min) and the supernatant decanted to remove lysed cellular debris. Isolated PMNs were resuspended in 0.5 ml of cold Rosewell Park Memorial Institute (RPMI) media supplemented with 2% heat-inactivated human plasma until use. Cell counts were performed with an equal volume of Trypan blue to ascertain viable cells (>99% for all experiments).

2.16.3 In vitro infection of human PMNs with GAS

GAS cultures were routinely prepared for *in vitro* human PMN infection via growth to mid-logarithmic phase (OD_{600}: 0.4), washing twice with sterile 1X PBS and dilution to the required inoculum in RPMI containing 2% heat-inactivated human plasma. Human PMNs were purified as described previously (2.16.1), seeded into the wells of either

tissue culture treated sterile 96-well (GAS killing, phagocytosis, cytotoxicity, ψ_M depolarisation assays) or 24-well plates (double immunofluorecence, TUNEL, microarray and western blot assays) (Greiner bio-one, Germany) and GAS added to the appropriate multiplicity of infection (MOI) (PMNs:GAS). PMNs were brought into close proximity with GAS via centrifugation (380 *x g,* 8 min, 4°C) prior to incubation at 37°C in 5% CO_2.

2.16.4 PMN bactericidal assay

Measurement of GAS resistance to PMN-mediated killing *in vitro* was conducted essentially as previously (Hollands *et al.*, 2008). *In vitro* infection of 2 x 10^5 PMNs with 2 x 10^4 GAS CFU was conducted as described above (2.16.2). After 30 min incubation, PMNs were hypotonically lysed and surviving GAS enumerated via serial dilution and overnight incubation on THYA. GAS survival was calculated as a percentage of GAS surviving following PMN incubation compared with growth controls incubated without PMNs.

2.16.5 Phagocytosis of GAS

To measure GAS uptake by PMNs, 5 x 10^5 PMNs were infected with 5 x 10^6 CFU of eGFP expressing GAS (2.16.2) and incubated for varying times (5, 40, 80, 120 min) or for 40 min at varying MOIs (1:5, 1:10, 1:20, 1:40). Post-incubation, assays were transferred to FACS tubes, resuspended in 1 ml PBS and pelleted (380 *x g*, 8 min, 4ºC), prior to resuspension in 500 µl 1X PBS containing 5 mM sodium azide and 5 mg/ml BSA. Association of GAS with PMNs was measured using an LSRII (BD Biosciences, USA) flow cytometer. A single gate was used to exclude debris, free GAS cells and isolate PMNs (Appendix F). Association of fluorescent GAS with PMNs was calculated as the percentage of PMNs with GAS eGFP fluorescence (510_20$^+$ population). The relative quantity of GAS associated with PMNs was estimated by the

mean fluorescence intensity (MFI) of eGFP positive PMNs. Data were analysed using Flowjo (Treestar, USA)

2.16.6 Double immunofluorescence microscopy

Visualisation of PMN phagocytosis of GAS was conducted by double immunofluorescence microscopy as described previously (Goldmann *et al.*, 2004). Sterile coverslips were prepared in 24 well tissue culture plates and covered with 200 µl 10% Poly-L-lysine solution for 30 min at 37°C. Post-incubation, excess Poly-L-lysine solution was aspirated and coverslips rinsed twice with sterile 1X PBS before being allowed to dry. 1 x 10^6 PMNs were purified as previously described, and infected with 1 x 10^7 CFU of GAS (2.16.2). Post-incubation, assays were fixed with 4% paraformaldehyde. Coverslips were then rinsed twice with 1X PBS, and non-specific antibody binding of GAS was blocked using 1X PBS with 10% FCS for 45 min at room temperature, and coverslips rinsed twice with 1X PBS. Extracellular GAS were labelled with polyclonal rabbit anti-GAS antiserum (kindly provided by M. Rohde) at a dilution of 1:300 in 1X PBS containing 10% FCS for 45 min at room temperature. After primary labelling, coverslips were rinsed twice with 1X PBS containing 10% FCS and goat anti-rabbit IgG Alexa 488 conjugate antibody (Dako, Denmark) diluted 1:300 in 1X PBS containing 10% FCS added for 45 min at room temperature. Coverslips were then rinsed twice with 1X PBS containing 10% FCS and PMN membranes permeabilised with 0.1% Triton-X 100 (v/v) in 1X PBS for 5 min at room temperature. Coverslips were then rinsed thrice with 1X PBS, and intracellular and extracellular GAS labelled with polyclonal rabbit anti-GAS antiserum at a dilution of 1:150 in 1X PBS containing 10% FCS for 45 min at room temperature. Coverslips were then rinsed twice with 1X PBS containing 10% FCS and secondary goat anti-rabbit IgG Alexa 568 conjugate (Dako, Denmark) added at a dilution of 1:400 in 1X PBS containing 10% FCS for 1 h at room temperature. Coverslips were then rinsed twice with 1X PBS. A 5 µl volume of Prolong Gold mounting medium (Invitrogen, USA) containing DAPI as a PMN nuclear

counterstain was used to mount coverslips, then sealed with nail polish and visualised using an Axio Observer inverted microscope (Zeiss microscopy, Germany).

2.16.7 Reactive oxygen species production

Kinetic measurement of PMN ROS production was conducted essentially as previously (Kobayashi *et al.*, 2003a). Purified PMNs were loaded with 25 μM of dichlorofluorescein (DCF, Molecular Probes) for 40 min in the dark at room temperature, prior to infection of 5 x 10^5 PMNs with 5 x 10^6 GAS CFU (2.16.2) in a black-walled microtitre plate. PMN ROS production was measured spectrophotometrically (λ_{ex}: 488 nm, λ_{emm}: 515 nm) at 37ºC using a POLARstar Omega fluorescent plate reader (BMG Labtech, USA).

2.16.8 GAS-induced cytotoxicity

PMN cytotoxicity was assessed essentially as previously (Goldmann *et al.*, 2009). Briefly, 2 x 10^5 PMNs were infected with 2 x 10^6 GAS CFU (2.16.2) and incubated for varying time points, following which 50 μl aliquots of cell supernatants were sampled and the lactate *D*-hydrogenase (LDH) concentration measured using the CytoTox 96 kit (Promega) according to the manufacturer's instructions. Cytotoxicity was calculated as LDH release induced by either GAS strain over maximum LDH release (total LDH from lysed uninfected cells) minus spontaneous release of LDH from uninfected cells.

2.16.9 Western blot of cleaved caspase-3

Caspase-3 cleavage was detected via western blotting of cell lysates from uninfected and GAS-infected PMNs. *In vitro* infection of 2 x 10^6 PMNs with 2 x 10^7 GAS CFU was conducted as previously (2.16.2). Western blotting of caspase-3 and actin protein was conducted as previously (2.6).

2.16.10 TUNEL staining of purified PMNs

Assessment of apoptosis induced nuclear DNA fragmentation was measured using the DEADend fluorometric TUNEL kit (Promega, USA) instructions for suspension cells. *In*

vitro infection of 2 x 10^6 PMNs with 2 x 10^7 GAS CFU was conducted as previously (2.16.2). Post-incubation, assays were transferred to FACS tubes, resuspended in 1 ml PBS with 1% BSA and pelleted (380 *x g*, 10 min). Supernatant was discarded, and cells fixed in 1 ml 4% paraformaldehyde for 30 min on ice. Cells were subsequently washed with 2 ml of PBS (380 *x g*, 10 min) and stored overnight in 2 ml 70% ethanol at -20ºC. After overnight incubation, cells were pelleted (380 *x g*, 10 min), ethanol aspirated and washed with 1 ml of PBS (380 *x g*, 10 min). Samples were then transferred to 1.5 ml centrifuge tubes, and incubated for 5 min in 80 µl equilibration buffer. Cells were pelleted (400 *x g*, 10 min), buffer aspirated and samples incubated in 50 µl incubation buffer containing fluorescein-conjugated nucleotide mix and deoxynucleotidyl transferase enzyme for 90 min at 37ºC in the dark. Reactions were stopped via the addition of 1 ml 20 mM EDTA and samples pelleted (400 *x g*, 10 min). Samples were then permeabilised using 1 ml 0.1% Triton-X 100 in PBS with 5 mg/ml BSA, pelleted (400 *x g*, 10 min) and finally resuspended in 0.5 ml PBS, transferred to FACS tubes and read using a LSRII flow cytometer (BD Bioscience, USA). A single gate was used to remove debris, and apoptotic cells with incorporated fluorescein (515_20^+) were quantified (Appendix F). Data were analysed using Flowjo (Treestar, USA)

2.16.11 Estimation of PMN mitochondrial membrane potential (Ψ_m)

Depolarisation of mitochondrial membranes of infected PMNs was estimated as previously (Goldmann *et al.*, 2009). Purified PMNs were loaded with 5 µM of 3,3'-Dihexyloxacarbocyanine [$DiOC_6(3)$] iodide for 20 min at room temperature prior to infection of 5 x 10^5 PMNs with 5 x 10^7 GAS CFU (2.16.2) for 2 h. Perturbation of Ψ_m was indicated as a loss of $DiOC_6(3)$ fluorescence (FL1 channel) compared to time 0 uninfected PMNs as determined using a FACSCalibur flow cytometer (Appendix F) (BD Bioscience, USA). Data were analysed using Flowjo (Treestar, USA)

2.17 Animal infection studies

2.17.1 Ethics statement

All animal use and procedures were approved by the University of Wollongong Animal Ethics Committee protocol numbers AE11/09 and AE12/05.

2.17.1 Subcutaneous GAS challenge

Subcutaneous GAS challenge of C57BL/6 mice has been described previously (Maamary *et al.*, 2010). Mid-logarithmic GAS cultures were prepared in cold sterile 0.7% (w/v) NaCl at an inoculum of 9 x 10^8 CFU/100 µl. For each strain, 10 gender matched C57BL/6 wild-type mice were prepared for infection via shaving and application of depilatory cream to the rear right flank. Mice were anaesthetised via isoflurane inhalation and GAS injections given in 100 µl subcutaneously to the shaven flank. Estimation of GAS virulence was determined by observation of mouse mortality over a 10-day period post-injection.

2.17.2 Intradermal phagocytosis of GAS and GAS survival

Estimation of GAS survival *in vivo* and GAS interaction with murine PMNs were conducted by the method of (Ly *et al.*, 2014). C57BL/6 mice were mice were prepared for infection via shaving and application of depilatory cream to the rear left and right flanks. Mice were then anaesthetised via isoflurane inhalation and 2 x 10^7 CFU of mid-logarithmic phase eGFP expressing GAS were injected intradermally into the shaven flanks prior to incubation for 6 h. Mice were subsequently euthanised via CO_2 asphyxiation and the sites of injection lavaged with two 1 ml quantities of sterile 0.7% saline. Lavage fluid was adjusted to a fixed volume and bacterial survival estimated via serial dilution of lavage fluid in dH_2O, plating out and enumeration of recovered bacteria after overnight incubation. Survival was calculated as [recovered GAS CFU/CFU of inoculum]*100%. Remaining lavage fluid was washed once with sterile PBS, labelled with 0.2 µg rat anti-mouse Ly6-G PE-conjugated IgG (clone: 1A8,

Biolegend, USA) for 20 min in the dark, and murine PMN (575_26^{+}) phagocytosis of GAS assessed as previously using a LSRII flow cytometer (Appendix F) (2.16.4). Data were analysed using Flowjo (Treestar, USA)

2.17.3 Immunohistochemistry and histology

Immunohistochemical determination of murine PMN apoptosis and inflammation was conducted via bilateral injection of 5 x 10^7 GAS CFU into the dermis of C57BL/6 mice as previously (2.17.2). Infected murine dermal tissue was harvested 24 h post-infection using a 12 mm biopsy punch and fixed in ice cold neutral buffered formalin for 3 h. Tissue processing was conducted using an ASP200 automated vacuum tissue processor (Leica, Germany) using the protocol listed in Table 2.2, and tissue biopsies embedded in paraffin using a EG1150 paraffin embedding station (Leica, Germany).

Table 2.2 Automated tissue processing protocol.

Solution	Time (h.min)	Temperature (ºC)
1. Formalin	00.05	37
2. 70% ethanol	00.10	37
3. 90% ethanol	00.10	37
4. 100% ethanol	00.20	37
5. 100% ethanol	00.20	37
6. 100% ethanol	00.30	37
7. 100% ethanol	00.45	37
8. Xylene	00.20	37
9. Xylene	00.30	37
10. Xylene	00.45	37
11. Paraffin	00.20	65
12. Paraffin	00.30	65
13. Paraffin	00.45	65

Paraffin embedded tissue blocks were sectioned (5 µm thickness) using a microtome (Leica, Germany). Sections were regressively haematoxylin and eosin (H&E) stained using the protocol listed in Table 2.3. Immunofluorescent identification of apoptotic murine cells was conducted by deparaffinising tissue sections with two xylene washes (5 min each), rehydrating sections using a graded series of ethanol (100%, 5 min; 100%, 95%, 85%, 70%, 50%, 3 min each) and washing in 0.85% NaCl (5 min).

Enzymatic antigen retrieval was conducted using 20 µg/ml proteinase K in PBS for 10 min at room temperature, followed by identification of apoptotic cells using the DEADend fluorometric TUNEL kit (Promega, USA) instructions for paraffin embedded tissues. Slides were covered with 100 µl of equilibration buffer for 10 min, followed by aspiration of equilibration buffer and treatment with 50 µl incubation buffer containing fluorescein-conjugated nucleotide mix and deoxynucleotidyl transferase enzyme for 60 min at 37ºC in the dark. Slides were washed in 2X SSC buffer (15 min), followed by washing twice in PBS (5 min each). Coverslips were then mounted on samples using Slowfade gold mounting medium (Invitrogen, USA) and sealed with nail polish. Analysis of cells was conducted using a TCS SP5 confocal microscope (Leica, Germany).

Table 2.3 Haematoxylin and eosin (H&E) staining protocol.

Solution	Time (min.s)
1. Xylene	1.30
2. Xylene	1.00
3. 100% ethanol	1.30
4. 100% ethanol	0.10
5. Water bath	1.00
6. Harris haematoxylin	2.00
7. Water bath	2.00
8. Acid alcohol	0.01
9. Water bath	1.00
10. Scotts blueing solution	1.00
11. Water bath	1.00
12. 1% aqueous eosin	0.20
13. 100% ethanol	1.00
14. 100% ethanol	0.45
15. Xylene	0.10
16. Xylene	1.00

CHAPTER 3: ASSEMBLY AND ANALYSIS OF THE NS88.2 DRAFT GENOME SEQUENCE

A part of this work has been published in *FASEB J.*

Reference:

James A. Tsatsaronis, Andrew Hollands, Jason N. Cole, Peter G. Maamary, Christine M. Gillen, Nouri L. Ben Zakour, Malak Kotb, Victor Nizet, Scott A. Beatson, Mark J. Walker, Martina L. Sanderson-Smith (2013). Streptococcal collagen-like protein A and general stress protein 24 are immuno-modulating virulence factors of group A Streptococcus. *FASEB J.* **7:** 2633-43.

3.1 Introduction

Recent increases in the incidences of life-threatening invasive GAS infections highlight the need to identify bacterial factors that explain this epidemic behaviour. Extensive research has focused on GAS serotypes associated with outbreaks in urbanised regions (Kansal *et al.*, 2010; Sumby *et al.*, 2005). In contrast, comparatively few studies have focused on disparate GAS strains originating from less developed areas. In many cases, rates of severe GAS diseases from these areas far exceed those observed in urban centres (Carapetis *et al.*, 1996). The diversity of GAS strains isolated from regions of endemic GAS disease also prompts greater interest into the mechanisms underlying this epidemiology.

Genomic sequencing and comparative bioinformatics has enabled high-throughput screening of M2, M4, M6, M12 and M28 GAS strains (Musser and Shelburne, 2009). These techniques have identified genetic features that distinguish virulent subclones of these strains from closely related, avirulent strains (Beres *et al.*, 2006; Green *et al.*, 2005). Such features, which include the acquisition of prophages, direct recombination of core chromosomal elements between GAS serotypes and from other streptococcal species, have bestowed recipient strains with enhanced virulence capacity or disease predilection (Green *et al.*, 2005; Sumby *et al.*, 2005). Currently, genomic research has

focused exclusively on GAS serotypes which are more prevalent in developed countries such as M1, M3, M12 and M28 (Musser and Shelburne, 2009). Whilst these serotypes are frequently isolated from severe infections in more developed regions, and/or are associated with distinct disease pathologies, the majority of GAS infections nonetheless occur in developing areas (Carapetis *et al.*, 2005). Furthermore, prior to 2010 no representative *emm*-pattern D GAS (skin tropic) isolate had undergone whole-genome sequencing (Musser and Shelburne, 2009; Smeesters *et al.*, 2010). Since then, only a single study has described whole-genomic analysis of an *emm*-pattern D isolate (Bessen *et al.*, 2011). This highlights the underrepresented nature of GAS strains from developing regions in genomic research.

Whole-genome shotgun sequencing, facilitated by next-generation sequencing (NGS) technologies, represents a viable method to use in the rapid and comprehensive genetic characterisation of candidate strains which display remarkable disease propensity. The clinical GAS isolate NS88.2 (*emm*98.1, *emm*-pattern D) is highly-encapsulated, acquires cell-surface plasmin activity, is resistant to killing by human neutrophils and is hypervirulent in a humanised plasminogen mouse model (Maamary *et al.*, 2010; Sanderson-Smith *et al.*, 2008). As such, NS88.2 exhibits a virulent phenotype suitable to use as a model strain for interrogative genomic analyses. As such, we utilised whole-genome shotgun sequencing and comparative bioinformatics to assist in identifying virulence factors that distinguish the neutrophil resistant GAS isolate NS88.2 from other GAS serotypes.

3.2 Results

3.2.1 Assembly of NS88.2 draft genome

Genomic sequence analysis of the NS88.2 strain was instigated via the generation of a genomic sequence draft. RNA-free, genomic NS88.2 DNA was isolated from overnight liquid culture; genomic fragment libraries constructed for whole-genome shotgun

sequencing at the Australian Genome Research Facility, and sequenced using a Genome Analyser II instrument (Illumina, USA). A total of 1,857,922 75-bp read pairs were generated, giving estimated genome coverage of approximately 75X, based upon an average genome size of 1.85 Mb according to other fully sequenced GAS.

To facilitate screening for potential NS88.2 virulence determinants and novel nucleotide sequence, read pairs were assembled *de novo* using Velvet 1.0.13, a de Brujin graph-based assembly algorithm designed for short-read sequences (Zerbino and Birney, 2008). Iterative refinement of the `-hash_length` argument (kmer value) was conducted, utilising genome draft length, contig n50 (a metric describing the length for which the collection of all contigs of that length or longer contains at least half of the sum of the lengths of the contigs), number of nodes (contigs) and maximum contig length as approximate indicators of assembly quality (Fig. 3.1). A kmer value of 31 was selected, as this value produced the longest relative genome and max contig length and a lower relative number of nodes (Fig. 3.1). As such the following Velveth command was used for sequence hashing.

```
./velveth NS882gen 31 -fastq -shortPaired -
NS882/s_1_1_sequence.txt NS882/s_1_2_sequence.txt
```

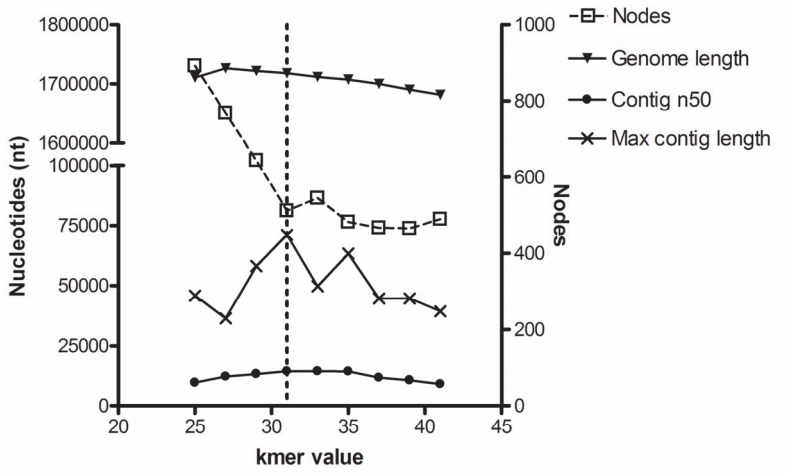

Fig 3.1 Optimisation of kmer value for velveth hashing of NS88.2 read pairs. Iterative refinement of the kmer value for velveth was conducted to optimise several draft genome parameters including number of nodes, genome length (nt), contig n50 (nt) and maximum contig length (nt). The optimum kmer value of 31 is indicated.

A similar approach was taken for de Brujin graph construction, error removal and repeat resolution, whereby iterative refinement of the `-cov_cutoff` argument was used to remove low coverage nodes after assembly (Fig 3.2). As such a `-cov_cutoff` value of 6 was chosen, resulting in the following command being used for the second step of *de novo* genome assembly.

```
./velvetg NS882gen -exp_cov 70 -read_trkg yes -cov_cutoff 6 -ins_length 300
```

Using this approach, a 1,731,197 bp genome draft of NS88.2 was generated, with 73-fold average sequence coverage over 482 nodes, an n50 score of 14,205 bp and max contig length of 63,219 bp. Nodes shorter than 100 bp were then manually removed from the draft to reduce background noise in later homology searches, resulting in a scaffold of 298 nodes over 1,727,974 bp.

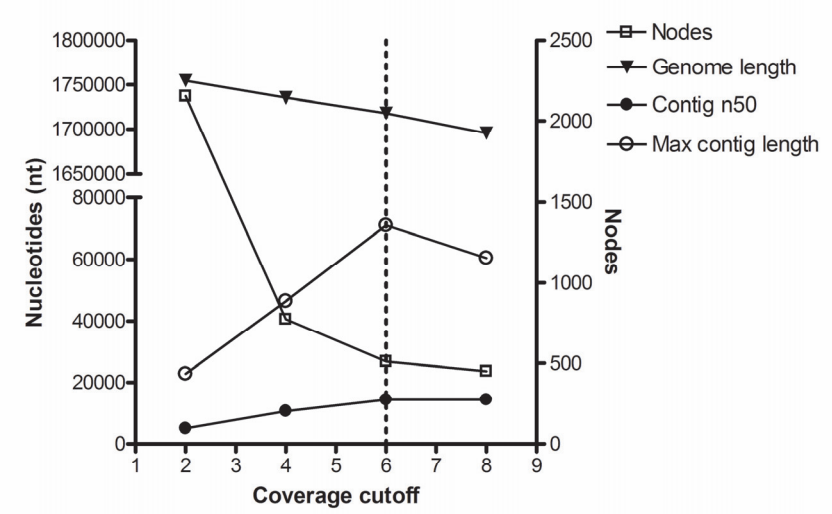

Fig. 3.2 Optimisation of coverage cutoff (-cov_cuttoff) for velvetg de Brujin graph generation, error removal and repeat resolution. Iterative refinement of the -cov_cutoff value for velvetg was conducted to optimise several draft genome parameters including number of nodes, genome length (nt), contig n50 (nt) and maximum contig length (nt). The optimum –cov_cutoff value of 6 is indicated.

The unordered scaffold was used to calculate genomic distances between the NS88.2 draft genome sequence and publically available fully sequenced genomes, as given by DNA maximal unique matches indices (MUMi) (Deloger *et al.*, 2009), calculated using

MUMmer3 (Kurtz *et al.*, 2004) (Table 3.1). The GAS genome with the lowest MUMi ratio (indicating closest sequence similarity), MGAS315 (accession number: NC_004070), was then used as the reference for reordering the nodes using the contig mover tool of Mauve (Darling *et al.*, 2004). These contigs were concatenated and submitted to the RAST server (http://rast.nmpdr.org) (Aziz *et al.*, 2008) for automated annotation, wherein open reading frames (ORFs) were called using the built in Glimmer3 algorithm (Delcher *et al.*, 2007), and putative protein function for each ORF assigned from FIGfam subsystem families (Meyer *et al.*, 2009). Manual curation and analysis of the draft genome was conducted using Artemis 12.0 (Rutherford *et al.*, 2000) and read coverage mapped using BAMview (Carver *et al.*, 2010).

Table 3.1 DNA maximal unique match indices (MUMi) calculated between the NS88.2 draft scaffold and fully sequenced GAS genomes.

Strain (**Serotype**)	Genbank Accession number	MUMi ratio
SF370 (**M1**)	NC_002737	0.2955
MGAS5005 (**M1**)	NC_007297	0.2960
MGAS10270 (**M2**)	NC_008022	0.3217
MGAS315 (**M3**)	NC_004070	0.2685
SSI-1 (**M3**)	NC_004606	0.2690
MGAS10750 (**M4**)	NC_008024	0.3201
MGAS10394 (**M6**)	NC_006086	0.3384
Manfredo (**M5**)	NC_009332	0.2870
MGAS2096 (**M12**)	NC_008023	0.3183
MGAS9469 (**M12**)	NC_008021	0.3052
MGAS8232 (**M18**)	NC_003485	0.3220
MGAS6180 (**M28**)	NC_007296	0.3005
NZ131 (**M49**)	NC_011375	0.3129

3.2.2 General features of the NS88.2 genome

The NS88.2 draft genome consists of a single circular chromosome with a sequence length of 1.7 Mbp, G +C content of 39.35% and estimated 1659 protein coding sequences (CDS), which account for 86.3% of the genome. The NS88.2 genome encodes many previously characterised virulence factors, including streptolysin O (*slo*), Mac-1-like protein (*mac*), SmeZ, cysteine protease SpeB and C5a peptidase (*scpA*), though not streptococcal inhibitor of complement nor serum opacity factor, as expected for an *emm* pattern D GAS isolate. Relatedness to other GAS was determined by multi-locus sequence typing (MLST). The NS88.2 glucokinase (*gki*), glutamine transporter protein (*glnQ*), glutamate racemase (*murI*), DNA mismatch repair protein (*mutS*), transketolase (*recP*), xanthine phosphoriboyl transferase (*xpt*) and acetyl-CaA acetyltransferase (*yiqL*) gene sequences were used to interrogate the MLST database (http://spyogenes.mlst.net). These sequence data gave the following sequence types: *gki*, 16; *glnQ*, 2; *murI*, 8; *mutS*, 3; *recP*, 2; *xpt*, 3, *yiqL*, 2; corresponding to a MLST sequence type (ST) of 205. The relative abundances of sequence types and connectedness of ST 205 to other GAS MLST types was then visualised using the eBURST v3 tool (http://eburst.mlst.net) (Fig. 3.3). A population snapshot representing all 602 known STs from 2343 typed isolates in the MLST database illustrates the disparate evolutionary pathways that GAS appears to have undergone, demonstrated by few single locus variations (SLV) which link separate ST clusters together (Fig. 3.3). ST205 is connected by a SLV in *gki* to ST340, a founder for a small cluster of STs primarily comprising *emm*53 GAS isolates.

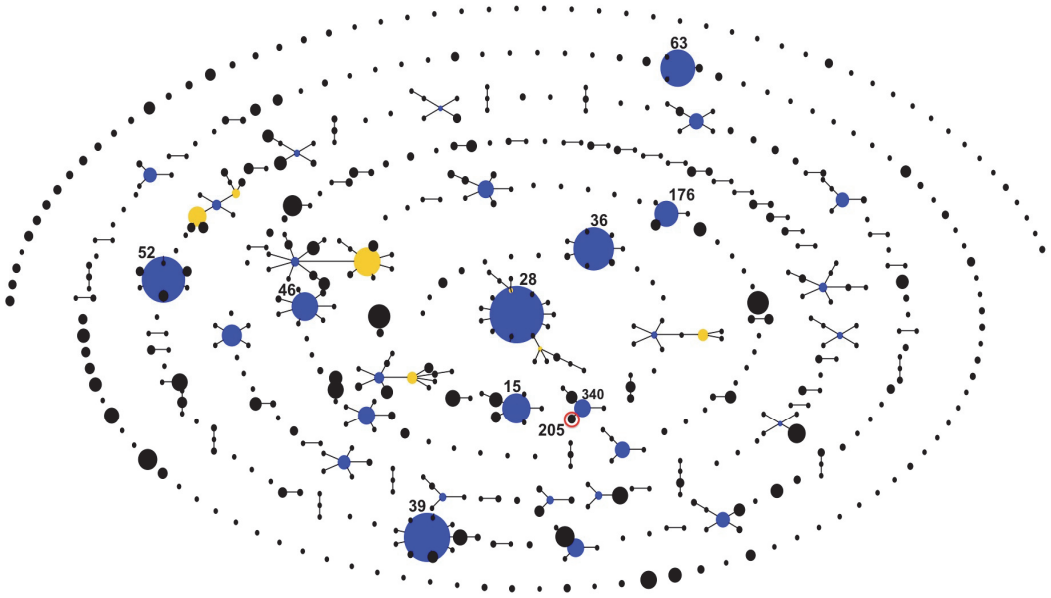

Fig. 3.3 Population snapshot of all 2343 GAS isolates in the MLST database. Each circle represents a single ST, with the relative abundance of each ST indicated by the size of each circle. Circles connected by lines are separated by a single variation in one of the seven loci used to group STs together. Blue circles represent putative founders for each cluster, with sub-founders coloured yellow. ST 205 (NS88.2 strain, indicated in red) and other STs representing clinically prevalent *emm*-types; 28 (*emm*1), 52 (*emm*28), 36 (*emm*12), 39 (*emm*4), 15 (*emm*3), 176 (*emm*58), 63 (*emm*77), 340 (*emm*53); are indicated.

3.2.3 BLAST comparison of NS88.2 to other fully sequenced GAS genomes

Identification of novel NS88.2 genomic sequence and genes was conducted by whole genome BLAST analysis and comparison to other fully sequenced GAS genomes using the BLAST Ring Image Generator (BRIG) (Fig. 3.4) (Alikhan *et al.*, 2011). The majority of genetic variation (nucleotide sequence identity <80%) was localised to a prophage-like region situated between base pairs 908,594 – 939,872. Closer inspection of the core NS88.2 genome (excluding exogenous prophage-like sequence) showed high similarity between NS88.2 and other GAS genomes, excepting the NS88.2 MGA and FCT loci. Manual curation of BLAST results identified several genes containing regions of variation with <80% sequence identity to all other fully sequenced GAS genomes, including streptococcal collagen-like protein A, streptococcal collagen-like protein B, M protein and extra-cellular protein factor (Appendix G).

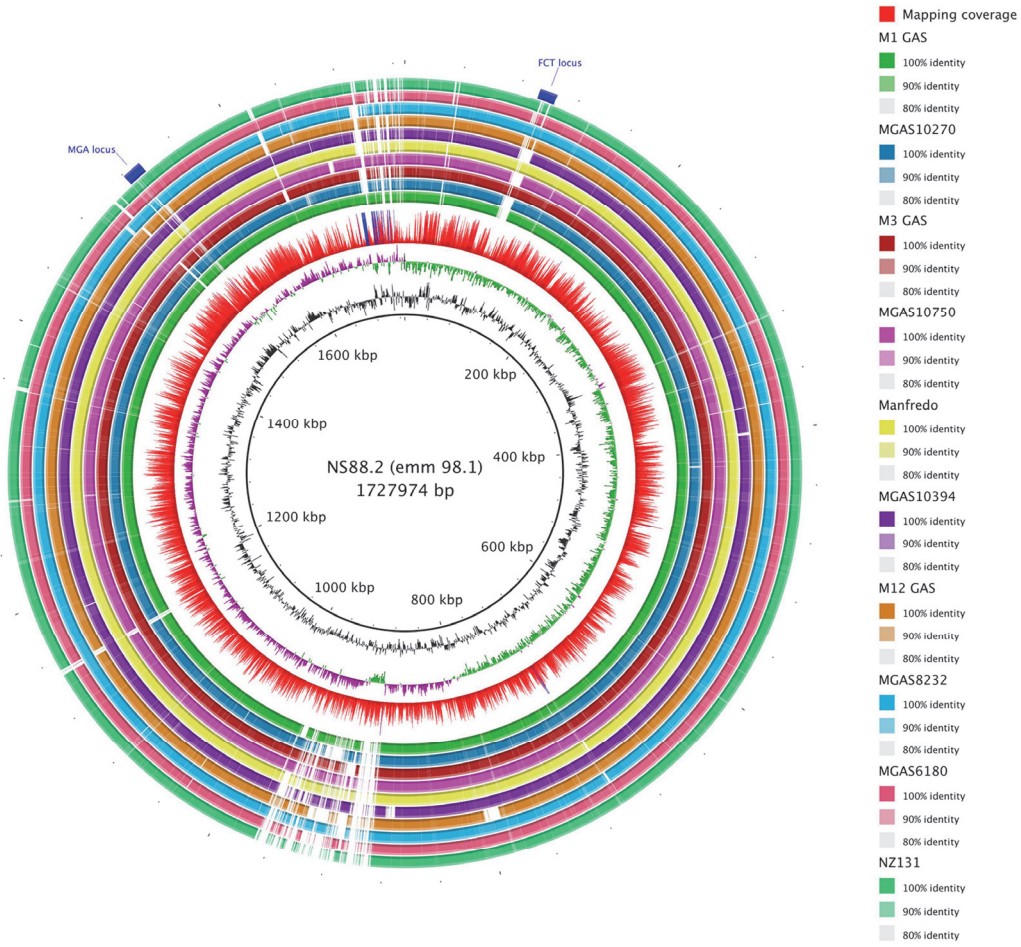

Fig. 3.4 Genome-wide BLAST comparison of the NS88.2 draft genome to publicly available fully sequenced GAS genomes. Rings are annotated from outermost to innermost. Location of the variable fibronectin-binding, collagen-binding, T antigen (FCT) locus and MGA regulatory region (ring 1). Coloured blocks denoting BLAST matches of 80% - 100% nucleotide identity between NS88.2 and query genomes (rings 2 - 11; Genbank accession numbers are indicated in parentheses): NZ131 (NC_011375), MGAS6180 (NC_007296), MGAS8232 (NC_003485), MGAS9469 (NC_008021) and MGAS2096 (NC_008023), MGAS10394 (NC_006086), Manfredo (NC_009332), MGAS10750 (NC_008024), SSI-1 (NC_004606) and MGAS315 (NC_004070), MGAS10270 (NC_008022), MGAS5005 (NC_007297) and SF370 (NC_002737). Mapping coverage, red bars denote <200 fold coverage, blue bars denote >200 fold coverage (ring 12). Guanine and cytosine deviation (ring 13). Percent guanine and cytosine content (ring 14). NS88.2 genome draft concatenated backbone in kilo base pairs (kbp, ring 15).

3.2.4 Comparison of the NS88.2 FCT and MGA loci

GAS genomes are known to contain a Fibrinogen, Collagen and T-antigen (FCT) locus that contains genes responsible for the assembly of a pilus structure (Mora *et al.*,

2005). GAS pili are responsible for adherence to the host cells and binding of host ECM components (Falugi *et al.*, 2008; Manetti *et al.*, 2007). Classification of the NS88.2 FCT locus by the previously established FCT typing scheme corresponds to FCT-3, which encode a collagen-binding protein Cpa and fibronectin-binding protein PrtF2 (Kratovac *et al.*, 2007). Comparison of the NS88.2 FCT sequence to other GAS was conducted via BLASTn analysis and visualised using EasyFIG (Sullivan *et al.*, 2011) (Figure 3.4A). As expected, the NS88.2 FCT locus showed the highest sequence identity with FCT-3 loci from other fully sequenced GAS strains (SSI-1, Manfredo, MGAS8232 and NZ131) and low identity to strains bearing FCT types 1 (MGAS10394), 2 (SF370), 4 (MGAS6180) and 5 (MGAS10750) (Fig. 3.5A). Two genes comprising the NS88.2 *cpa* and *fctA* also exhibited variability relative to other FCT type 3 GAS (SSI-1, Manfredo, MGAS8232 and NZ131) as has been previously described (Kratovac *et al.*, 2007).

GAS express multiple anti-phagocytic virulence factors, many of which are encoded within or regulated by the Multiple Gene regulator in group A Streptococci (MGA) locus (Hollingshead *et al.*, 1993). This region encodes the well-characterised M protein (*emm*), in addition to M-like proteins (*enn* and *mrp*) and C5a peptidase (*scpA*). As an *emm*-pattern D isolate, NS88.2 encodes both the plasminogen-binding M protein-like protein, Prp, and two M-family proteins, Enn and Mrp in the MGA regulon (McKay *et al.*, 2004). Comparison of the NS88.2 MGA region to other GAS was conducted by BLASTn analysis and visualised as previously (Fig. 3.4B). These data indicated high sequence identity between NS88.2 *scpA*, *mga*, *isp* and the *irk-irr* operon to other GAS, but limited homology between NS88.2 *emm*, and where present, *enn* and *mrp* in other GAS (Fig. 3.5B). These data support current understanding of the hypervariable nature of GAS M and M-like proteins.

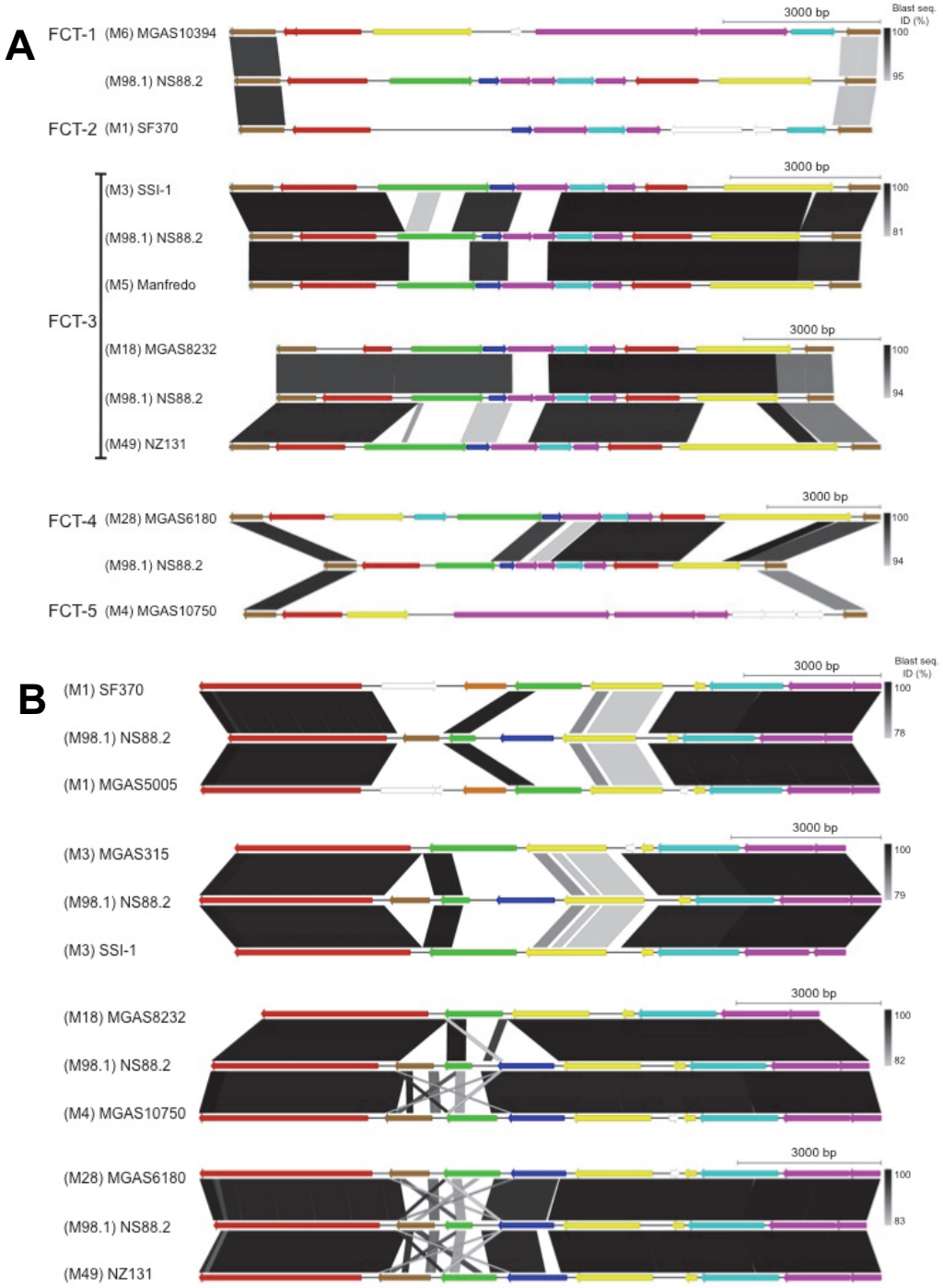

Fig. 3.5 Comparison of the NS88.2 FCT and MGA loci to other GAS strains. The NS88.2 FCT (**A**) and MGA (**B**) loci were compared with those of other GAS strains via BLASTn analysis and shaded by percent sequence identity. **A** Brown, *hsp33* and *M1_0136* FCT locus flanking genes; red, transcriptional regulators (*nra*, *rofA*, *msmR*); magenta, surface exposed proteins (*fctA*. *fctB*); yellow, genes encoding fibronectin binding proteins (*prtF1*, *prtF2*, *fbaB*); green, *cpa* collagen-binding protein; cyan, sortases (*srtC1*, *srtC2*, *srtB*); blue, *lepA* signal peptidase; white, other ORFs. **B** Red, *scpA* C5a peptidase; orange, *sic* streptococcal inhibitor of complement; cyan, *isp* immunogenic secreted protein; magenta, *irk-irr* two-component regulator; yellow, *mga* and *mga*-associated protein; green, *emm* streptococcal M protein; blue, *mrp* M protein-related protein; brown, *enn* M-like protein. Genes are displayed as 5'-3' left to right, with arrows indicating gene direction. Nucleotide scale bars are drawn to the sizes indicated in base pairs (bp) and BLASTn sequence identify (Blast seq. ID %) are shaded as indicated.

3.2.5 Analysis of NS88.2 prophage-like sequence

Bacterial outbreaks and variations in virulence capacity are often driven by lateral gene transfer of novel genes that bestow antibiotic resistance or additional survivability within the host. In GAS, the acquisition of exogenous DNA is primarily mediated via bacteriophages, which have been previously associated with GAS epidemics and acquisition of novel virulence factors, such as *sda1* in M1T1 GAS (Maamary *et al.*, 2012). The NS88.2 draft genome contains at least one lysogenised prophage-like element, with many contigs containing putative phage genes situated between base pairs 908,594 – 939,872. Manual interrogation of this region (Appendix G) identified the presence of a paratox (*prx*) gene in this region. Particular *prx* alleles have been previously shown to be genetically associated with specific phage-encoded toxins, such as *speA2* and *sda1* (Aziz *et al.*, 2005). Analysis of the genes flanking *prx* showed that a streptococcal pyrogenic exotoxin L (*speL*) is encoded adjacent to *prx*, which has been previously associated with M89 isolates and is reported to bind mammalian MHC class II molecules in a Zn-dependent manner (Proft *et al.*, 2003).

As an additional screen for the presence of known phage-encoded virulence factors unable to be assembled via the previously described pipeline, a read pair mapping approach was applied. This method involved construction of a pan-prophage sequence using the already defined prophage-like elements from fully sequenced GAS, and using Maq software (http://maq.sourceforge.net), mapped the original raw read pairs from NS88.2 Illumina sequencing to the concatenated phage sequence and visualised the stacked reads using BAMview. Manual interrogation of this sequence showed that mapped reads were primarily situated on nodes containing putative phage structural genes, phage integrases, AttL and AttR integration sites and the previously described *prx* and *speL* genes (Appendix G).

3.2.6 Secretion signal peptide and cell-surface anchor prediction

To identify genes encoding secreted proteins, protein coding sequences from NS88.2 were interrogated using the SignalP 4.1 algorithm (http://www.cbs.dtu.dk/services/SignalP/) (Bendtsen *et al.*, 2004) using the gram-positive bacteria option and default D-cutoff values. By this approach, 190 genes encoding proteins with putative secretion signal peptides were identified, including genes encoding previously characterised secreted virulence factors such as streptolysin O, streptolysin S and streptokinase (Appendix G). Cell-surface bound proteins were also bioinformatically predicted via the `hmmsearch` function of the hmmer3 package (http://hmmer.janelia.org/). Analysis using hidden Markov model for Gram-positive anchor motifs identified 10 genes encoding putative cell-surface anchored proteins, including NS88.2 M protein, M-like proteins and streptococcal collagen-like protein A (Appendix G).

3.3 Discussion

The methods by which bacterial phenotypes are analysed have evolved over the last decade to harness the technologies that are now available. Whole-genome shotgun sequencing offers a rapid and comprehensive approach to genetically screen bacteria, and characterise their evolution and acquisition of novel genetic content (Parkhill and Wren, 2011). More so, NGS technologies such as Illumina's sequencing by synthesis, 454 Life Science's pyrosequencing or Applied Biosystem's SOLiD sequencing method, produce a profusion of data that enables comprehensive, genomic based screening approaches to be undertaken (Metzker, 2010). In this study, we utilised Illumina based sequencing technology to assemble a draft genome sequence of the hypervirulent NS88.2 GAS isolate. The construction of this sequence permitted calculation of relatedness to other GAS, secreted and cell-surface protein prediction, in-depth analysis of prophage-like elements and whole genome sequence comparison between NS88.2 and other fully sequenced GAS.

Analysis of other fully sequenced GAS reveals that the GAS core genome (excluding all prophage-like material and other exogenous genetic elements) is highly conserved, whereas variation in these genetic elements may account for up to 10% of the genome (Musser and Shelburne, 2009). The source of this variation is primarily from the integration of prophage elements, which are responsible for intra- and inter-serotype circulation of GAS virulence factors (Aziz *et al.*, 2005; Beres *et al.*, 2002; Nakagawa *et al*., 2003). Analysis of NS88.2 prophage-like sequence did not elucidate any factors that have obvious roles in bestowing resistance to neutrophil killing. However, read coverage of this region was also lower than in more conserved areas, and a more targeted approach to sequencing and analysing NS88.2 prophage-like material may be necessary to fully deconvolute the number, position and content of NS88.2 prophages. Other individual, non-phage related genes in the NS88.2 genome also display divergence from other fully sequenced GAS (Fig. 3.5). Some of these genes, including *emm*, *mrp* and *enn*, encode proteins with secretion signal peptides, cell-wall surface anchors and have known anti-phagocytic roles in pathogenesis (Horstmann *et al.*, 1988; Podbielski *et al*., 1994), and support putative roles for other genes in mediating host-pathogen interactions.

Several recent studies have employed large scale, high-throughput sequencing to characterise GAS epidemics (Beres *et al*., 2010; Fittipaldi *et al*., 2012; Shea *et al*., 2011). Such analyses greatly enhance our knowledge of GAS genome biology, with the addition of 396 M3 genomes and 601 M59 genomes to genome databases (Fittipaldi *et al*., 2012; Shea *et al*., 2011). The ability to rapidly sequence and analyse epidemic strains (<10 days from strain isolation to full-genome sequencing), and comprehensively characterise their genetic makeup through comparative genomics and single nucleotide polymorphism (SNP) profiling, allows the precise evolution of epidemics to be traced (Fittipaldi *et al*., 2012; Maamary *et al*., 2012; Tse *et al*., 2012). These approaches can also be applied within smaller clinical scenarios to determine

causal bacterial clones, and thus make more informed inferences regarding sources of bacterial transmission within hospitals (Ben Zakour *et al.*, 2012; Walker and Beatson, 2012).

Full genome shotgun sequencing of NS88.2 will enable other systematic analyses of this isolate, to comprehensively define the complete genomic, transcriptional and proteomic factors which underlie the virulent and immuno-modulating qualities it exhibits.

CHAPTER 4: STREPTOCOCCAL COLLAGEN-LIKE PROTEIN A AND GENERAL STRESS PROTEIN 24 ARE IMMUNO-MODULATING VIRULENCE FACTORS OF GROUP A STREPTOCOCCUS

A major part of this work has been published in *FASEB J* and is formatted accordingly.

Reference:

James A. Tsatsaronis, Andrew Hollands, Jason N. Cole, Peter G. Maamary, Christine M. Gillen, Nouri L. Ben Zakour, Malak Kotb, Victor Nizet, Scott A. Beatson, Mark J. Walker, Martina L. Sanderson-Smith (2013). Streptococcal collagen-like protein A and general stress protein 24 are immuno-modulating virulence factors of group A Streptococcus. *FASEB J.* **7:** 2633-43.

4.1 Abstract

In Western countries, invasive infections caused by M1T1 serotype group A *Streptococcus* (GAS) are epidemiologically linked to mutations in the control of virulence regulatory two-component operon (*covRS*). In indigenous communities and developing countries, severe GAS disease is associated with genetically diverse non-M1T1 GAS serotypes. Hypervirulent M1T1 *covRS* mutant strains arise through selection by human polymorphonuclear cells for increased expression of GAS virulence factors such as the DNase Sda1, which promotes neutrophil resistance. The GAS bacteraemia isolate NS88.2 (*emm* 98.1), is a *covS* mutant that exhibits a hypervirulent phenotype and neutrophil resistance, yet lacks the phage-encoded Sda1. Here, we have employed a comprehensive systems biology approach to identify NS88.2 virulence determinants that enhance neutrophil resistance in the non-M1T1 GAS genetic background. Using this approach, we have identified streptococcal collagen-like protein A and general stress protein 24 proteins as NS88.2 determinants that contribute to survival in whole blood and neutrophil resistance in non-M1T1 GAS. This study has revealed new factors that contribute to GAS pathogenicity that may play important roles in resisting innate immune defences and the development of human invasive infections.

4.2 Introduction

Streptococcus pyogenes (group A *Streptococcus*, GAS) infection is responsible for human mortality and morbidity on a global scale. Severe disease pathologies caused by GAS include acute suppurative invasive conditions such as bacteraemia, streptococcal toxic shock-like syndrome (STSS), and necrotising fasciitis, as well as post-infectious immune-mediated sequelae in the form of acute rheumatic fever and glomerulonephritis (Cole *et al.*, 2011). Epidemiologically, severe GAS infections in developed countries are dominated by a handful of serotypes (Schwartz *et al.*, 1990). Notably, the well-characterised M1T1 GAS clone is frequently isolated from invasive infection (Chatellier *et al.*, 2000). A resurgence in the rates of severe GAS disease over the last three decades has been paralleled by the global emergence of clonal hypervirulent M1T1 and M3 isolates (Ikebe *et al.*, 2002; Sharkawy *et al.*, 2002). In contrast, diverse GAS serotypes are endemic in indigenous and developing communities, where no serotype predominates (Carapetis *et al.*, 1999). Necrotising fasciitis isolates from tropical northern Australia exhibit *emm* diversity, and serotypes that monopolise disease epidemiology in the Western hemisphere are seldom encountered (Hassell *et al.*, 2004). Thus isolates from indigenous and developing areas make ideal model organisms for the study of emergent, invasive GAS strains.

Multiple factors appear to underlie the pandemic spread of M1T1, including the recent acquisition of phage-encoded virulence factors that dampen innate immune responses (Aziz and Kotb, 2008; Sumby *et al.*, 2005). Bacteriophage-encoded deoxyribonuclease Sda1 enables M1T1 GAS to degrade neutrophil extracellular traps (NETs) (Buchanan *et al.*, 2006), and the transfer of Sda1 to M1T1 provides a selective trigger for acquiring mutations in the control of virulence *covRS* regulator (Walker *et al.*, 2007). Certain mutations of *covRS* result in the up-regulation of many GAS virulence factor genes including *sda1* and those encoding streptolysin O and hyaluronic acid capsule (Aziz *et al.*, 2010; Kansal *et al.*, 2010; Sumby *et al.*, 2006). Furthermore, expression of the

broad spectrum cysteine protease SpeB is also abrogated as a result of *covRS* mutation, preserving the integrity of many GAS virulence proteins (Aziz *et al.*, 2004b) and allowing the pathogen to acquire cell-surface plasmin activity capable of degrading fibrin clots which impede bacterial dissemination (Cole *et al.*, 2006). Thus, the *in vivo* selection for GAS *covRS* mutants by the host innate immune system inadvertently initiates a permanent genetic switch to a hypervirulent phenotype, capable of resisting neutrophil-mediated killing and subverting the host plasminogen activation system for systemic infection (Cole *et al.*, 2011).

The mechanisms coordinating the virulence of non-M1T1 GAS are less defined. It has recently been shown that mutation of *covRS* in a range of GAS M-types results in a genetic switch analogous to that seen in M1T1 (Maamary *et al.*, 2010), and that GAS of divergent M-types with mutations in *covRS* and/or the regulatory *ropB* gene are frequently isolated from STSS patients (Ikebe *et al.*, 2010). However, the mechanisms underlying the hypervirulent phenotype in the absence of the bacteriophage encoded DNase Sda1 are yet to be characterised. The clinical isolate NS88.2 (*emm*98.1) encodes a mutated *covS* gene, is highly-encapsulated, acquires cell-surface plasmin activity, is resistant to killing by human neutrophils and is hypervirulent in a humanised plasminogen mouse model (Maamary *et al.*, 2010; Sanderson-Smith *et al.*, 2008). Here, we apply a comprehensive systems biology approach to analyse this representative non-M1 isolate, in order to identify virulence determinants contributing to GAS neutrophil resistance, leading to invasive infection in the absence of *sda1*.

4.3 Materials and methods

4.3.1 Ethics statement

Permission to collect human blood under informed consent was approved by the UCSD Human Research Protections Program and the University of Wollongong Human Ethics Committee. All animal use and procedures were approved by the UCSD Institutional

Animal Care and Use Committee and the University of Wollongong Animal Ethics Committee.

4.3.2 Biofilm formation

Measurement of biofilm formation on polystyrene essentially as previously described (Hollands *et al.*, 2010). Briefly, 12 individual wells of a tissue culture treated 96-well microtitre plate were inoculated with 150 µl of overnight culture diluted 1:100 in THB and incubated for 24 h at 37°C. Plates were washed with sterile phosphate-buffered saline (PBS), and cells were fixed with 4% paraformaldehyde. Wells were stained with 0.2% crystal violet, extracted in ethanol/acetone (80:20), and assayed for crystal violet absorbance at 595 nm for biofilm quantification.

4.3.3 Epithelial cell adherence and invasion assay

Assays measuring the adherence of GAS to human keratinocyte cells (HaCaT) were performed as previously described (Hollands *et al.*, 2010). Mid-logarithmic phase GAS (2×10^6 CFU) were added to HaCaT cells (2×10^5 cells) in the wells of a 24 well plate, centrifuged for 10 min at 500 *x g* and incubated at 37°C in 5% CO_2. For adherence assays, plates were incubated for 30 min prior to washing with PBS with subsequent release and lysing of cells. Bacteria were serially diluted and plated on THYA for enumeration. For invasion assays, plates were incubated for 2 h. Plates were then washed as previously described and treated with gentamicin and penicillin G. Plates were then incubated for a further 2 h, prior to washing and treating as described above. Bacterial adherence and invasion was calculated as a percentage of the original inoculum. Statistical significance was determined using one-way ANOVA with the Tukey post-hoc test.

4.3.4 Murine skin adherence assay

Adherence of GAS to mice flank was assessed *in vivo* as previously conducted (Hollands *et al.*, 2010). Mid-logarithmic phase GAS culture (2×10^5 CFU) was spotted

onto THYA plates, air-dried and agar disks containing the bacteria excised using a biopsy punch. Bacterial agar disks were affixed to a total of 10 CD1 mice, each with 3 disks (one each of the wild type NS88.2, NS88.2*rep* and NS88.2*covS*). After 1 h, the mice were euthanised and skin under the bacterial disks was excised. Tissue was thoroughly washed with sterile PBS to remove non-adherent bacteria prior to homogenisation. Homogenate was serially diluted in sterile PBS and plated on THYA for enumeration. Bacterial adherence was calculated as a percentage of the original inoculum. Statistical significance was determined using one-way ANOVA with the Tukey post-hoc test.

4.3.5 Transcriptional Microarray

The oligonucleotide microarray used in this study and the method for *in vitro* transcriptional microarray has been described previously (Maamary *et al.*, 2010). Mid-logarithmic phase GAS cultures were grown in THBY and RNA extracted using the RNeasy Mini Kit (Qiagen, Germany). RNA was DNase-treated and converted to dendrimer-labeled cDNA using the Genisphere 3DNA Array 900MPX Kit according the manufacturer's guidelines. Dendrimer-labeled cDNA was hybridised to the array and labelled with Alexa Fluor 546 or Alexa Fluor 647. Sliders were scanned with a GenePix 4000B scanner (Molecular Devices, USA) and images processed using GenePixPro 4.0 software (Molecular Devices, USA). Transcriptional analyses were performed with GeneSpring GX 10 (Agilent, USA). All transcriptional microarray data were submitted to the NCBI Gene Expression Omnibus (GEO) according to the MIAME standards (GEO accession No. GSE23825).

4.3.6 NET Degradation

Visualisation of NET degradation was conducted as previously (Buchanan *et al.*, 2006). Human neutrophils were purified from venous blood using a PolyMorphPrep kit (Axis-Shield, Norway) as per the manufacturer's instructions and seeded at 2 x 10^5 cells per

well in 96-well plates. GAS were added to the wells at a multiplicity of infection of 1:100 (GAS:neutrophils) and Sytox Orange (Invitrogen, USA) added at a final concentration of 0.1 μM. Cells were visualised without fixation or washing using a Zeiss Axiovert 100 inverted microscope with appropriate fluorescent filters, and images captured with a CCD camera. For quantification, NETs were enumerated for each treatment by counting one transect after staining from 3 independent wells; a NET was defined as a discrete area of bright orange fluorescence larger than the size of a neutrophil. Statistical significance was determined using one-way ANOVA with the Tukey post-hoc test.

4.4 Results

4.4.1 Reduction of NS88.2 colonisation potential due to covS mutation

Similar to the globally disseminated M1T1 GAS, mutation of *covS* in non-M1T1 GAS results in a hypervirulent, neutrophil resistant phenotype (Maamary *et al.*, 2010). Such mutations in the M1T1 background have come with a potential fitness cost, as the *covS* mutant displays reduced capacity for biofilm formation and epithelial adherence and invasion (Hollands *et al.*, 2010). To determine whether this phenomenon occurred in the non-M1T1 background, clinical *covS* mutant GAS isolate NS88.2 (*emm*98.1) from a case of severe bacteraemia in Australia's Northern Territory (McKay *et al.*, 2004) was compared to isogenic derivative strains with the *covS* mutation repaired (NS88.2*rep*) and the *covS* regulator returned to non-functionality via reverse complementation (NS88.2*covS*) (Maamary *et al.*, 2010). Restoration of functional *covS* in NS88.2*rep* resulted in a significant increase in biofilm formation compared to the wild-type NS88.2 or the reverse complemented mutant NS88.2*covS*, which each express truncated CovS ($P < 0.001$) (Fig. 4.1A). A similar result was observed with respect to the ability of the NS88.2 strains to adhere to and invade epithelial cells. The intact *covS* NS88.2*rep* strain showed a significant increase in adherence to and invasion of the HaCaT

keratinocyte cell line over the *covS* mutant NS88.2 and NS88.2*covS* strains ($P < 0.001$) (Fig. 4.1B). This *in vitro* data was further corroborated by *in vivo* assays, as adhesion to live mouse skin was also compromised by *covS* mutation in NS88.2 and NS88.2*covS* ($P < 0.01$) (Fig. 4.1C).

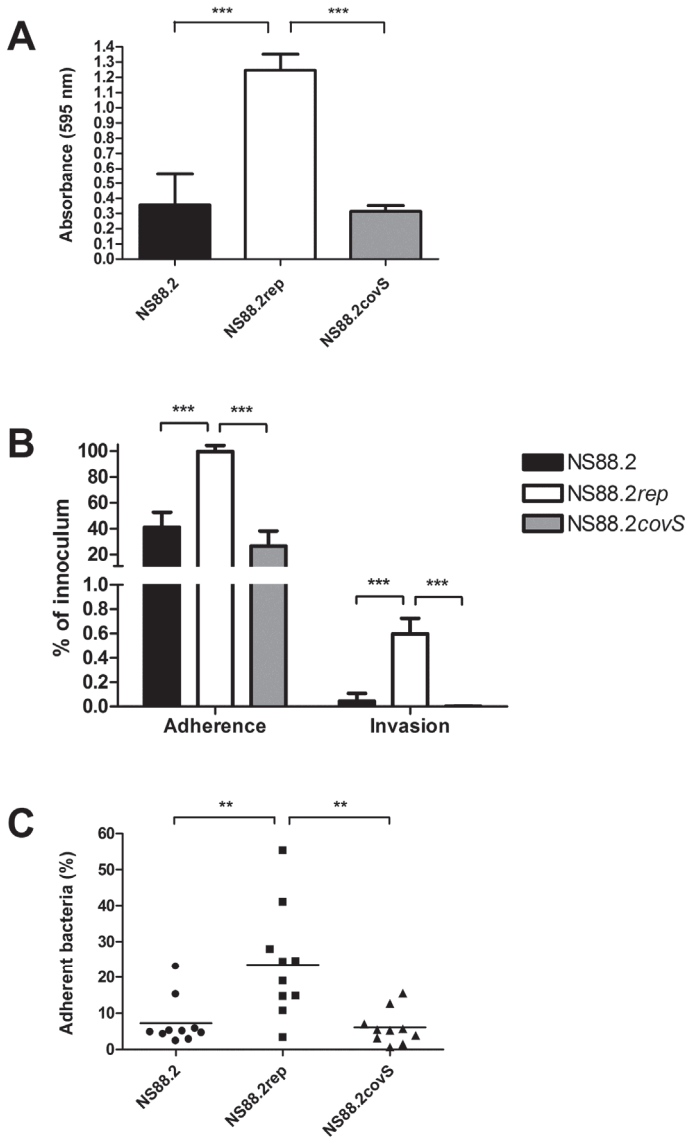

Fig. 4.1 Reduction of colonisation propensity due to *covS* inactivation in NS88.2. A Biofilm formation of *covS* inactive strains NS88.2 and NS88.2*covS* and *covS* intact strain NS88.2*rep*. **B** Adherence and invasion of HaCaT human keratinocytes by NS88.2, NS88.2*rep* and NS88.2*covS*. **C** Adherence of NS88.2, NS88.2*rep* and NS88.2*covS* to live mouse flanks. Panels B and C are expressed as a percentage of adherent/invasive bacteria of the original inoculum. Values shown for panels A and B are means ± standard deviations. *** indicates $P < 0.001$, ** indicates $P < 0.01$.

4.4.2 NS88.2 neutrophil resistance does not require neutrophil extracellular trap degradation

NS88.2 is highly resistant to neutrophil killing (Maamary *et al.*, 2010); however PCR and genomic screening indicates that NS88.2 does not contain the *sda1* gene (Chapter 3). The ability of NS88.2 and the isogenic *covS* derivative mutants NS88.2*rep* and complemented mutant NS88.2*covS* to degrade NETs was examined. We observed no significant differences in NET degradation between NS88.2, the NS88.2 derivative strains or 5448Δ*sda1*, an M1T1 GAS strain with *sda1* deleted via precise allelic exchange (Fig. 4.2). In contrast, the *covRS* mutant animal-passaged 5448AP strain exhibited significantly higher NET degradation in comparison to all of the NS88.2 strains and 5448Δ*sda1* ($P < 0.001$). We conclude that in the absence of Sda1, other virulence factors play a role in NS88.2 neutrophil resistance. To test this hypothesis, we undertook a systems biology approach to identify virulence determinants contributing to neutrophil resistance in this genetic background.

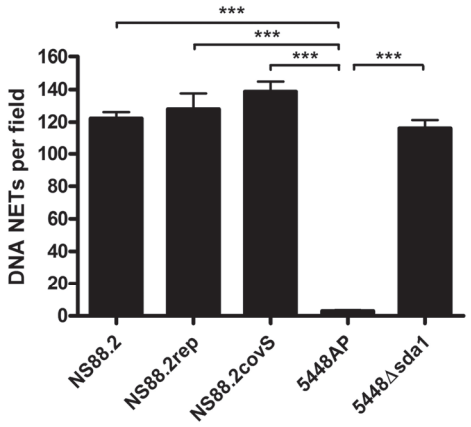

Fig. 4.2 GAS mediated degradation of extracellular neutrophil DNA NETs. NET degradation by GAS strains NS88.2, NS88.2*rep* and NS88.2*covS* and M1T1 GAS strains 5448AP (animal passaged 5448 encoding a truncated *covS* protein) and 5448Δ*sda1* (a 5448 derivative with *sda1* isogenically deleted). Values shown are means ± standard deviations. *** indicates $P < 0.001$.

4.4.3 Screening of the NS88.2 secretome

GAS secrete many proteins which play immune-modulating roles during infection. Screening of the NS88.2, NS88.2*rep* and NS88.2*covS* supernatant protein fractions was conducted via two-dimensional electrophoresis to experimentally confirm the surface exposure of putatively secreted proteins (Fig. 4.3). To analyse peptide mass fingerprinting data, we used CDS data from the NS88.2 draft genome sequence (Chapter 3), and formatted this information as a database which could be interrogated by the Mascot search engine (2.11) (Perkins *et al.*, 1999). Multiple putatively cytoplasmic proteins were detected in the supernatant, as has been noted previously (Lei *et al.*, 2000). Notably, of the 42 supernatant proteins identified (Table 4.1), SclA and general stress protein 24 (Gls24) were both found in the supernatants of NS88.2 and NS88.2*covS*, but not in NS88.2*rep*. As with M1T1 GAS (Aziz *et al.*, 2004b), expression of cysteine protease SpeB resulted in the degradation of much of the NS88.2*rep* secretome, including Gls24 and SclA, when grown in the absence of cysteine protease inhibitor E64 (data not shown).

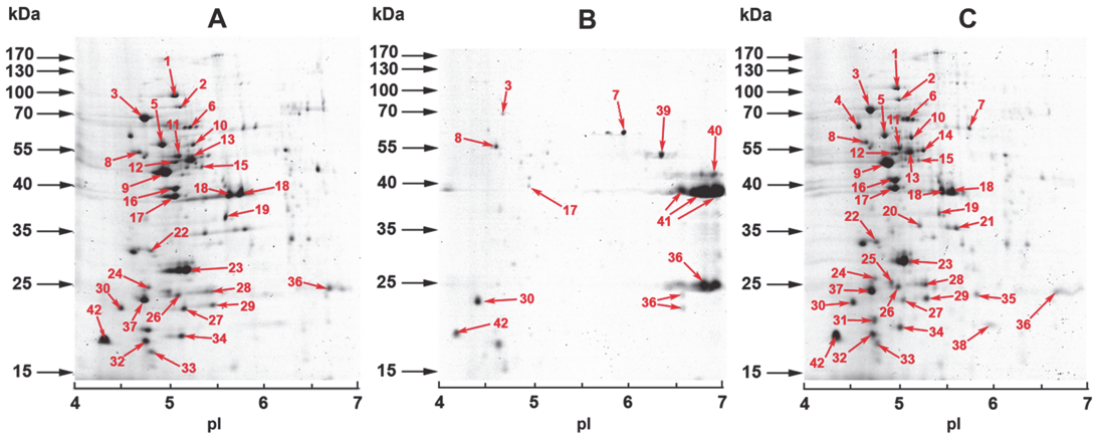

Fig. 4.3 Screening of the NS88.2 secretome. Secreted proteomic profiles of **A** NS88.2, **B** NS88.2*rep* and **C** NS88.2*covS*. Proteins identified via MALDI-TOF MS are indicated with numbered arrows (Table 4.1). Molecular masses of marker proteins (expressed as kilo Daltons, kDa) and approximate isoelectric point (pI) values of each gel are indicated. Results shown are representative of duplicate gels from two independent protein isolations.

Table 4.1 List of proteins identified in the supernatant of NS88.2, NS88.2rep and NS88.2covS.

	Protein	pI[a]	Size (kDa)	Peptide Match[b]	Coverage[c]
1	Translation elongation factor G	4.83	76.5	9	22
2	Transketolase	4.98	71.4	3	6
3	Chaperone protein DnaK	4.62	64.9	8	19
4	Cell division trigger factor	4.48	47.1	3	16
5	Heat shock protein 60 family chaperone GroEL	4.75	42.1	8	32
6	Collagen-like surface protein A	5.39	32.2	3	13
7	Immunogenic secreted protein	5.42	54.1	4	10
8	Group B streptococcal surface immunogenic protein	4.62	40.8	4	18
9	Enolase	4.80	47.3	12	41
10	Pyruvate kinase	4.96	54.5	10	24
11	Xaa-His dipeptidase	4.87	51.3	6	19
12	SSU ribosomal protein S1p	4.90	43.8	7	20
13	Translation elongation factor Tu	4.89	43.9	9	36
14	Non-phosphorylating glyceraldehyde-3-phosphate dehydrogenase	5.06	50.4	6	19
15	Arginine deiminase	4.99	46.3	6	18
16	Phosphoglycerate kinase	4.82	42.1	11	42
17	Translation elongation factor Ts	4.86	37.3	7	28
18	Glyceraldehyde-3-phosphate dehydrogenase (GAPDH)	5.34	35.9	5	15
19	L-lactate dehydrogenase	5.14	35.3	5	22
20	Phosphate acetyltransferase	4.85	35.9	4	15
21	6-phosphofructokinase	5.34	35.7	4	11
22	Manganese-dependent inorganic pyrophosphatase	4.47	33.9	4	20
23	Fructose-bisphosphate aldolase class II	4.98	31.2	5	32
24	Protein serine/threonine phosphatase PrpC	4.60	27	5	31
25	Adenylate kinase	4.74	23.7	4	29
26	Translation elongation factor P	4.85	20.4	4	27
27	Manganese superoxide dismutase	4.87	22.7	6	45
28	Phosphoglycerate mutase	5.10	26	7	41
29	Ribosomal subunit interface protein	4.45	21.1	4	34
30	Peptidoglycan hydrolase, Autolysin2	4.66	25.5	4	31
31	Alkyl hydroperoxide reductase protein C	4.65	20.5	3	22
32	Sortase A, LPXTG specific	9.17	27.7	5	18
33	Transcription elongation factor GreA	4.67	17.6	3	31
34	General stress protein, Gls24 family	4.93	12.6	5	50
35	Peptide deformylase	5.50	22.9	3	22
36	Streptodornase B; Mitogenic factor 1	8.61	28.7	6	33
37	Triosephosphate isomerase	4.57	26.6	6	33
38	Ribosome recycling factor	5.58	20.6	4	22
39	Streptokinase	5.58	50.2	9	28
40	Secreted antigen GbpB/SagA/PcsB, putative peptidoglycan hydrolase	8.42	42	3	15
41	Streptococcal pyrogenic exotoxin B (SpeB)	8.76	43.2	8	28
42	M1_SPy_1686	4.40	12.6	2	24

[a] Isoelectric point calculated using Expasy compute pI/Mw tool
[b] Number of tryptic peptides from mass spectrum matched to theoretical tryptic digest of protein sequence
[c] Percentage coverage of protein sequence covered by Peptide Matches

4.4.4 Expression of the NS88.2 transcriptome

The *covRS* operon has been shown to control ~10-15% of the GAS genome, including many genes which have proven or putative roles in host-pathogen interactions (Sumby *et al.*, 2006). We subjected the parental NS88.2 strain bearing a mutated *covS* gene and the derivative NS88.2*rep* with intact *covS* to transcriptional microarray analysis during mid-logarithmic phase growth (Appendix H). Comparison of the transcriptional profile of NS88.2 to NS88.2*rep* showed significant de-repression of many virulence genes associated with resistance to innate immune responses, including *emm*, *scpA*, *slo* and the hyaluronic acid capsule biosynthesis genes *hasA* and *hasB* (Fig. 4.4). The *sclA* gene was also found to be highly up-regulated in NS88.2 compared with NS88.2*rep*. A putative antibiotic resistance gene *norA*, and *speB* were found to be repressed in NS88.2 as a result of *covS* mutation, in accordance with previous studies (Maamary *et al.*, 2010; Sumby *et al.*, 2006).

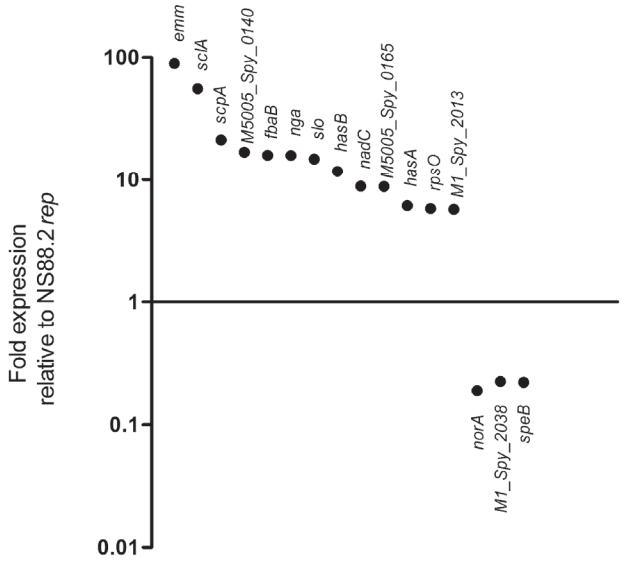

Fig. 4.4 Differential regulation of genes between the parental NS88.2 wild-type strain, which contains a *covS* inactivating mutation and derivative NS88.2*rep* which encodes a functional *covS* gene. Selected genes are significantly differentially expressed ($P < 0.05$).

To validate the microarray data, a panel of five genes was chosen for interrogation using quantitative real-time PCR analysis (Fig. 4.5A). The strong up-regulation of the *emm*, *sclA* and *hasA* genes, and down-regulation of *speB* in wild-type NS88.2 relative

to the NS88.2*rep* strain were found to be consistent with the microarray analysis. In addition, expression of the *gls24* gene was analysed and did not show significant differences in regulation between the two *covS* variants. However, 2D-PAGE data described previously (Fig. 4.5) and *in vitro* assays utilising purified Gls24 protein suggest that expression of Gls24 may be regulated at the protein level via SpeB-mediated degradation (Fig. 4.6). Exposure of GAS to whole blood is likely to play an important role in the regulation of GAS genes during infection, and gene expression levels were also investigated following 1 h incubation *in sanguis* (Fig. 4.5B). Transcripts were quantified relative to the *proS* housekeeping gene, and the relative transcript abundance between NS88.2 and NS88.2*rep* cultured in THY and cultured in blood was estimated. Growth of NS88.2 and NS88.2*rep* in blood resulted in a significant (P < 0.001) up-regulation of *gls24* expression relative to growth of the same strains in THY. Other NS88.2 genes (*sclA*, *emm*) also displayed increased expression in response to exposure to blood, whilst *speB* showed consistent down-regulation in response to growth in whole blood and *covS* mutation.

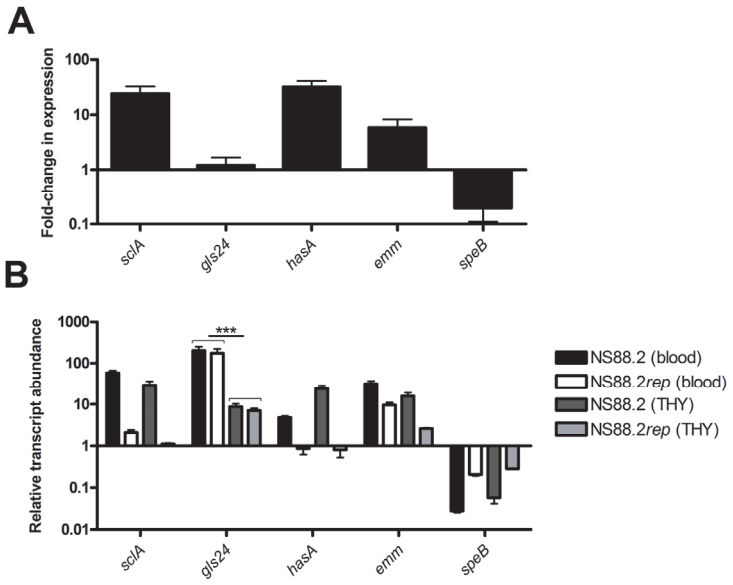

Fig. 4.5 *SclA* and *Gls24* are up-regulated in response to growth in whole blood. A Quantitative real-time PCR analysis of NS88.2 genes during mid-logarithmic phase growth. Fold-change in expression between NS88.2 relative to NS88.2*rep* is indicated. **B** Quantitative real-time PCR analysis of NS88.2 genes during mid-logarithmic phase growth in THY or after 1 h incubation in whole blood. Transcript abundance is expressed relative to the house-keeping gene *proS*. *** indicates P < 0.001.

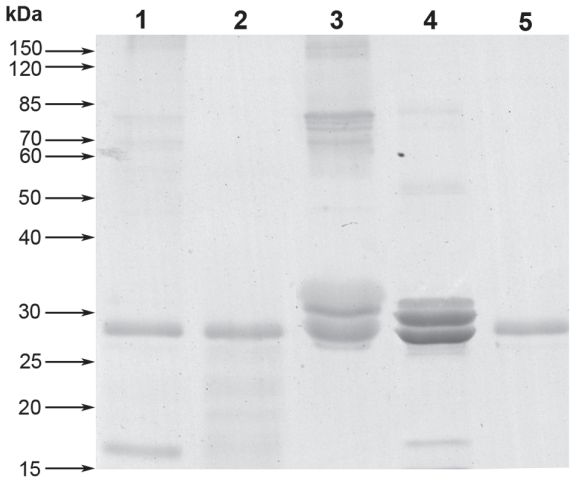

Fig. 4.6 Gls24 protein is degraded by GAS cysteine protease SpeB *in vitro*. Lane 1: SpeB and Casein; Lane 2: SpeB and Gls24; Lane 3: Casein; Lane 4: Gls24; Lane 5: SpeB. Molecular weight markers are given in kilo-Daltons (kDa).

4.4.5 SclA and Gls24 contribute to NS88.2 survival in whole blood and neutrophil resistance

Taken collectively, the presence of SclA and Gls24 in the NS88.2 secretome; up-regulation of *sclA* as a result of *covS* mutation; up-regulation of Gls24 after incubation in whole blood, the presence of secretion signal peptides in both proteins and their putative roles in virulence indicated these factors may function alone or in synergy as virulence determinants of NS88.2. SclA exhibits a variety of binding propensities including alternative complement factor H (FH) and FH-related protein 1 (Caswell *et al.*, 2008), thrombin-activatable fibrinolysis inhibitor (Pahlman *et al.*, 2007), low-density lipoproteins (Han *et al.*, 2006) and $\alpha_2\beta_1$ integrins (Humtsoe *et al.*, 2005). It has also been shown that SclA is expressed during human infection, and that SclA elicits a humoral immune response against the collagen-like region of this protein (Hoe *et al.*, 2007). Gls24 contributes to the virulence of *Enterococcus faecalis* in an endocarditis model and is involved in stress tolerance of that pathogen (Nannini *et al.*, 2005; Teng *et al.*, 2005). To assess the effect of these proteins on NS88.2 innate immune resistance, the *sclA* and *gls24* genes were isogenically deleted from the NS88.2 genome via precise allelic replacement with the *cat* gene (Appendix D).

Complementation of the *sclA* and *gls24* deficient strains was conducted via transformation with *sclA* or *gls24* expressing pDCerm variants (Appendix D).

The ability of NS88.2 and the *sclA* and *gls24* isogenic deletion mutants to replicate in whole blood was assessed via Lancefield bactericidal assays (Humtsoe *et al.*, 2005) (Fig. 4.7A-B). Deletion of either *sclA* or *gls24* significantly impaired the survival of the isogenic mutants in comparison to NS88.2 (NS88.2Δ*sclA*, $P < 0.001$; NS88.2Δ*gls24*, $P < 0.01$). Complementation of the *sclA* or *gls24* deletion via heterologous expression restored survival in whole blood to both isogenic mutants ($P > 0.05$) (Fig. 4.7A-B). These changes were resultant of the activity of SclA and Gls24 in whole blood, as the growth kinetics of the isogenic mutants and complemented strains in THY were unchanged relative to the wild-type NS88.2 (Fig. 4.8A). Further examination of the role of SclA and Gls24 in innate immune responses was studied via measurement of the NS88.2 strains resistance to neutrophil mediated killing (Fig. 4.7C-D). In comparison with the NS88.2 wild type, both NS88.2Δ*sclA* and NS88.2Δ*gls24* displayed significantly reduced neutrophil resistance ($P < 0.05$) whilst the complemented isogenic mutants exhibited neutrophil resistance equivalent to the wild-type ($P > 0.05$) (Fig. 4.7C-D). This difference in resistance to neutrophil killing was independent of capsule expression as the isogenic deletion mutations and complemented strains express equivalent amounts of hyaluronic acid (Fig. 4.8B).

4.5 Discussion

Genetic integrity of the two-component gene regulator *covRS* is a major determining factor of GAS virulence and colonisation. M1T1 GAS that bear the intact form of this operon are more highly suited to adherence and colonisation of host tissues (Hollands *et al.*, 2010). In this study we have characterised the *emm*98.1 invasive isolate NS88.2. Phenotypically, this isolate is hypervirulent and neutrophil resistant (Maamary *et al.*, 2010), whilst the *covS* intact derivative (NS88.2*rep*) is avirulent, and exhibits increased biofilm formation and adhesion to epithelial cells. However, NS88.2 does not contain

sda1 nor does it degrade neutrophil NETs, and so the mechanism of neutrophil resistance exhibited by NS88.2 is unaccounted for. Transcriptomic and proteomic data generated here demonstrates a cohort of immunomodulating virulence factors is up-regulated as a result of *covS* mutation in NS88.2, including the antiphagocytic M protein and SclA.

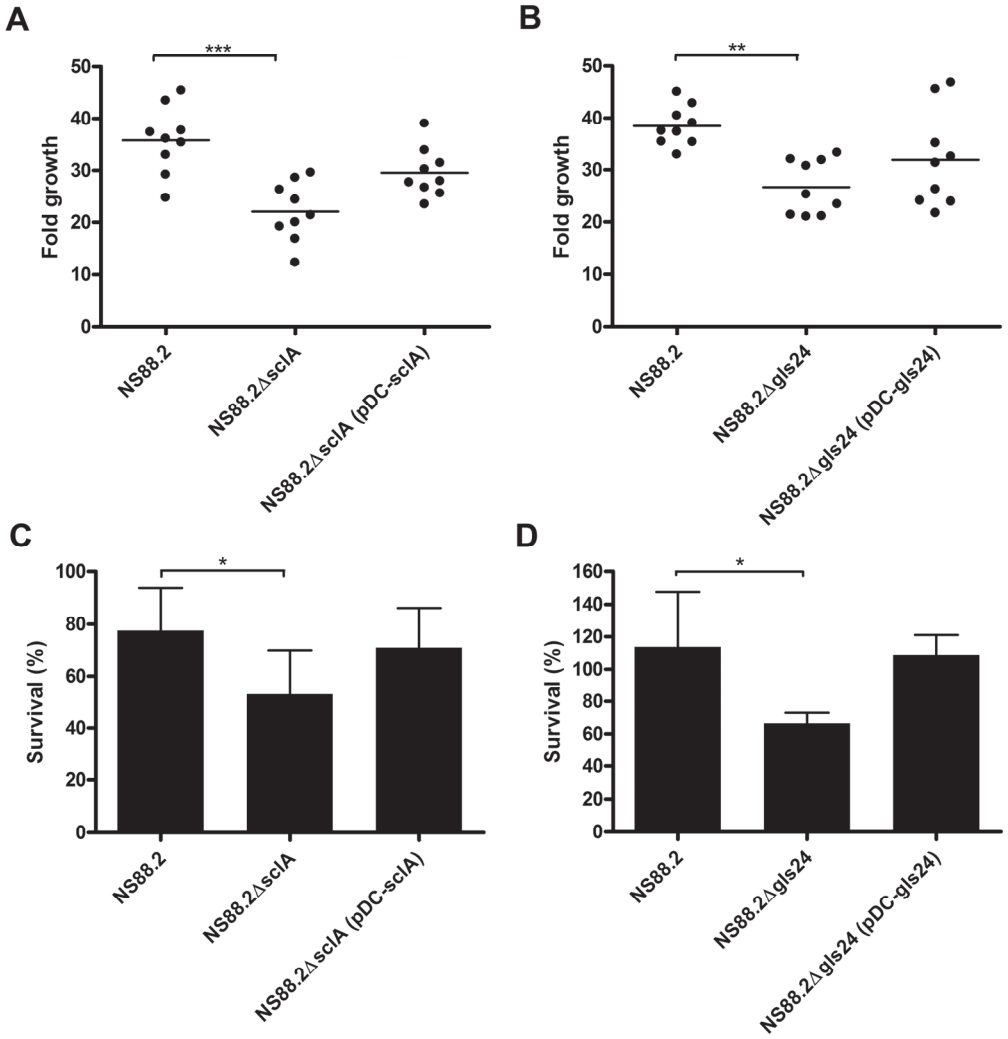

Fig. 4.7 Deletion of *sclA* or *gls24* impairs NS88.2 growth in whole blood and resistance to neutrophil-mediated killing. Fold growth of NS88.2, the *sclA* deficient mutant NS88.2Δ*sclA* and complemented derivative NS88.2Δ*sclA* (pDC-sclA) (**A**); the *gls24* deficient mutant NS88.2Δ*gls24* and complemented derivative NS88.2Δ*gls24* (pDC-gls24) (**B**) after 3 h incubation in human whole blood. Ability of NS88.2, NS88.2Δ*sclA*, NS88.2Δ*sclA* (pDC-sclA) (**C**), NS88.2Δ*gls24* and NS88.2Δ*gls24* (pDC-gls24) (**D**) to survive neutrophil-mediated killing following co-culture with purified human PMNs. All assays were performed with a minimum of 3 donors and all assays were conducted in triplicate. Values shown for all panels are means ± standard deviations of triplicate assays**.** *** indicates $P < 0.01$, ** indicates $P < 0.01$, * indicates $P < 0.05$.

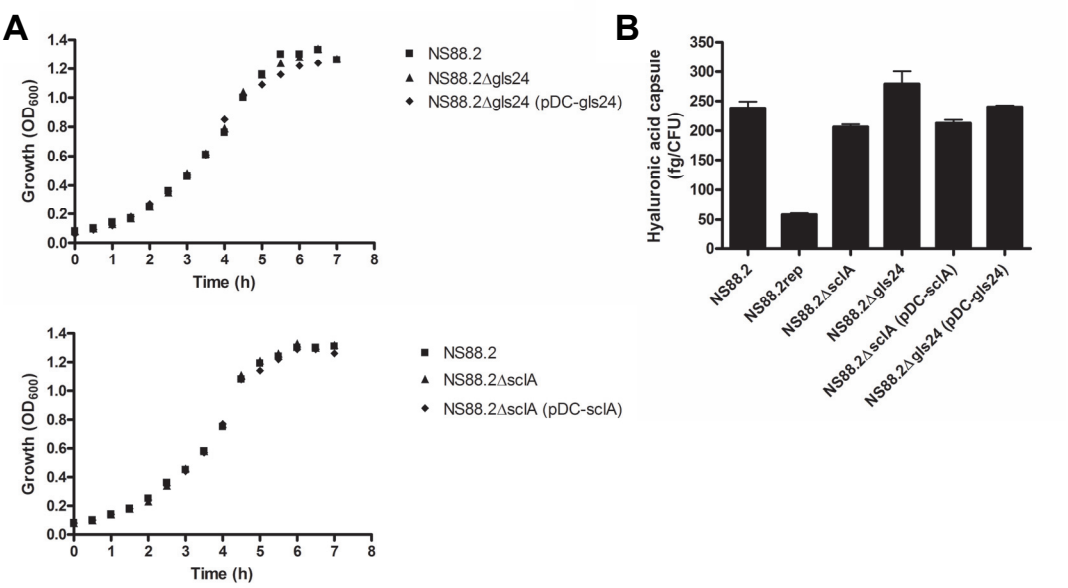

Fig. 4.8 Deletion of NS88.2 *sclA* or *gls24* does not impact growth in Todd-Hewitt broth or capsule synthesis. A Growth of NS88.2, *sclA* and *gls24* isogenic knock-mutant mutants and complemented strains growth kinetics in Todd-Hewitt broth. **B** NS88.2, *sclA* and *gls24* isogenic knock-out and complemented strains hyaluronic acid capsule biosynthesis. Capsule is expressed as femtograms of hyaluronic acid per colony forming unit (fg/CFU). Values shown for panel B are means ± standard deviations.

Isogenic deletion of *sclA* and *gls24* from the NS88.2 genome was conducted to investigate their role in providing resistance to innate immune responses. Multiple attempts to generate a double-knockout mutant were unsuccessful. This is a noteworthy finding as it may indicate such a knockout is lethal in GAS. The finding that loss of *sclA* expression results in attenuated growth in whole blood and increased neutrophil sensitivity, is consistent with previous work describing the binding of complement regulatory factors to SclA (Caswell *et al.*, 2008; Pahlman *et al.*, 2007; Reuter *et al.*, 2010). SclA is ubiquitously distributed in GAS strains; however *sclA* shows evidence of recombination and immune-selection analogous to the gene encoding M protein (Hoe *et al.*, 2007; Rasmussen *et al.*, 2000). This gives credence to a potential anti-phagocytic role in pathogenesis, as *sclA* hyper-variability could drive antigenic variation on the GAS cell surface and thus enhanced immune evasion through decreased FcR-mediated bacterial uptake. GAS binding of mammalian integrins with SclA may also facilitate escape from phagolysosomal killing via uptake

into the cytoplasm (Humtsoe *et al.*, 2005). Previous work implicates Gls24 in the survival of *E. faecalis* during culture in human blood and in urine (Vebo *et al.*, 2009; Vebo *et al.*, 2010). Gls24 was also found to be up-regulated at a protein level in response to growth of GAS in hyaluronic acid enriched media simulating an infection scenario (Zhang *et al.*, 2007) and during microarray analysis of murine soft tissue GAS infection (Graham *et al.*, 2006). To date this is the first work demonstrating the direct impact of *gls24* mutation on GAS survival and work is currently ongoing to determine the precise mechanism of action of Gls24 in systemic GAS infection.

Mutations in *covRS* have been linked to the hypervirulence of GAS in animal models of infection (Cole *et al.*, 2006; Maamary *et al.*, 2010). Moreover, the recently published recovery of an *emm*81.0 *covS* mutant GAS isolate following 13 days of human carriage, supports a model which predicts that such mutations occur clinically in a range of serotypes and in doing so escalate the severity of infection (Garcia *et al.*, 2010; Ikebe *et al.*, 2010; Maamary *et al.*, 2010). Recent work has shown that functional *emm* and *hasA* genes, are also essential for the acquisition of *covRS* mutations (Cole *et al.*, 2010). Data from this study supports a model in which GAS utilise a cohort of immune modulating virulence factors to attain a highly neutrophil resistant phenotype, leading to more severe infection.

Despite ongoing research effort, the burden of GAS infection in developing areas and indigenous populations remains high, and is likely to be underestimated. Here, we demonstrate the utility of systems biology approaches to identify novel bacterial virulence factors. Such virulence factors may prove valuable targets for future therapeutic or vaccine interventions to treat this globally important pathogen.

CHAPTER 5: GROUP A STREPTOCOCCUS MODULATES TISSUE INFLAMMATION BY MANIPULATING POLYMORPHONUCLEAR LEUKOCYTE CELL DEATH RESPONSES

The results presented are in preparation for submission to the Journal of Infectious Diseases and are formatted accordingly.

Reference:

James A. Tsatsaronis, Oliver Goldmann, Manfred Rohde, Jude Taylor, Diane Ly, Robert Geffers, Mark J. Walker, Eva Medina, Martina L. Sanderson-Smith. (2014) Group A Streptococcus modulates tissue inflammation by manipulating polymorphonuclear leukocyte cell death responses.

5.1 Abstract

The nature of polymorphonuclear leukocyte (PMN) cell death can strongly influence resolution of inflammatory episodes, and may also exacerbate tissue damage resulting from immunopathology in response to infection. Virulent group A *Streptococcus* (GAS) strains generally induce robust inflammatory responses that underlie the pathophysiology of suppurative GAS diseases. In this study we examined the influence of PMN cell death induced by avirulent and virulent GAS in the modulation of tissue inflammation. PMNs phagocytosed virulent GAS less efficiently in *in vitro* infection assays, produced less reactive oxygen species, and underwent reduced mitochondrial membrane depolarisation than avirulent GAS strains. Morphological and biochemical analyses revealed a dichotomy in GAS-infected PMN cell death responses, whereby PMNs infected with avirulent GAS exhibited nuclear fragmentation and caspase-3 activation consistent with an anti-inflammatory PMN apoptotic phenotype. Conversely, virulent GAS induced PMN vacuolisation and plasma membrane permeabilisation, leading to oncotic cell death. Cutaneous infection of C57BL/6 mice with virulent GAS engendered localised infiltration of neutrophils exhibiting reduced apoptotic potential,

whereas avirulent GAS infection was associated with tissue PMN apoptosis. We propose differences in PMN cell death mechanisms influence inflammatory responses to infection by GAS.

5.2 Introduction

Polymorphonuclear leukocytes (PMNs) are highly abundant, phagocytic immune cell indispensable for host defence against infection. Massive numbers of PMNs are rapidly recruited to sites of bacterial infection, which utilise highly potent mechanisms to destroy infecting pathogens (Nathan, 2006). Resolution of such infections depends greatly upon the ability of recruited PMNs to quickly eliminate infecting bacteria. This is accomplished in part by the release of cytotoxic granules. The recruitment and degranulation of PMNs are key processes that underlie initiation of acute phase inflammation. PMN responses during inflammation are required to provide host defence, however this process is implicated in contributing to tissue damage during infections (Gautam *et al.*, 2001; Johansson *et al.*, 2009). As such, the cytotoxic granule components with which PMNs are equipped, and the inherent risk of collateral damage to the host, necessitates tightly regulated control systems to reign in PMN activity.

Programmed cell death determines the ultimate fate of circulating PMNs and those recruited to sites of infection. PMNs are rapidly and spontaneously apoptotic under physiological conditions, a phenotype also prominent during bacterial infection (Kennedy and DeLeo, 2009). Post-phagocytosis, senescent PMNs initiate an apoptotic program that shuts down cellular processes and blunts inflammatory potential (Kobayashi *et al.*, 2003a; Kobayashi *et al.*, 2003b). Initiation of phagocytosis induced cell death triggers the expression of “eat-me” signals on these cells and marks them for phagocytosis by tissue resident and recruited macrophages, termed efferocytosis (Silva, 2011). Macrophage efferocytosis of apoptotic PMNs reduces accidental release of stored PMN granules, and thus prevents the potential for PMN-mediated collateral damage to surrounding tissues (Bratton and Henson, 2011). However, numerous

pathogens have been shown capable of prompting alternative leukocyte cell death mechanisms; including pyroptosis and oncosis (Fink and Cookson, 2007; Goldmann *et al.*, 2009). Whilst induction of PMN apoptosis and efferocytosis impart strong anti-inflammatory effects on surrounding tissues, pathogenic stimulation of pyroptosis and oncosis prompt pro-inflammatory cell phenotypes that lead to eventual cell death. Thus, dysregulation of native PMN apoptosis may stimulate gratuitous inflammatory responses via uncontrolled release of granular contents and other pro-inflammatory cytosolic factors (Kono and Rock, 2008).

Group A *Streptococcus* (*Streptococcus pyogenes*; GAS) is the etiological agent of severe diseases with inflammatory involvement, including necrotising fasciitis (NF) and septic shock (Cole *et al.*, 2011). Epidemiologically, GAS disease accounts for more than 663,000 cases of invasive infections globally (Carapetis *et al.*, 2005). Almost a third of NF cases lead to mortality in developed countries, a fraction that rises to 50% in NF cases with associated toxic shock (Lamagni *et al.*, 2008). Severe inflammation and destruction of focal tissues is a hallmark of NF infection. Furthermore, GAS sepsis is accompanied by systemic release of numerous pro-inflammatory mediators, with the magnitude of inflammatory cytokine response strongly correlated to the severity of disease (Norrby-Teglund *et al.*, 2000). GAS alteration of PMN cell death therefore may strongly influence clinical manifestations of inflammatory GAS disease. Here, we examine the potential of virulent and avirulent GAS strains to modulate PMN cell death responses, and the associated effect of GAS-induced PMN cell death on tissue inflammation.

5.3 Materials and methods

5.3.1 Ethics approval

All work involving the use of human blood and blood products was conducted with the informed consent of volunteers and was approved by the University of Wollongong

Human Ethics Committee. All animal use and procedures were approved by the University of Wollongong Animal Ethics Committee.

5.3.2 Electron Microscopy

For scanning electron microscopy, 5 x 10^6 PMNs were infected with 5 x 10^7 GAS CFU as described (2.16.2) for 5 h. Samples were fixed with 5% formaldehyde and 2% glutaraldehyde in HEPES buffer, kept at 4°C before dehydrating with a graded series of acetone, critical point dried with CO_2 and sputter coated with gold-palladium. Samples were examined in a Zeiss Merlin (Oberkochen, Germany) at an acceleration voltage of 5 kV using the Everhart-Thornley SE-detector and the Inlens SE-detector in a 25:75 ratio. For transmission electron microscopy, PMNs were infected and samples fixed as above, and treated with 1% aqueous osmium tetroxide for 1 h prior to dehydration with a graded series of acetone, treatment with 2% uranyl acetate in 70% acetone for overnight, dehydrated further with acetone, and embedded in the Spurr epoxide resin. Ultrathin sections were cut with a diamond knife, counterstained with uranyl acetate and observed in a Zeiss EM910 at an acceleration voltage of 80 kV. Images were recorded digitally with a Slow-Scan CCD-Camera (ProScan, 1024 x 1024) with ITEM-Software (Olympus Soft Imaging Solutions). Contrast and brightness of images were adjusted with Adobe Photoshop.

5.4 Results

5.4.1 PMN phagocytosis, ROS production and mitochondrial membrane depolarisation are differentially modulated by virulent GAS

The initial interactions of PMNs with GAS are mediated via phagocytosis of the infecting bacteria. Incubation of eGFP expressing virulent GAS (NS88.2) and avirulent GAS (NS88.2*rep*) with PMNs revealed that phagocytosis occurred rapidly for both NS88.2 and NS88.2*rep* GAS (<5 min), with a higher percentage of PMNs tending to associate with NS88.2*rep* compared with NS88.2 (Fig. 5.1A). The relative quantity of

NS88.2*rep* associated with each PMN cell was significantly higher than NS88.2, an effect that was exaggerated at increasing MOIs (Fig. 5.1B, $P < 0.001$ for all). NS88.2 was frequently visualised in the extracellular space during PMN infection, whereas NS88.2*rep* was more often localised within infected PMNs (Fig. 5.1C-D).

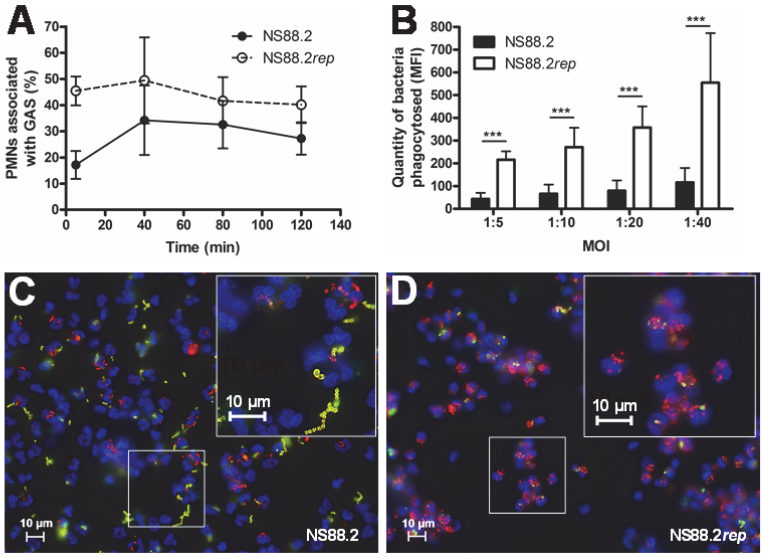

Fig. 5.1 PMN phagocytosis of virulent GAS is impaired *in vitro*. A PMN phagocytosis of virulent GAS strain NS88.2 and avirulent GAS strain NS88.2*rep* at a constant multiplicity of infection (MOI). **B** Relative quantification of NS88.2 and NS88.2*rep* phagocytosis at increasing MOIs. **C**-**D** Double immunofluorescence microscopy of PMNs infected with NS88.2 (**C**) or NS88.2*rep* (**D**), with inset pictures drawn to a higher magnification. Extra-cellular GAS are depicted in yellow, intra-cellular GAS in red, and PMN nuclei in blue. Scale bars in panels **C**-**D** are drawn to the sizes indicated. Microscope images were altered for brightness to highlight infecting GAS cells. Results shown for panels **A** and **B** are pooled means ± standard deviations ($n = 3$). Images shown in panels **C** and **D** are representative of duplicate experiments. Asterisks indicate statistical significance, *** $P < 0.001$.

The PMN respiratory burst against ingested pathogens plays a key role in the destruction of phagocytosed microbes, and in regulation of down-stream cell death pathways (Galluzzi *et al*., 2012). Kinetic measurement of PMN ROS production during phagocytosis of GAS revealed avirulent NS88.2*rep* GAS stimulated higher ROS activity than the virulent NS88.2 strain (Fig. 5.2A). ROS also play an important function in regulation of the mitochondrial membrane potential (Ψ_M), which in turn reflects cellular viability, as uncoupling of this proton gradient plays a central role in multiple cell death pathways (Galluzzi *et al*., 2012). Incubation with NS88.2*rep* elicited a large, significant reduction in Ψ_M compared with uninfected PMNs and cells infected with NS88.2 ($P <$

0.001) (Fig. 5.2B). Infection of PMNs with NS88.2 also elicited a significant, albeit smaller reduction in Ψ_M compared to uninfected cells (P < 0.001) (Fig. 5.2B). Collectively, these results suggest that downstream PMN cell death responses, such as apoptosis, may be influenced by differential ROS generation and Ψ_M depolarisation post-phagocytosis of GAS.

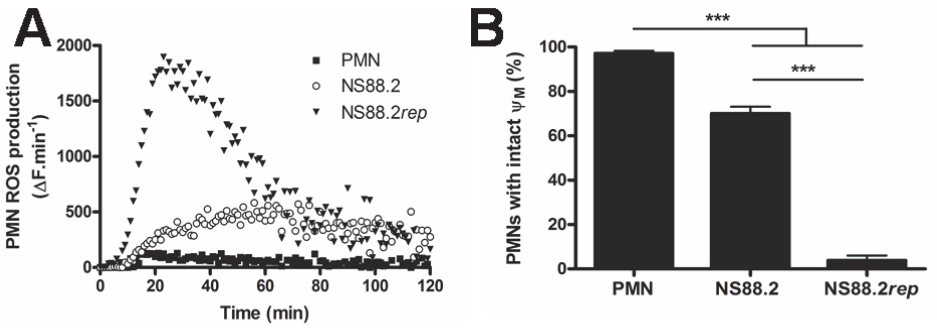

Fig. 5.2 Virulent GAS differentially modulate PMN ROS production and mitochondrial membrane depolarisation. A GAS-induced PMN reactive oxygen species (ROS) production during NS88.2 or NS88.2*rep* infection. ROS production is expressed as a change in relative fluorescence units over time ($\Delta F.min^{-1}$). **B** Determination of mitochondrial membrane potential (ψ_M) of GAS-infected PMNs. Results shown for panel **A** are means pooled from multiple experiments (n = 4). Results shown for panel **B** are pooled means ± standard deviations (n = 3). Asterisks indicate statistical significance, *** P < 0.001.

5.4.2 Avirulent GAS infection induces an apoptotic PMN phenotype

During many forms of cell death pathways, cells undergo characteristic alterations in external cell morphology which are indicative of the cell death mechanisms occurring (Kroemer *et al.*, 2009). Visualisation of GAS-induced PMN cell death was conducted by scanning electron microscopy. Uninfected PMNs exhibited typical neutrophil exterior morphology with few membrane irregularities (Fig. 5.3A). Comparatively, NS88.2 infected PMNs exhibited slight cellular swelling but similar membrane morphology to uninfected cells (Fig. 5.3B). In contrast, NS88.2*rep* infected PMNs exhibited both cellular shrinkage and extensive membrane blebbing, features indicative of apoptotic cell death (Fig. 5.3C).

Biochemical interrogation of GAS-induced cell death was conducted via fluorescent measurement of nuclear DNA fragmentation (TUNEL staining) and caspase-3 cleavage. Infection of human PMNs with the avirulent NS88.2*rep* strain induced

significantly higher TUNEL staining at 4 h ($P < 0.01$) and 6 h ($P < 0.001$) post-infection compared to both NS88.2 and uninfected PMNs (Fig. 5.3D), whereas NS88.2 infection induced comparable TUNEL staining to uninfected cells ($P > 0.05$). An increased amount of the active caspase-3 protein was present in NS88.2*rep* infected cells relative to uninfected and NS88.2 infected cells 5 h post-infection (Fig. 5.3E), further indicating an apoptotic cellular response in PMNs exposed to NS88.2*rep*.

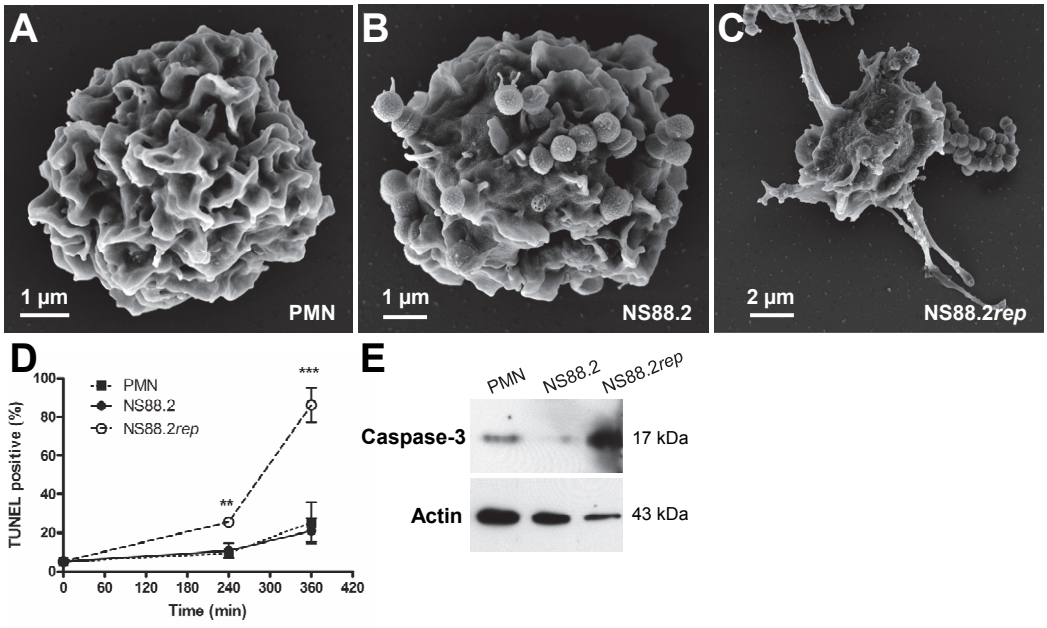

Fig. 5.3 Avirulent group A Streptococcus promotes PMN apoptotic responses. Uninfected PMNs (**A**), PMNs infected with NS88.2 (**B**) or PMNs infected with NS88.2*rep* (**C**) analysed by scanning electron microscopy 5 h post-infection. Scale bars in panels **A**-**B** are drawn to the sizes indicated. **D** Quantification of oligonucleosomal DNA fragmentation of uninfected PMNs and PMNs infected with NS88.2 and NS88.2*rep* by TUNEL. **E** Detection of active caspase-3 protein in uninfected (PMN), NS88.2 and NS88.2*rep* infected PMNs by western blot. Results shown in panel **D** are pooled means ± standard deviations ($n = 3$), results shown in panel **E** are representative of duplicate experiments. Asterisks indicate statistical significance, ** $P < 0.01$; *** $P < 0.001$.

5.4.3 PMNs infected by virulent GAS exhibit plasma membrane disintegration and oncosis

Oncotic leukocyte mechanisms (also referred to as regulated necrosis) have been previously shown to result in proinflammatory phenotypes, and precede cell death following infection by other pathogens (Bergsbaken and Cookson, 2009; Dacheux *et al.*, 2000). To investigate potential oncotic consequences of GAS infection of PMNs,

cell membrane integrity (LDH release) was assayed (Fig. 5.4A). Infection of PMNs with NS88.2*rep* resulted in minimal LDH release and maintenance of plasma membrane impermeability, in contrast to NS88.2 infected PMNs, which provoked significantly higher LDH release ($P < 0.05$). Substantiating this biochemical data, transmission electron microscopy revealed a large degree of vacuolisation and evidence of cell membrane disintegration in NS88.2 infected PMNs in comparison to uninfected cells (Fig. 5.4B-C). Both extensive vacuolisation and loss of cell membrane integrity have been previously associated with oncotic cell death processes, leading to proinflammatory cell responses (Fink and Cookson, 2005). Although proinflammatory PMN cell-death responses are well characterised *in vitro*, the *in vivo* role of GAS-induced oncotic PMN cell death and oncotic PMN-mediated cutaneous inflammation is less well defined.

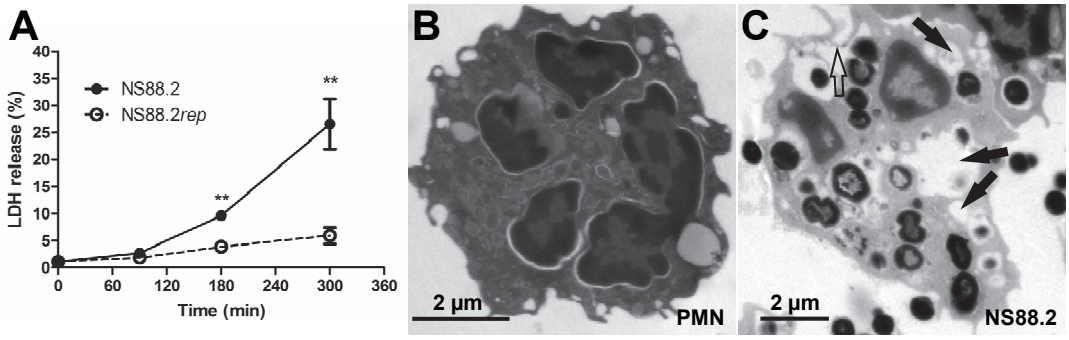

Fig. 5.4 PMN cell death induced by virulent GAS is associated with loss of membrane integrity and vacuolization consistent with oncosis. A Quantification of NS88.2 and NS88.2*rep*-induced PMN plasma membrane permeabilisation via LDH measurement. **B** and **C** Transmission electron microscopy of uninfected (**B**) and NS88.2 infected (**C**) human PMNs. Filled arrowheads indicate PMN vacuoles and unfilled arrowheads indicate cell membrane disruption. Scale bars in panels **B** and **C** are drawn to the sizes indicated. Results shown in panel **A** are representative means ± standard deviations ($n = 4$). Asterisks indicate statistical significance, ** $P < 0.01$.

5.4.4 PMNs recruited to virulent GAS infection have impaired apoptotic ability and accompany heightened inflammatory responses

Oncotic PMN cell death results in eventual cell lysis, and as such the release of damage-associated molecular pattern (DAMPs) molecules from these injured and dying cells (Kono and Rock, 2008). GAS-induced dysregulation from a more

physiological apoptotic PMN response may contribute to destructive tissue pathologies noted in murine infection models, and in clinical manifestations of severe GAS disease (Stevens *et al.*, 2005). To characterise the dynamics of PMNs recruited to virulent GAS infection *in vivo*, C57BL/6 mice were intradermally injected with eGFP expressing NS88.2 and NS88.2*rep*, and the infection site lavaged 6 h post-infection. Murine neutrophils (Ly6-G^+ cells) showed increased uptake of NS88.2*rep* compared with NS88.2 (Fig. 5.5A, $P < 0.001$), corroborating previous data described above using human PMNs (Fig. 1). Reduced phagocytic uptake of NS88.2 by murine neutrophils is likely to contribute to the significantly enhanced survival of this strain within the dermis of infected mice at 6 h (Fig. 5.5B, $P < 0.01$), and to NS88.2 virulence during 10-day infection, relative to NS88.2*rep* (Fig. 5.5C, $P < 0.001$).

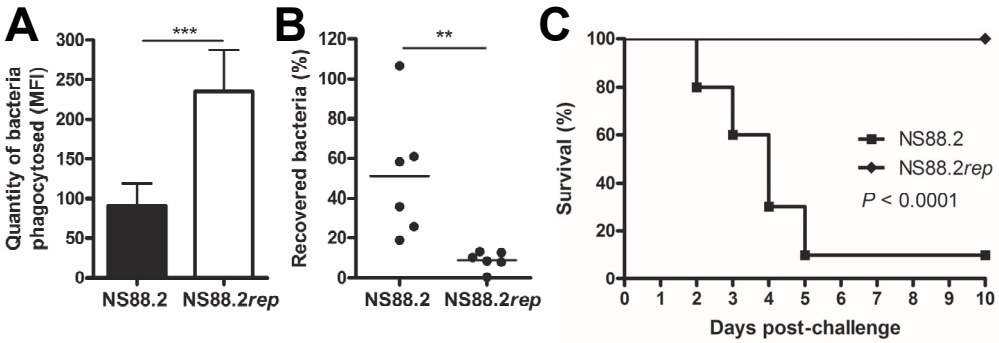

Fig. 5.5 Murine PMN phagocytosis and killing of virulent GAS is impaired *in vivo*, leading to mortality. A Relative quantification of NS88.2 and NS88.2*rep* phagocytosis by murine Ly6-G^+ neutrophils. **B** NS88.2 and NS88.2*rep* cutaneous survival *in vivo*. Survival is expressed as percentage recovered bacteria over inoculum. **C** Survival of wild-type C57BL/6 mice sub-cutaneously infected with NS88.2 or NS88.2*rep*. Results shown for panels **A**-**B** are pooled means ± standard deviations ($n = 3$). Asterisks indicate statistical significance, ** $P < 0.01$; *** $P < 0.001$.

Histopathological assessment of H&E stained infected murine dermal tissues was undertaken 24 h post-infection. Saline injection engendered no adverse histopathologies. (Fig. 5.6A-C). Infection with virulent NS88.2 elicited suppurative inflammation manifested by disintegration of the extracellular matrix and PMN infiltration (Fig. 5.6D; Fig. 5E, black arrowheads). Infiltrating PMNs exhibited a high degree of pyknotic (Fig. 5.6F, red arrowheads) and karyorrhexic (Fig. 5.6F, unfilled

arrowheads) nuclei morphologies. Intradermal infection with avirulent NS88.2*rep* also elicited robust inflammation, however in contrast to NS88.2, gross histological architecture was maintained (Fig. 5.6G). Infiltrates to the site of NS88.2*rep* infection were primarily PMNs (Fig. 5.6H, black arrowheads), and displayed frequent pyknotic cell morphology (Fig. 5.6I, red arrowheads) with the appearance of numerous apoptotic body structures (Fig. 5.6I, white arrowheads).

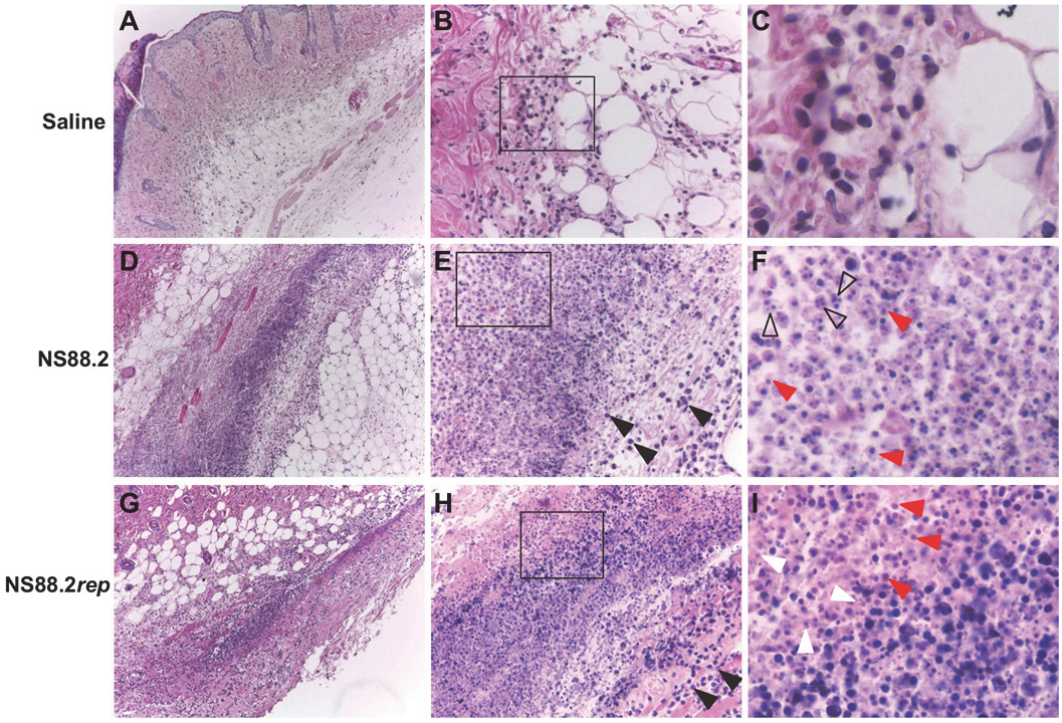

Fig. 5.6 Murine PMNs exhibit degeneracy and adverse histopathologies during cutaneous infection by virulent GAS. Murine dermis injected with sterile saline (**A**-**C**), NS88.2 (**D**-**F**) or NS88.2*rep* (**G-I**) was H&E stained 24 h post-injection. **E**, **H** black arrowheads, PMNs; **F**, **I** red arrowheads, pyknotic cells; **F** unfilled arrowheads, karyorrhexic cells; **I** white arrowheads, apoptotic bodies. Results shown are depicted at the following magnifications; **A**, **D**, **G,** 10x; **B**, **E**, **H,** 40x; **C**, **F**, **I,** 460x.

Biochemical analysis of murine infiltrates associated with GAS infection was assessed via TUNEL to confirm apoptotic nuclear DNA fragmentation (Fig. 5.7A-I). Saline injection was not associated with significant TUNEL staining (Fig. 5.7A-C). Cells associated with NS88.2 infection were infrequently TUNEL positive, indicating a paucity of apoptotic cell nuclei (Fig. 5.7D-F). Infiltrating cells within and surrounding the bolus of NS88.2*rep* infection exhibited stronger and more frequent positive TUNEL staining

(Fig. 5.7G-I). Thus, immuno-histological evidence supports previous *in vitro* data described above, and demonstrates that PMNs recruited to cutaneous, virulent GAS infection display a reduced apoptotic phenotype.

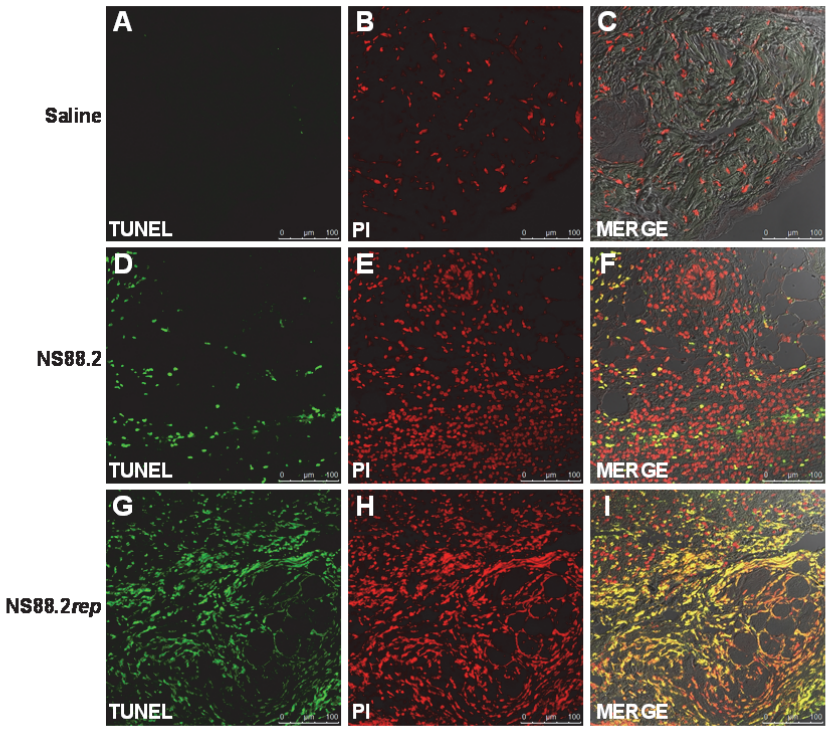

Fig. 5.7 PMN responses during cutaneous infection by virulent GAS infection exhibit decreased apoptosis. Murine dermis injected with sterile saline (**A**-**C**), NS88.2 (**D**-**F**) or NS88.2*rep* (**G**-**I**) was stained 24 h post-injection using TUNEL to detect apoptotic cells (**A**, **D**, **G**); propidium iodide (PI) as a counter stain for the total cell population (**B**, **E**, **H**) and merged channels with differential interference (**C**, **F**, **I**). Results shown are representative of quadruplicate sections taken from six flanks of three animals per condition. Scale bars are drawn to the sizes indicated.

5.5 Discussion

Induction of PMN apoptosis is critical to resolution of inflammation in a variety of non-infectious and infectious scenarios, including wound healing, meningitis and pneumonia (Fox *et al.*, 2010). This process is essential to preventing excessive inflammatory reactions, whereby aging cells and those recruited to sites of infection may be disposed of safely without sustained stimulation of immune responses. In animal models of meningitis, the persistence of PMNs lacking crucial apoptotic factors is strongly associated with adverse clinical outcomes (Garrison *et al.*, 2010). The present study indicates that phagocytosis of avirulent GAS elicits a programmed PMN

cell death mechanism which is apoptotic in nature. Avirulent GAS are rapidly phagocytosed by PMNs and elicit robust ROS production, triggering downstream mitochondrial membrane depolarisation and activation of the primary apoptotic effector, caspase-3. These data indicate that phagocytosis of avirulent GAS elicits a regulated PMN cell death mechanism reflective of the caspase-dependent, intrinsic apoptotic pathway (Elmore, 2007). The induction of apoptotic PMN cell-death by avirulent GAS could be crucial to preventing excessive inflammatory reactions, whereby PMNs exhausted from microbicidal responsibilities may be disposed of safely without undue immune stimulation (Fox *et al.*, 2010). As apoptotic cell death does not induce further inflammatory responses, it is considered to be immunologically silent (Labbe and Saleh, 2008). However, exposure to virulent GAS appears to elicit a distinct PMN cell death process that lacks typical apoptotic markers.

Leukocyte oncosis results in a pro-inflammatory phenotype, and precedes leukocyte cell-death following infection by other pathogens (Bergsbaken and Cookson, 2009; Dacheux *et al.*, 2000; Kroemer *et al.*, 2005). However, a dearth of knowledge remains in the literature concerning the mechanisms by which PMN oncosis proceeds, and the relationship between infection-mediated PMN cell death responses and tissue damage during disease. Here, we show that in contrast to avirulent GAS, PMNs infected with virulent GAS undergo mitochondrial membrane depolarisation, as shown for avirulent GAS, but this event precedes early loss of plasma membrane integrity and vacuolisation, which are all morphological features indicative of oncotic cell death (Fink and Cookson, 2005). *In vivo* data describing the pathophysiological relevance of leukocyte oncotic cell death has been lacking. We propose that the manner of PMN cell death by either apoptotic or oncotic demise affects the magnitude and nature of subsequent host immune responses.

Multiple reports have described a pivotal role for pore-forming toxins in shaping host leukocyte cell death, including the GAS cytotoxins SLO and SLS (Miyoshi-Akiyama *et*

al., 2005; Sierig *et al.*, 2003), and GAS different serotypes can acquire *covRS* mutations (Maamary *et al.*, 2010; Ikebe *et al.*, 2010). Virulent GAS bestowed with *covRS* mutations are highly encapsulated, and express higher levels of SLO (Chapter 4). As such, this suggests a role for GAS-induced PMN oncosis in the pathogenesis of multiple GAS serotypes.

Induction of PMN apoptosis has been postulated as a viable strategy to reduce harmful pathologies during acute inflammation (Fox *et al.*, 2010; Rossi *et al.*, 2006). Attempts to induce PMN apoptosis *in vivo*, and therapeutically reduce inflammation caused by GAS infection as part of this study were unsuccessful (data not shown). However, treatment of mice with a cyclin-dependent kinase inhibitor (CDKi) inducing PMN apoptosis has been previously shown to improve resolution of inflammation and clinical symptoms during experimental pneumococcal infection (Hoogendijk *et al.*, 2012; Koedel *et al.*, 2009). CDKi drugs show promise as a novel class of anti-inflammatory therapeutics, which combined with traditional antibiotics, could be used as adjunctive treatments to reduce harmful immune-mediated pathologies during severe GAS infection (Fox *et al.*, 2010; Leitch *et al.*, 2009).

In summary, this work describes dynamic host PMN cell death responses to GAS infection. PMN cell death in response to avirulent GAS infection is associated with an apoptotic program resulting from intra-cellular triggers, post-phagocytosis. Whereas PMNs recruited to virulent GAS infection in the dermis lack apoptotic markers, and bear hallmarks of proinflammatory cell death, which may amplify immune reactions during infection.

CHAPTER 6: CONCLUSIONS AND FUTURE DIRECTIONS

Streptococcus pyogenes inflicts a devastating global burden of mortality through severe, invasive infections. The World Health Organisation has placed GAS in the top 10 human pathogens, and of this list of organisms, GAS occupies the 4th most deadly bacterial pathogen by cause of mortality (Carapetis *et al.*, 2005). Severe GAS disease imparts a large burden of death and morbidity; however more mild afflictions, such as streptococcal pharyngitis, impart a large financial cost. The societal cost of paediatric pharyngitis in the USA alone has been estimated to be up to $538 million (Pfoh *et al.*, 2008). Multiple GAS serotypes are associated with severe GAS disease, however the M1T1 serotype is epidemiologically overrepresented from invasive and non-invasive infections, and has disseminated on a global scale (Aziz and Kotb, 2008). The precise molecular triggers for M1T1 invasive disease have been recently described, and highlight the importance of a combination of factors including phage-mediated lateral gene transfer and interactions with PMNs, in determining disease severity (Walker *et al.*, 2007). This multi-faceted nature of the disease process requires a complementary multi-disciplinary approach to identifying both host and bacterial factors that influence GAS immune survival and disease pathologies. High-throughput techniques such as genomics, transcriptomics, proteomics; as well as traditional molecular and immunological functional assays, are requisite to identifying and characterising factors that influence GAS immune resistance and the host mechanisms that act in response to GAS infection.

The recent advent of NGS technologies has revolutionised the manner and speed at which we conduct full genomic characterisation of bacterial isolates. Small genetic modifications such as SNPs, transfer of larger genetic elements from other streptococcal species, and prophage-mediated gene transfer can be rapidly identified in response to bacterial outbreaks (Musser and Shelburne, 2009). NGS enables the

precise tracking of GAS evolution, which can be linked to epidemiological data in the reconstruction of pathogen disseminations (Maamary *et al.*, 2012). This study utilised NGS technologies to genetically characterise a virulent and neutrophil resistant GAS isolate, NS88.2, which represents a skin tropic *emm*-pattern D strain from a remote region of Australia's Northern Territory (McKay *et al.*, 2004). Data from this study suggest that this isolate, similar to M1T1 and other serotypes of GAS, harbours at least one lysogenised prophage-like element; however no factors with obvious roles in mediating neutrophil responses were identified in this region. Further bioinformatic analyses of genes divergent from other fully sequenced GAS, and prediction of secreted and cell surface proteins, indicated that a number of virulence factors may mediate host-pathogen interactions. However, the positive confirmation of these putative functions required further experimental verification. The genome constructed as part of this study provides a useful starting point for such studies.

Mutations of the two-component regulator *covRS* result in enhanced virulence in the M1T1 GAS serotype (Sumby *et al.*, 2006). These mutations are selected for by GAS interactions with PMNs, due to the preservation of extracellular DNase Sda1 activity (Walker *et al.*, 2007). Although no obvious phage-acquired factor influencing PMN resistance was identified by NS88.2 genomic sequencing (Chapter 3), it has been shown that multiple virulence factors encoded by the GAS core genome, including M protein and capsule, are essential for *covRS* phase-switching to occur (Cole *et al.*, 2010). In addition, mutations of *covRS* in a variety of serotypes result in a unanimous increase in virulence potential (Maamary *et al.*, 2010). The NS88.2 isolate encodes a non-functional *covS* gene, exhibits hypervirulence in humanised plasminogen murine infection models, and is highly resistant to PMN killing (Maamary *et al.*, 2010). Inactivation of the *covRS* in virulent M1T1 exerts a counterbalancing decrease in the ability to adhere and colonise murine dermal tissues (Hollands *et al.*, 2010). Data presented in this study demonstrates that this compensatory aspect of GAS virulence

is also noted in the non-M1T1 NS88.2, as NS88.2*rep,* a functional *covS* encoding derivative mutant, exhibits enhanced biofilm formation and colonisation potential. Expansion of the previous genomic characterisation of NS88.2 through transcriptomic and proteomic analyses suggested that the activity of NS888.2 *gls24* and *sclA* are regulated both directly by *covRS* mutation and indirectly through SpeB-mediated degradation, and bestow enhanced survival in human blood and resistance to PMN killing. It is feasible that SclA interacts with PMN integrins in order to assist bacterial survival (Caswell *et al*., 2007), however potential mechanisms of Gls24-mediated PMN resistance are currently unknown. Future work should focus on determining potential metabolic functions of Gls24, as multiple studies of *E. faecalis* Gls24 and Gls24-homologs have shown a role for this protein in providing resistance to bile salt stress and involvement in pyruvate metabolism (Giard *et al.*, 2000).

Multiple reports have described mechanisms by which GAS resists killing by innate immune responses, while comparatively less attention has been given to differences in host cellular responses to virulent and avirulent GAS, and host processes underlying pathophysiologies during GAS infections. Previous studies indicate that multiple leukocyte cell death responses are triggered by GAS infection (Cortes and Wessels, 2009; Goldmann *et al.*, 2009; Kobayashi *et al*., 2003a). However, data elucidating the relevance of these processes to inflammation and disease pathophysiology have been elusive. Results presented in this study demonstrate that avirulent and PMN-sensitive NS88.2*rep* induces a morphologically, biochemically and immunologically distinct PMN cell death program which is characterised by an apoptotic phenotype. Infection by the virulent and PMN resistant NS88.2 strain triggers an oncotic cell death mechanism, leading to amplified immune responses and adverse histopathologies. This polarity in cell death responses may underlie differences in clinical GAS disease outcomes, as oncotic PMN cell death is pro-inflammatory and may perpetuate excessive immune responses. Further work should assess the potential of modulating PMN cell death as

an adjunctive therapeutic intervention to alleviate damaging GAS disease symptoms, as has been applied to other pathogens and inflammatory syndromes (Fox *et al.*, 2010; Hoogendijk *et al.*, 2012). This work also has implications for the pathogenesis of other GAS serotypes, and further studies should investigate whether manipulation of PMN cell death is a general pathogenic mechanism utilised by other GAS serotypes.

The economic pressure and large burden of mortality imparted by both M1T1 and non-M1T1 GAS diseases necessitate in-depth study of GAS pathogenesis. GAS interaction with host immune mediators, in particular PMNs, determines the ability of GAS to persist in the host and severity of disease. The use of high-throughput techniques greatly assists the identification of critical factors that determine GAS virulence and immune resistance. Host cellular responses also govern inflammatory reactions to GAS infection and resolution of inflammation. This study describes the generation of a new GAS genomic sequence draft and the identification of new roles for factors that influence GAS interactions with human PMNs. In addition, a divergence in PMN cell death is described in response to virulent and avirulent forms of a non-M1T1 GAS isolate. These data provide key insights into a variety of aspects of GAS biology, including the genomic makeup, secreted proteome, transcriptional behaviour, virulence determinants, and manipulation of the host innate immune responses to cause disease. The results described here expand our understanding of the bacterium in of itself, and how clinical manifestations of GAS disease are generated.

REFERENCES

Abbas, A.K. and Lichtman, A.H. (2009). Basic Immunology, Updated Edition, 3rd edn (Saunders Elsevier Publishers).

Abbot, E.L., Smith, W.D., Siou, G.P., Chiriboga, C., Smith, R.J., Wilson, J.A., Hirst, B.H., and Kehoe, M.A. (2007). Pili mediate specific adhesion of *Streptococcus pyogenes* to human tonsil and skin. *Cell. Microbiol. 9*, 1822-1833.

Abdeltawab, N.F., Aziz, R.K., Kansal, R., Rowe, S.L., Su, Y., Gardner, L., Brannen, C., Nooh, M.M., Attia, R.R., Abdelsamed, H.A.*, et al.* (2008). An unbiased systems genetics approach to mapping genetic loci modulating susceptibility to severe streptococcal sepsis. *PLoS Pathog. 4*, e1000042.

Adams, D.O., and Hamilton, T.A. (1984). The cell biology of macrophage activation. *Ann. Rev. Immunol. 2*, 283-318.

Agniswamy, J., Lei, B., Musser, J.M., and Sun, P.D. (2004). Insight of host immune evasion mediated by two variants of group a Streptococcus Mac protein. *J. Biol. Chem. 279*, 52789-52796.

Aikawa, C., Nozawa, T., Maruyama, F., Tsumoto, K., Hamada, S., and Nakagawa, I. (2010). Reactive oxygen species induced by *Streptococcus pyogenes* invasion trigger apoptotic cell death in infected epithelial cells. *Cell. Microbiol. 12*, 814-830.

Akesson, P., Schmidt, K.H., Cooney, J., and Bjorck, L. (1994). M1 protein and protein H: IgGFc- and albumin-binding streptococcal surface proteins encoded by adjacent genes. *Biochem. J. 300*, 877-886.

Akesson, P., Sjoholm, A.G., and Bjorck, L. (1996). Protein SIC, a novel extracellular protein of *Streptococcus pyogenes* interfering with complement function. *J. Biol. Chem. 271*, 1081-1088.

Alikhan, N.F., Petty, N.K., Ben Zakour, N.L., and Beatson, S.A. (2011). BLAST Ring Image Generator (BRIG): simple prokaryote genome comparisons. *BMC Genomics. 12*.

Almengor, A.C., and McIver, K.S. (2004). Transcriptional activation of sclA by Mga requires a distal binding site in *Streptococcus pyogenes*. *J. Bacteriol. 186*, 7847-7857.

Ashbaugh, C.D., Alberti, S., and Wessels, M.R. (1998). Molecular analysis of the capsule gene region of group A Streptococcus: the hasAB genes are sufficient for capsule expression. *J. Bacteriol. 180*, 4955-4959.

Ashbaugh, C.D., and Wessels, M.R. (2001). Absence of a cysteine protease effect on bacterial virulence in two murine models of human invasive group A streptococcal infection. *Infect. Immun. 69*, 6683-6688.

Athens, J.W., Haab, O.P., Raab, S.O., Mauer, A.M., Ashenbrucker, H., Cartwright, G.E., and Wintrobe, M.M. (1961). Leukokinetic studies. IV. The total blood, circulating and marginal granulocyte pools and the granulocyte turnover rate in normal subjects. *J. Clin. Invest. 40*, 989-995.

Aziz, R.K., Bartels, D., Best, A.A., DeJongh, M., Disz, T., Edwards, R.A., Formsma, K., Gerdes, S., Glass, E.M., Kubal, M.*, et al.* (2008). The RAST server: Rapid Annotations using Subsystems Technology. *BMC gen. 9*.

Aziz, R.K., Edwards, R.A., Taylor, W.W., Low, D.E., McGeer, A., and Kotb, M. (2005). Mosaic prophages with horizontally acquired genes account for the emergence and diversification of the globally disseminated M1T1 clone of *Streptococcus pyogenes*. *J. Bacteriol. 187*, 3311-3318.

Aziz, R.K., Ismail, S.A., Park, H.W., and Kotb, M. (2004a). Post-proteomic identification of a novel phage-encoded streptodornase, Sda1, in invasive M1T1 *Streptococcus pyogenes*. *Mol. Microbiol. 54*, 184-197.

Aziz, R.K., Kansal, R., Aronow, B.J., Taylor, W.L., Rowe, S.L., Kubal, M., Chhatwal, G.S., Walker, M.J., and Kotb, M. (2010). Microevolution of group A streptococci in vivo: capturing regulatory networks engaged in sociomicrobiology, niche adaptation, and hypervirulence. *PLoS One 5*, e9798.

Aziz, R.K., and Kotb, M. (2008). Rise and persistence of global M1T1 clone of *Streptococcus pyogenes*. *Emerg. Infect. Dis. 14*, 1511-1517.

Aziz, R.K., Pabst, M.J., Jeng, A., Kansal, R., Low, D.E., Nizet, V., and Kotb, M. (2004b). Invasive M1T1 group A Streptococcus undergoes a phase-shift in vivo to prevent proteolytic degradation of multiple virulence factors by SpeB. *Mol. Microbiol. 51*, 123-134.

Barnett, T.C., Liebl, D., Seymour, L.M., Gillen, C.M., Lim, J.Y., LaRock, C.N., Davies, M.R., Schulz, B.L., Nizet, V., Teasdale, R.D., and Walker, M.J. (2013). The globally disseminated M1T1 clone of group A Streptococcus evades autophagy for intracellular replication. *Cell Host Microbe 14*, 675-682.

Baruch, M., Belotserkovsky, I., Hertzog, B.B., Ravins, M., Dov, E., McIver, K.S., Le Breton, Y.S., Zhou, Y., Chen, C.Y., and Hanski, E. (2014). An extracellular bacterial pathogen modulates host metabolism to regulate its own sensing and proliferation. *Cell 156*, 97-108.

Baxter, F., and McChesney, J. (2000). Severe group A streptococcal infection and streptococcal toxic shock syndrome. *Can. J. Anaesth. 47*, 1129-1140.

Beall, B., Facklam, R., and Thompson, T. (1996). Sequencing emm-specific PCR products for routine and accurate typing of group A streptococci. *J. Clin. Microbiol. 34*, 953-958.

Ben Zakour, N.L., Venturini, C., Beatson, S.A., and Walker, M.J. (2012). Analysis of a *Streptococcus pyogenes* puerperal sepsis cluster by use of whole-genome sequencing. *J. Clin. Microbiol. 50*, 2224-2228.

Bendtsen, J.D., Nielsen, H., Heijne, G.V., and Brunak, S. (2004). Improved prediction of signal peptides: SignalP 3.0. *J. Mol. Biol. 340*, 783-795.

Beres, S.B., Carroll, R.K., Shea, P.R., Sitkiewicz, I., Martinez-Gutierrez, J.C., Low, D.E., McGeer, A., Willey, B.M., Green, K., Tyrrell, G.J. et al. (2010). Molecular complexity of successive bacterial epidemics deconvoluted by comparative pathogenomics. *Proc. Natl. Acad. Sci. U.S.A.* 107, 4371-4376.

Beres, S.B., Richter, E.W., Nagiec, M.J., Sumby, P., Porcella, S.F., DeLeo, F.R., and Musser, J.M. (2006). Molecular genetic anatomy of inter- and intraserotype variation in the human bacterial pathogen group A Streptococcus. *Proc. Natl. Acad. Sci. U.S.A. 103*, 7059-7064.

Beres, S.B., Sylva, G.L., Barbian, K.D., Lei, B., Hoff, J.S., Mammarella, N.D., Liu, M.Y., Smoot, J.C., Porcella, S.F., Parkins, L.D.*, et al.* (2002). Genome sequence of a serotype M3 strain of group A Streptococcus: phage-encoded toxins, the high-virulence phenotype, and clone emergence. *Proc. Natl. Acad. Sci. U.S.A. 99*, 10078-10083.

Berge, A., and Bjorck, L. (1995). Streptococcal cysteine proteinase releases biologically active fragments of streptococcal surface proteins. *J. Biol. Chem. 270*, 9862-9867.

Berge, A., and Sjobring, U. (1993). PAM, a novel plasminogen-binding protein from *Streptococcus pyogenes*. *J. Biol. Chem. 268*, 25417-25424.

Bergsbaken, T., and Cookson, B.T. (2009). Innate immune response during Yersinia infection: critical modulation of cell death mechanisms through phagocyte activation. *J. Leukoc. Biol. 86*, 1153-1158.

Bessen, D.E., Carapetis, J.R., Beall, B., Katz, R., Hibble, M., Currie, B.J., Collingridge, T., Izzo, M.W., Scaramuzzino, D.A., and Sriprakash, K.S. (2000). Contrasting molecular epidemiology of group A streptococci causing tropical and nontropical infections of the skin and throat. *J. Infect. Dis. 182*, 1109-1116.

Bessen, D.R., Kumar, N., Hall, G.S., Riley, D.R., Luo, F., Lizano, S., Ford, C.N., McShan, M., Nguyen, S.V., Dunning Hotopp, J.C., and Tettelin, H. (2011). Whole genome association study on tissue tropism phenotypes in group A *Streptococcus*. *J. Bacteriol. 10, 3*512-3523

Bessen, D.E., McGregor, K.F., and Whatmore, A.M. (2008). Relationships between emm and multilocus sequence types within a global collection of *Streptococcus pyogenes*. *BMC Microbiol. 8*, 59.

Bessen, D.E., Sotir, C.M., Readdy, T.L., and Hollingshead, S.K. (1996). Genetic correlates of throat and skin isolates of group A streptococci. *J. Infect. Dis. 173*, 896-900.

Betschel, S.D., Borgia, S.M., Barg, N.L., Low, D.E., and De Azavedo, J.C. (1998). Reduced virulence of group A streptococcal Tn916 mutants that do not produce streptolysin S. *Infect. Immun. 66*, 1671-1679.

Bisno, A.L. (2001). Acute pharyngitis. *N. Engl. J. Med. 344*, 205-211.

Bisno, A.L., and Stevens, D.L. (1996). Streptococcal infections of skin and soft tissues. *N. Engl. J. Med. 334*, 240-245.

Bratton, D.L., and Henson, P.M. (2011). Neutrophil clearance: when the party is over, clean-up begins. *Trends Immunol. 32*, 350-357.

Brinkmann, V., Reichard, U., Goosmann, C., Fauler, B., Uhlemann, Y., Weiss, D.S., Weinrauch, Y., and Zychlinsky, A. (2004). Neutrophil extracellular traps kill bacteria. *Science 303*, 1532-1535.

Bryant, A.E., Bayer, C.R., Chen, R.Y., Guth, P.H., Wallace, R.J., and Stevens, D.L. (2005). Vascular dysfunction and ischemic destruction of tissue in *Streptococcus pyogenes* infection: the role of streptolysin O-induced platelet/neutrophil complexes. *J. Infect. Dis. 192*, 1014-1022.

Buchanan, J.T., Simpson, A.J., Aziz, R.K., Liu, G.Y., Kristian, S.A., Kotb, M., Feramisco, J., and Nizet, V. (2006). DNase expression allows the pathogen group A Streptococcus to escape killing in neutrophil extracellular traps. *Curr. Biol. 16*, 396-400.

Burns, E.H., Jr., Lukomski, S., Rurangirwa, J., Podbielski, A., and Musser, J.M. (1998). Genetic inactivation of the extracellular cysteine protease enhances in vitro internalization of group A streptococci by human epithelial and endothelial cells. *Microb. Pathog. 24*, 333-339.

Burns, E.H., Jr., Marciel, A.M., and Musser, J.M. (1996). Activation of a 66-kilodalton human endothelial cell matrix metalloprotease by *Streptococcus pyogenes* extracellular cysteine protease. *Infect. Immun. 64*, 4744-4750.

Carapetis, J.R., Steer, A.C., Mulholland, E.K., and Weber, M. (2005). The global burden of group A streptococcal diseases. *Lancet Infect. Dis. 5*, 685-694.

Carapetis, J.R., Walker, A.M., Hibble, M., Sriprakash, K.S., and Currie, B.J. (1999). Clinical and epidemiological features of group A streptococcal bacteraemia in a region with hyperendemic superficial streptococcal infection. *Epidemiol. Infect. 122*, 59-65.

Carapetis, J.R., Wolff, D.R., and Currie, B.J. (1996). Acute rheumatic fever and rheumatic heart disease in the top end of Australia's Northern Territory. Med. J. Aust. *164*, 146-149.

Carver, T., Bohme, U., Otto, T.D., Parkhill, J., and Berriman, M. (2010). BamView: viewing mapped read alignment data in the context of the reference sequence. *Bioinformatics 26*, 676-677.

Caswell, C.C., Han, R., Hovis, K.M., Ciborowski, P., Keene, D.R., Marconi, R.T., and Lukomski, S. (2008). The Scl1 protein of M6-type group A Streptococcus binds the human complement regulatory protein, factor H, and inhibits the alternative pathway of complement. *Mol. Microbiol. 67*, 584-596.

Caswell, C.C., Lukomska, E., Seo, N.S., Hook, M., and Lukomski, S. (2007). Scl1-dependent internalization of group A Streptococcus via direct interactions with the alpha2beta(1) integrin enhances pathogen survival and re-emergence. *Mol. Microbiol. 64*, 1319-1331.

Chang, C.W., Tsai, W.H., Chuang, W.J., Lin, Y.S., Wu, J.J., Liu, C.C., Tsai, P.J., and Lin, M.T. (2009). Procaspase 8 and Bax Are up-regulated by distinct pathways in streptococcal pyrogenic exotoxin B-induced apoptosis. *J. Biol. Chem. 284*, 33195-33205.

Chatellier, S., Ihendyane, N., Kansal, R.G., Khambaty, F., Basma, H., Norrby-Teglund, A., Low, D.E., McGeer, A., and Kotb, M. (2000). Genetic relatedness and superantigen expression in group A streptococcus serotype M1 isolates from patients with severe and nonsevere invasive diseases. *Infect. Immun. 68*, 3523-3534.

Chaussee, M.S., Cole, R.L., and van Putten, J.P. (2000). Streptococcal erythrogenic toxin B abrogates fibronectin-dependent internalization of *Streptococcus pyogenes* by cultured mammalian cells. *Infect. Immun. 68*, 3226-3232.

Chaussee, M.S., Somerville, G.A., Reitzer, L., and Musser, J.M. (2003). Rgg coordinates virulence factor synthesis and metabolism in *Streptococcus pyogenes*. *J. Bacteriol. 185*, 6016-6024.

Cleary, P.P., Prahbu, U., Dale, J.B., Wexler, D.E., and Handley, J. (1992). Streptococcal C5a peptidase is a highly specific endopeptidase. *Infect. Immun. 60*, 5219-5223.

Cole, J.N., Barnett, T.C., Nizet, V., and Walker, M.J. (2011). Molecular insight into invasive group A streptococcal disease. *Nat. Rev. Microbiol. 9*, 724-736.

Cole, J.N., McArthur, J.D., McKay, F.C., Sanderson-Smith, M.L., Cork, A.J., Ranson, M., Rohde, M., Itzek, A., Sun, H., Ginsburg, D.*, et al.* (2006). Trigger for group A streptococcal M1T1 invasive disease. *FASEB J. 20*, 1745-1747.

Cole, J.N., Pence, M.A., von Kockritz-Blickwede, M., Hollands, A., Gallo, R.L., Walker, M.J., and Nizet, V. (2010). M protein and hyaluronic acid capsule are essential for *in vivo* selection of *covRS* mutations characteristic of invasive serotype M1T1 group A *Streptococcus*. *MBio 1*.

Collin, M., and Olsen, A. (2001). Effect of SpeB and EndoS from *Streptococcus pyogenes* on human immunoglobulins. *Infect. Immun. 69*, 7187-7189.

Collin, M., and Olsen, A. (2003). Extracellular enzymes with immunomodulating activities: variations on a theme in *Streptococcus pyogenes*. *Infect. Immun. 71*, 2983-2992.

Cook, S.M., Skora, A., Gillen, C.M., Walker, M.J. and McArthur, J.D. (2012). Streptokinase variants from *Streptococcus pyogenes* display altered plasminogen activation characteristics - implications for pathogenesis. *Mol. Microbiol.* 86, 1052-1062.

Cortes, G., and Wessels, M.R. (2009). Inhibition of dendritic cell maturation by group A Streptococcus. *J. Infect. Dis. 200*, 1152-1161.

Courtney, H.S., Dale, J.B., and Hasty, D.I. (1996). Differential effects of the streptococcal fibronectin-binding protein, FBP54, on adhesion of group A streptococci to human buccal cells and HEp-2 tissue culture cells. *Infect. Immun. 64*, 2415-2419.

Courtney, H.S., Hasty, D.L., and Dale, J.B. (2002). Molecular mechanisms of adhesion, colonization, and invasion of group A streptococci. *Ann. Med. 34*, 77-87.

Courtney, H.S., Hasty, D.L., and Dale, J.B. (2006). Anti-phagocytic mechanisms of *Streptococcus pyogenes*: binding of fibrinogen to M-related protein. *Mol. Microbiol. 59*, 936-947.

Courtney, H.S., Hasty, D.L., Dale, J.B., and Poirier, T.P. (1992). A 28-kilodalton fibronectin-binding protein of group A streptococci. *Curr. Microbiol. 25*, 245-250.

Courtney, H.S., Li, Y., Dale, J.B., and Hasty, D.L. (1994). Cloning, sequencing, and expression of a fibronectin/fibrinogen-binding protein from group A streptococci. *Infect. Immun. 62*, 3937-3946.

Courtney, H.S., Ofek, I., and Hasty, D.L. (1997). M protein mediated adhesion of M type 24 *Streptococcus pyogenes* stimulates release of interleukin-6 by HEp-2 tissue culture cells. *FEMS Microbiol. 151*, 65-70.

Courtney, H.S., Ofek, I., Penfound, T., Nizet, V., Pence, M.A., Kreikemeyer, B., Podbielbski, A., Hasty, D.L., and Dale, J.B. (2009). Relationship between Expression of the Family of M Proteins and Lipoteichoic Acid to Hydrophobicity and Biofilm Formation in *Streptococcus pyogenes*. *PLoS One 4*, -.

Courtney, H.S., Simpson, W.A., and Beachey, E.H. (1983). Binding of streptococcal lipoteichoic acid to fatty acid-binding sites on human plasma fibronectin. *J. Bacteriol. 153*, 763-770.

Cox, K.H., Ruiz-Bustos, E., Courtney, H.S., Dale, J.B., Pence, M.A., Nizet, V., Aziz, R.K., Gerling, I., Price, S.M., and Hasty, D.L. (2009). Inactivation of DltA modulates virulence factor expression in *Streptococcus pyogenes*. *PLoS One 4*, e5366.

Cue, D., Lam, H., and Cleary, P.P. (2001). Genetic dissection of the *Streptococcus pyogenes* M1 protein: regions involved in fibronectin binding and intracellular invasion. *Microb. Pathog. 31*, 231-242.

Cunningham, M.W. (2000). Pathogenesis of group A streptococcal infections. *Clin. Microbiol. Rev. 13*, 470-511.

Cunningham, M.W. (2008). Pathogenesis of group A streptococcal infections and their sequelae. *Adv. Exp. Med. Biol. 609*, 29-42.

Cywes Bentley, C., Hakansson, A., Christianson, J., and Wessels, M.R. (2005). Extracellular group A Streptococcus induces keratinocyte apoptosis by dysregulating calcium signalling. *Cell. Microbiol. 7*, 945-955.

Cywes, C., Stamenkovic, I., and Wessels, M.R. (2000). CD44 as a receptor for colonization of the pharynx by group A Streptococcus. *J. Clin. Invest. 106*, 995-1002.

D'Costa, S.S., and Boyle, M.D. (1998). Interaction of a group A Streptococcus within human plasma results in assembly of a surface plasminogen activator that contributes to occupancy of surface plasmin-binding structures. *Microb. Pathog. 24*, 341-349.

Dacheux, D., Toussaint, B., Richard, M., Brochier, G., Croize, J., and Attree, I. (2000). Pseudomonas aeruginosa cystic fibrosis isolates induce rapid, type III secretion-dependent, but ExoU-independent, oncosis of macrophages and polymorphonuclear neutrophils. *Infect. Immun. 68*, 2916-2924.

Dale, J.B., Washburn, R.G., Marques, M.B., and Wessels, M.R. (1996). Hyaluronate capsule and surface M protein in resistance to opsonization of group A streptococci. *Infect. Immun. 64*, 1495-1501.

Darling, A.C.E., Mau, B., Blattner, F.R., and Perna, N.T. (2004). Mauve: Multiple alignment of conserved genomic sequence with rearrangements. *Gen. Research 14*, 1394-1403.

Datta, V., Myskowski, S.M., Kwinn, L.A., Chiem, D.N., Varki, N., Kansal, R.G., Kotb, M., and Nizet, V. (2005). Mutational analysis of the group A streptococcal operon encoding streptolysin S and its virulence role in invasive infection. *Mol. Microbiol. 56*, 681-695.

Delcher, A.L., Bratke, K.A., Powers, E.C., and Salzberg, S.L. (2007). Identifying bacterial genes and endosymbiont DNA with Glimmer. *Bioinformatics 23*, 673-679.

Deloger, M., El Karoui, M., and Petit, M.A. (2009). A genomic distance based on MUM indicates discontinuity between most bacterial species and genera. *J. Bacteriol. 191*, 91-99.

Diamond, G., Beckloff, N., Weinberg, A., and Kisich, K.O. (2009). The roles of antimicrobial peptides in innate host defense. *Curr. Pharm. Des. 15*, 2377-2392.

Dinkla, K., Rohde, M., Jansen, W.T., Kaplan, E.L., Chhatwal, G.S., and Talay, S.R. (2003). Rheumatic fever-associated *Streptococcus pyogenes* isolates aggregate collagen. *J. Clin. Invest. 111*, 1905-1912.

Dinkla, K., Talay, S.R., Morgelin, M., Graham, R.M., Rohde, M., Nitsche-Schmitz, D.P., and Chhatwal, G.S. (2009). Crucial role of the CB3-region of collagen IV in PARF-induced acute rheumatic fever. *PLoS One 4*, e4666.

Donaldson, P.M., Naylor, B., Lowe, J.W., and Gouldesbrough, D.R. (1993). Rapidly fatal necrotising fasciitis caused by *Streptococcus pyogenes*. *J. Clin. Pathol. 46*, 617-620.

Edwards, R.J., Taylor, G.W., Ferguson, M., Murray, S., Rendell, N., Wrigley, A., Bai, Z., Boyle, J., Finney, S.J., Jones, A.*, et al.* (2005). Specific C-terminal cleavage and inactivation of interleukin-8 by invasive disease isolates of *Streptococcus pyogenes*. *J. Infect. Dis. 192*, 783-790.

Efstratiou, A. (2000). Group A streptococci in the 1990s. *J. Antimicrob. Chemother. 45*, 3-12.

Elmore, S. (2007). Apoptosis: a review of programmed cell death. *Toxicol. Pathol. 35*, 495-516.

Facklam, R. (2002). What happened to the streptococci: overview of taxonomic and nomenclature changes. *Clin. Microbiol. Rev. 15*, 613-630.

Factor, S.H., Levine, O.S., Schwartz, B., Harrison, L.H., Farley, M.M., McGeer, A., and Schuchat, A. (2003). Invasive group A streptococcal disease: risk factors for adults. *Emerg. Infect. Dis. 9*, 970-977.

Fae, K.C., da Silva, D.D., Oshiro, S.E., Tanaka, A.C., Pomerantzeff, P.M., Douay, C., Charron, D., Toubert, A., Cunningham, M.W., Kalil, J., and Guilherme, L. (2006). Mimicry in recognition of cardiac myosin peptides by heart-intralesional T cell clones from rheumatic heart disease. *J. Immunol. 176*, 5662-5670.

Falugi, F., Zingaretti, C., Pinto, V., Mariani, M., Amodeo, L., Manetti, A.G., Capo, S., Musser, J.M., Orefici, G., Margarit, I.*, et al.* (2008). Sequence variation in group A Streptococcus pili and association of pilus backbone types with lancefield T serotypes. *J. Infect. Dis. 198*, 1834-1841.

Fernandez, H.N., and Hugli, T.E. (1978). Primary structural analysis of the polypeptide portion of human C5a anaphylatoxin. Polypeptide sequence determination and assignment of the oligosaccharide attachment site in C5a. *J. Biol. Chem. 253*, 6955-6964.

Fernie-King, B.A., Seilly, D.J., Davies, A., and Lachmann, P.J. (2002). Streptococcal inhibitor of complement inhibits two additional components of the mucosal innate immune system: secretory leukocyte proteinase inhibitor and lysozyme. *Infect. Immun. 70*, 4908-4916.

Fernie-King, B.A., Seilly, D.J., Willers, C., Wurzner, R., Davies, A., and Lachmann, P.J. (2001). Streptococcal inhibitor of complement (SIC) inhibits the membrane attack complex by preventing uptake of C567 onto cell membranes. *Immunology 103*, 390-398.

Fink, S.L., and Cookson, B.T. (2005). Apoptosis, pyroptosis, and necrosis: mechanistic description of dead and dying eukaryotic cells. *Infect. Immun. 73*, 1907-1916.

Fink, S.L., and Cookson, B.T. (2007). Pyroptosis and host cell death responses during Salmonella infection. *Cell. Microbiol. 9*, 2562-2570.

Fiorentino, T.R., Beall, B., Mshar, P., and Bessen, D.E. (1997). A genetic-based evaluation of the principal tissue reservoir for group A streptococci isolated from normally sterile sites. *J. Infect. Dis. 176*, 177-182.

Fischetti, V.A. (1989). Streptococcal M protein: molecular design and biological behavior. *Clin. Microbiol. Rev. 2*, 285-314.

Fittipaldi, N., Beres, S.B., Olsen, R.J., Kapur, V., Shea, P.R., Watkins, M. E., Cantu, C.C., Laucirica, D.R., Jenkins, L., Flores, A.R. *et al*. (2012). Full-genome dissection of an epidemic of severe invasive disease caused by a hypervirulent, recently emerged clone of group A *Streptococcus*. *Am. J. Pathol.* 180, 1522-1534.

Fontaine, M.C., Lee, J.J., and Kehoe, M.A. (2003). Combined contributions of streptolysin O and streptolysin S to virulence of serotype M5 *Streptococcus pyogenes* strain Manfredo. *Infect. Immun. 71*, 3857-3865.

Fox, S., Leitch, A.E., Duffin, R., Haslett, C., and Rossi, A.G. (2010). Neutrophil apoptosis: relevance to the innate immune response and inflammatory disease. *J. Innate Immun. 2*, 216-227.

Frick, I.M., Akesson, P., Rasmussen, M., Schmidtchen, A., and Bjorck, L. (2003). SIC, a secreted protein of *Streptococcus pyogenes* that inactivates antibacterial peptides. *J. Biol. Chem. 278*, 16561-16566.

Gallo, R.L. and Nizet, V. (2008). Innate barriers against infection and associated disorders. *Drug Disc. Today Dis Mech 5*, e145-152.

Galluzzi, L., Vitale, I., Abrams, J.M., Alnemri, E.S., Baehrecke, E.H., Blagosklonny, M.V., Dawson, T.M., Dawson, V.L., El-Deiry, W.S., Fulda, S.*, et al.* (2012). Molecular definitions of cell death subroutines: recommendations of the Nomenclature Committee on Cell Death 2012. *Cell Death Diff. 19*, 107-120.

Garcia, A.F., Abe, L.M., Erdem, G., Cortez, C.L., Kurahara, D., and Yamaga, K. (2010). An insert in the covS gene distinguishes a pharyngeal and a blood isolate of *Streptococcus pyogenes* found in the same individual. *Microbiology 156*, 3085-3095.

Gardiner, D., Hartas, J., Currie, B., Mathews, J.D., Kemp, D.J., and Sriprakash, K.S. (1995). Vir typing: a long-PCR typing method for group A streptococci. *PCR Methods Appl. 4*, 288-293.

Gardiner, D.L., Goodfellow, A.M., Martin, D.R., and Sriprakash, K.S. (1998). Group A streptococcal Vir types are M-protein gene (emm) sequence type specific. *J. Clin. Microbiol. 36*, 902-907.

Gardiner, D.L., and Sriprakash, K.S. (1996). Molecular epidemiology of impetiginous group A streptococcal infections in aboriginal communities of northern Australia. *J. Clin. Microbiol. 34*, 1448-1452.

Garrison, S.P., Thornton, J.A., Hacker, H., Webby, R., Rehg, J.E., Parganas, E., Zambetti, G.P., and Tuomanen, E.I. (2010). The p53-target gene puma drives neutrophil-mediated protection against lethal bacterial sepsis. *PLoS Pathog. 6*, e1001240.

Gautam, N., Olofsson, A.M., Herwald, H., Iversen, L.F., Lundgren-Akerlund, E., Hedqvist, P., Arfors, K.E., Flodgaard, H., and Lindbom, L. (2001). Heparin-binding protein (HBP/CAP37): A missing link in neutrophil-evoked alteration of vascular permeability. *Nat. Med. 7*, 1123-1127.

Giard, J.C., Rince, A., Capiaux, H., Auffray, Y., and Hartke, A. (2000). Inactivation of the stress- and starvation-inducible gls24 operon has a pleiotrophic effect on cell morphology, stress sensitivity, and gene expression in *Enterococcus faecalis*. *J. Bacteriol. 182*, 4512-4520.

Gillen, C.M., Courtney, H.S., Schulze, K., Rohde, M., Wilson, M.R., Timmer, A.M., Guzman, C.A., Nizet, V., Chhatwal, G.S., and Walker, M.J. (2008). Opacity factor activity and epithelial cell binding by the serum opacity factor protein of *Streptococcus pyogenes* are functionally discrete. *J. Biol. Chem. 283*, 6359-6366.

Goldmann, O., Chhatwal, G.S., and Medina, E. (2003). Immune mechanisms underlying host susceptibility to infection with group A streptococci. *J. Infect. Dis. 187*, 854-861.

Goldmann, O., Chhatwal, G.S., and Medina, E. (2005a). Contribution of natural killer cells to the pathogenesis of septic shock induced by *Streptococcus pyogenes* in mice. *J. Infect. Dis. 191*, 1280-1286.

Goldmann, O., Hertzen, E., Hecht, A., Schmidt, H., Lehne, S., Norrby-Teglund, A., and Medina, E. (2010). Inducible cyclooxygenase released prostaglandin E2 modulates the severity of infection caused by *Streptococcus pyogenes*. *J. Immunol. 185*, 2372-2381.

Goldmann, O., Lengeling, A., Bose, J., Bloecker, H., Geffers, R., Chhatwal, G.S., and Medina, E. (2005b). The role of the MHC on resistance to group a streptococci in mice. *J. Immunol. 175*, 3862-3872.

Goldmann, O., Rohde, M., Chhatwal, G.S., and Medina, E. (2004). Role of macrophages in host resistance to group A streptococci. *Infect. Immun. 72*, 2956-2963.

Goldmann, O., Sastalla, I., Wos-Oxley, M., Rohde, M., and Medina, E. (2009). *Streptococcus pyogenes* induces oncosis in macrophages through the activation of an inflammatory programmed cell death pathway. *Cell. Microbiol. 11*, 138-155.

Graham, M.R., Smoot, L.M., Migliaccio, C.A., Virtaneva, K., Sturdevant, D.E., Porcella, S.F., Federle, M.J., Adams, G.J., Scott, J.R., and Musser, J.M. (2002). Virulence control in group A Streptococcus by a two-component gene regulatory system: global expression profiling and in vivo infection modeling. *Proc. Natl. Acad. Sci. U.S.A. 99*, 13855-13860.

Graham, M.R., Virtaneva, K., Porcella, S.F., Gardner, D.J., Long, R.D., Welty, D.M., Barry, W.T., Johnson, C.A., Parkins, L.D., Wright, F.A., and Musser, J.M. (2006). Analysis of the transcriptome of group A Streptococcus in mouse soft tissue infection. *Am. J. Pathol. 169*, 927-942.

Gratz, N., Hartweger, H., Matt, U., Kratochvill, F., Janos, M., Sigel, S., Drobits, B., Li, X.D., Knapp, S., and Kovarik, P. (2011). Type I interferon production induced by *Streptococcus pyogenes*-derived nucleic acids is required for host protection. *PLoS Pathog. 7*, e1001345.

Gratz, N., Siller, M., Schaljo, B., Pirzada, Z.A., Gattermeier, I., Vojtek, I., Kirschning, C.J., Wagner, H., Akira, S., Charpentier, E., and Kovarik, P. (2008). Group A streptococcus activates type I interferon production and MyD88-dependent signaling without involvement of TLR2, TLR4, and TLR9. *J. Biol. Chem. 283*, 19879-19887.

Green, N.M., Zhang, S., Porcella, S.F., Nagiec, M.J., Barbian, K.D., Beres, S.B., LeFebvre, R.B., and Musser, J.M. (2005). Genome sequence of a serotype M28 strain of group a streptococcus: potential new insights into puerperal sepsis and bacterial disease specificity. *J. Infect. Dis. 192*, 760-770.

Hakansson, A., Bentley, C.C., Shakhnovic, E.A., and Wessels, M.R. (2005). Cytolysin-dependent evasion of lysosomal killing. *Proc. Natl. Acad. Sci. U.S.A. 102*, 5192-5197.

Han, R., Caswell, C.C., Lukomska, E., Keene, D.R., Pawlowski, M., Bujnicki, J.M., Kim, J.K., and Lukomski, S. (2006). Binding of the low-density lipoprotein by streptococcal collagen-like protein Scl1 of *Streptococcus pyogenes*. *Mol. Microbiol. 61*, 351-367.

Hanski, E., and Caparon, M. (1992). Protein F, a fibronectin-binding protein, is an adhesin of the group A streptococcus *Streptococcus pyogenes*. *Proc. Natl. Acad. Sci. U.S.A. 89*, 6172-6176.

Hanski, E., Horwitz, P.A., and Caparon, M.G. (1992). Expression of protein F, the fibronectin-binding protein of *Streptococcus pyogenes* JRS4, in heterologous streptococcal and enterococcal strains promotes their adherence to respiratory epithelial cells. *Infect. Immun. 60*, 5119-5125.

Harder, J., Franchi, L., Munoz-Planillo, R., Park, J.H., Reimer, T., and Nunez, G. (2009). Activation of the Nlrp3 inflammasome by *Streptococcus pyogenes* requires streptolysin O and NF-kappa B activation but proceeds independently of TLR signaling and P2X7 receptor. *J. Immunol. 183*, 5823-5829.

Hassell, M., Fagan, P., Carson, P., and Currie, B.J. (2004). Streptococcal necrotising fasciitis from diverse strains of *Streptococcus pyogenes* in tropical northern Australia: case series and comparison with the literature. *BMC Infect. Dis. 4*, 60.

Hasty, D.L., Ofek, I., Courtney, H.S., and Doyle, R.J. (1992). Multiple adhesins of streptococci. *Infect. Immun. 60*, 2147-2152.

Herwald, H., Collin, M., Muller-Esterl, W., and Bjorck, L. (1996). Streptococcal cysteine proteinase releases kinins: a virulence mechanism. *J. Exp. Med. 184*, 665-673.

Herwald, H., Cramer, H., Morgelin, M., Russell, W., Sollenberg, U., Norrby-Teglund, A., Flodgaard, H., Lindbom, L., and Bjorck, L. (2004). M protein, a classical bacterial virulence determinant, forms complexes with fibrinogen that induce vascular leakage. *Cell 116*, 367-379.

Hidalgo-Grass, C., Dan-Goor, M., Maly, A., Eran, Y., Kwinn, L.A., Nizet, V., Ravins, M., Jaffe, J., Peyser, A., Moses, A.E., and Hanski, E. (2004). Effect of a bacterial pheromone peptide on host chemokine degradation in group A streptococcal necrotising soft-tissue infections. *Lancet 363*, 696-703.

Hidalgo-Grass, C., Mishalian, I., Dan-Goor, M., Belotserkovsky, I., Eran, Y., Nizet, V., Peled, A., and Hanski, E. (2006). A streptococcal protease that degrades CXC chemokines and impairs bacterial clearance from infected tissues. *EMBO J. 25*, 4628-4637.

Hoe, N.P., Lukomska, E., Musser, J.M., and Lukomski, S. (2007). Characterization of the immune response to collagen-like proteins Scl1 and Scl2 of serotype M1 and M28 group A Streptococcus. *FEMS Microbiol. Lett. 277*, 142-149.

Hollands, A., Aziz, R.K., Kansal, R., Kotb, M., Nizet, V., and Walker, M.J. (2008). A Naturally Occurring Mutation in ropB suppresses SpeB expression and reduces M1T1 group A streptococcal systemic virulence. *PLoS One 3*.

Hollands, A., Pence, M.A., Timmer, A.M., Osvath, S.R., Turnbull, L., Whitchurch, C.B., Walker, M.J., and Nizet, V. (2010). Genetic switch to hypervirulence reduces colonization phenotypes of the globally disseminated group A Streptococcus M1T1 clone. *J. Infect. Dis. 202*, 11-19.

Hollingshead, S.K., Readdy, T.L., Yung, D.L., and Bessen, D.E. (1993). Structural heterogeneity of the emm gene cluster in group A streptococci. *Mol. Microbiol. 8*, 707-717.

Holm, S.E. (1988). The pathogenesis of acute post-streptococcal glomerulonephritis in new lights. *APMIS. 96*, 189-193.

Hoogendijk, A.J., Roelofs, J.J., Duitman, J., van Lieshout, M.H., Blok, D.C., van der Poll, T., and Wieland, C.W. (2012). R-roscovitine reduces lung inflammation induced by lipoteichoic acid and Streptococcus pneumoniae. *Mol. Med. 18*, 1086-1095.

Horst, S.A., Linner, A., Beineke, A., Lehne, S., Holtje, C., Hecht, A., Norrby-Teglund, A., Medina, E., and Goldmann, O. (2013). Prognostic Value and Therapeutic Potential of TREM-1 in *Streptococcus pyogenes*- Induced Sepsis. J. Innate Immun. *5*, 581-590.

Horstmann, R.D., Sievertsen, H.J., Knobloch, J., and Fischetti, V.A. (1988). Antiphagocytic activity of streptococcal M protein: selective binding of complement control protein factor H. *Proc. Natl. Acad. Sci. U.S.A. 85*, 1657-1661.

Humtsoe, J.O., Kim, J.K., Xu, Y., Keene, D.R., Hook, M., Lukomski, S., and Wary, K.K. (2005). A streptococcal collagen-like protein interacts with the alpha2beta1 integrin and induces intracellular signaling. *J. Biol. Chem. 280*, 13848-13857.

Hynes, W. (2004). Virulence factors of the group A streptococci and genes that regulate their expression. *Front. Biosci. 9*, 3399-3433.

Hytonen, J., Haataja, S., Gerlach, D., Podbielski, A., and Finne, J. (2001). The SpeB virulence factor of *Streptococcus pyogenes*, a multifunctional secreted and cell surface molecule with strepadhesin, laminin-binding and cysteine protease activity. *Mol. Microbiol. 39*, 512-519.

Ikebe, T., Ato, M., Matsumura, T., Hasegawa, H., Sata, T., Kobayashi, K., and Watanabe, H. (2010). Highly frequent mutations in negative regulators of multiple virulence genes in group A streptococcal toxic shock syndrome isolates. *PLoS Pathog. 6*, e1000832.

Ikebe, T., Wada, A., Inagaki, Y., Sugama, K., Suzuki, R., Tanaka, D., Tamaru, A., Fujinaga, Y., Abe, Y., Shimizu, Y.*, et al.* (2002). Dissemination of the phage-associated novel superantigen gene speL in recent invasive and noninvasive *Streptococcus pyogenes* M3/T3 isolates in Japan. *Infect. Immun. 70*, 3227-3233.

Jaffe, J., Natanson-Yaron, S., Caparon, M.G., and Hanski, E. (1996). Protein F2, a novel fibronectin-binding protein from *Streptococcus pyogenes*, possesses two binding domains. *Mol. Microbiol. 21*, 373-384.

Jeng, A., Sakota, V., Li, Z., Datta, V., Beall, B., and Nizet, V. (2003). Molecular genetic analysis of a group A Streptococcus operon encoding serum opacity factor and a novel fibronectin-binding protein, SfbX. *J. Bacteriol. 185*, 1208-1217.

Ji, Y., Carlson, B., Kondagunta, A., and Cleary, P.P. (1997). Intranasal immunization with C5a peptidase prevents nasopharyngeal colonization of mice by the group A Streptococcus. *Infect. Immun. 65*, 2080-2087.

Ji, Y., McLandsborough, L., Kondagunta, A., and Cleary, P.P. (1996). C5a peptidase alters clearance and trafficking of group A streptococci by infected mice. *Infect. Immun. 64*, 503-510.

Johansson, L., Linner, A., Sunden-Cullberg, J., Haggar, A., Herwald, H., Lore, K., Treutiger, C.J., and Norrby-Teglund, A. (2009). Neutrophil-derived hyperresistinemia in severe acute streptococcal Infections. *J. Immunol. 183*, 4047-4054.

Johansson, L., Thulin, P., Low, D.E., and Norrby-Teglund, A. (2010). Getting under the skin: the immunopathogenesis of *Streptococcus pyogenes* deep tissue infections. *Clin. Infect. Dis. 51*, 58-65.

Johnson, D.R., Kaplan, E.L., VanGheem, A., Facklam, R.R. and Beall, B. (1996). Characterisation of group A streptococci (*Streptococcus pyogenes*): correlation of M-protein and *emm*-gene type with T-protein agglutination pattern and serum opacity factor. *J Med. Microbiol. 55*, 157-164.

Johnsson, E., Thern, A., Dahlback, B., Heden, L.O., Wikstrom, M., and Lindahl, G. (1996). A highly variable region in members of the streptococcal M protein family binds the human complement regulator C4BP. *J. Immunol. 157*, 3021-3029.

Jones, K.F., Schneewind, O., Koomey, J.M., and Fischetti, V.A. (1991). Genetic diversity among the T-protein genes of group A streptococci. *Mol. Microbiol. 5*, 2947-2952.

Joosten, L.A., Koenders, M.I., Smeets, R.L., Heuvelmans-Jacobs, M., Helsen, M.M., Takeda, K., Akira, S., Lubberts, E., van de Loo, F.A., and van den Berg, W.B. (2003). Toll-like receptor 2 pathway drives streptococcal cell wall-induced joint inflammation: critical role of myeloid differentiation factor 88. *J. Immunol. 171*, 6145-6153.

Joubert, P.E., Meiffren, G., Gregoire, I.P., Pontini, G., Richetta, C., Flacher, M., Azocar, O., Vidalain, P.O., Vidal, M., Lotteau, V.*, et al.* (2009). Autophagy induction by the pathogen receptor CD46. *Cell Host Microbe 6*, 354-366.

Kahn, F., Morgelin, M., Shannon, O., Norrby-Teglund, A., Herwald, H., Olin, A.I., and Bjorck, L. (2008). Antibodies against a surface protein of *Streptococcus pyogenes* promote a pathological inflammatory response. *PLoS Pathog. 4*, e1000149.

Kansal, R.G., Datta, V., Aziz, R.K., Abdeltawab, N.F., Rowe, S., and Kotb, M. (2010). Dissection of the molecular basis for hypervirulence of an in vivo-selected phenotype of the widely disseminated M1T1 strain of group A Streptococcus bacteria. *J. Infect. Dis. 201*, 855-865.

Kansal, R.G., McGeer, A., Low, D.E., Norrby-Teglund, A., and Kotb, M. (2000). Inverse relation between disease severity and expression of the streptococcal cysteine protease, SpeB, among clonal M1T1 isolates recovered from invasive group A streptococcal infection cases. *Infect. Immun. 68*, 6362-6369.

Kapur, V., Majesky, M.W., Li, L.L., Black, R.A., and Musser, J.M. (1993). Cleavage of interleukin 1 beta (IL-1 beta) precursor to produce active IL-1 beta by a conserved extracellular cysteine protease from *Streptococcus pyogenes*. *Proc. Natl. Acad. Sci. U.S.A. 90*, 7676-7680.

Kennedy, A.D., and DeLeo, F.R. (2009). Neutrophil apoptosis and the resolution of infection. *Immunol. Res. 43*, 25-61.

Klenk, M., Koczan, D., Guthke, R., Nakata, M., Thiesen, H.J., Podbielski, A., and Kreikemeyer, B. (2005). Global epithelial cell transcriptional responses reveal *Streptococcus pyogenes* Fas regulator activity association with bacterial aggressiveness. *Cell. Microbiol. 7*, 1237-1250.

Klenk, M., Nakata, M., Podbielski, A., Skupin, B., Schroten, H., and Kreikemeyer, B. (2007). *Streptococcus pyogenes* serotype-dependent and independent changes in infected HEp-2 epithelial cells. *ISME J. 1*, 678-692.

Kobayashi, S.D., Braughton, K.R., Palazzolo-Ballance, A.M., Kennedy, A.D., Sampaio, E., Kristosturyan, E., Whitney, A.R., Sturdevant, D.E., Dorward, D.W., Holland, S.M.*, et al.* (2010). Rapid neutrophil destruction following phagocytosis of *Staphylococcus aureus*. *J. Innate. Immun. 2*, 560-575.

Kobayashi, S.D., Braughton, K.R., Whitney, A.R., Voyich, J.M., Schwan, T.G., Musser, J.M., and DeLeo, F.R. (2003a). Bacterial pathogens modulate an apoptosis differentiation program in human neutrophils. *Proc. Natl. Acad. Sci. U.S.A. 100*, 10948-10953.

Kobayashi, S.D., Voyich, J.M., Braughton, K.R., and DeLeo, F.R. (2003b). Down-regulation of proinflammatory capacity during apoptosis in human polymorphonuclear leukocytes. *J. Immunol. 170*, 3357-3368.

Kobayashi, S.D., Voyich, J.M., Burlak, C., and DeLeo, F.R. (2005). Neutrophils in the innate immune response. *Arch. Immunol. Ther. Exp. (Warsz.) 53*, 505-517.

Kobayashi, S.D., Voyich, J.M., Somerville, G.A., Braughton, K.R., Malech, H.L., Musser, J.M., and DeLeo, F.R. (2003c). An apoptosis-differentiation program in human polymorphonuclear leukocytes facilitates resolution of inflammation. *J. Leukoc. Biol. 73*, 315-322.

Koedel, U., Frankenberg, T., Kirschnek, S., Obermaier, B., Hacker, H., Paul, R., and Hacker, G. (2009). Apoptosis is essential for neutrophil functional shutdown and determines tissue damage in experimental pneumococcal meningitis. *PLoS Pathog. 5*, e1000461.

Kono, H., and Rock, K.L. (2008). How dying cells alert the immune system to danger. *Nat. Rev. Immunol. 8*, 279-289.

Kotb, M. (1995). Bacterial pyrogenic exotoxins as superantigens. *Clin. Microbiol. Rev. 8*, 411-426.

Kotb, M., Norrby-Teglund, A., McGeer, A., El-Sherbini, H., Dorak, M.T., Khurshid, A., Green, K., Peeples, J., Wade, J., Thomson, G.*, et al.* (2002). An immunogenetic and molecular basis for differences in outcomes of invasive group A streptococcal infections. *Nat. Med. 8*, 1398-1404.

Kratovac, Z., Manoharan, A., Luo, F., Lizano, S., and Bessen, D.E. (2007). Population genetics and linkage analysis of loci within the FCT region of *Streptococcus pyogenes*. *J. Bacteriol. 189*, 1299-1310.

Kreikemeyer, B., Nakata, M., Oehmcke, S., Gschwendtner, C., Normann, J., and Podbielski, A. (2005). *Streptococcus pyogenes* collagen type I-binding Cpa surface protein. Expression profile, binding characteristics, biological functions, and potential clinical impact. *J. Biol. Chem. 280*, 33228-33239.

Kristian, S.A., Datta, V., Weidenmaier, C., Kansal, R., Fedtke, I., Peschel, A., Gallo, R.L., and Nizet, V. (2005). D-alanylation of teichoic acids promotes group a streptococcus antimicrobial peptide resistance, neutrophil survival, and epithelial cell invasion. *J. Bacteriol. 187*, 6719-6725.

Kroemer, G., El-Deiry, W.S., Golstein, P., Peter, M.E., Vaux, D., Vandenabeele, P., Zhivotovsky, B., Blagosklonny, M.V., Malorni, W., Knight, R.A.*, et al.* (2005). Classification of cell death: recommendations of the Nomenclature Committee on Cell Death. *Cell Death Differ. 12 Suppl 2*, 1463-1467.

Kroemer, G., Galluzzi, L., Vandenabeele, P., Abrams, J., Alnemri, E.S., Baehrecke, E.H., Blagosklonny, M.V., El-Deiry, W.S., Golstein, P., Green, D.R.*, et al.* (2009).

Classification of cell death: recommendations of the Nomenclature Committee on Cell Death 2009. *Cell Death Differ*. *16*, 3-11.

Kurtz, S., Phillippy, A., Delcher, A.L., Smoot, M., Shumway, M., Antonescu, C., and Salzberg, S.L. (2004). Versatile and open software for comparing large genomes. *Gen. Biol. 5*, R12.

Kwinn, L.A., and Nizet, V. (2007). How group A Streptococcus circumvents host phagocyte defenses. *Future Microbiol. 2*, 75-84.

Labbe, K., and Saleh, M. (2008). Cell death in the host response to infection. *Cell Death Differ. 15*, 1339-1349.

Lamagni, T.L., Darenberg, J., Luca-Harari, B., Siljander, T., Efstratiou, A., Henriques-Normark, B., Vuopio-Varkila, J., Bouvet, A., Creti, R., Ekelund, K.*, et al.* (2008). Epidemiology of severe *Streptococcus pyogenes* disease in Europe. *J. Clin. Microbiol. 46*, 2359-2367.

Lancefield, R.C. (1928). The Antigenic Complex of Streptococcus Haemolyticus : I. Demonstration of a Type-Specific Substance in Extracts of Streptococcus Haemolyticus. *J. Exp. Med. 47*, 91-103.

Lancefield, R.C. (1962). Current knowledge of type-specific M antigens of group A streptococci. *J. Immunol. 89*, 307-313.

Lappin, E., and Ferguson, A.J. (2009). Gram-positive toxic shock syndromes. *Lancet Infect. Dis. 9*, 281-290.

Lauth, X., von Kockritz-Blickwede, M., McNamara, C.W., Myskowski, S., Zinkernagel, A.S., Beall, B., Ghosh, P., Gallo, R.L., and Nizet, V. (2009). M1 protein allows Group A streptococcal survival in phagocyte extracellular traps through cathelicidin inhibition. *J. Innate Immun. 1*, 202-214.

Lee, W.T., and Chang, C.W. (2010). Bax is upregulated by p53 signal pathway in the SPE B-induced apoptosis. *Mol. Cell. Biochem. 343*, 271-279.

Lei, B., DeLeo, F.R., Hoe, N.P., Graham, M.R., Mackie, S.M., Cole, R.L., Liu, M., Hill, H.R., Low, D.E., Federle, M.J.*, et al.* (2001). Evasion of human innate and acquired immunity by a bacterial homolog of CD11b that inhibits opsonophagocytosis. *Nat. Med*. *7*, 1298-1305.

Lei, B., DeLeo, F.R., Reid, S.D., Voyich, J.M., Magoun, L., Liu, M., Braughton, K.R., Ricklefs, S., Hoe, N.P., Cole, R.L.*, et al.* (2002). Opsonophagocytosis-inhibiting mac protein of group a streptococcus: identification and characteristics of two genetic complexes. *Infect. Immun. 70*, 6880-6890.

Lei, B., Mackie, S., Lukomski, S., and Musser, J.M. (2000). Identification and immunogenicity of group A Streptococcus culture supernatant proteins. *Infect. Immun. 68*, 6807-6818.

Leitch, A.E., Haslet, C., and Rossi, A.G. (2009). Cyclin-dependent kinase inhibitors as potential novel anti-inflammatory and pro-resolution agents. *Brit. J. Pharm. 158,* 1004-1016.

Limbago, B., Penumalli, V., Weinrick, B., and Scott, J.R. (2000). Role of streptolysin O in a mouse model of invasive group A streptococcal disease. *Infect. Immun. 68*, 6384-6390.

Loof, T.G., Goldmann, O., Gessner, A., Herwald, H., and Medina, E. (2010). Aberrant inflammatory response to *Streptococcus pyogenes* in mice lacking myeloid differentiation factor 88. *Am. J. Pathol. 176*, 754-763.

Loof, T.G., Goldmann, O., and Medina, E. (2008). Immune recognition of *Streptococcus pyogenes* by dendritic cells. *Infect. Immun. 76*, 2785-2792.

Loof, T.G., Rohde, M., Chhatwal, G.S., Jung, S., and Medina, E. (2007). The contribution of dendritic cells to host defenses against *Streptococcus pyogenes*. *J. Infect. Dis. 196*, 1794-1803.

Lukomski, S., Burns, E.H., Jr., Wyde, P.R., Podbielski, A., Rurangirwa, J., Moore-Poveda, D.K., and Musser, J.M. (1998). Genetic inactivation of an extracellular cysteine protease (SpeB) expressed by *Streptococcus pyogenes* decreases resistance to phagocytosis and dissemination to organs. *Infect. Immun. 66*, 771-776.

Lukomski, S., Hoe, N.P., Abdi, I., Rurangirwa, J., Kordari, P., Liu, M., Dou, S.J., Adams, G.G., and Musser, J.M. (2000a). Nonpolar inactivation of the hypervariable streptococcal inhibitor of complement gene (sic) in serotype M1 *Streptococcus pyogenes* significantly decreases mouse mucosal colonization. *Infect. Immun. 68*, 535-542.

Lukomski, S., Nakashima, K., Abdi, I., Cipriano, V.J., Ireland, R.M., Reid, S.D., Adams, G.G., and Musser, J.M. (2000b). Identification and characterization of the scl gene encoding a group A Streptococcus extracellular protein virulence factor with similarity to human collagen. *Infect. Immun. 68*, 6542-6553.

Ly, D., Taylor, J.M., Tsatsaronis, J.A., Monteleone, M.M., Skora, A.S., Donald, C.A., Maddocks, T., Nizet, V., West, N.P., Ranson, M.*, et al.* (2014). Plasmin(ogen) Acquisition by Group A Streptococcus Protects against C3b-Mediated Neutrophil Killing. *J. Innate Immun.*. 6, 240-250.

Maamary, P.G., Ben Zakour, N.L., Cole, J.N., Hollands, A., Aziz, R.K., Barnett, T.C., Cork, A.J., Henningham, A., Sanderson-Smith, M., McArthur, J.D.*, et al.* (2012). Tracing the evolutionary history of the pandemic group A streptococcal M1T1 clone. *FASEB J. 26*, 4675-4684.

Maamary, P.G., Sanderson-Smith, M.L., Aziz, R.K., Hollands, A., Cole, J.N., McKay, F.C., McArthur, J.D., Kirk, J.K., Cork, A.J., Keefe, R.J.*, et al.* (2010). Parameters governing invasive disease propensity of non-M1 serotype group A streptococci. *J. Innate Immun. 2*, 596-606.

Macheboeuf, P., Buffalo, C., Fu, C.Y., Zinkernagel, A.S., Cole, J.N., Johnson, J.E., Nizet, V., and Ghosh, P. (2011). Streptococcal M1 protein constructs a pathological host fibrinogen network. *Nature. 472*, 64-68.

Manetti, A.G., Zingaretti, C., Falugi, F., Capo, S., Bombaci, M., Bagnoli, F., Gambellini, G., Bensi, G., Mora, M., Edwards, A.M.*, et al.* (2007). *Streptococcus pyogenes* pili promote pharyngeal cell adhesion and biofilm formation. *Mol. Microbiol. 64*, 968-983.

McArthur, J.D., Cook, S.M., Venturini, C., and Walker, M.J. (2012). The role of streptokinase as a virulence determinant of *Streptococcus pyogenes*--potential for therapeutic targeting. *Curr. Drug Targets 13*, 297-307.

McCormick, J.K., Yarwood, J.M., and Schlievert, P.M. (2001). Toxic shock syndrome and bacterial superantigens: an update. *Annu. Rev. Microbiol. 55*, 77-104.

McKay, F.C., McArthur, J.D., Sanderson-Smith, M.L., Gardam, S., Currie, B.J., Sriprakash, K.S., Fagan, P.K., Towers, R.J., Batzloff, M.R., Chhatwal, G.S.*, et al.* (2004). Plasminogen binding by group A streptococcal isolates from a region of hyperendemicity for streptococcal skin infection and a high incidence of invasive infection. *Infect. Immun. 72*, 364-370.

McNamara, C., Zinkernagel, A.S., Macheboeuf, P., Cunningham, M.W., Nizet, V., and Ghosh, P. (2008). Coiled-coil irregularities and instabilities in group A Streptococcus M1 are required for virulence. **Science** *319*, 1405-1408.

Medina, E., Molinari, G., Rohde, M., Haase, B., Chhatwal, G.S., and Guzman, C.A. (1999). Fc-mediated nonspecific binding between fibronectin-binding protein I of *Streptococcus pyogenes* and human immunoglobulins. *J. Immunol. 163*, 3396-3402.

Metzker, M.L. (2010). Sequencing technologies - the next generation. *Nat. Rev. Genet. 11*, 31-46.

Meyer, F., Overbeek, R., and Rodriguez, A. (2009). FIGfams: yet another set of protein families. *Nucleic acids res. 37*, 6643-6654.

Miyoshi-Akiyama, T., Takamatsu, D., Koyanagi, M., Zhao, J., Imanishi, K., and Uchiyama, T. (2005). Cytocidal effect of *Streptococcus pyogenes* on mouse neutrophils in vivo and the critical role of streptolysin S. *J. Infect. Dis. 192*, 107-116.

Mora, M., Bensi, G., Capo, S., Falugi, F., Zingaretti, C., Manetti, A.G., Maggi, T., Taddei, A.R., Grandi, G., and Telford, J.L. (2005). Group A Streptococcus produce pilus-like structures containing protective antigens and Lancefield T antigens. *Proc. Natl. Acad. Sci. U.S.A. 102*, 15641-15646.

Musser, J.M., Kapur, V., Szeto, J., Pan, X., Swanson, D.S., and Martin, D.R. (1995). Genetic diversity and relationships among *Streptococcus pyogenes* strains expressing serotype M1 protein: recent intercontinental spread of a subclone causing episodes of invasive disease. *Infect. Immun. 63*, 994-1003.

Musser, J.M., and Shelburne, S.A., 3rd (2009). A decade of molecular pathogenomic analysis of group A Streptococcus. *J. Clin. Invest. 119*, 2455-2463.

Nakagawa, I., Amano, A., Mizushima, N., Yamamoto, A., Yamaguchi, H., Kamimoto, T., Nara, A., Funao, J., Nakata, M., Tsuda, K.*, et al.* (2004a). Autophagy defends cells against invading group A Streptococcus. *Science 306*, 1037-1040.

Nakagawa, I., Nakata, M., Kawabata, S., and Hamada, S. (2001). Cytochrome c-mediated caspase-9 activation triggers apoptosis in *Streptococcus pyogenes*-infected epithelial cells. *Cell. Microbiol. 3*, 395-405.

Nakagawa, I., Nakata, M., Kawabata, S., and Hamada, S. (2004b). Transcriptome analysis and gene expression profiles of early apoptosis-related genes in *Streptococcus pyogenes*-infected epithelial cells. *Cell. Microbiol. 6*, 939-952.

Nakagawa, I., Kurokawa, K., Yamashita, A., Nakata, M., Tomiyasu, Y., Okahashi, N., Kawabata, S., Yamazaki, K., Shiba, T., Yasunaga, T. *et al*. (2003). Genome sequence of an M3 strain of *Streptococcus pyogenes* reveals a large-scale genomic rearrangement in invasive strains and new insights into phage evolution. *Gen. Res.* 13, 1042-1055.

Nannini, E.C., Teng, F., Singh, K.V., and Murray, B.E. (2005). Decreased virulence of a gls24 mutant of *Enterococcus faecalis* OG1RF in an experimental endocarditis model. *Infect. Immun. 73*, 7772-7774.

Nathan, C. (2006). Neutrophils and immunity: challenges and opportunities. *Nat. Rev. Immunol. 6*, 173-182.

Nilsson, M., Sorensen, O.E., Morgelin, M., Weineisen, M., Sjobring, U., and Herwald, H. (2006). Activation of human polymorphonuclear neutrophils by streptolysin O from *Streptococcus pyogenes* leads to the release of proinflammatory mediators. *Thromb. Haemost. 95*, 982-990.

Nitsche-Schmitz, D.P., Rohde, M., and Chhatwal, G.S. (2007). Invasion mechanisms of Gram-positive pathogenic cocci. *Thromb. Haemost. 98*, 488-496.

Nizet, V. (2007). Understanding how leading bacterial pathogens subvert innate immunity to reveal novel therapeutic targets. *J. Allergy Clin. Immunol. 120*, 13-22.

Norrby-Teglund, A., Chatellier, S., Low, D.E., McGeer, A., Green, K., and Kotb, M. (2000). Host variation in cytokine responses to superantigens determine the severity of invasive group A streptococcal infection. Eur *J. Immunol. 30*, 3247-3255.

Norrby-Teglund, A., and Johansson, L. (2013). Beyond the traditional immune response: bacterial interaction with phagocytic cells. *Int. J. Antimicrob. Agents 42*, S13-16.

Nozawa, T., Aikawa, C., Goda, A., Maruyama, F., Hamada, S., and Nakagawa, I. (2012). The small GTPases Rab9A and Rab23 function at distinct steps in autophagy during Group A Streptococcus infection. *Cell. Microbiol. 14*, 1149-1165.

O'Connor, S.P., and Cleary, P.P. (1986). Localization of the streptococcal C5a peptidase to the surface of group A streptococci. *Infect. Immun. 53*, 432-434.

O'Seaghdha, M., and Wessels, M.R. (2013). Streptolysin O and its co-toxin NAD-glycohydrolase protect group A Streptococcus from Xenophagic killing. *PLoS Pathog. 9*, e1003394.

Okada, N., Pentland, A.P., Falk, P., and Caparon, M.G. (1994). M protein and protein F act as important determinants of cell-specific tropism of *Streptococcus pyogenes* in skin tissue. *J. Clin. Invest. 94*, 965-977.

Olsen, R.J., Shelburne, S.A., and Musser, J.M. (2009). Molecular mechanisms underlying group A streptococcal pathogenesis. *Cell. Microbiol. 11*, 1-12.

Pahlman, L.I., Marx, P.F., Morgelin, M., Lukomski, S., Meijers, J.C., and Herwald, H. (2007). Thrombin-activatable fibrinolysis inhibitor binds to *Streptococcus pyogenes* by interacting with collagen-like proteins A and B. *J. Biol. Chem. 282*, 24873-24881.

Pahlman, L.I., Morgelin, M., Eckert, J., Johansson, L., Russell, W., Riesbeck, K., Soehnlein, O., Lindbom, L., Norrby-Teglund, A., Schumann, R.R.*, et al.* (2006). Streptococcal M protein: a multipotent and powerful inducer of inflammation. *J. Immunol. 177*, 1221-1228.

Pancholi, V., and Fischetti, V.A. (1992). A major surface protein on group A streptococci is a glyceraldehyde-3-phosphate-dehydrogenase with multiple binding activity. *J. Exp. Med. 176*, 415-426.

Park, J.M., Ng, V.H., Maeda, S., Rest, R.F., and Karin, M. (2004). Anthrolysin O and other gram-positive cytolysins are toll-like receptor 4 agonists. *J. Exp. Med. 200*, 1647-1655.

Parkhill, J., and Wren, B.W. (2011). Bacterial epidemiology and biology--lessons from genome sequencing. *Gen. Biol. 12*, 230.

Perea-Mejia, L.M., Inzunza-Montiel, A.E., and Cravioto, A. (2002). Molecular characterization of group A Streptococcus strains isolated during a scarlet fever outbreak. *J. Clin. Microbiol. 40*, 278-280.

Perkins, D.N., Pappin, D.J., Creasy, D.M., and Cottrell, J.S. (1999). Probability-based protein identification by searching sequence databases using mass spectrometry data. *Electrophoresis 20*, 3551-3567.

Pfaffl, M.W. (2001). A new mathematical model for relative quantification in real-time RT-PCR. *Nucleic Acids Res. 29*, e45.

Pfoh, E., Wessels, M.R., Goldmann, D., and Lee, G.M. (2008). Burden and economic cost of group A streptococcal pharyngitis. *Pediatrics 121*, 229-234.

Plow, E.F., Herren, T., Redlitz, A., Miles, L.A., and Hoover-Plow, J.L. (1995). The cell biology of the plasminogen system. *FASEB J. 9*, 939-945.

Podbielski, A., Hawlitzky, J., Pack, T.D., Flosdorff, A., and Boyle, M.D. (1994). A group A streptococcal Enn protein potentially resulting from intergenomic recombination exhibits atypical immunoglobulin-binding characteristics. *Mol. Microbiol. 12*, 725-736.

Podbielski, A., Woischnik, M., Leonard, B.A., and Schmidt, K.H. (1999). Characterization of nra, a global negative regulator gene in group A streptococci. *Mol. Microbiol. 31*, 1051-1064.

Pommerville, J.C. (2010). Alcamo's Fundamentals of Microbiology, 9th edn (Jones and Bartlett Publishers).

Proft, T., Webb, P.D., Handley, V., and Fraser, J.D. (2003). Two novel superantigens found in both group A and group C Streptococcus. *Infect. Immun. 71*, 1361-1369.

Radek, K., and Gallo, R. (2007). Antimicrobial peptides: natural effectors of the innate immune system. *Semin. Immunopathol. 29*, 27-43.

Ramachandran, V., McArthur, J.D., Behm, C.E., Gutzeit, C., Dowton, M., Fagan, P.K., Towers, R., Currie, B., Sriprakash, K.S., and Walker, M.J. (2004). Two distinct genotypes of prtF2, encoding a fibronectin binding protein, and evolution of the gene family in *Streptococcus pyogenes*. *J. Bacteriol. 186*, 7601-7609.

Rasmussen, M., Eden, A., and Bjorck, L. (2000). SclA, a novel collagen-like surface protein of *Streptococcus pyogenes*. *Infect. Immun. 68*, 6370-6377.

Relf, W.A., Martin, D.R., and Sriprakash, K.S. (1992). Identification of sequence types among the M-nontypeable group A streptococci. *J. Clin. Microbiol. 30*, 3190-3194.

Remijsen, Q., Kuijpers, T.W., Wirawan, E., Lippens, S., Vandenabeele, P., and Vanden Berghe, T. (2011). Dying for a cause: NETosis, mechanisms behind an antimicrobial cell death modality. *Cell Death Differ. 18*, 581-588.

Ren, Y., Xie, Y., Jiang, G., Fan, J., Yeung, J., Li, W., Tam, P.K., and Savill, J. (2008). Apoptotic cells protect mice against lipopolysaccharide-induced shock. *J. Immunol. 180*, 4978-4985.

Reuter, M., Caswell, C.C., Lukomski, S., and Zipfel, P.F. (2010). Binding of the human complement regulators CFHR1 and factor H by streptococcal collagen-like protein 1 (Scl1) via their conserved C termini allows control of the complement cascade at multiple levels. *J. Biol. Chem. 285*, 38473-38485.

Rezcallah, M.S., Boyle, M.D., and Sledjeski, D.D. (2004). Mouse skin passage of *Streptococcus pyogenes* results in increased streptokinase expression and activity. *Microbiology 150*, 365-371.

Rosch, J., and Caparon, M. (2004). A microdomain for protein secretion in Gram-positive bacteria. *Science 304*, 1513-1515.

Rossi, A.G., Sawatzky, D.A., Walker, A., Ward, C., Sheldrake, T.A., Riley, N.A., Caldicott, A., Martinez-Losa, M., Walker, T.R., Duffin, R*., et al.* (2006). Cyclin-dependent kinase inhibitors enhance the resolution of inflammation by promoting inflammatory cell apoptosis. *Nat. Med. 12*, 1056-1064.

Rutherford, K., Parkhill, J., Crook, J., Horsnell, T., Rice, P., Rajandream, M.-A., and Barrell, B. (2000). Artemis: sequence visualization and annotation. *Bioinformatics 16*, 944-945.

Sakurai, A., Maruyama, F., Funao, J., Nozawa, T., Aikawa, C., Okahashi, N., Shintani, S., Hamada, S., Ooshima, T., and Nakagawa, I. (2010). Specific behavior of intracellular *Streptococcus pyogenes* that has undergone autophagic degradation is associated with bacterial streptolysin O and host small G proteins Rab5 and Rab7. *J. Biol. Chem. 285*, 22666-22675.

Sanderson-Smith, M.L., Dinkla, K., Cole, J.N., Cork, A.J., Maamary, P.G., McArthur, J.D., Chhatwal, G.S., and Walker, M.J. (2008). M protein-mediated plasminogen binding is essential for the virulence of an invasive *Streptococcus pyogenes* isolate. *FASEB J. 22*, 2715-2722.

Schmidtchen, A., Frick, I.M., Andersson, E., Tapper, H., and Bjorck, L. (2002). Proteinases of common pathogenic bacteria degrade and inactivate the antibacterial peptide LL-37. *Mol. Microbiol. 46*, 157-168.

Schrager, H.M., Alberti, S., Cywes, C., Dougherty, G.J., and Wessels, M.R. (1998). Hyaluronic acid capsule modulates M protein-mediated adherence and acts as a ligand for attachment of group A Streptococcus to CD44 on human keratinocytes. *J. Clin. Inves. 101*, 1708-1716.

Schrager, H.M., Rheinwald, J.G., and Wessels, M.R. (1996). Hyaluronic acid capsule and the role of streptococcal entry into keratinocytes in invasive skin infection. *J. Clin. Invest. 98*, 1954-1958.

Schwartz, B., Facklam, R.R., and Breiman, R.F. (1990). Changing epidemiology of group A streptococcal infection in the USA. *Lancet 336*, 1167-1171.

Sharkawy, A., Low, D.E., Saginur, R., Gregson, D., Schwartz, B., Jessamine, P., Green, K., McGeer, A., and Ontario Group, A.S.S.G. (2002). Severe group a streptococcal soft-tissue infections in Ontario: 1992-1996. *Clin. Infect. Dis. 34*, 454-460.

Shea, P.R., Beres, S.B., Flores, A.R. Ewbank, A.L., Gonzalez-Lugo, J.H., Martagon-Rosado, A.J., Martinez-Gutierrez, J.C., Rehman, H.A., Serrano-Gonzalez, M., Fittipaldi, N. et al. (2011). Distinct signatures of diversifying selection revealed by genome analysis of respiratory tract and invasive bacterial populations. *Proc. Natl. Acad. Sci. U.S.A.*. 108, 5039-5044.

Shelburne, S.A., 3rd, Granville, C., Tokuyama, M., Sitkiewicz, I., Patel, P., and Musser, J.M. (2005). Growth characteristics of and virulence factor production by group A Streptococcus during cultivation in human saliva. *Infect. Immun. 73*, 4723-4731.

Shelburne, S.A., 3rd, Keith, D.B., Davenport, M.T., Horstmann, N., Brennan, R.G., and Musser, J.M. (2008). Molecular characterization of group A Streptococcus maltodextrin catabolism and its role in pharyngitis. *Mol. Microbiol. 69*, 436-452.

Schottmüller, H. (1903). Die Artunterscheidung der für den menschen Pathogen Streptokokken durch Blutagar. *Munch. Med. Wochenschr. 50*, 849-853.

Sierig, G., Cywes, C., Wessels, M.R., and Ashbaugh, C.D. (2003). Cytotoxic effects of streptolysin o and streptolysin s enhance the virulence of poorly encapsulated group A streptococci. *Infect. Immun. 71*, 446-455.

Silva, M.T. (2010). Bacteria-induced phagocyte secondary necrosis as a pathogenicity mechanism. *J. Leukoc. Biol. 88*, 885-896.

Silva, M.T. (2011). Macrophage phagocytosis of neutrophils at inflammatory/infectious foci: a cooperative mechanism in the control of infection and infectious inflammation. *J. Leukoc. Biol. 89*, 675-683.

Simpson, W.A., Ofek, I., Sarasohn, C., Morrison, J.C., and Beachey, E.H. (1980). Characteristics of the binding of streptococcal lipoteichoic acid to human oral epithelial cells. *J. Infect. Dis. 141*, 457-462.

Sitkiewicz, I., and Musser, J.M. (2006). Expression microarray and mouse virulence analysis of four conserved two-component gene regulatory systems in group a streptococcus. *Infect. Immun. 74*, 1339-1351.

Sitkiewicz, I., Nagiec, M.J., Sumby, P., Butler, S.D., Cywes-Bentley, C., and Musser, J.M. (2006). Emergence of a bacterial clone with enhanced virulence by acquisition of a phage encoding a secreted phospholipase A2. *Proc. Natl. Acad. Sci. U.S.A. 103*, 16009-16014.

Smeesters, P.R., McMillan, D.J., and Sriprakash, K.S. (2010). The streptococcal M protein: a highly versatile molecule. *Trends Microbiol. 18*, 275-282.

Soehnlein, O., Oehmcke, S., Ma, X., Rothfuchs, A.G., Frithiof, R., van Rooijen, N., Morgelin, M., Herwald, H., and Lindbom, L. (2008). Neutrophil degranulation mediates severe lung damage triggered by streptococcal M1 protein. *Eur. Respir. J. 32*, 405-412.

Staali, L., Bauer, S., Morgelin, M., Bjorck, L., and Tapper, H. (2006). *Streptococcus pyogenes* bacteria modulate membrane traffic in human neutrophils and selectively inhibit azurophilic granule fusion with phagosomes. *Cell. Microbiol. 8*, 690-703.

Staali, L., Morgelin, M., Bjorck, L., and Tapper, H. (2003). *Streptococcus pyogenes* expressing M and M-like surface proteins are phagocytosed but survive inside human neutrophils. *Cell. Microbiol. 5*, 253-265.

Stevens, D.L., Bisno, A.L., Chambers, H.F., Everett, E.D., Dellinger, P., Goldstein, E.J., Gorbach, S.L., Hirschmann, J.V., Kaplan, E.L., Montoya, J.G.*, et al.* (2005). Practice guidelines for the diagnosis and management of skin and soft-tissue infections. *Clin. Infect. Dis. 41*, 1373-1406.

Sullivan, M.J., Petty, N.K., and Beatson, S.A. (2011). Easyfig: a genome comparison visualizer. *Bioinformatics 27*, 1009-1010.

Sumby, P., Porcella, S.F., Madrigal, A.G., Barbian, K.D., Virtaneva, K., Ricklefs, S.M., Sturdevant, D.E., Graham, M.R., Vuopio-Varkila, J., Hoe, N.P., and Musser, J.M. (2005). Evolutionary origin and emergence of a highly successful clone of serotype M1 group a Streptococcus involved multiple horizontal gene transfer events. *J. Infect. Dis. 192*, 771-782.

Sumby, P., Whitney, A.R., Graviss, E.A., DeLeo, F.R., and Musser, J.M. (2006). Genome-wide analysis of group a streptococci reveals a mutation that modulates global phenotype and disease specificity. *PLoS Pathog. 2*, e5.

Sumby, P., Zhang, S., Whitney, A.R., Falugi, F., Grandi, G., Graviss, E.A., Deleo, F.R., and Musser, J.M. (2008). A chemokine-degrading extracellular protease made by group A Streptococcus alters pathogenesis by enhancing evasion of the innate immune response. *Infect. Immun. 76*, 978-985.

Sun, H., Ringdahl, U., Homeister, J.W., Fay, W.P., Engleberg, N.C., Yang, A.Y., Rozek, L.S., Wang, X., Sjobring, U., and Ginsburg, D. (2004). Plasminogen is a critical host pathogenicity factor for group A streptococcal infection. *Science 305*, 1283-1286.

Svensson, M.D., Sjobring, U., and Bessen, D.E. (1999). Selective distribution of a high-affinity plasminogen-binding site among group A streptococci associated with impetigo. *Infect. Immun. 67*, 3915-3920.

Svensson, M.D., Sjobring, U., Luo, F., and Bessen, D.E. (2002). Roles of the plasminogen activator streptokinase and the plasminogen-associated M protein in an experimental model for streptococcal impetigo. *Microbiology 148*, 3933-3945.

Takeda, K., Kaisho, T., and Akira, S. (2003). Toll-like receptors. *Annu. Rev. Immunol. 21*, 335-376.

Teng, F., Nannini, E.C., and Murray, B.E. (2005). Importance of gls24 in virulence and stress response of *Enterococcus faecalis* and use of the Gls24 protein as a possible immunotherapy target. *J. Infect. Dis. 191*, 472-480.

Terao, Y., Kawabata, S., Kunitomo, E., Murakami, J., Nakagawa, I., and Hamada, S. (2001). Fba, a novel fibronectin-binding protein from *Streptococcus pyogenes*, promotes bacterial entry into epithelial cells, and the fba gene is positively transcribed under the Mga regulator. *Mol. Microbiol. 42*, 75-86.

Terao, Y., Kawabata, S., Kunitomo, E., Nakagawa, I., and Hamada, S. (2002a). Novel laminin-binding protein of *Streptococcus pyogenes*, Lbp, is involved in adhesion to epithelial cells. *Infect. Immun. 70*, 993-997.

Terao, Y., Kawabata, S., Nakata, M., Nakagawa, I., and Hamada, S. (2002b). Molecular characterization of a novel fibronectin-binding protein of *Streptococcus pyogenes* strains isolated from toxic shock-like syndrome patients. *J. Biol. Chem. 277*, 47428-47435.

Terao, Y., Okamoto, S., Kataoka, K., Hamada, S., and Kawabata, S. (2005). Protective immunity against *Streptococcus pyogenes* challenge in mice after immunization with fibronectin-binding protein. *J. Infect. Dis. 192*, 2081-2091.

Timmer, A.M., Kristian, S.A., Datta, V., Jeng, A., Gillen, C.M., Walker, M.J., Beall, B., and Nizet, V. (2006). Serum opacity factor promotes group A streptococcal epithelial cell invasion and virulence. *Mol. Microbiol. 62*, 15-25.

Timmer, A.M., Timmer, J.C., Pence, M.A., Hsu, L.C., Ghochani, M., Frey, T.G., Karin, M., Salvesen, G.S., and Nizet, V. (2009). Streptolysin O promotes group A Streptococcus immune evasion by accelerated macrophage apoptosis. *J. Biol. Chem. 284*, 862-871.

Tsai, P.J., Lin, Y.S., Kuo, C.F., Lei, H.Y., and Wu, J.J. (1999). Group A Streptococcus induces apoptosis in human epithelial cells. *Infect. Immun. 67*, 4334-4339.

Tsai, W.H., Chang, C.W., Chuang, W.J., Lin, Y.S., Wu, J.J., Liu, C.C., Chang, W.T., and Lin, M.T. (2004). Streptococcal pyrogenic exotoxin B-induced apoptosis in a549 cells is mediated by a receptor- and mitochondrion-dependent pathway. *Infect. Immun. 72*, 7055-7062.

Tsai, W.H., Chang, C.W., Lin, Y.S., Chuang, W.J., Wu, J.J., Liu, C.C., Tsai, P.J., and Lin, M.T. (2008). Streptococcal pyrogenic exotoxin B-induced apoptosis in A549 cells is mediated through alpha(v)beta(3) integrin and Fas. *Infect. Immun. 76*, 1349-1357.

Tse, H., Bao, J.Y., Davies, M.R., Maamary, P., Tsoi, H.W., Tong, A.H., Ho, T.C., Lin, C.H., Gillen, C.M., Barnett, T.C*., et al.* (2012). Molecular characterization of the 2011 Hong Kong scarlet fever outbreak. *J. Infect. Dis. 206*, 341-351.

Valentin-Weigand, P., Grulich-Henn, J., Chhatwal, G.S., Muller-Berghaus, G., Blobel, H., and Preissner, K.T. (1988). Mediation of adherence of streptococci to human endothelial cells by complement S protein (vitronectin). *Infect. Immun. 56*, 2851-2855.

Vebo, H.C., Snipen, L., Nes, I.F., and Brede, D.A. (2009). The transcriptome of the nosocomial pathogen *Enterococcus faecalis* V583 reveals adaptive responses to growth in blood. *PLoS One 4*, e7660.

Vebo, H.C., Solheim, M., Snipen, L., Nes, I.F., and Brede, D.A. (2010). Comparative genomic analysis of pathogenic and probiotic *Enterococcus faecalis* isolates, and their transcriptional responses to growth in human urine. *PLoS One 5*, e12489.

Virtaneva, K., Porcella, S.F., Graham, M.R., Ireland, R.M., Johnson, C.A., Ricklefs, S.M., Babar, I., Parkins, L.D., Romero, R.A., Corn, G.J.*, et al.* (2005). Longitudinal analysis of the group A Streptococcus transcriptome in experimental pharyngitis in cynomolgus macaques. *Proc. Natl. Acad. Sci. U.S.A. 102*, 9014-9019.

Vitali, L.A., Zampaloni, C., Prenna, M., and Ripa, S. (2002). PCR m typing: a new method for rapid typing of group a streptococci. *J. Clin. Microbiol. 40*, 679-681.

von Bernuth, H., Picard, C., Jin, Z., Pankla, R., Xiao, H., Ku, C.L., Chrabieh, M., Mustapha, I.B., Ghandil, P., Camcioglu, Y.*, et al.* (2008). Pyogenic bacterial infections in humans with MyD88 deficiency. *Science 321*, 691-696.

von Pawel-Rammingen, U., Johansson, B.P., and Bjorck, L. (2002). IdeS, a novel streptococcal cysteine proteinase with unique specificity for immunoglobulin G. *EMBO J. 21*, 1607-1615.

Voyich, J.M., Braughton, K.R., Sturdevant, D.E., Vuong, C., Kobayashi, S.D., Porcella, S.F., Otto, M., Musser, J.M., and DeLeo, F.R. (2004). Engagement of the pathogen survival response used by group A Streptococcus to avert destruction by innate host defense. *J. Immunol. 173*, 1194-1201.

Walker, M.J., and Beatson, S.A. (2012). Epidemiology. Outsmarting outbreaks. *Science 338*, 1161-1162.

Walker, M.J., Barnett, T.C., McArthur, J.D., Cole, J.N., Gillen, C.M., Henningham, A., Sriprakash, K.S., Sanderson-Smith, M.L., and Nizet, V. (2014). Disease manifestations and pathogenic mechanisms of group A Streptococcus. *Clin. Micro. Rev. 27, 264-301.*

Walker, M.J., Hollands, A., Sanderson-Smith, M.L., Cole, J.N., Kirk, J.K., Henningham, A., McArthur, J.D., Dinkla, K., Aziz, R.K., Kansal, R.G.*, et al.* (2007). DNase Sda1 provides selection pressure for a switch to invasive group A streptococcal infection. *Nat. Med. 13*, 981-985.

Walker, M.J., McArthur, J.D., McKay, F., and Ranson, M. (2005). Is plasminogen deployed as a *Streptococcus pyogenes* virulence factor? *Trends Microbiol. 13*, 308-313.

Wang, H., Lottenberg, R., and Boyle, M.D. (1995). Analysis of the interaction of group A streptococci with fibrinogen, streptokinase and plasminogen. *Microb. path. 18*, 153-166.

Wang, J.R., and Stinson, M.W. (1994). M protein mediates streptococcal adhesion to HEp-2 cells. *Infect. Immun. 62*, 442-448.

Wannamaker, L.W., and Yasmineh, W. (1967). Streptococcal nucleases. I. Further studies on the A, B, and C enzymes. *J. Exp. Med. 126*, 475-496.

Wessels, M.R., and Bronze, M.S. (1994). Critical role of the group A streptococcal capsule in pharyngeal colonization and infection in mice. *Proc. Natl. Acad. Sci. U.S.A. 91*, 12238-12242.

Wessels, M.R., Moses, A.E., Goldberg, J.B., and DiCesare, T.J. (1991). Hyaluronic acid capsule is a virulence factor for mucoid group A streptococci. *Proc. Natl. Acad. Sci. U.S.A. 88*, 8317-8321.

Winter, J.E., and Bernheimer, A.W. (1964). The deoxyribonucleases of *Streptococcus pyogenes*. *J. Biol. Chem. 239*, 215-221.

Witko-Sarsat, V., Rieu, P., Descamps-Latscha, B., Lesavre, P., and Halbwachs-Mecarelli, L. (2000). Neutrophils: molecules, functions and pathophysiological aspects. *Lab. Invest. 80*, 617-653.

Xu, Y., Keene, D.R., Bujnicki, J.M., Hook, M., and Lukomski, S. (2002). Streptococcal Scl1 and Scl2 proteins form collagen-like triple helices. *J. Biol. Chem. 277*, 27312-27318.

Yamaguchi, H., Nakagawa, I., Yamamoto, A., Amano, A., Noda, T., and Yoshimori, T. (2009). An initial step of GAS-containing autophagosome-like vacuoles formation requires Rab7. *PLoS Pathog. 5*, e1000670.

Zerbino, D.R., and Birney, E. (2008). Velvet: Algorithms for *de novo* short read assembly using de Bruijn graphs. *Gen. Res. 18*, 821-829.

Zhang, M., McDonald, F.M., Sturrock, S.S., Charnock, S.J., Humphery-Smith, I., and Black, G.W. (2007). Group A streptococcus cell-associated pathogenic proteins as revealed by growth in hyaluronic acid-enriched media. *Proteomics 7*, 1379-1390.

Zinkernagel, A.S., Hruz, P., Uchiyama, S., von Kockritz-Blickwede, M., Schuepbach, R.A., Hayashi, T., Carson, D.A., and Nizet, V. (2012). Importance of Toll-like receptor 9 in host defense against M1T1 group A Streptococcus infections. *J. Innate Immun. 4*, 213-218.

APPENDIX A: MEDIA AND GENERAL BUFFER COMPONENTS

Unless noted otherwise, all media and buffers were made up to volume with distilled H_2O.

Media

Lysogeny-Broth (LB)

Tryptone	10 g/L
Yeast Extract	5 g/L
NaCl	10 g/L

LB Agar

LB	
Agar	15 g/L

Todd-Hewitt Broth (THY)

Todd-Hewitt Broth	30 g/L
Yeast Extract	10 g/L

THY Agar (THYA)

THY	
Agar	15 g/L

TSS Media

Tryptone	1.25 g/250 ml
Yeast Extract	2.5 g/250 ml
NaCl	1.25 g/250 ml
Polyethylene Glycol (PEG) 3330	25 g/250 ml

Make up to 225ml volume with dH_2O, just before culture add 12.5 ml sterile DMSO and 12.5 ml sterile 1 M $MgCl_2$

General buffers

1X Phosphate buffered saline (PBS)

NaCl	8 g/L
KCl	0.2 g/L
Na_2HPO_4	1.44 g/L
KH_2PO_4	0.24 g/L

Make up to 800 ml volume with dH_2O, adjust to pH 7.4 and expand to 1L with dH_2O

1X Phosphate buffered saline with 0.05% Tween-20 (PBST)
PBS

Tween-20	500 µl/L

Alkaline Lysis Solution 1

Glucose	0.9 g/100 ml
Tris-HCl	2.5 g/100 ml
EDTA	0.29 g/100 ml

Alkaline Lysis Solution 2

NaOH	0.8 g/100 ml
SDS	1 g/100 ml

Alkaline Lysis Solution 3

Potassium acetate	29.4 g/100 ml
Glacial acetic acid	11.5 ml/100 ml

1X Tris-Acetate-EDTA (TAE) buffer

Tris-base	4.84 g/L
Glacial acetic acid	1.14 ml/L
EDTA	0.292 g/L

DNA Loading Buffer

Bromophenol Blue	5 mg/10 ml
Glycerol	7.5 ml/10 ml

Make up to 10 ml volume with TAE buffer.

Ethidium Bromide Staining Solution

Ethidium bromide	1 µg/100 ml

5X Protein Cracking Buffer

Tris-HCl (pH 6.8)	4.5 ml/10 ml
Glycerol	5 ml/10 ml
SDS	0.5 g/10 ml
Bromophenol blue	5 mg/10 ml

Coomassie Blue Rapid Stain

Coomassie Blue R-250	2 g/L
Methanol	400 ml/L
Glacial Acetic Acid	100 ml/L

Make up to 1 L with dH_2O.

Rapid Destain

Methanol	400 ml/L
Glacial Acetic Acid	100 ml/L

Make up to 1 L with dH_2O.

1X SDS-PAGE Running Buffer

Tris base	3.03 g/L
Glycine	14.33 g/L
SDS	1 g/L

Western Transfer Buffer

Glycine	14.4 g/L
Tris base	3.02 g/L
Methanol	200 ml/L

Make up to 1 L with dH_2O.

Native Cell Lysis Buffer

Lysozyme	50 mg/50 ml
DNase I	25 µg/50 ml
PMSF	8.725 mg/ 50 ml
$MgCl_2$	476 µg/50 ml
$CaCl_2$	1.4 µg/50 ml
Triton X-100	50 µl/50 ml
NaCl	1.055 g/50 ml
NaH_2PO_4	0.3 g/50 ml
Imidazole	85 µg/50 ml

Native Wash Buffer

NaCl	17.5 g/L
NaH_2PO_4	6.9 g/L
Imidazole	1.36 g/L

Native Elution Buffer

NaCl	17.5 g/L
NaH_2PO_4	6.9 g/L
Imidazole	17 g/L

Standard Sample Solubilisation (SSS) Buffer

Urea	9.6 g/20 ml
DTT	0.308 g/20 ml
CHAPS	0.8 g/20 ml
Carrier ampholytes	400 µl/20 ml
Tris base	0.097 g/20 ml

Make up to 20 ml with ddH_2O.

5X Tris HCl Gel buffer

Tris HCl	56.8 g/250 ml

Adjust to pH 8.8 with HCl. Make up to volume with ddH_2O.

Equilibration Buffer

Urea	3.6 g/10 ml
SDS	0.2 g/10 ml
Glycerol	4 ml/10 ml
Acrylamide (25%)	1 ml/10 ml
5X Tris HCl gel buffer	2 ml/10 ml

Make up to volume with ddH_2O.

Colloidal Coomassie Blue Stain

Ammonium sulphate	170 g/L
Orthophosphoric acid (85%)	36 ml/L
Coomassie G-250	1 g/L
Methanol	340 ml/L

Mix $(NH_4)_2SO_4$, methanol, phosphoric acid and 500 ml of ddH_2O in a 1 L Schott bottle. Add Coomassie G-250 and stir with heating (60-70ºC) until Coomassie is completely dissolved (overnight). Make up to 1 L with ddH_2O.

Colloidal Coomassie Destain

Glacial acetic acid	1 ml/L

Make up to volume with ddH_2O.

MALDI Mass Spectrometry Matrix

Acetonitrile	3.5 ml/5 ml
Trifluoroacetic acid	25 µl/5 ml

Make up to volume with ddH_2O.

Acid alcohol

Ethanol	70 ml/100 ml
HCl	437 mg/100 ml

Scott's blueing solution

$MgSO_4$	2 g/100 ml
$NaHCO_3$	370 mg/100 ml

APPENDIX B: LIST OF PRIMERS USED IN THIS STUDY

Table B.1 List of primers used in this study.

Primer name	Sequence (5'-3')
Cloning primers	
GLS24-X F	CGCGCATGCCTGGTTCCGCGTGGCTCTGTGGAAGTTGGAAAAAAACAAGTTGCCGTT GATCTTG
GLS24-X R	GGCCCCGGGTTATTTTACACGTGGCTCAGCTTTTTGATC
pDC-SCLA F	CCGGTCTAGATAAAGGAGGACTCTTCATGTTGACATCAAAACACCACAA
pDC-SCLA R	ATATGAATTCTTAGTTGTTTTCTTTGCGTTTTGT
pDC-GLS24 F	CCGGTCTAGATAAAGGAGGACTCTTCGTGGAAGTTGGAAAAAAACAAGTTGCCG
pDC-GLS24 R	ATATGAATTCTTATTTTACACGTGGCTCAGCTTTTTGATC
LIC primers	
SCLA-LIC 1 F	TTCTTCCTGTCTGTTTACATTTCAAAAAAGAGTGACC
SCLA-LIC 1 R	GTGGCTTTTTTCTCCATATGTTGTTCTCTCTTTCTCT
SCLA-LIC 2 F	GTGGCTGGGCGGGGCGTAATCCTCTAAATTGAGAGGCCT
SCLA-LIC 2 R	TTGTCCTCTTCTGTTTTCGTTCCTCATCTAGCATTT
GLS24-LIC 1 F	TTCTTCCTGTCTGTTTAAGGTATTATTGATCAATTTC
GLS24-LIC 1 R	GTGGCTTTTTTCTCCATGTTCACGCCATCACGTACAG
GLS24-LIC 2 F	GTGGCTGGGCGGGGCGTAATCATATGTCGTCAATTAGGT
GLS24-LIC 2 R	TTGTCCTCTTCTGTTTATGTCCCCTTTATTTATCTT
CAT LIC F	GGAGAAAAAAGCCACTGGATATACCACC
CAT LIC R	ACGCCCCGCCCAGCCACTCATCGCAATACTGTT
Screening and sequencing primers	
pHY304 F	GATTAAGTTGGGTAACGCCAG
pHY304 R	CAGGAAACAGCTATGACCATG
M223 F	CCCAGTCACGACGTTGTAAA
M224 R	AGCGGATAACAATTTCACACA
pQE30 F	CGGATAACAATTTCACACAG
pQE30 R	GTTCTGAGGTCATTACTGG
ERMB F	GAAGGAGTGATTACATGAAC
ERMB R	CATAGAATTATTTCCTCCCG
SCLA-X F	CGCGCATGCCTGGTTCCGCGTGGCTCTGAGGCTGCTTCTACGATTATGACGT
SCLA-X R	GGCCCCGGGTAGACGTCTGTGGTTGTTAGCTACAG
RT-PCR primers	
PROS F	GCCTTGGCAGAAGTTGAGAC
PROS R	GCAAAGCAACAACAGGTTCA
GLS24 F	TCGATCGTTGAAGAAGAAGTGA
GLS24 R	GAACGTGCCATGTCTGAAAC
SCLA F	CTGAGGCTGCTTCTACGATTATG
SCLA R	TTGTATCCCAAAAGGCCACTC
HASA F	AGCGTGCTGCTCAATCATTA
HASA R	CATCCCCAATGCTAACAGGT
SPEB F	CCAAATCAACCGTAGCGACT
SPEB R	AGAAGTTACGTCCGTCAGCA
EMM F	GACTCACAAACCCCTGATGC
EMM R	GCTGCTTCACCTGTTGATGG

APPENDIX C: VECTOR CONSTRUCTION, ALLELIC EXCHANGE AND PROTEIN EXPRESSION

Primer pairs used for all PCR reactions listed here are given in parentheses, and sequences are given in Appendix C.

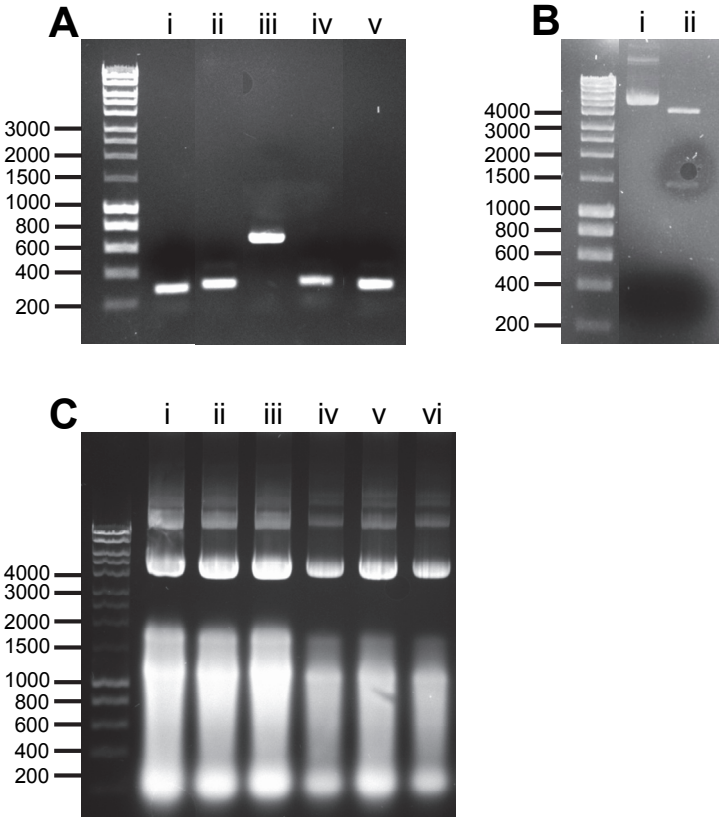

Fig. C.1 Construction of pHY-Δ*sclA* and pHY-Δ*gls24* via ligation independent cloning. **A** PCR amplicons of 250 bp NS88.2 genomic flanks upstream (**i**, **iv**) and downstream (**ii**, **v**) of *gls24* (**i**, GLS24-LIC 1 F and R; **ii**, GLS24-LIC 2 F and R) and *sclA* (**iv**, SCLA-LIC 1 F and R; **v**, SCLA-LIC 2 F and R), and the *cat* coding sequence (**iii**, CAT LIC F and R). **B** Agarose gel showing uncut pHY304-LIC (i) and *Pme*I digested pHY304-LIC (ii). **C** Representative agarose gel of pHY304-LIC transformants screened by alkaline lysis for pHY-Δ*gls24* (**i**-**iii**) and pHY-Δ*sclA* (**iv**-**vi**). All agarose gels are 1% (w/v). Molecular size markers are from Hyperladder I (Bioline, Australia), with sizes indicated in base pairs.

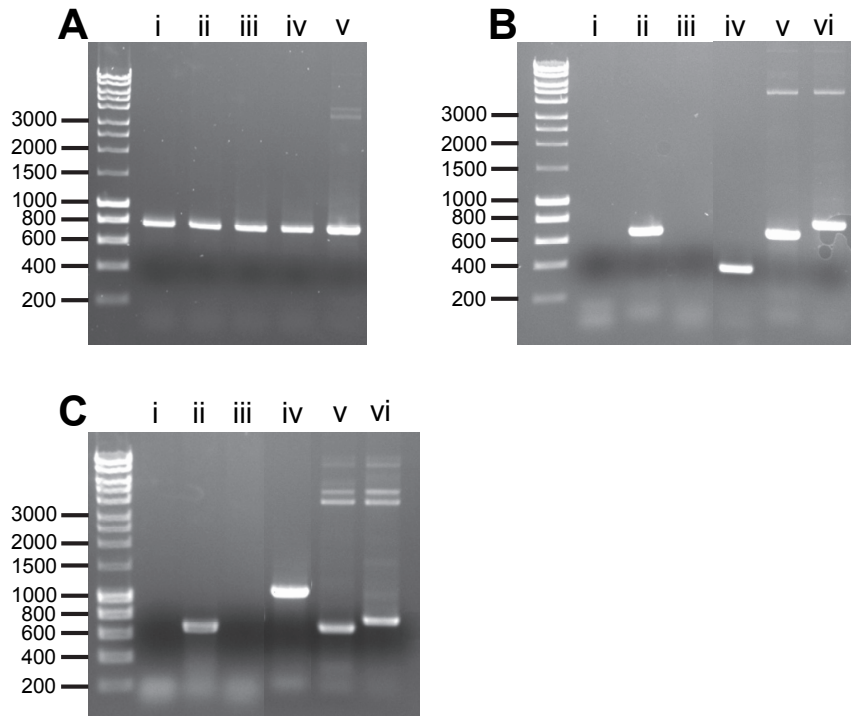

Fig. C.2 Generation of NS88.2Δ*gls24* and NS88.2Δ*sclA* by precise allelic replacement using pHY-Δ*gls24* and pHY-Δ*sclA*. A Representative agarose gel showing NS88.2 transformants screened by PCR for the presence of *ermB* (ERMB F and R) from pHY-Δ*gls24* (**i**-**ii**) or pHY-Δ*sclA* (**iii**-**iv**) and the positive control from pHY304-LIC plasmid. **B** Representative agarose gel of putative NS88.2Δ*gls24* mutants (**i**-**iii**) screened by PCR for the presence of *gls24* (**i**, **iv**; GLS24-X F and R), *cat* (**ii, v**; CAT LIC F and R) and *ermB* (**iii, vi**; ERMB F and R), with positive controls from NS88.2 gDNA (**iv**) and pure pHY-Δ*gls24* DNA (**v**-**vi**). **C** Representative agarose gel of putative NS88.2Δ*sclA* mutants (**i**-**iii**) screened by PCR for the presence of *sclA* (**i**, **iv;** SCLA-X F and R), *cat* (**ii, v**; CAT LIC F and R) and *ermB* (**iii, vi**; ERMB F and R), with positive controls from NS88.2 gDNA (**iv**) and pure pHY-Δ*sclA* DNA (**v**-**vi**). All agarose gels are 1% (w/v). Molecular size markers are from Hyperladder I (Bioline, Australia), with sizes indicated in base pairs.

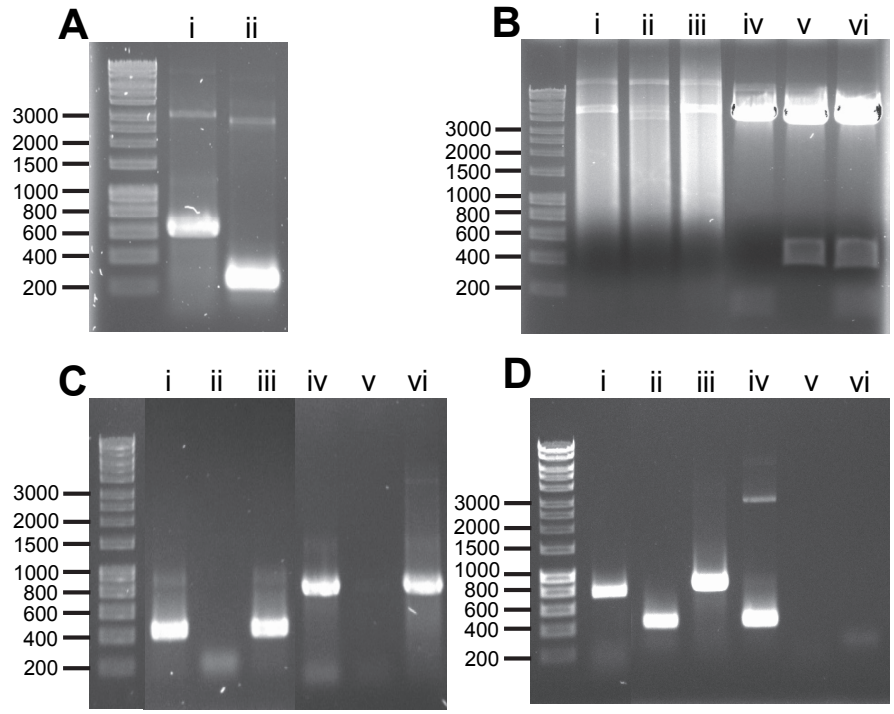

Fig. C.3 Construction of pDC-*gls24* and generation of NS88.2Δ*gls24* (pDC-*gls24*). A Representative agarose gel of pCR2.1 PCR screening for *gls24* (**i**-**ii**; M223 F and M224 R) from positive (**i**) or negative (**ii**) clones. **B** Restriction enzyme digestion of pDCerm (**i**-**iii**) and pCR-*gls24* (**iv**-**vi**) using *Xba*I (**i**, **iv**), *Eco*RI (**ii**, **v**) or *Xba*I and *Eco*RI (**iii**, **vi**). **C** Representative agarose gel of pDCerm PCR screening for *gls24* (**i-iii**; GLS-X F and R) or *ermB* (**iv-vi**; ERMB F and R) from transformant *E. coli* colonies (**i**, **iv**), sterile water (**ii**, **v**) or positive control pCR-*gls24* DNA (**iii**, **vi**). **D** Representative agarose gel of PCR screening for *gls24* (**ii, iv, v**; GLS24-X F and R) or *ermB* (**i, iii, vi**; ERMB F and R) from transformant GAS colonies (**i**-**ii**), positive control pCR-*gls24* DNA (**iii**-**iv**) or sterile water (**v**, **vi**). All agarose gels are 1% (w/v). Molecular size markers are from Hyperladder I, with sizes indicated in base pairs.

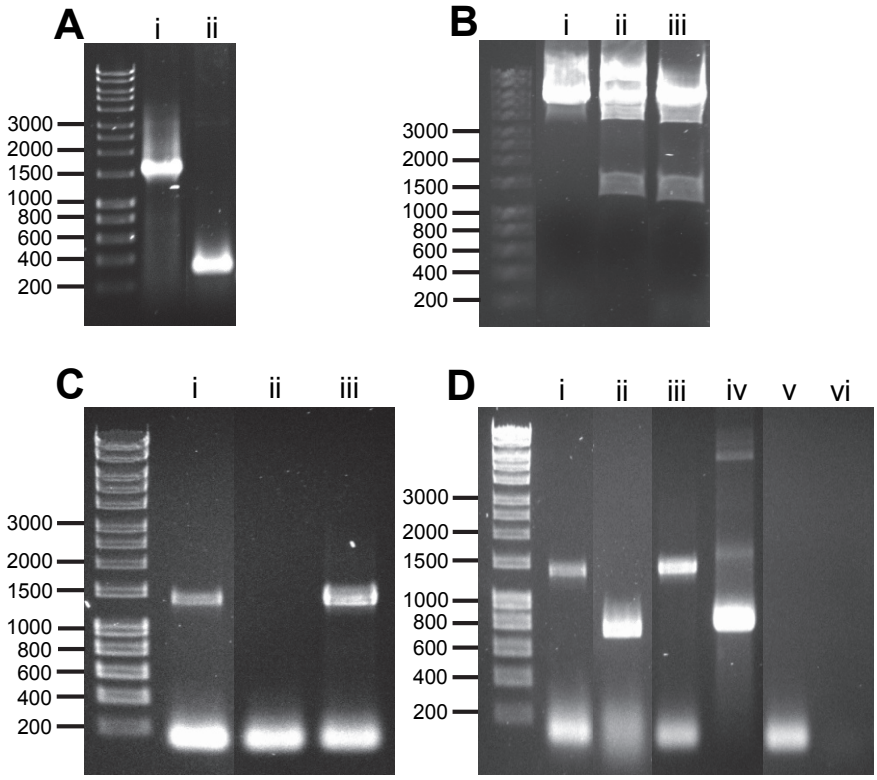

Fig. C.4 Construction of pDC-*sclA* and NS88.2Δ*sclA* (pDC-*sclA*) A Representative agarose gel of pCR2.1 transformants PCR screened for *sclA* (M223 F and M224 R) from either positive (**i**) or negative clones (**ii**). **B** Restriction enzyme digestion of pCR-*sclA* using *Xba*I (**i**), *Eco*RI (**ii**) or *Xba*I and *Eco*RI (**iii**). **C** Representative agarose gel of pDCerm PCR screening for *sclA* (SCLA-X F and R) from transformant *E. coli* colonies (**i**), sterile water (**ii**) or positive control pCR-*sclA* DNA (**iii**). **D** Representative agarose gel of pDCerm PCR screening for *sclA* (**i, iii, v**; SCLA-X F and R) or *ermB* (**ii, iv, vi**; ERMB F and R) from transformant GAS colonies (**i**-**ii**), positive control pCR-*sclA* DNA (**iii**-**iv**) or sterile water (**v**, **vi**). All agarose gels are 1% (w/v). Molecular size markers are from Hyperladder I, with sizes indicated in base pairs.

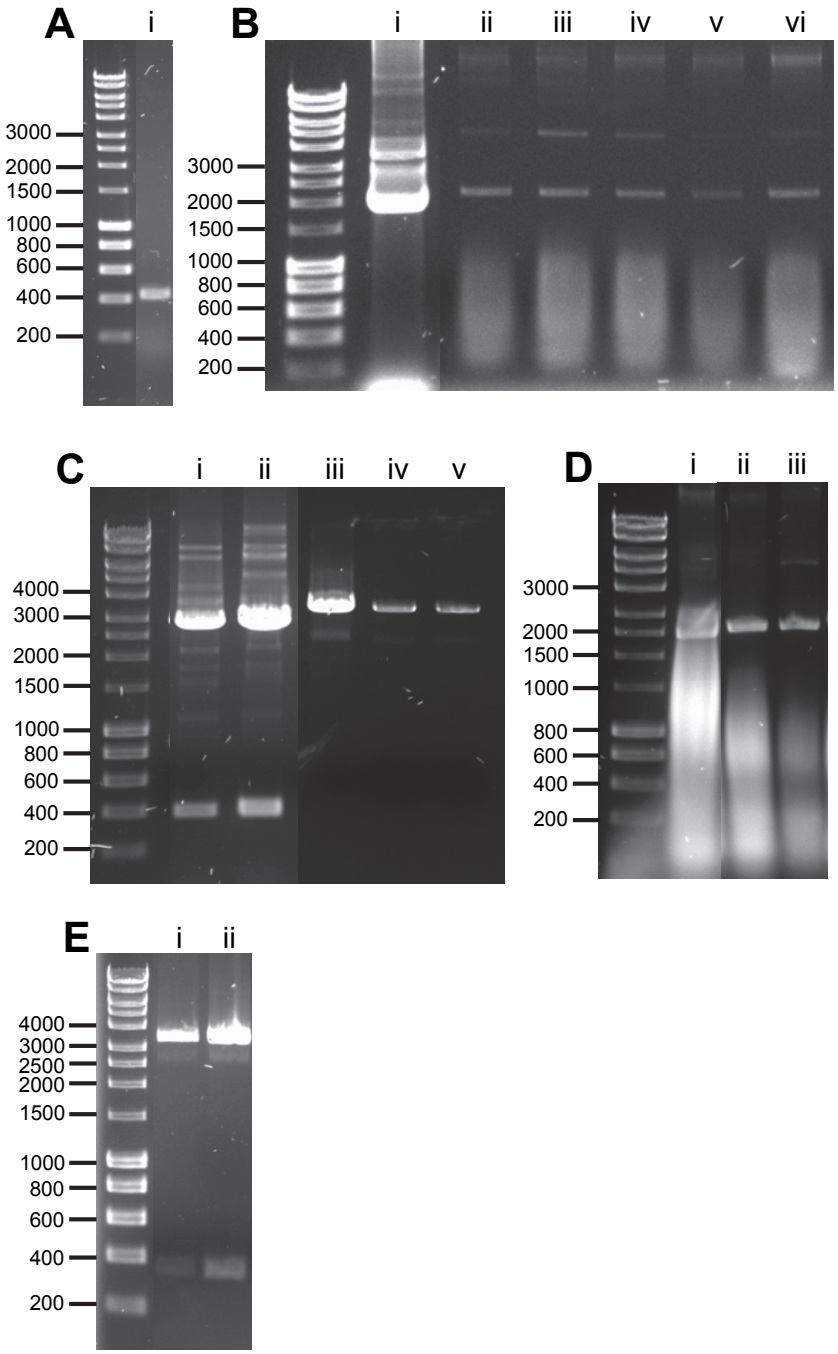

Fig. C.5 Construction of the pQE-*gls24* expression vector. A Agarose gel showing *gls24* PCR amplicon (**i**, GLS24-X F and R). **B** Representative agarose gel of pPCRscript transformants screened via alkaline lysis for blue colonies containing, self-ligated pPCRScript (**i**) and white colonies with *gls24* insert (**ii**-**vi**). **C** *Pae*I/*Sma*I double digest of pPCRscript clones showing excision of *gls24* insert (**i**-**ii**), *Pae*I/*Sma*I double digest of pQE-30 vector (**iii**), *Pae*I digest of pQE-30 (**iv**), *Sma*I digest of pQE-30 (**v**). **D** Representative agarose gel of pQE-30 transformants screened by alkaline lysis containing self-ligated pQE-30 (**i**) or colonies with *gls24* insert (**ii**-**iii**). **E** *Pae*I/*Sma*I double digest of pQE-30 clones showing excision of *gls24* insert (**i**-**ii**). All agarose gels are 1% (w/v). Molecular size markers are from Hyperladder I, with sizes indicated in base pairs.

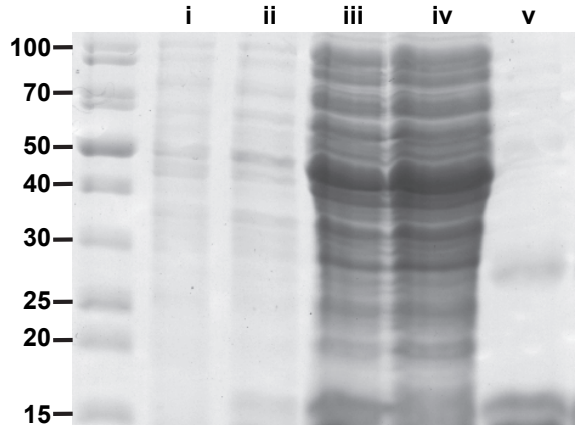

Fig. C.6 Expression and purification of NS88.2 Gls24 protein. Representative expression of the pQE-*gls24* vector in M15 (pREP4) *E. coli* showing crude lysate from uninduced culture (i) and culture induced with 1 µM IPTG for 4 h (ii). Induced *E. coli* culture were pelleted and stored at -20°C prior to thawing and lysing. Samples were added in batch to 2 ml 50% Nickel-NTA resin, incubated for 1 h at 4°C with agitation and purified over Nickel-NTA column with samples taken pre-purification (iii), after batch addition (iv) and post-elution (v). Results shown are from a 12% SDS-PAGE gel. Molecular weight markers are from Unstained Pageruler, with weights indicated in kilo-Daltons.

APPENDIX D: MALDI-TOF SPECTRUM AND PMF

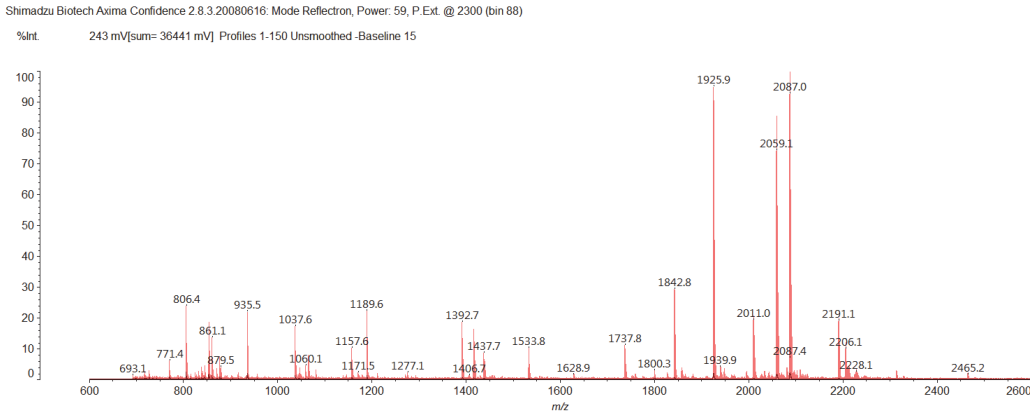

Fig. D.1 Example spectrum of streptococcal enolase (SEN) protein identified in the supernatant of NS88.2.

MASCOT Search Results

Protein View: ENO_STRP1

Enolase OS=Streptococcus pyogenes serotype M1 GN=eno PE=3 SV=2

Database: SwissProt
Score: 131
Expect: 4.8e-09
Nominal mass (M_r): 47327
Calculated pI: 4.74
Taxonomy: Streptococcus pyogenes serotype M1

Sequence similarity is available as an NCBI BLAST search of ENO_STRP1 against nr.

Search parameters

Enzyme: Trypsin: cuts C-term side of KR unless next residue is P.
Mass values searched: 14
Mass values matched: 12

Protein sequence coverage: 41%

Matched peptides shown in ***bold red***.

```
  1 MSIITDVYAR EVLDSRGNPT LEVEVYTESG AFGRGMVPSG ASTGEHEAVE
 51 LRDGDKSRYL GLGTQKAVDN VNNIIAEAII GYDVRDQQAI DRAMIALDGT
101 PNKGKLGANA ILGVSIAVAR AAADYLEVPL YTYLGGFNTK VLPTPMMNII
151 NGGSHSDAPI AFQEFMIMPV GAPTFKEGLR WGAEVFHALK KILKERGLVT
201 AVGDEGGFAP KFEGTEDGVE TILKAIEAAG YEAGENGIMI GFDCASSEFY
251 DKERKVYDYT KFEGEGAAVR TSAEQVDYLE ELVNKYPIIT IEDGMDENDW
301 DGWKVLTERL GKRVQLVGDD FFVTNTEYLA RGIKENAANS ILIKVNQIGT
351 LTETFEAIEM AKEAGYTAVV SHRSGETEDS TIADIAVATN AGQIKTGSLS
401 RTDRIAKYNQ LLRIEDQLGE VAQYKGIKSF YNLKK
```

Unformatted sequence string: 435 residues (for pasting into other applications).

Sort peptides by ◉ Residue Number ○ Increasing Mass ○ Decreasing Mass

Show predicted peptides also

Start – End	Observed	Mr(expt)	Mr(calc)	Delta	M	Peptide
2 – 10	1037.5900	1036.5827	1036.5553	0.0274	0	M.SIITDVYAR.E
17 – 34	1925.9100	1924.9027	1924.9167	-0.0139	0	R.GNPTLEVEVYTESGAFGR.G
67 – 85	2059.0600	2058.0527	2058.0745	-0.0218	0	K.AVDNVNNIIAEAIIGYDVR.D
121 – 140	2206.0900	2205.0827	2205.0994	-0.0166	0	R.AAADYLEVPLYTYLGGFNTK.V
181 – 190	1157.6000	1156.5927	1156.6029	-0.0102	0	R.WGAEVFHALK.K
197 – 211	1417.7100	1416.7027	1416.7249	-0.0222	0	R.GLVTAVGDEGGFAPK.F
212 – 224	1437.6900	1436.6827	1436.7035	-0.0208	0	K.FEGTEDGVETILK.A
271 – 285	1737.8300	1736.8227	1736.8468	-0.0241	0	R.TSAEQVDYLEELVNK.Y
314 – 331	2087.0300	2086.0227	2086.0371	-0.0144	0	R.VQLVGDDFFVTNTEYLAR.G
363 – 373	1189.6100	1188.6027	1188.5887	0.0140	0	K.EAGYTAVVSHR.S
374 – 395	2191.0800	2190.0727	2190.0652	0.0076	0	R.SGETEDSTIADIAVATNAGQIK.
414 – 425	1392.6700	1391.6627	1391.6932	-0.0305	0	R.IEDQLGEVAQYK.G

No match to: 1842.8500, 2010.9900

Fig. D.2 Example Mascot peptide mass finger print search results for streptococcal Enolase protein.

APPENDIX E: QPCR PRIMER EFFICIENCIES AND ANALYSIS

Efficiency calculation

Primer efficiencies were calculated via serial 10-fold dilution of NS88.2 cDNA, and subsequent qPCR quantification using the thermocycling program described previously (2.12). Crossing threshold cycles (Cp) were plotted against the logarithm of the template quantity and simple linear regression performed for each primer. Efficiency (Ep) of each primer was then calculated as follows:

$$\text{Efficiency (Ep)} = (10^{(-1/\text{Slope of linear regression line})} - 1) \times 100\%$$

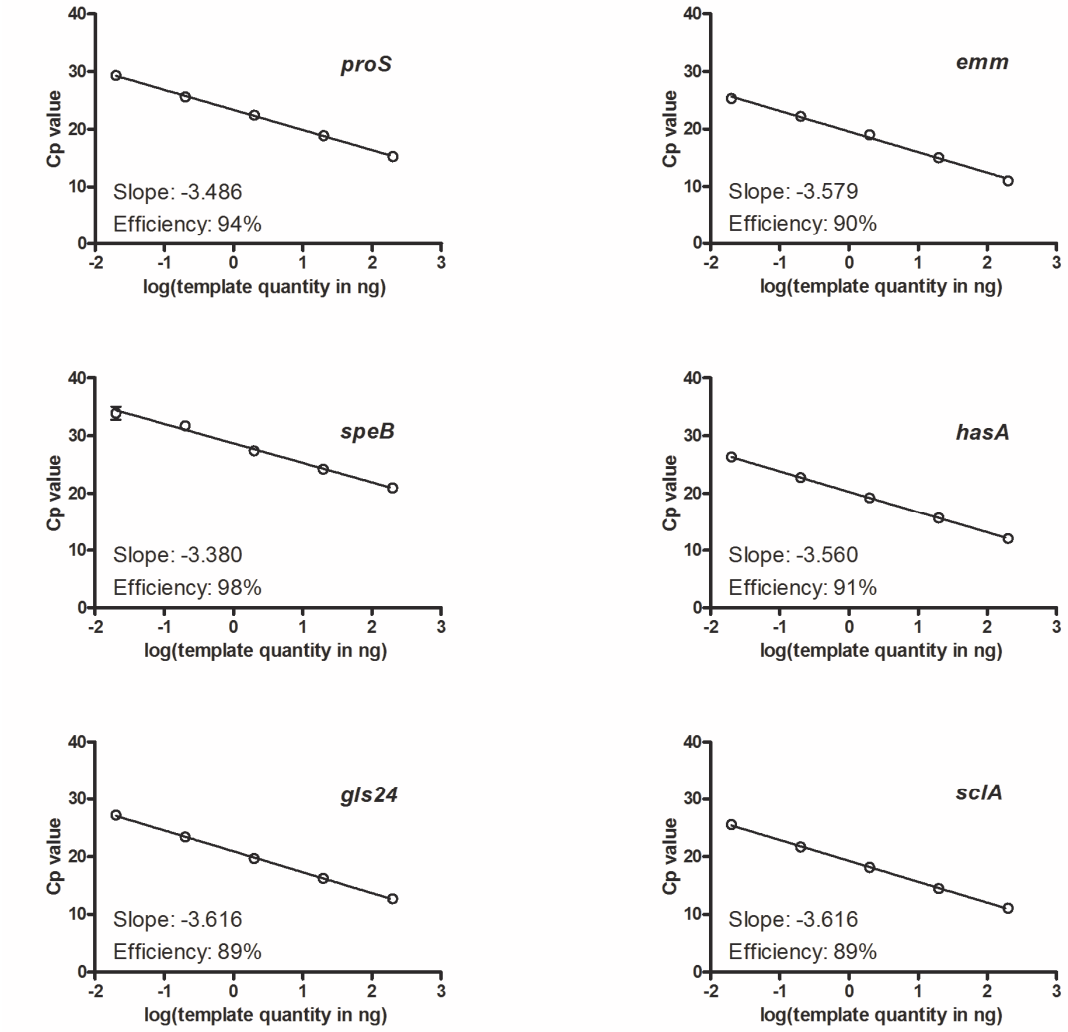

Fig. E.1 Crossing threshold cycles (Cp) of serially diluted NS88.2 cDNA used to calculate primer efficiencies. NS88.2 200 ng of cDNA was diluted ten-fold 5 times and subject to qPCR quantification. Cp cycles for each dilution were then plotted against the logarithm of template quantity, and the slope of the resulting regression line used to calculate relative primer efficiencies. Results shown are means ± standard deviations of triplicate determinations.

Melt curve analyses

Melt curves analyses were performed for each qPCR primer set (Appendix C) to ensure that single amplicons were generated from each gene. Single amplicons are demonstrated by sharp, singular peaks in the measured change in fluorescence (-[d/dT]fluorescence) resulting from SYBR green disassociation from heat denatured, single stranded DNA.

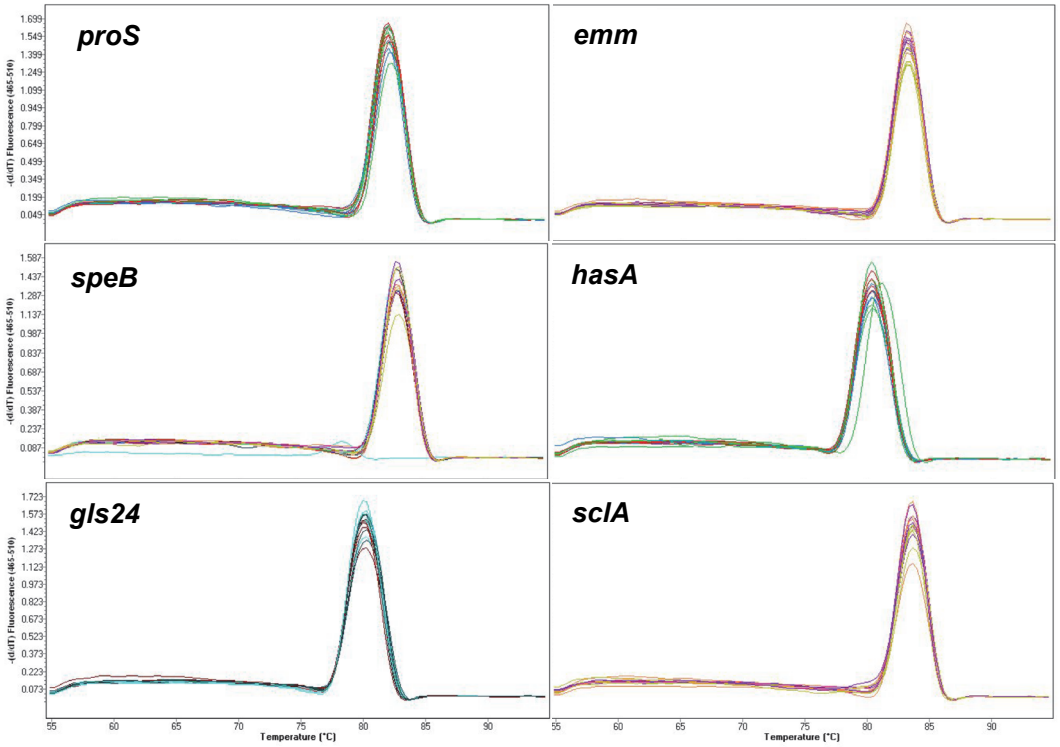

Fig. E.2 Melt curve analyses generated for each primer set used to quantify GAS gene expression. Melt curves were generated following amplification of serially ten-fold diluted cDNA template used to calculate primer efficiencies.

Calculation of normalised gene expression

Expression of GAS genes were normalised to the *proS* house-keeping gene and primer efficiency according to the equation:

Normalised fold change = $(Ep\text{-}_{target})^{\Delta Cp\text{-}target}/(Ep\text{-}_{proS})^{\Delta Cp\text{-}proS}$

Eg: *hasA:* $Cp\text{-}_{NS88.2}$: 14.2, $Cp\text{-}_{NS88.2rep}$: 20.6. Efficiency: 91% (1.91)

proS: $Cp\text{-}_{NS88.2}$: 18.9, $Cp\text{-}_{NS88.2rep}$: 19.2. Efficiency: 94% (1.94)

$\Delta Cp\text{-}_{hasA} = (Cp\text{-}_{NS88.2rep} - Cp_{NS88.2}) = 20.6 - 14.2 = 6.4$

$\Delta Cp\text{-}_{proS} = (Cp\text{-}_{NS88.2rep} - Cp_{NS88.2}) = 19.2 - 18.9 = 0.3$

Normalised *hasA* fold change (NS88.2 relative to NS88.2*rep*): $(1.91)^{6.4}/(1.94)^{0.3} = 51.6$

APPENDIX F: FLOW CYTOMETRY GATING STRATEGIES

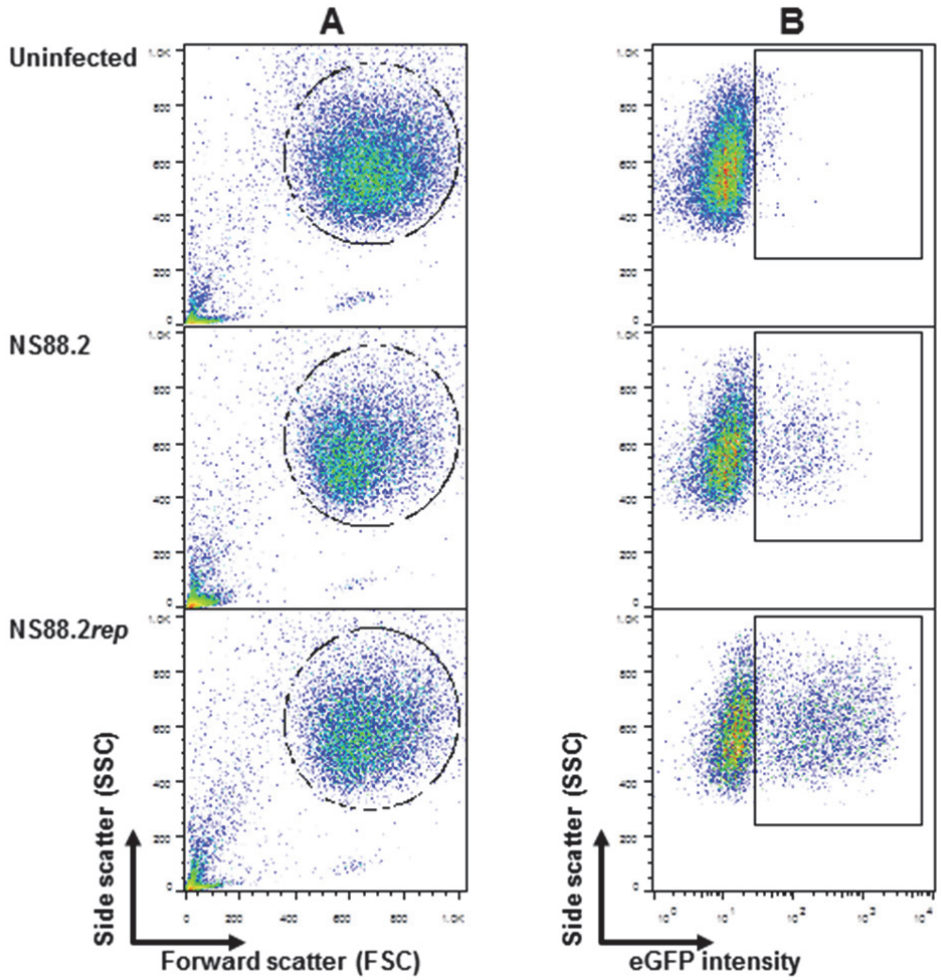

Fig. F.1 Gating strategy to assess *in vitro* purified PMN phagocytosis of eGFP expressing GAS. *In vitro* infections of PMNs with eGFP expressing GAS was conducted as described to assess PMN phagocytosis dynamics (2.16.2, 2.16.4). PMNs were identified by their characteristic forward and side scatter profile, and a single gate used to exclude debris, free GAS and other cell types (**A,** marked region). Gated PMNs (**B**, 20,000 events) were analysed for eGFP fluorescence using a 515_20 filter (**B**, marked region) to quantify association of PMNs with eGFP GAS and measure mean fluorescence intensity. Data shown are representative of six experiments; analysed results are presented in Fig 5.1A-B.

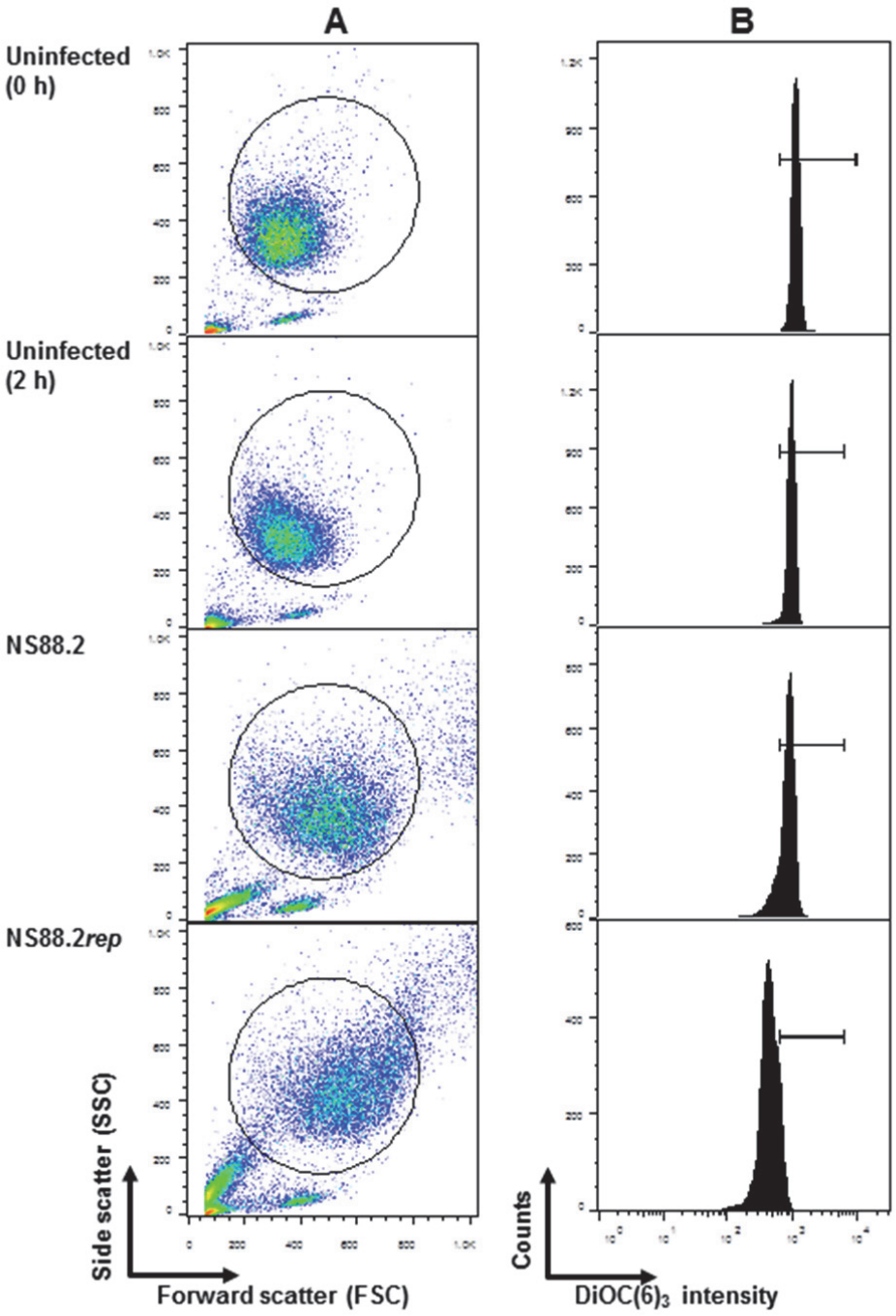

Fig. F.2 Gating strategy to assess *in vitro* purified PMN mitochondrial membrane depolarisation post-phagocytosis of GAS. *In vitro* infections of PMNs with GAS was conducted as described to assess PMN mitochondrial membrane potential (ψ_m) (2.16.2, 2.16.10). PMNs were identified by their characteristic forward and side scatter profile, and a single gate used to exclude debris, free GAS and other cell types (**A,** marked region). Gated PMNs (**B**, 10,000 events) were analysed for $DiOC(6)_3$ fluorescence using the FL-1 channel. A shift in $DiOC(6)_3$ fluorescence relative to uninfected PMNs at 0 h was used to determine ψ_m integrity (**B**, marked region). Data shown are representative of three experiments; analysed results are presented in Fig 5.2D.

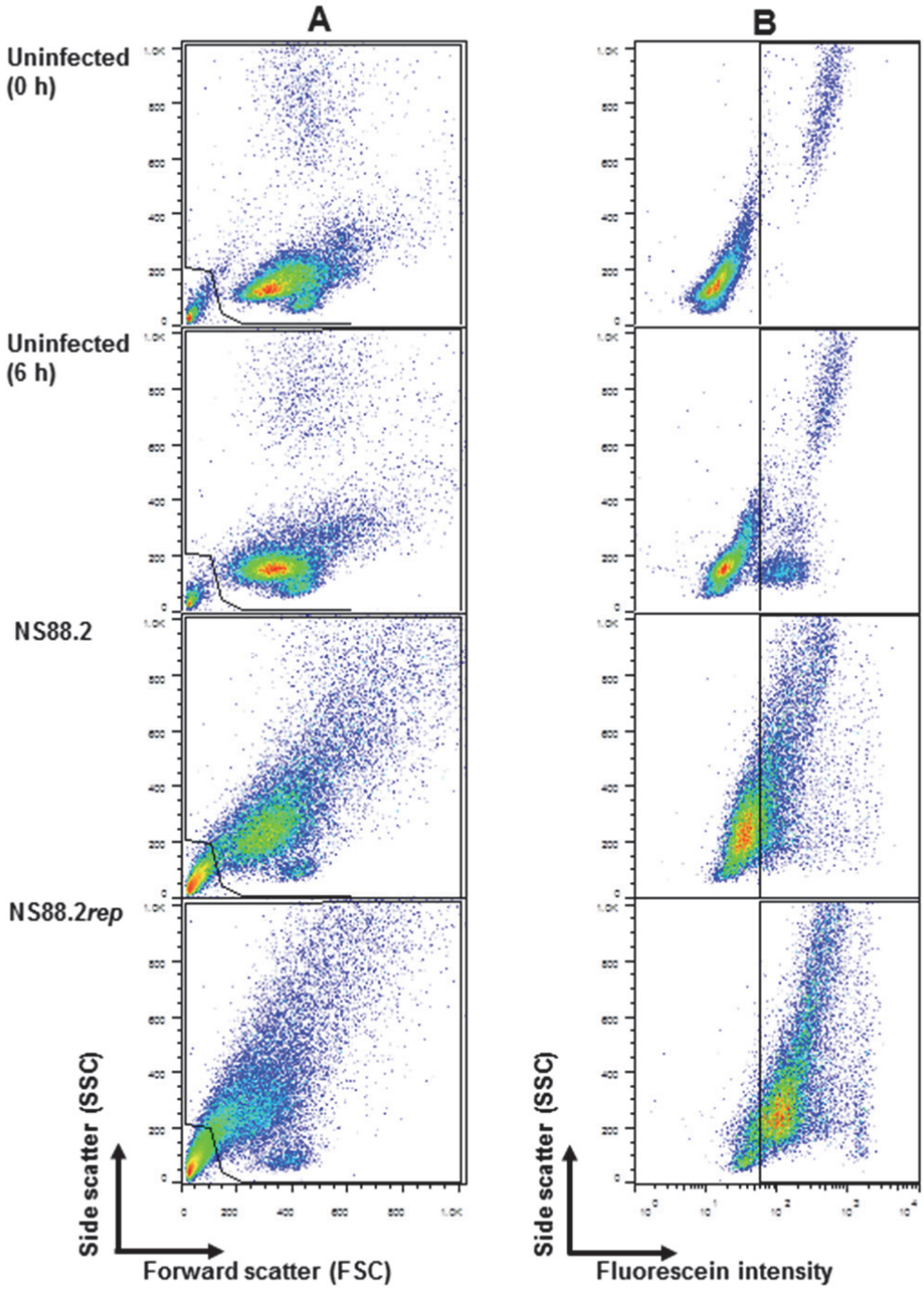

Fig. F.3 Gating strategy to assess *in vitro* purified PMN apoptosis by TUNEL staining post-phagocytosis of GAS. *In vitro* infections of PMNs with GAS was conducted as described to assess PMN apoptosis (2.16.2, 2.16.9). PMNs were identified by their characteristic forward and side scatter profile, and a single gate used to exclude debris (**A,** marked region). Note that the forward and side scatter profile of TUNEL stained PMNs differs from other experiments due to fixation and overnight ethanol incubation. Gated PMNs (**B**, 20,000 events) were analysed for fluorescein fluorescence using a 515_20 filter (**B**, marked region) to quantify TUNEL staining of apoptotic PMN nuclei. Data shown are representative of five experiments; analysed results are presented in Fig 5.2D.

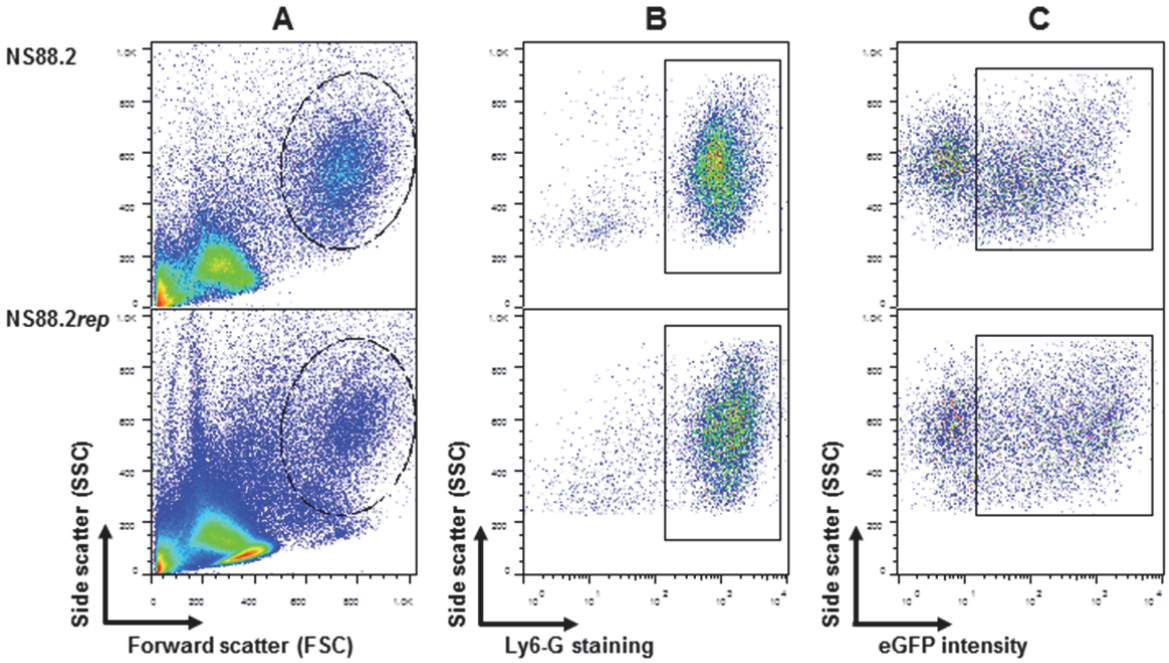

Fig. F.4 Gating strategy to assess *in vivo* murine neutrophil phagocytosis of eGFP expressing GAS. Intradermal infection of C57BL/6 mice with eGFP expressing GAS was conducted as described (2.17.2) to quantify murine neutrophil phagocytosis of eGFP expressing GAS *in vivo*. PMNs were identified in lavage fluid by their characteristic forward and side scatter profile, and a single gate used to exclude debris, free GAS and other cell types (**A,** marked region). Gated PMNs (**B**, 10,000 events) were analysed for the murine neutrophil specific Ly6-G antigen using a 575_26 filter (**B,** marked region). Ly6-G^{+} cells (**C**) were analysed for eGFP fluorescence as described for human PMNs (2.16.4) using a 515_20 filter (**C**, marked region). Data shown are representative of three experiments; analysed results are presented in Fig 5.4A.

APPENDIX G: SUPPLEMENTARY GENOME ANALYSES

Table G.1 Genes contained within the NS88.2 prophage-like region.

Loci	Genome annotation	Significant matches to Pfam motifs
888122	Paratox	None
888425	SpeL	streptococcal toxin, beta-grasp domain
889080	Phage holin	Bacteriophage holin
889304	Phage holin	Bacteriophage holin
889595	Phage protein	None
890274	Hypothetical phage protein	N-6 DNA Methylase
891100	Phage protein	None
891546	Phage terminase, large subunit	None
892802	Phage portal	Phage portal protein, SPP1 Gp6-like
894273	Hypothetical protein	Phage Mu protein F like protein
895203	Hypothetical protein	None
895612	Phage capsid and scaffold	None
896155	Putative structural phage protein	None
896559	Phage major capsid protein	Phage major capsid protein E
897645	Hypothetical phage protein	None
897901	Conserved hypothetical protein, phage associated	Phage QLRG family, putative DNA packaging
898251	Conserved hypothetical protein, 370.2 phage	None
898547	Hypothetical protein	Bacteriophage tail protein family
898900	Hypothetical protein	None
899286	Phage tail protein	Phage major tail protein 2
899865	Hypothetical protein	Phage protein
900254	Hypothetical protein	None
900572	Phage tail length tape-measure protein	Phage-related minor tail protein
901441	Putative human platelet-binding protein - phage associated	None
903318	Tail protein, putative	Siphovirus Phage tail protein
904085	Minor structural protein	None
904575	Phage endopeptidase	None
906114	Phage hyaluronidase	gp58-like protein
908241	Phage protein	Protein of unknown function (DUF1617)
908967	Hypothetical protein	None
909529	Hypothetical protein	None
910029	Hypothetical protein	None
910219	Hypothetical protein	None
910679	Putative DNA primase, phage associated	D5 proteins of DNA viruses and bacteriophage P4 DNA primases phages
912336	Phage protein	Primase C terminal 1
913194	Hypothetical protein	None
913469	Hypothetical protein	None
913795	Unknown phage protein	None
914169	Hypothetical protein	None
914360	Hypothetical protein	None
914937	Prophage ps3 protein 13	Phage regulatory protein Rha
915741	Phage protein	None
915876	Phage protein	None
916304	Transcriptional regulator	Helix-turn-Helix

916538	Conserved hypothetical protein, phage associated	Helix-turn-Helix
916898	Putative repressor protein, phage associated	Helix-turn-Helix
917334	Hypothetical protein	None
917513	Unknown phage protein	None
917871	Phage antirepressor protein	ORF6C domain (anti-repressor from Lactococcus phage)
918323	ORF2	Protein of unknown function (Possible Mu DNA binding domain)
919275	Hypothetical protein	Helix-turn-helix domain
919596	Hypothetical protein	None
920070	Hypothetical protein	None
920460	Repressor protein	Helix-turn-Helix
920898	Hypothetical protein	Protein of unknown function (DUF1617)
921363	Phage hyaluronidase	gp58-like protein
923157	Hyaluronate lyase, phage associated	Hyaluronidase protein (HylP)
923824	Phage hyaluronidase, phage endopeptidase	None
925752	Phage associated protein	None
926444	Phage minor tail protein #GP26 human platelet-binding protein	None
928759	Hypothetical protein	NUMOD4 motif (found in homing endonucleases)
929102	Phage minor tail protein #GP26 human platelet-binding protein	None
929701	Phage protein	None
930087	Phage protein	None
930361	Phage major tail protein	None
930965	Phage associated protein	None
931301	Phage associated protein	Phage minor tail protein
931530	Phage protein	None
931828	Phage protein	Phage protein Gp19/Gp15/Gp42
932264	Hypothetical protein	None
932476	Phage major capsid protein	Phage capsid family
933381	Phage capsid and scaffold	None
933956	Phage terminase	Phage Terminase
935435	Hypothetical protein	None
935697	Hypothetical phage protein	None
935926	Phage associated protein	None
936156	Phage protein	None
937642	Phage portal protein; phage capsid and scaffold	Phage portal protein, SPP1 Gp6-like
938907	Phage protein	No sig matches
939839	Phage protein	Protein of unknown function
940680	Phage protein	None
942031	Conserved hypothetical protein, phage associated	None
942750	Phage protein	N-6 DNA Methylase
943190	Putative methyltransferase	DNA methylase
943678	Hypothetical protein	None
943944	Hypothetical phage protein	None
944125	Hypothetical protein	None
944634	Hypothetical protein	None
945168	Conserved hypothetical protein, phage associated	Protein of unknown function (DUF1351)
946206	Phage related protein lin1242	RecT family (ssDNA binding)

947000	Hypothetical protein	None
947385	Hypothetical protein	None
947600	Hypothetical protein	None
947737	Hypothetical protein	None
947951	Dna replication protein dnaD	Replication initiation and membrane attachment protein (DnaB)
949069	Phage transcriptional regulator Cro/CI	Helix-turn-Helix
949420	Conserved hypothetical protein, phage associated	Domain of unknown function (DUF955)
949812	Hypothetical protein	None
950205	Phage integrase	Phage integrase family
951580	Phage protein	None
952241	Phage lysin	CHAP domain, SH3 domain
952995	Phage protein	AP2 domain (DNA binding)
953920	Phage lysin	Mannosyl-glycoprotein endo-beta-N-acetylglucosaminidase
954599	Phage protein	None
954781	Phage protein	None
955091	Hypothetical protein	None
955391	Hypothetical protein	None
955663	Putative ABC transporter	None (Weak match to ABC transporter family)
956319	Hypothetical protein	None
956601	Conserved hypothetical protein, phage associated	ParB-like nuclease domain
957042	Hypothetical protein	None
957816	Hypothetical protein	None
958003	Phage excisionase	None
958457	Hypothetical phage protein	No sig matches (weak match to phage minor tail protein)
958835	Putative protein Ymh	Protein of unknown function (associated with phage/plasmids)
959874	Phage antirepressor protein	AntA/AntB antirepressor, Phage antirepressor protein KilAC domain
960602	Conserved hypothetical protein, phage assocaited	None
961661	Hypothetical phage protein	None
961828	Phage protein	Protein of unknwon function (DUF3310)
962306	Hypothetical protein	None
962646	Conserved hypothetical protein, phage assocaited	VRR-NUC domain (associated with members of the PD-(D/E)XK nuclease superfamily)
963211	DNA primase	Poxvirus D5 protein-like
964682	Phage protein	Bifunctional DNA primase/polymerase, N-terminal, Primase C terminal 1 (PriCT-1)
965497	Conserved hypothetical protein, phage assocaited	Protein of unknown function (DUF669)
965971	Putative helicase, phage associated	Type III restriction enzyme - res subunit, Helicase conserved C-terminal domain
967302	NTP binding protein	ATPase family associated with various cellular activities (Often act as chaperones)
967983	Hypothetical protein	Siphovirus Gp157 (Sfi type)
968692	Hypothetical phage protein	Helix-turn-Helix
969022	Conserved hypothetical protein, phage associated	None
969153	Unknown phage protein	None
969527	Hypothetical phage protein	Helix-turn-Helix
969852	Hypothetical protein	None
970110	Integrase	None
970615	Integrase	Phage integrase family
971544	Lipoprotein, putative	None

Table G.2 List of phage regions from fully sequenced GAS genomes Maq mapped by NS88.2 read pairs

Phage	Region of mapped reads		
	Start	End	Size (bp)
315.1	10506	11141	635
315.1	31101	31265	164
315.1	33927	34208	281
315.1	34663	35258	595
315.2	39550	40873	1323
315.2	44890	45106	216
315.2	45691	46141	450
315.2	46511	50561	4050
315.2	50813	51308	495
315.2	54635	55688	1053
315.2	72161	72737	576
315.2	74384	74627	243
315.2	74825	75374	549
315.3	93262	94387	1125
315.3	94828	96547	1719
315.3	97474	98959	1485
315.3	102013	102895	882
315.3	103966	106738	2772
315.4	127231	128095	864
315.4	128599	130741	2142
315.4	146785	147379	594
315.5	161446	167647	6201
315.6	227794	228703	909
370.1	249178	249934	756
370.1	268210	268813	603
370.2	275970	277119	1149
370.2	283048	283381	333
370.2	305884	313120	7236
370.2	317392	318481	1089
370.3	335332	336790	1458
370.3	337537	338185	648
370.3	339769	341497	1728
370.4	352027	355690	3663
370.4	358528	364081	5553
370.4	365287	365647	360
2069.1	379381	380515	1134
2069.2	None		
5005.1	447769	448354	585
5005.1	473389	475216	1827
5005.1	484852	486148	1296
5005.2	486159	486477	318
5005.2	500292	501768	1476
5005.2	502488	504144	1656
5005.2	504747	506439	1692
5005.2	512697	518430	5733
5005.3	None		
6180.1	560724	561471	747
6180.1	580587	581217	630
6180.1	591099	592908	1809

6180.1	606018	608277	2259
6180.2	None		
6180.3	650796	652083	1287
6180.3	652884	656025	3141
6180.3	658266	659409	1143
6180.3	661833	663840	2007
6180.3	664686	665163	477
6180.4	None		
8232.1	687348	688257	909
8232.2	721881	723537	1656
8232.3	757449	758907	1458
8232.3	760857	764340	3483
8232.3	796605	797181	576
8232.4	812856	818490	5634
8232.4	821514	822981	1467
8232.4	823929	827898	3969
8232.5	864522	866007	1485
9429.1	None		
9429.2	922824	925272	2448
9429.2	926319	933600	7281
9429.2	942789	943392	603
9429.3	962436	963246	810
10270.1	1010118	1011099	981
10270.1	1011312	1012113	801
10270.2	1072071	1072701	630
10270.2	1075464	1079694	4230
10270.2	1080255	1082190	1935
10270.2	1084746	1086024	1278
10270.3	None		
10270.4	1127967	1133160	5193
10270.4	1138959	1141137	2178
10270.5	1143141	1150035	6894
10394.1	None		
10394.2	None		
10394.3	1210802	1212095	1293
10394.3	1215477	1217205	1728
10394.3	1239360	1240593	1233
10394.3	1243797	1246209	2412
10394.4	None		
10394.5	1307526	1309875	2349
10394.5	1315368	1318158	2790
10394.5	1334859	1336206	1347
10394.6	None		
10394.7	1367883	1368918	1035
10394.7	1379955	1380549	594
10394.8	1383999	1392288	8289
10394.8	1394094	1396446	2352
10750.1	None		
10750.2	1440330	1441608	1278
10750.2	1444134	1451046	6912
10750.3	1483242	1483926	684
10750.3	1484520	1485069	549

10750.3	1488609	1491543	2934
10750.3	1495980	1497816	1836
10750.4	1514124	1516293	2169
10750.4	1519386	1520745	1359
PhiMan1	1538625	1540452	1827
PhiMan1	1541901	1542792	891
PhiMan1	1562448	1563870	1422
PhiMan2	1575552	1577379	1827
PhiMan3	1605543	1607217	1674
PhiMan3	1639752	1641111	1359
PhiMan4	None		
PhiMan5	1686186	1686942	756
131.1	1699812	1700964	1152
131.1	1707930	1708578	648
131.1	1714401	1714644	243
131.2	1749927	1752555	2628
131.3	1772754	1773483	729
SPsP1	1832781	1833789	1008
SPsP2	1843992	1850733	6741
SPsP3	None		
SPsP4	1932237	1938240	6003
SPsP4	1943247	1946019	2772
SPsP5	1954347	1955634	1287
SPsP5	1961268	1966038	4770
SPsP5	1987905	1990326	2421
SPsP5	1995222	1995627	405

Table G.3 List of proteins with putative secretion signal peptides from SignalP

Loci	Signal peptide containing proteins (SignalP)
7511 - 8797	Hypothetical protein
12889 - 14148	Cationic amino acid transporter - APC Superfamily
15939 - 17135	Secreted antigen GbpB SagA PcsB, putative peptidoglycan hydrolase
30538 - 31662	Putative choline binding protein
58741 - 60045	Preprotein translocase secY subunit TC 3.A.5.1.1
82349 - 82675	Late competence protein ComGC, access of DNA to ComEA, FIG007487
83083 - 83319	Late competence protein ComGE, FIG075573
83730 - 84056	Late competence protein ComGG, FIG068335
95904 - 97478	Putative collagen binding protein
98014 - 98595	Hypothetical protein
99823 - 100410	Hypothetical protein
102159 - 103943	Protein F2-like protein
105468 - 106874	Short chain fatty acids transporter
111859 - 112878	Transcriptional regulator pfoR
115644 - 116123	V-type ATP synthase subunit K EC 3.6.3.14
123564 - 124442	Hypothetical protein spyM18_0155
126499 - 127542	Nucleoside-binding protein
128626 - 129981	Nicotine adenine dinucleotide glycohydrolase NADGH EC 3.2.2.5
130485 - 132209	Thiol-activated cytolysin pneumolysin
132348 - 132566	Hypothetical protein
133005 - 133148	Hypothetical protein
156498 - 157037	Substrate-specific component BioY of biotin ECF transporter
159085 - 160305	S-layer homology domain putative murein endopeptidase
160718 - 161191	streptococcal pyrogenic exotoxin G SpeG
165785 - 166486	Integral membrane protein Rhomboid family
166586 - 167485	UTP--glucose-1-phosphate uridylyltransferase EC 2.7.7.9
170983 - 172767	Lipid A export ATP-binding permease protein MsbA
186683 - 188002	ABC transporter, predicted N-acetylneuraminate-binding protein
188107 - 188994	ABC transporter, predicted N-acetylneuraminate transport system permease protein 1
189007 - 189837	ABC transporter, predicted N-acetylneuraminate transport system permease protein 2
201997 - 204618	Surface exclusion protein
210810 - 212378	Amino acid ABC transporter, glutamine-binding protein permease protein
212576 - 214501	Hypothetical protein
223024 - 224205	D-alanyl-D-alanine carboxypeptidase EC 3.4.16.4
224373 - 225605	D-alanyl-D-alanine carboxypeptidase EC 3.4.16.4
225936 - 227906	Oligopeptide ABC transporter, periplasmic oligopeptide-binding protein oppA TC 3.A.1.5.1
227971 - 229473	Oligopeptide transport system permease protein oppB TC 3.A.1.5.1
240786 - 241628	Cysteine ABC transporter, substrate-binding protein
241955 - 242800	Methionine ABC transporter substrate-binding protein
246465 - 247679	Dicarboxylate amino acid cation Na or H symporter
251346 - 252242	Heat shock protein HtpX protease EC 3.4.24
253974 - 255476	Transmembrane histidine kinase CsrS
268549 - 269472	OxaI YidC membrane insertion protein
279538 - 280101	Substrate-specific component RibU of riboflavin ECF transporter
280103 - 280756	Membrane-associated phospholipid phosphatase
288778 - 289710	Ferrichrome-binding periplasmic protein precursor TC 3.A.1.14.3
318523 - 318909	Hypothetical protein
327369 - 327710	Hypothetical protein
328614 - 329546	Manganese ABC transporter, periplasmic-binding protein SitA
331368 - 332174	Peptidyl-prolyl cis-trans isomerase EC 5.2.1.8
332391 - 334796	Cell division protein FtsK
340237 - 341397	Group B streptococcal surface immunogenic protein

351376 - 352440	Hypothetical protein
360270 - 360506	Preprotein translocase subunit SecG TC 3.A.5.1.1
418560 - 418988	General stress protein, putative
427804 - 428652	Phage lysin, glycosyl hydrolase, family 25
428977 - 429480	Substrate-specific component SCO2325 of predicted cobalamin ECF transporter
429464 - 429847	Additional lipoprotein component of predicted cobalamin ECF transporter
462403 - 463332	Cell division protein FtsX
475711 - 477258	Candidate zinc-binding lipoprotein ZinT
498025 - 499152	Streptolysin S export transmembrane permease SagH
500852 - 503584	Endonuclease Exonuclease phosphatase family protein
521883 - 522959	ABC transporter permease protein
533048 - 533410	Large-conductance mechanosensitive channel
554083 - 556254	Phosphoglycerol transferase
566064 - 567257	Capsule biosynthesis protein capA
579005 - 580276	periplasmic component of efflux system
580998 - 582218	ABC transporter permease protein
585828 - 587165	Cell surface protein
589459 - 590334	Cobalt-zinc-cadmium resistance protein CzcD
593572 - 593775	Membrane protein
600228 - 600935	Peptidoglycan hydrolase, Autolysin2 EC 3.5.1.28
601892 - 602917	Immunoglobulin G-endopeptidase IdeS Mac Secreted immunoglobulin binding protein Sib38
609417 - 611429	5 -nucleotidase EC 3.1.3.5
612987 - 614219	Two component system histidine kinase EC 2.7.3.-
622641 - 622811	Hypothetical protein
638772 - 639635	Cystine-binding periplasmic protein precursor
653717 - 654625	Exfoliative toxin A
654743 - 654919	Hypothetical protein
674498 - 675496	ABC transporter substrate-binding protein
689186 - 691603	Hyaluronate lyase precursor EC 4.2.2.1
696023 - 696289	uncharacterized secreted protein, YBBR Bacillus subtilis homolog
706686 - 707735	Hypothetical protein
722764 - 723999	D-alanyl-D-alanine carboxypeptidase EC 3.4.16.4
724115 - 725077	Polysaccharide deacetylase
732575 - 733648	ABC transporter, periplasmic spermidine putrescine-binding protein potD TC 3.A.1.11.1
739936 - 740667	Class B acid phosphatase precursor EC 3.1.3.2
777814 - 778563	Sortase A, LPXTG specific
779690 - 780058	Hypothetical protein
794026 - 795432	Mg2 citrate complex transporter
798259 - 799146	Citrate lyase beta chain EC 4.1.3.6
811327 - 811755	Hypothetical protein
820449 - 821999	Cardiolipin synthetase EC 2.7.8.-
834196 - 835152	Putative deoxyribose-specific ABC transporter, permease protein
835154 - 836218	Putative deoxyribose-specific ABC transporter, permease protein
837882 - 838934	Nucleoside-binding protein
850502 - 851368	Phosphate ABC transporter, periplasmic phosphate-binding protein PstS TC 3.A.1.7.1
859452 - 862013	ABC transporter permease protein
865721 - 866308	Hypothetical protein
872840 - 873613	CAMP factor
873982 - 874818	Amino acid ABC transporter, amino acid-binding protein
878742 - 879299	Signal peptidase I EC 3.4.21.89
886549 - 887037	ABC transporter, ATP-binding protein
889080 - 889307	Phage holin
971544 - 972164	lipoprotein, putative
977591 - 977704	Maltose maltodextrin ABC transporter, substrate binding periplasmic protein MalE

982811 - 984061	Poly glycerophosphate chain D-alanine transfer protein DltD
989735 - 991909	Glutamine ABC transporter, glutamine-binding protein permease protein
995287 - 995598	PTS system, cellobiose-specific IIB component EC 2.7.1.69
1000449 - 1001144	Ribosyl nicotinamide transporter, PnuC-like
1002746 - 1002874	Hypothetical protein
1022129 - 1022497	Protein G-related alpha 2 macroglobulin-binding protein GRAB
1025938 - 1028304	internalin, putative
1032896 - 1033114	Hypothetical protein
1035958 - 1036443	Peptidoglycan N-acetylglucosamine deacetylase EC 3.5.1.-
1044295 - 1045521	Chloride channel protein
1047117 - 1047878	Hypothetical protein
1051456 - 1052511	Foldase protein prsA 1 precursor EC 5.2.1.8
1067262 - 1067924	Late competence protein ComEA, DNA receptor
1081695 - 1082237	Substrate-specific component NiaX of predicted niacin ECF transporter
1085195 - 1087057	Lead, cadmium, zinc and mercury transporting ATPase EC 3.6.3.3 EC 3.6.3.5 Copper-translocating P-type ATPase EC 3.6.3.4
1087796 - 1088383	YfaA
1088361 - 1089203	Lipase Acylhydrolase with GDSL-like motif
1090885 - 1091238	Hypothetical protein
1129138 - 1130175	Lon-like protease with PDZ domain
1132610 - 1133560	Carbamate kinase EC 2.7.2.2
1134928 - 1136421	Arginine ornithine antiporter ArcD
1145580 - 1146686	Peptide methionine sulfoxide reductase MsrA EC 1.8.4.11
1146729 - 1147352	Thiol disulfide oxidoreductase associated with MetSO reductase
1147365 - 1148075	Cytochrome c-type biogenesis protein CcdA homolog, associated with MetSO reductase
1167182 - 1168906	Two-component sensor kinase YesM EC 2.7.3.-
1169807 - 1171252	Multiple sugar ABC transporter, substrate-binding protein
1171333 - 1172259	Multiple sugar ABC transporter, membrane-spanning permease protein MsmG
1172269 - 1173219	Multiple sugar ABC transporter, membrane-spanning permease protein MsmF
1207151 - 1208758	Hydrolase HAD superfamily
1220091 - 1222256	Multimodular transpeptidase-transglycosylase EC 2.4.1.129 EC 3.4.-.- Penicillin-binding protein 1A 1B PBP1
1253228 - 1253572	Hypothetical protein
1276009 - 1276995	putative esterase
1287507 - 1288790	Cell envelope-associated transcriptional attenuator LytR-CpsA-Psr, subfamily F2 as in PMID19099556
1289921 - 1291381	Guanine-hypoxanthine permease
1327794 - 1328363	ABC transporter permease protein
1334598 - 1336268	Putative ABC transporter ATP-binding protein, spy1790 homolog
1338854 - 1339876	Heme ABC transporter Streptococcus , permease protein
1341817 - 1345644	streptococcal cell surface hemoprotein receptor Shr
1354169 - 1357132	Secreted Endo-beta-N-acetylglucosaminidase EndoS
1388916 - 1389761	Integral membrane protein
1411405 - 1411956	Hypothetical protein
1413608 - 1414462	Acid phosphatase EC 3.1.3.2
1436355 - 1436489	Hypothetical protein
1455925 - 1456722	Hypothetical protein, Spy1939 homolog
1458695 - 1458925	Hypothetical protein
1481795 - 1485292	Pullulanase EC 3.2.1.41
1489850 - 1491172	Streptokinase
1494199 - 1495125	Collagen-like surface protein
1497283 - 1499469	PTS system, maltose and glucose-specific component EC 2.7.1.69
1502246 - 1504219	6-aminohexanoate-cyclic-dimer hydrolase EC 3.5.2.12
1508634 - 1509287	streptococcal mitogenic exotoxin Z SmeZ
1509957 - 1511585	Dipeptide-binding ABC transporter, periplasmic substrate-binding component TC 3.A.1.5.2
1511698 - 1512675	Dipeptide transport system permease protein DppB TC 3.A.1.5.2

1517854 - 1518774	Laminin-binding surface protein
1519408 - 1519935	Cell surface protein
1520032 - 1523493	C5a peptidase EC 3.4.21.
1523828 - 1524637	Antiphagocytic M protein
1525960 - 1527126	CDS Antiphagocytic M protein
1529593 - 1529844	Mga-associated protein
1529922 - 1531511	Immunogenic secreted protein
1535638 - 1536906	periplasmic component of efflux system
1537330 - 1537734	Hypothetical protein
1538808 - 1539737	Peptidylproline cis-trans-isomerase EC 5.2.1.8 Proteinase maturation protein RopA
1540523 - 1541719	Strepotococcal cysteine protease SpeB
1549901 - 1551244	PTS system, cellobiose-specific IIC component EC 2.7.1.69
1551254 - 1551562	PTS system, cellobiose-specific IIB component EC 2.7.1.69
1559918 - 1561558	Hypothetical protein SPy2065
1561842 - 1563341	Dipeptidase EC 3.4
1624727 - 1625599	Transporter
1625642 - 1626520	Membrane protein, putative
1636106 - 1636948	Membrane protein
1638699 - 1639778	Hypothetical protein
1646322 - 1648298	Phosphoesterase, DHH family protein
1654679 - 1655293	Immunodominant antigen A
1658143 - 1658685	CDP-diacylglycerol--glycerol-3-phosphate 3-phosphatidyltransferase EC 2.7.8.5
1664443 - 1665357	UTP--glucose-1-phosphate uridylyltransferase EC 2.7.7.9
1674190 - 1675905	ABC transporter, permease protein
1678922 - 1680145	Serine protease, DegP HtrA, do-like EC 3.4.21.
1689580 - 1692978	Extracellular Protein Factor, epf
1698719 - 1699006	Hypothetical protein
1710326 - 1710646	Hypothetical protein
1713949 - 1715313	Competence-stimulating peptide ABC transporter permease protein ComB
1717615 - 1717845	Hypothetical protein
1721798 - 1721920	Hypothetical protein

Table G.4 List of NS88.2 genes with putative cell-surface anchor HMM motifs

Loci	Signal peptide containing proteins (SignalP)
705653	Collagen-like surface protein SclB
1090263	Hypothetical protein
1481795	Pullulanase
1494199	Collagen-like surface protein
1519026	Cell surface protein
1523828	Antiphagocytic M protein
1524846	M protein
1525960	Antiphagocytic M protein
1696680	Extracellular Protein Fator, epf
1698781	Endonuclease/exonuclease/phosphatase family protein

Table G.5 List of NS88.2 genes bearing <80% sequence identity to other fully sequenced GAS genomes

Loci	Genome annotation	Significant matches to Pfam motifs
98014	FctA	None
319582	Phage protein	None
705357	SclB	Collagen triple helix
891546	Phage terminase, large subunit	Terminase family
894273	Hypothetical protein	Phage Mu protein F like protein
896155	Putative structural phage protein	None
898251	Conserved hypothetical protein, 370.2 phage	None
898547	Hypothetical protein	Bacteriophage tail protein family
898900	Hypothetical protein	None
899286	Phage tail protein	Phage major tail protein 2
899865	Hypothetical protein	Phage protein
900254	Hypothetical protein	None
900572	Phage tail length tape-measure protein	Phage-related minor tail protein
901441	Putative human platelet-binding protein, phage associated	None
903318	Tail protein, putative	Siphovirus Phage tail protein
904085	Minor structural protein	None
904575	Phage endopeptidase	None
917871	Phage antirepressor protein	ORF6C domain)
918323	ORF2	DUF3102
919596	Hypothetical protein	None
920070	Hypothetical protein	None
932264	Hypothetical protein	None
932476	Phage major capsid protein	Phage capsid family
939839	Phage protein	Protein of unknown function
1494199	streptococcal collagen-like protein A (sclA)	Collagen triple helix
1523828	M protein	Gram positive anchor
1689580	Extra-cellular protein factor (epf)	DUF1542

APPENDIX H: TRANSCRIPTIONAL MICROARRAY ANALYSIS

Table H.1 Greater than 2.0 fold differential transcription in the *covRS* mutant NS88.2 relative to NS88.2*rep*. (All genes significantly differentially expressed, $P < 0.05$ by Student's unpaired T-test)

Array Spot ID	Description	Fold change NS88.2/NS88.2*rep*	P value
NT01SP0378_1P8	Hypothetical M6 protein	88.229614	>0.0001
NT01SP1759_5I1	Collagen-like protein (Scl1/SclA)	55.097668	0.0002
NT01SP1784_5J2	C5a peptidase precursor	20.991302	0.0015
NT01SP1761_5I3	Hypothetical protein	19.6434	0.0401
NT01SP1785_5J3	C5a peptidase	18.886713	0.0012
7M14	Putative acetyl-CoA acetyltransferase	16.645632	0.0007
NT01SP1783_5J1	Fibronectin- and factor H-binding protein FbaB	15.769812	0.0010
7M12	NAD glycohydrolase	15.673019	0.0002
7M16	Streptolysin O	14.658403	0.0004
NT01SP0151_1G5	Streptolysin O precursor	13.490279	0.0007
NT01SP1949_5P21	UDP-glucose 6-dehydrogenase HasB	11.588559	0.0000
7M22	Hypothetical protein	10.115629	0.0007
NT01SP0154_1G8	Nicotinate-nucleotide pyrophosphorylase (carboxylating)	8.680448	0.0105
NT01SP0149_1G3	Nicotine adenine dinucleotide/Transposase	8.645583	0.0001
SpyM3_1703_6H6	Putative collagen-like protein (SclA protein)	7.2604804	0.0276
NT01SP1948_5P20	Hyaluronate synthase hasA	6.0195627	0.0104
NT01SP1736_5H2	Ribosomal protein S15	5.670866	0.0020
NT01SP1786_5J4	Transposase	5.5987473	0.0097
NT01SP0079_1D5	Kinase, GHMP family, putative	-5.5788984	0.0247
NT01SP1644_5D8	Putative antibiotic resistance protein NorA	-5.3511586	0.0218
NT03SP0426_6I18	Putative uncharacterized protein	4.91205	0.0123
NT01SP1923_5O21	Hypothetical membrane associated protein (DUF1700)	4.818099	0.0126
NT01SP1804_5J22	Pyrogenic exotoxin B SpeB	-4.5816684	0.0341
NT01SP1803_5J21	Inhibitor of SpeB; co-transcribed	-4.518096	0.0479
NT01SP1788_5J6	M1 protein precursor	4.3725247	0.0260
NT01SP0380_1P10	Hypothetical protein (signal peptide)	4.189857	0.0261
NT01SP1801_5J19	Gene regulated by Mga	4.066102	0.0374
NT01SP0756_2P2	Exotoxin type C precursor	3.8816411	0.0009
NT01SP1307_4F17	Conserved hypothetical protein	-3.6440828	0.0026
NT01SP1375_4I6	Aspartate-ammonia ligase	-3.6189883	0.0398
NT01SP0645_2K11	SagC (Streptolysin S)	-3.506283	0.0284
NT01SP1922_5O20	30S ribosomal protein S14 homolo	3.496096	0.0225
NT01SP1140_3P1	Glucosamine--fructose-6-phosphate aminotransferase [isomerizing]	3.4258008	0.0171
NT01SP0123_1F1	Hypothetical protein	-3.3847964	0.0011
NT01SP0230_1J8	Putative N-acetylmannosamine-6-phosphate 2-Epimerase	-3.3678224	0.0437
NT01SP0643_2K9	Streptolysin S associated protein	-3.0084574	0.0245
NT03SP0690_6L2	Hypothetical phage protein	2.9954643	0.0464
NT01SP0757_2P3	IgG-degrading protease	2.9946172	0.0120
NT01SP1790_5J8	Hypothetical protein	2.9226377	0.0150
NT01SP0299_1M4	YlbN-like protein	2.8479881	0.0360

NT01SP1321_4F24	Excisionase-related protein	-2.7499423	0.0200
NT01SP1807_5K1	Putative transcription regulator (RopB/Rgg)	-2.7335727	0.0355
NT01SP1296_4F6	Conserved hypothetical protein	-2.7113366	0.0390
NT01SP1300_4F10	Hypothetical protein (Prophage)	-2.693816	0.0166
NT01SP0846_3C19	Hypothetical protein (Prophage)	-2.565225	0.0224
NT01SP1645_5D9	PrfA, putative	2.4824119	0.0441
SpyM3_0694_6A21	Putative uncharacterized protein	-2.418434	0.0292
SpyM3_0102_6A17	Putative uncharacterized protein	-2.3645484	0.0250
NT01SP1627_5C15	A/G-specific adenine glycosylase	2.3582458	0.0044
NT01SP1876_5M22	Hypothetical protein (Prophage)	-2.294977	0.0144
NT01SP1777_5I19	Peptide ABC transporter, ATP-binding	2.2753694	0.0126
NT01SP0651_2K17	Conserved hypothetical protein	2.2155092	0.0158
NT01SP1850_5L20	Endopeptidase O	-2.2019196	0.0174
NT01SP0647_2K13	Hypothetical protein	-2.1831903	0.0204
NT01SP0648_2K14	Hypothetical protein	-2.1643605	0.0033
NT03SP0350_6I8	Exotoxin type A (SpeA)	2.1022217	0.0138
NT03SP1629_6P1	Hypothetical phage protein	2.0912435	0.0016
SpyM3_1260_6D14	Putative uncharacterized protein	-2.0735266	0.0500
NT01SP0891_3E16	Exotoxin H precursor (Prophage)	2.0626948	0.0446

APPENDIX I: PUBLICATIONS ARISING FROM PHD CANDIDATURE

The FASEB Journal article fj.12-226662. Published online March 26, 2013.

The FASEB Journal • Research Communication

Streptococcal collagen-like protein A and general stress protein 24 are immunomodulating virulence factors of group A *Streptococcus*

James A. Tsatsaronis,[*,†] Andrew Hollands,[‡,§,‖] Jason N. Cole,[‡,§,‖] Peter G. Maamary,[§,‖] Christine M. Gillen,[§,‖] Nouri L. Ben Zakour,[§,‖] Malak Kotb,[¶,#] Victor Nizet,[‡] Scott A. Beatson,[§,‖] Mark J. Walker,[§,‖,1] and Martina L. Sanderson-Smith[*,†,1,2]

*Illawarra Health and Medical Research Institute and [†]School of Biological Sciences, University of Wollongong, Wollongong, New South Wales, Australia; [‡]Department of Pediatrics, University of California–San Diego, La Jolla, California, USA; [§]Australian Infectious Diseases Research Centre and [‖]School of Chemistry and Molecular Biosciences, University of Queensland, St. Lucia, Queensland, Australia; and [¶]Veterans Affairs Medical Center and [#]Department of Molecular Genetics, Biochemistry, and Microbiology, University of Cincinnati, Cincinnati, Ohio, USA

ABSTRACT **In Western countries, invasive infections caused by M1T1 serotype group A *Streptococcus* (GAS) are epidemiologically linked to mutations in the control of virulence regulatory 2-component operon (*covRS*). In indigenous communities and developing countries, severe GAS disease is associated with genetically diverse non-M1T1 GAS serotypes. Hypervirulent M1T1 *covRS* mutant strains arise through selection by human polymorphonuclear cells for increased expression of GAS virulence factors such as the DNase Sda1, which promotes neutrophil resistance. The GAS bacteremia isolate NS88.2 (*emm* 98.1) is a *covS* mutant that exhibits a hypervirulent phenotype and neutrophil resistance yet lacks the phage-encoded Sda1. Here, we have employed a comprehensive systems biology (genomic, transcriptomic, and proteomic) approach to identify NS88.2 virulence determinants that enhance neutrophil resistance in the non-M1T1 GAS genetic background. Using this approach, we have identified streptococcal collagen-like protein A and general stress protein 24 proteins as NS88.2 determinants that contribute to survival in whole blood and neutrophil resistance in non-M1T1 GAS. This study has revealed new factors that contribute to GAS pathogenicity that may play important roles in resisting innate immune defenses and the development of human invasive infections—Tsatsaronis, J. A., Hollands, A., Cole, J. N., Maamary, P. G., Gillen, C. M., Ben Zakour, N. L., Kotb, M., Nizet, V., Beatson, S. A. Walker, M. J., Sanderson-Smith, M. L. Streptococcal collagen-like protein A and general stress protein 24 are immunomodulating virulence factors of group A *Streptococcus*. *FASEB J.* 27, 000–000 (2013). www.fasebj.org**

Key Words: systems biology · next-generation sequencing · innate immunity